



UNIVERSIDAD MICHOACANA DE
SAN NICOLÁS DE HIDALGO

Facultad de Ingeniería Eléctrica
División de Estudios de Posgrado

*“METHODOLOGY FOR THE ANALYSIS AND
SIMULATION OF ELECTRIC CIRCUITS AND
COMPONENTS BASED ON A FINITE ELEMENT ANALYSIS
AND APPLICATION OF PARALLEL PROCESSING”*

by

RAUL EDUARDO DOMINGUEZ MEZA

THESIS

REQUIREMENT FOR THE DEGREE OF
DOCTOR OF SCIENCE
IN ELECTRICAL ENGINEERING

ADVISOR:
J. AURELIO MEDINA RIOS, PhD.

MORELIA, MICHOACÁN

AUGUST 2014





METHODOLOGY FOR THE ANALYSIS AND SIMULATION OF ELECTRIC CIRCUITS AND COMPONENTS BASED ON A FINITE ELEMENT ANALYSIS AND APPLICATION OF PARALLEL PROCESSING

Los Miembros del Jurado de Examen de Grado aprueban
la Tesis de Doctorado en Ciencias en Ingeniería Eléctrica Opción en Sistemas Eléctricos
de *Raúl Eduardo Domínguez Meza*

Dra. Elisa Espinosa Juárez
Presidente del Jurado

Dr. J. Aurelio Medina Ríos
Director de Tesis

Dr. Antonio Ramos Paz
Vocal

Antonio Ramos Paz

Dr. Roberto Tapia Sánchez
Vocal

Roberto

Dr. Juan Felipe Soriano Peña
Revisor Externo

Dr. J. Aurelio Medina Ríos
*Jefe de la División de Estudios de Posgrado
de la Facultad de Ingeniería Eléctrica. UMSNH
(Por reconocimiento de firmas)*

Table of Contents

Nomenclature	i
Nomenclature (Greek symbols).....	vii
List of Tables	ix
List of Figures	x
List of Publications	xii
Abstract	xiii
Resumen	xiv
Acknowledgment	xv
1 Introduction.....	1
1.1 Solution of electromagnetic fields of electrical machines	1
1.1.1 Variables of electric and magnetic fields.....	2
1.1.1.1 Current density field	2
1.1.1.2 Magnetic flux density field	2
1.1.1.3 Magnetic vector potential field	3
1.1.1.4 Magnetic field strength	3
1.1.1.5 Electric fields	4
1.1.1.5.1 Maxwell's electrical field	4
1.1.1.5.2 Lorentz electrical field	5
1.1.1.5.3 Motional electric field	5
1.1.1.5.4 Total electric field	5
1.1.1.6 Total current density	5
1.1.2 Summary of main features of variables	6
1.1.2.1 Coulomb's position	6
1.1.2.2 Displacement current neglected	6
1.1.2.3 Defining magnetic vector potential	6
1.1.2.4 Defining electric field	6
1.1.2.5 Defining total current density	6
1.1.3 Field equations	7
1.1.3.1 Laplace and Poisson field equations	7
1.1.3.2 Helmholtz field equation	7
1.2 Justification of the present research	10
1.3 Objectives	11
1.4 Description of the methodology	12
1.5 Thesis content	13

2	Finite element analysis and computational techniques	14
2.1	Introduction	14
2.2	The Galerkin finite element method	15
2.2.1	Application of the finite element method by two-dimensional fields	15
2.2.1.1	Two dimensional field defined by a planar symmetry	16
2.2.1.1.1	Poisson equation, current density as the forcing function	16
2.2.1.1.2	Current density defined by an electrical field	17
2.2.1.1.3	Poisson equation, voltage as the forcing function	17
2.2.1.1.4	Defining the current as the forcing function	17
2.2.1.2	Two dimensional field defined by a axisymmetric symmetry	18
2.2.1.2.1	Poisson equation, current density as the forcing function	18
2.2.1.2.2	Current density defined by an electrical field	19
2.2.1.2.3	Poisson equation, voltage as the forcing function	19
2.2.1.2.4	Defining the current as the forcing function	20
2.2.2	Solution of field equation using Galerkin method	20
2.2.2.1	Field problems with boundary conditions	20
2.2.2.1.1	Boundary conditions of field equations	21
2.2.2.1.1.1	Dirichlet boundary condition	21
2.2.2.1.1.2	Neumann boundary condition	22
2.2.2.2	Solution of field problems using residual equation (Galerkin method)	22
2.2.2.2.1	Defining an approximate solution of residual equation	22
2.2.2.2.2	Defining the weigh functions of the residual equation	23
2.2.2.2.3	Substitution of approximate solution and weigh function in residual equation	23
2.2.2.2.4	Deriving matrix equation from residual expression	23

2.2.3	Solution of field problems using the finite element method/analysis -----	24
2.2.3.1	Partition of the domain -----	25
2.2.3.2	Choice of the interpolating function -----	26
2.2.3.2.1	Finite elements for a planar symmetry -----	27
2.2.3.2.1.1	Triangular finite element in planar symmetry with three nodes -----	27
2.2.3.2.1.2	Triangular finite element in planar symmetry with six nodes -----	28
2.2.3.2.2	Finite elements for an axisymmetric symmetry -----	30
2.2.3.2.2.1	Triangular finite element in axisymmetric symm with three nodes -----	30
2.2.3.2.3	Using alternative system of coordinates for finite element calculation -----	31
2.2.3.2.3.1	Reference and local finite elements planar symmetry -----	31
2.2.3.2.3.2	Reference and local finite elements axisymmetric symmetry -----	35
2.2.3.3	Formulation of the system to solve a field equation derived from a planar symmetry and an axisymmetric symmetry -----	37
2.2.3.3.1	Formulation of the system to solve a field equation derived from a planar symmetry assumption -----	37
2.2.3.3.1.1	Solution of a field equation derived from a plannar symm. using Galerkin weak formulation -----	38
2.2.3.3.2	Formulation of the system to solve a field equation derived from a axisymmetric symmetry assumption -----	40
2.2.3.3.2.1	Solution of a field equation derived from an axisymmetric symm. using Galerkin weak formulation -----	41
2.2.3.4	Deriving final matrix equation that contains the solution of the problem -----	43
2.2.3.5	Deriving field equation with time varying terms -----	44
2.2.3.5.1	Time varying terms of the planar symmetry, current and voltage as the forcing function -----	44
2.2.3.5.2	Time varying terms of the axisymmetric symmetry, current and voltage as the forcing function -----	46
2.3	FEM equations features -----	48
2.3.1	Assumptions of the FEM equations -----	48
2.3.2	FEM field equation of a device with voltages known -----	49
2.3.3	FEM field equation of a device with currents known -----	49

2.3.4	FEM circuit coupled equation of a device -----	50
2.3.4.1	Voltage-current circuit equation -----	50
2.3.4.2	Deriving the FEM-circuit coupled equation -----	51
2.4	Parallel processing -----	51
2.4.1	The CUDA platform -----	52
2.4.2	Using the CUDA platform to solve a FEM matrix equation -----	52
2.4.2.1	General form of the normal FEM equation -----	52
2.4.2.2	Preprocessing step of the FEM equation -----	53
2.4.2.3	Calculating step of the FEM equation -----	54
2.5	Conclusions -----	54
3	Proposed methodology -----	56
3.1	Introduction -----	56
3.1.1	Field equations-----	56
3.1.2	FEM field equations-----	57
3.1.2.1	FEM field equation with voltages known -----	57
3.1.2.2	FEM field equation with currents known -----	58
3.1.3	FEM-circuit coupled equation -----	58
3.2	Proposed methodology -----	59
3.2.1	Methodology applied on a FEM field equation with voltage known -----	59
3.2.1.1	Renumbering the nodes of the FEM field equations -----	59
3.2.1.2	Deriving a new FEM field equation based on the nodal renumbering -----	60
3.2.1.3	Identifying submatrices and formulating matrix equations -----	60
3.2.1.4	Deriving two matrix equations -----	61
3.2.1.5	Calculating the reduced equation -----	61
3.2.2	Methodology applied on a FEM field equation with currents known -----	62
3.2.2.1	Deriving a new FEM field equation based on the nodal renumbering -----	62
3.2.2.2	Performing an arrangement of the time varying variables -----	62
3.2.2.3	Identifying submatrices and formulating matrix equations -----	63
3.2.2.4	Deriving matrix equations -----	64
3.2.2.5	Calculating the reduced equation -----	64
3.2.3	Methodology applied on a FEM circuit coupled equation-----	64
3.2.3.1	Performing an arrangement of the time varying variables -----	64
3.2.3.2	Identifying submatrices and formulating matrix equations -----	65
3.2.3.3	Calculating the matrix equations -----	66
3.2.3.4	Calculating the reduced equation -----	66
3.3	Solution of the equation derived by the methodology -----	66
3.3.1	Time domain solution -----	67
3.3.3.1	Explicit methods -----	67

3.3.3.1.1	Euler method (forward difference)-----	68
3.3.3.1.2	Backwards Euler (backwards difference) -----	68
3.3.3.1.3	Runge Kutta method -----	69
3.3.3.2	Implicit method: Newton method -----	70
3.3.2	Frequency domain solution -----	72
3.3.2.1	Preprocessing step -----	74
3.3.2.2	Calculating step -----	75
3.3.2.3	Parallel computing using the LU method -----	75
3.3.2.3.1	Preprocessing steps implemented by a parallel computing -----	76
3.3.2.3.2	Calculating steps implemented by a parallel computing -----	77
3.3.2.3.2.1	CUBLAS decomposition LU -----	77
3.3.2.3.2.2	Final solution of equation using CUBLAS -----	77
3.4	Comparison between the ordinary and the proposed method -----	78
3.4.1	General aspects-----	78
3.4.1.1	FEM-field equation with voltages or currents known -----	78
3.4.1.2	FEM-circuit coupled equation -----	78
3.4.2	Comparison in the time domain-----	79
3.4.2.1	Euler method -----	79
3.4.2.2	Backwards Euler method -----	80
3.4.2.3	Runge Kutta method-----	80
3.4.2.4	Newton method -----	81
3.4.2.5	Summary of the time domain comparison -----	81
3.4.3	Comparison in the frequency domain-----	81
3.4.3.1	Summary of the frequency domain comparison -----	82
3.5	Conclusions -----	82
4	Sequential and parallel routines used in the finite element analysis-----	84
4.1	Introduction -----	84
4.2	Conventional FEM equations -----	84
4.2.1	Preprocessing FEM stage-----	84
4.2.1.1	FEM field equation with voltages known -----	85
4.2.1.2	FEM field equation with currents known -----	86
4.2.1.3	FEM-circuit coupled equation-----	87
4.2.2	Calculating stage-----	88
4.2.2.1	Solution in the frequency domain-----	89
4.2.2.2	Solution in the time domain-----	90
4.3	Proposed methodology-----	91
4.3.1	Preprocessing FEM stage-----	91
4.3.1.1	FEM field equation with voltages known -----	92
4.3.1.2	FEM field equation with currents known -----	94
4.3.1.3	FEM-circuit coupled equation-----	95
4.3.2	Calculating stage-----	96
4.3.2.1	Solution in the frequency domain-----	96
4.3.2.2	Solution in the time domain-----	97

4.4	Conclusion	99
5	Case studies	101
5.1	Introduction	101
5.2	Planar symmetry assumption cases	102
5.2.1	Case study 1. Slot embedded conductor modeled by a one dimension finite element analysis	102
5.2.1.1	Introduction	102
5.2.1.2	Two-loop circuit voltage-current equation	104
5.2.1.3	Field equations of the device	104
5.2.1.4	Finite element analysis	104
5.2.1.5	FEM-circuit coupled equation	105
5.2.1.6	Solution derived by the proposed methodology	106
5.2.1.7	Comparison results in frequency domain	108
5.2.1.8	Comparison in time domain	109
5.2.1.9	Performance comparison	111
5.2.2	Case study 2. Slot embedded conductor modeled by two dimension Finite element analysis	112
5.2.2.1	Introduction	112
5.2.2.2	Two-loop circuit voltage-current equation	112
5.2.2.3	Field equations of the device	112
5.2.2.4	Finite element analysis	112
5.2.2.5	FEM-circuit coupled equation	113
5.2.2.6	Solution derived by the proposed methodology	113
5.2.2.7	Comparison in frequency domain	115
5.2.2.8	Comparison in time domain	115
5.2.2.9	Performance comparison	117
5.2.3	Case study 3. T Slot embedded conductor modeled by a two dimension Finite element analysis	119
5.2.3.1	Introduction	119
5.2.3.2	Field equations of the device	120
5.2.3.3	Finite element analysis	121
5.2.3.4	Solution obtained by the proposed methodology	121
5.2.3.5	Comparison results	123
5.2.3.6	Performance comparison	124
5.2.3.7	Parallel solution using CUBLAS	125
5.2.3.7.1	Performance comparison between the sequential and the parallel solution	126
5.3	Axisymmetric symmetry assumption cases	128
5.3.1	Case study 4. Air series reactor modeled by a two dimension Finite element analysis	128
5.3.1.1	Introduction	128
5.3.1.2	Field equations	129
5.3.1.3	Finite element analysis	130
5.3.1.3.1	Conventional finite element analysis	130
5.3.1.3.2	Finite element analysis using proposed methodology	132
5.3.1.3.3	Finite element analysis using ANSYS	133
5.3.1.4	Calculating the inductances of the reactors 1 and 2	133

5.3.1.5	Calculating the inductance ratio	134
5.3.1.6	Comparison results	134
5.3.1.7	Performance comparison	137
5.3.2	Case study 5. Parallel solution of the air series reactors	138
5.3.2.1	Introduction	138
5.3.2.2	Parallel calculating process	138
5.3.2.3	Performance comparison between the Sequential and the parallel solutions	139
5.4	Conclusions	142
6	Conclusions	144
6.1	Summary of results	144
6.2	Recommendation for further investigations	146
	Bibliography	147
A	Appendix A	152
A.1	Planar symmetry's FEM matrices and vectors	152
A.1.1	Finite elements	152
A.1.1.1	Triangular linear finite element with three nodes	152
A.1.1.2	Triangular linear finite element with six nodes	152
A.1.2	Field equation with current density as the forcing function	153
A.1.2.1	Matrixes derived from applying FEA	153
A.1.2.1.1	Matrixes and vectors for Finite element of three nodes	153
A.1.2.1.2	Matrixes and vectors for Finite element of six nodes	154
A.1.3	Field equation with voltages as the forcing function	155
A.1.3.1	Matrixes derived from applying FEA	155
A.1.3.1.1	Matrixes and vectors for Finite element of three nodes	155
A.1.3.1.2	Matrixes and vectors for Finite element of six nodes	155
A.1.4	Field equation with currents as the forcing function	156
A.1.4.1	Matrixes derived from applying FEA and Newton C	156
A.1.4.1.1	Vectors for finite element of three nodes	156
A.1.4.1.2	Vectors for finite element of six nodes	156
A.2	Axisymmetric symmetry FEM matrixes and vectors	157
A.2.1	Finite elements	157
A.2.1.1	Triangular linear finite element with three nodes	157
A.2.2	Field equation with current density as the forcing function	157
A.2.2.1	Matrixes derived from applying FEA	157

A.2.2.1.1	Matrices and vectors for finite element of three nodes -----	158
A.2.3	Field equation with voltages as the forcing function-----	158
A.2.3.1	Matrixes derived from applying FEA -----	158
A.2.3.1.1	Matrices and vectors for Finite element of three nodes -----	158
A.2.4	Field equation with currents as the forcing function-----	159
A.2.4.1	Matrixes derived from applying FEA-----	159
A.2.4.1.1	Vectors for finite element of three nodes -----	159
B	Appendix B -----	160
B.1	Frequency domain solution-----	161
B.2	Time domain solution-----	163
B.2.1	Explicit methods -----	163
B.2.1.1	Euler method (forward difference)-----	163
B.2.1.2	Backwards method (backwards difference)-----	165
B.2.1.3	Fourth order Runge Kutta methods-----	167
B.2.2	Implicit methods-----	169
B.2.2.1	Newton method -----	169
B.2.2.2	Numerical Differentiation method -----	172
C	Appendix C -----	174
C.1	Case study 2 -----	174
C.1.1	GSL program -----	174
C.1.2	CUBLAS program -----	176
C.2	Case study 4 -----	176
C.2.1	Air series reactor 1-----	176
C.2.1.1	GSL program -----	174
C.2.1.2	CUBLAS program -----	178
C.2.2	Air series reactor 2 -----	178
C.2.2.1	GSL program -----	178
C.2.2.2	CUBLAS program -----	180

Nomenclature

A	Tm	magnetic vector potential
A_i	—	magnetic vector potentials of the conductor region
A_j	—	magnetic vector potentials of the non-conductor region
A_x	—	magnetic vector potentials, planar and axisymmetric symmetries
A_z	Tm	magnetic vector potential, planar symmetry
A_ρ	Tm	magnetic vector potential, axisymmetric symmetry
$[A_f], [L_f], [U_f]$	—	matrices of equation $Ax=b$
$[A_g], [L_g], [U_g]$	—	matrices of equation $Ax=b$
$[A_T]_{(t)}, [A_T], [L_T], [U_T]$	—	matrices of equation $Ax=b$
$[A]_{(t)}, [L]_{(t)}, [U]_{(t)}$	—	matrices of equation $Ax=b$
$[A_z]^e$	—	vector of a triangle finite element, planar symmetry
$[A_\rho]^e$	—	vector of a triangle finite element, axisymmetric symmetry
$\{A_x\}, \{A_{x,T}\}$	—	magnetic vector potentials vector, planar and axisymmetric symmetries
a, b, c	—	components of the interpolation function of triangular finite element
B	T	magnetic flux density
$\{b_f\}, \{b_T\}, \{b_T\}_{(t)}$	—	vector solution of equation $Ax=b$
D	C/m ²	electric displacement
Dx_i, Dx_{i+1}	—	variational variables of Newton method
E_z	V/m	electric field, planar symmetry
E	V/m	electric field
E_c	V/m	coulombian electric field
E_i	V/m	induced electric field
E_m	V/m	motional electric field

E_p	V/m	electric field, axisymmetric symmetry
F_i	—	component i-th of excitation vector
f	—	forcing functional
f_J	—	excitation of field equation, planar and axisymmetric symmetry
f_p	—	excitation of field equation, axisymmetric symmetry
f_i	—	subvector of the proposed method
$f_b, \{f_T\}, \{F_T\}, \{F_{T,x}\}$	—	vector of the proposed method
f_1, f_2	—	subvectors of the proposed method
$[f_{1,x}], [f_{2,x}]$	—	subvectors of the proposed method
$\{f_b^{(I)}\}$	—	Neumann boundary conditions vector
$\{f_b^{(II)}\}$	—	Dirichlet boundary conditions vector
$\{f_{gij}, f_{guj}, \{f_g\}, \{f_U\}$	—	excitation vector derived by finite element analysis
$\{f_x\}$	—	excitation vector, planar and axisymmetric symmetry
$\{f_z\}^e$	—	excitation of a triangle finite element, planar symmetry
$\{f_p\}^e$	—	excitation of a triangle finite element, axisymmetric symmetry
F_i	—	component i-th of excitation vector
$\{F\}$	—	excitation vector
$\{F\}_{(t+\Delta t)}, \{F\}_{(n+1)}$	—	variable discretized in time domain
$\{F\}_{(t)}, \{F\}_{(n)}$	—	variable discretized in time domain
$\{F\}_{(t-\Delta t)}, \{F\}_{(n-1)}$	—	variable discretized in time domain
$\{F_T\}_{(t+\Delta t)}, \{F_T\}_{(n+1)}$	—	variable of proposed method discretized in time domain
$\{F_T\}_{(t)}, \{F_T\}_{(n)}$	—	variable of proposed method discretized in time domain
$\{F_T\}_{(t-\Delta t)}, \{F_T\}_{(n-1)}$	—	variable of proposed method discretized in time domain
$[G]$	—	stiffness matrix derived by finite element analysis
$G_b, [G_T], [G_{T,x}], [G_T]_{(t)}$	—	matrix of the proposed method
G_{11}, G_{12}	—	submatrices of the proposed method
$[G_{11,x}], [G_{12,x}]$	—	submatrices of the proposed method
H	A/m	magnetic field strength

l, l_x, l_t	m	conductor length
I	A	current
$\{I\}$	—	currents vector
I_c	A	conductor current
I_z	A	current, planar symmetry
I_ρ	A	current, axisymmetric symmetry
H	A/m	magnetic field strength
J, J_{tot}	A/m ²	current density
J_z	A/m ²	current density, planar symmetry
J_ρ	A/m ²	current density, axisymmetric symmetry
$J(t)$	—	jacobian matrix of Newton method
k_1, k_2, k_3, k_4	—	coefficients of Runge Kutta methods
$K_{12}, K_{12}, K_{21}, K_{22}$	—	submatrices of the proposed method
$[K_{12,x}], [K_{12,x}], [K_{21,x}], [K_{22,x}]$	—	submatrices of the proposed method
$K, [K_T], [K_{T,x}], [K_T]_{(t)}$	—	matrix of the proposed method
$[K]$	—	stiffness matrix derived by finite element analysis
$\{k_1\}, \{k_2\}, \{k_3\}, \{k_4\}$	—	coefficients vectors of Runge Kutta methods
$\{k_{1,T}\}, \{k_{2,T}\}, \{k_{3,T}\}, \{k_{4,T}\}$	—	proposed method, coefficients vectors of Runge Kutta methods
$\{k_{1T}\}_{(t)}, \{k_{2T}\}_{(t)}, \{k_{3T}\}_{(t)}, \{k_{4T}\}_{(t)}$	—	proposed method, coefficients vectors of Runge Kutta methods
L	—	generic differential operator
$[L]$	—	inductances matrices
$L_1, L_2, L_3, L_4, L_5, L_6$	—	components of the interpolation function of triangular finite element
$[M_c], [M_i], [M_c^x]$	—	matrix derived by Newton Cotes analysis
$[M_c^z]$	—	matrix derived by Newton Cotes analysis, planar symmetry
$[M_c^p]$	—	matrix derived by Newton Cotes analysis, axisymmetric symmetry

$[M_c]^e$	—	vector of a triangle finite element, planar symmetry
$\{M_c\}$	—	matrix derived by Newton Cotes
n_x, n_y	—	normal unit vector, planar symmetry
n_r, n_z	—	normal unit vector, axisymmetric symmetry
N_i, N_j	—	i-th and j-th weight function
N_{mj}	—	j-th weight function of interpolating function
N_p, N_q	—	p-th and q-th weight function
$\{N_{mj}\}, \{N_i\}$	—	j-th weight function vector
$\{N_i\}$	—	i-th weight function vector
$\{N_z^e\}, \{N_\rho^e\}$	—	weight function vector of a triangle finite element
r, z, ρ	m	cartesian Coordinates axisymmetric symmetries
r_D, z_D	m	integration limits along surface, planar symmetry
r_i, r_j, z_i, z_j	m	limits of the integration surface τ_r
$r_1, r_2, r_3, z_1, z_2, z_3$	m	coordinates of the triangle finite element, axisymmetric symmetry
P	—	dependence on the point P, e.g. on the coordinate (x,y,z) or (r,z, ρ)
q	C	electric charge
R_c	R_e	ohms conductors resistance
$[R]$	—	resistances matrix
S_c, S	m^2	area
S_{ij}	—	component i-th, j-th of the matrix [S]
S_{ii}, S_{ij}, S_{jj}	—	submatrices of the proposed method
$[S], [T]$	—	stiffness matrices derived by the finite element analysis
$[S_x], [T_x]$	—	stiffness matrix derived by finite element analysis
$[S_z]^e$	—	stiffness matrix of a triangle finite element, planar symmetry

$[S_\rho]^e$	—	stiffness matrix of a triangle finite element, axisymmetric symmetry
t	s	time
t_n, t_{n+1}	s	discretized time
T_{ii}	—	submatrix of the proposed method
$[T_{T,x}]$	—	matrix of the proposed method
$[T_z]^e$	—	stiffness matrix of a triangle finite element, planar symmetry
$[T_\rho]^e$	—	stiffness matrix of a triangle finite element, axisymmetric symmetry
U_c	V	conductor voltage
$\{U_c\}$	—	voltage vector
ν	m/H	magnetic permeability
u, v	m	coordinates of isoparametric finite element
ν_q	m/s	speed of the electric charge
ν_m	m/s	speed of the medium on which the charge is bound
ν_ρ	m/seg	speed of the electrical charge density
$\{V\}$	—	excitation voltage vector
w	rad/seg	angular velocity
w_i, w_j	—	i-th, j-th weight function
x, y, z	m	cartesian Coordinates
x_i, x_f, y_i, y_f	m	limits of the integration surface τ
$x_1, x_2, x_3, y_1, y_2, y_3$	m	coordinates of triangle finite element, planar symmetry
x_D, y_D	m	integration limits along surface, planar symmetry
$X_{(t+\Delta t)}, X_{(n+1)}$	—	variable discretized in time domain
$X_{(t)}, X_{(n)}$	—	variable discretized in time domain
x, y, z	m	cartesian Coordinates
$X_{(t-\Delta t)}, X_{(n-1)}$	—	variable discretized in time domain
X_∞	—	vector of the cycle finite
x_1, x_2	—	subvectors of the proposed method

X_T	—	variable of proposed method
$\{X\}_{(t+\Delta t)}, \{X\}_{(n+1)}$	—	vector discretized in time domain
$\{X\}_\infty$	—	cycle limit of vector
$\{X_T\}_\infty$	—	cycle limit of vector of proposed method
$\{X_f\}, \{X_g\}, \{X_T\}$	—	vector solution of equation $Ax=b$
$\{X\}$	—	vector that contains magnetic vector potentials or currents
$\{X_T\}$	—	vector of proposed method that contains magnetic vector potentials or currents
$\{X\}_{(t+\Delta t)}, \{X\}_{(n+1)}$	—	vector discretized in time domain
$\{X\}_{(t)}, \{X\}_{(n)}$	—	vector discretized in time domain
$\{X\}_{(t-\Delta t)}, \{X\}_{(n-1)}$	—	vector discretized in time domain
$\{X_T\}_{(t+\Delta t)}, \{X_T\}_{(n+1)}$	—	vector of proposed method discretized in time domain
$\{X_T\}_{(t)}, \{X_T\}_{(n)}$	—	vector of proposed method discretized in time domain
$\{X_T\}_{(t-\Delta t)}, \{X_T\}_{(n-1)}$	—	vector of proposed method discretized in time domain
$\{Y_f\}, \{Y_g\}, \{Y_T\}$	—	vector solution of equation $Ax=b$

Nomenclature (Greek symbols)

$\alpha_x, \alpha_y, \alpha_z, \beta$	—	parameters of field equation, planar symmetry
$\alpha_i, \beta_i, \alpha_{si}, \beta_{si}$	°	phase angle
$\alpha_r, \alpha_z, \alpha_\rho, \beta$	—	parameters of field equation, axisymmetric symmetry
Δ	m ²	conductor area, planar symmetry
Δ_d	m ²	determinant of the triangle finite element, planar symmetry
Δ_d^r	m ²	determinant of the triangle finite element, axisymmetric symmetry
Δ_e, Δ_r	V/A	equivalent of resistance, axisymmetric
Δ_r	—	ratio V and I, axisymmetric symmetry
$\Delta x, \Delta x_i$	—	variables of Newton method
$[\Delta_x]$	—	vector of ratio V and I, planar and axisymmetric symmetry
ϕ_k	—	general potential, planar and axisymmetric symmetry
ϕ_ρ	—	potentials of field equation, axisymmetric symmetry
ϕ_z	—	potentials of field equation, planar symmetry
ϕ	—	unknown potential to be determined
ϕ_1, ϕ_2, ϕ_3	Tm	magnetic vector potentials of triangle finite element, planar symmetry
ϕ^*	—	function that approaches the unknown potential
ϕ_j	—	j-th coefficient to approach the potential ϕ
ϕ_i, ϕ_j	—	unknown coefficients
ϕ_m	—	interpolating function of finite element
ϕ_m^*	—	interpolating function
ϕ_{mj}	—	j-th unknown potential
$\{\phi_{mj}\}$	—	unknown potential vector

$\{\phi_j\}$	—	vector of the unknown coefficients ϕ
$\{\phi_m\}$	—	magnetic vector potentials vector in the triangle finite element, planar symmetry
Φ	—	matrix of Newton method
$[\Phi_T]$	—	matrix of Newton method of proposed method
Γ, Γ_d	m	boundary of the domain, planar and axisymmetric symmetry
μ	H/m	magnetic permeability
μ_r	—	relative magnetic permeability
ρ	c/m ²	volume density of electric charge
σ	S/m	electric conductivity
τ, τ_D	m ²	surface, planar symmetry
τ_s, τ_{sD}	m ²	surface, axisymmetric symmetry

List of Tables

Table 1.1 Classification of the electrical fields.....	4
Table 4.1 Routines and platforms used in the <i>preprocessing stage</i> of a FEM field equation with voltages known.....	86
Table 4.2 Routines and platforms used in the <i>preprocessing stage</i> of a FEM field equation with currents known.....	87
Table 4.3 Routines and Platforms Used in the <i>preprocessing stage</i> of FEM-circuit coupled equation.....	88
Table 4.4 Routines and platforms used in the frequency domain solution of a <i>conventional</i> FEM equation.....	90
Table 4.5 Routines and platforms used in the time domain solution of a <i>conventional</i> FEM equation using the Backwards Euler method.....	91
Table 4.6 Routines and platforms used in the preprocessing stage of the proposed method For a FEM-field equation with voltages known	93
Table 4.7 Routines and platforms used in the preprocessing stage of the proposed method For a FEM-field equation with currents known	94
Table 4.8 Routines and platforms used in the preprocessing stage of the proposed method for a FEM-circuit coupled equation	95
Table 4.9 Routines used in the frequency domain solution of the reduced equation derived from the proposed method.....	97
Table 4.10 Routines used in the time domain solution of a conventional FEM equation using the Backwards Euler, Euler and the 4 th order Runge Kutta methods.....	99
Table 5.1 Parameters of the conductors and the voltage-current equation	104
Table 5.2 Magnetic vector potentials (MVP) and currents in the frequency domain	108
Table 5.3 Magnetic vector potentials (MVP) and currents in the time domain using the Backwards-Euler method	109
Table 5.4 Magnetic vector potentials (MVP) and currents in the time domain using the Backwards Euler and the Runge Kutta methods.....	110
Table 5.5 Computing time to solve the equations in the time domain	111
Table 5.6 Magnetic vector potentials (MVP) and currents in the frequency domain	115
Table 5.7 Magnetic vector potentials (MVP) and currents in the time domain using the Backwards Euler method.....	116
Table 5.8 Magnetic vector potentials (MVP) and currents in the time domain using the Backwards Euler and the 4 th Runge Kutta methods.....	117
Table 5.9. Computing time to solve the equations in the time domain.....	118
Table 5.10 Reverse “T” slot-embedded conductor physical dimensions.....	119
Table 5.11 Electric and magnetic properties of the “T” slot embedded conductor.....	120
Table 5.12 Source current density in the frequency domain.....	123
Table 5.13 FEM equations to be solved in a frequency range.....	126
Table 5.14 Dimensions and properties of air reactors 1 and 2.....	129
Table 5.15 Parameters of air reactors 1 and 2.....	131
Table 5.16 Voltages at each turn of reactor 1.....	135
Table 5.17 Voltages at each turn of reactor 2.....	135
Table 5.18 Simulation time to solve the conventional and the proposed equation for reactor 1.....	137

Table 5.19 Simulation time to solve the conventional and the proposed equation for reactor 2.....	138
Table 5.20 FEM equations to be solved in a frequency range.....	139

List of Figures

Figure 2.1 A finite element defined in a local system of coordinates (u,v) and mapping to a global system of coordinates (x,y)	31
Figure 2.2 A finite element of six nodes defined in a local system of coordinates (u,v) and mapping to a global system of coordinates (x,y)	34
Figure 2.3 A finite element defined in a local system of coordinates (u,v) and mapping to a global system o coordinates (r,z)	35
Figure 2.4 Two dimension domain of a planar symmetry assumption.....	39
Figure 2.5 Two dimension domain of an axisymmetric symmetry assumption.....	42
Figure 2.6 <i>Preprocessing</i> steps of the FEM equation.....	54
Figure 3.1. <i>Calculating</i> process of the Newton method using ND approach.....	72
Figure 3.2. <i>Preprocessing</i> step of the <i>conventional</i> FEM equation.....	74
Figure 3.3. <i>Preprocessing</i> step of the <i>reduced</i> FEM equation.....	75
Figure 3.4. <i>Preprocessing</i> step of the <i>proposed</i> FEM equation.....	76
Figure 3.5. <i>LU</i> decomposition process implemented in <i>CUBLAS</i>	77
Figure 4.1 <i>Preprocessing FEM stage</i> of a conventional FEM equation performed by ANSYS... ..	85
Figure 4.2 <i>Preprocessing stage</i> of a FEM field equation with voltages known.....	86
Figure 4.3 <i>Preprocessing stage</i> of a FEM field equation with currents known.....	87
Figure 4.4 <i>Preprocessing stage</i> of a FEM-circuit coupled equation.....	88
Figure 4.5 <i>Calculating process</i> for the <i>conventional</i> FEM equations in the frequency domain.....	89
Figure 4.6. <i>Preprocessing FEM stage</i> of the proposed methodology using ANSYS	92
Figure 4.7 <i>Preprocessing stage</i> of the methodology applied to a FEM-field equation with voltages known.....	93
Figure 4.8 <i>Preprocessing stage</i> of the methodology applied to a FEM-field equation with currents known.....	94
Figure 4.9 <i>Preprocessing stage</i> of the methodology applied to FEM-Circuit coupled equation... ..	95
Figure 4.10. <i>Calculating stage</i> of the proposed method in the frequency domain.....	97
Figure 5.1 Scheme of the three slot embedded conductors.....	102
Figure 5.2 Two loop circuit used for the Example.....	103
Figure 5.3 FEM discretization of the conductors.....	103
Figure 5.4 Proposed FEM discretization of the conductors.....	106
Figure 5.5 FEM discretization of the three slot conductors.....	112
Figure 5.6 Proposed FEM discretization of the three slot conductors.....	113
Figure 5.7 “T” slot-embedded conductor.....	119
Figure 5.8 Magnetic model of the conductor, its boundary conditions and the FEM meshing.....	120
Figure 5.9 <i>CPU times</i> derived for the FEM equations solutions.....	124
Figure 5.10 <i>CPU times</i> derived for solving the “T” planar conductor.....	127
Figure 5.10a. <i>Ratio t_s/t_p</i> derived for solving the “T” planar conductor.....	127
Figure 5.11 Air reactors to be analyzed.....	128
Figure 5.12 Geometry of air reactors.....	129

Figure 5.13 Finite element model of air reactors.....	130
Figure 5.14 Inductances ratio of air reactor 1.....	136
Figure 5.15 Inductances ratio of air reactor 2.....	136
Figure 5.16 <i>CPU time</i> derived for reactor 1	140
Figure 5.17 <i>CPU time</i> derived for reactor 2	141
Figure 5.18 <i>Ratio t_s/t_p</i> derived for reactor 1	142
Figure 5.19 <i>Ratio t_s/t_p</i> derived for reactor 2	142
Figure B.1 Calculating process of the <i>Euler</i> method.....	162
Figure B.2 Backwards Euler method.....	164
Figure B.3 Fourth order Runge Kutta method.....	166
Figure B.4 Brute force method.....	167
Figure B.5 Orbit of a vector X.....	168
Figure B.6 Diagram of the <i>ND</i> Method	171

List of Publications

Published in international conferences registered in ISI Thomson

- Dominguez R., Medina A., “A Novel Method for the Solution of a Finite Element-Circuit Coupled Equation using a Reduced Equivalent Equation”, Proceedings of the 2013 IEEE International Electric Machines and Drives Conference (IEMDC), May 2013. Chicago IL. pp. 1061-1064.
- Dominguez R., Medina A., Ramos-Paz A., “The solution of a FEM equation in frequency domain using a parallel computing with CUBLAS”, Proceedings of the 2014 International Conference on Parallel and Distributed Processing Techniques and Applications (PDPTA), July 2014. Las Vegas NV.
- Dominguez R., Medina A., “A Method to Solve a FEM-Circuit Coupled Equation based on a Time Varying Approach”, Proceedings of the 2014 International Conference on Electrical Machines (ICEM), September 2014. Berlin.

Abstract

An alternative method for the solution of finite element (FEM) equations is presented. The solution of the equation is based on deriving an uncoupled equation which is expressed, in terms of the time varying variables of the FEM equations. It has been considered FEM equations derived from planar or axisymmetric symmetries assumptions. The method consists on performing a nodal reordering of the FEM Equations, and performing a reduced number of matrix operations. These steps permit to get an equation defined in terms of the time varying variables. The equation can be solved in the frequency and the time domain. The method developed has been also implemented in the CUBLAS parallel computing platform, in order to reduce the computing times of solving the matrix equation.

The method has been applied to several devices modelled by a planar and an axisymmetric symmetry assumption. The method permits to obtain accurate results in the frequency and the time domain but do not consider non-linear materials properties. The advantages of using the method are evident when large FEM equations are meant to be solved. The results obtained by the method agree well with results obtained by other investigations.

Keywords: Finite element analysis, finite element method, frequency-domain analysis, time-domain analysis, parallel processing.

Resumen

En esta tesis se presenta un método de solución de ecuaciones de elemento finito (ecuaciones FEM por sus siglas en inglés). La solución de las ecuaciones está basado en obtener una ecuación desacoplada, misma que está expresada en término de las variables de las ecuaciones FEM, que tienen derivación no nula respecto al tiempo. Las ecuaciones FEM consideradas han sido obtenidas a partir de una simplificación de simetría plana o axisimétrica. El método desarrollado consiste en realizar un reordenamiento nodal de las ecuaciones FEM, y realizar al mismo tiempo, un reducido número de operaciones matriciales. Los pasos antes mencionados permiten obtener una ecuación definida en términos de las variables con derivación no nula respecto al tiempo. La ecuación puede resolverse tanto en el dominio del tiempo como en el dominio de la frecuencia. Al mismo tiempo, el método desarrollado ha sido implementado en la plataforma de cómputo paralelo CUBLAS, con el objetivo de reducir el tiempo de cómputo requerido para resolver las ecuaciones matriciales. El método ha sido aplicado a varios dispositivos modelados por una simetría plana o axisimétrica. El método permite obtener resultados precisos en el dominio del tiempo y la frecuencia, pero no considera las propiedades no lineales de los materiales. La ventaja del uso del método es evidente cuando es utilizado para resolver ecuaciones FEM de gran dimensión. Los resultados obtenidos por el método concuerdan con aquellos resultados obtenidos por otros trabajos de investigación.

Palabras clave: Análisis de elemento finito, método de elemento finito, análisis en el dominio de la frecuencia, análisis en el dominio del tiempo, procesamiento en paralelo.

Acknowledgments

Dedico esta tesis a mis padres quienes me apoyaron todo el tiempo en todos los sentidos. Las palabras no alcanzan para describir todo lo que les debo y todo el apoyo recibido.

A mi asesor, por su continuo apoyo y orientación académica y personal; sin las cuales esta tesis no hubiera sido posible.

A los académicos y maestros del posgrado quienes estudiaron mi tesis.

A los maestros y alumnos del posgrado a quienes tuve la oportunidad de conocer en estos cuatro años.

A mis amigos y personas queridas que tuve el tiempo de conocer, durante mi estancia en Morelia.

A todas las personas que he tenido la oportunidad de conocer a lo largo de mis casi cuarenta años de vida. Todo lo bueno y malo que soy, es por ustedes. Aunque no los nombre y se me olvide sus nombres, algo de ustedes está en mí; y espero que algo mío esté en ustedes.

A todos los que me apoyaron para escribir y concluir esta tesis.

Para ellos es esta dedicatoria de tesis.

1 Introduction

1.1 Solution of electromagnetic fields of electrical machines or devices

In the actual times, it is very important to have electrical machines which have been properly optimized in their design, since an optimized design permits to have devices with high energy efficiency (Manna and Marwaha 2008). Thus, it is possible to use a lesser amount of materials on them. Moreover, it is also very important to assure the reliability in the performance of the devices. Although the Maxwell electromagnetic laws have been well-known for many years, the analysis and solution of their electric and magnetic equations that model an electrical machine or devices, have been difficult to achieve. The main reason is the geometry or the complexity of the device to be modeled (Manna and Marwaha 2008), (Chari and Sylvester 1980), (Arkkio 1987).

In order to overcome this situation, several forms of solution of the field equations. For example have been proposed; some methods of solution permit to calculate some parameters of the device, or models have been developed to allow the modeling of specific machines or devices (Engleman and Middendorf 1995), (Brauer, Sadegui and Oerterlei 1999). The recent computation advances have allowed the development of numerical methods, which can solve the magnetic and electric field equations (Chari and Sylvester 1980), (Engleman and Middendorf 1995), (Brauer, Sadegui and Oerterlei 1999).

The Finite Element Method (FEM) is a numerical method which has become a powerful tool, to solve the steady state and transient field equations of electrical machines or devices (Reece and Preston 2000), (Wang and Xie 2009), (Lubin, Mezani and Rezzoug 2011), (Li, Ho and Fu 2012), (Ho, Fu and Wong 1997), (Bianchi 2005). The method is now an important technique which supports the design of large machines, i.e. power transformers, large induction and synchronous motors; since it can solve the magnetic or electrical field of difficult geometries or configurations. Thus, the finite element method has allowed the improvement of the machines or devices efficiency, by optimizing their respective designs (Lubin, Mezani and Rezzoug 2011), (Li, Ho and Fu 2012), (Mihai and Benelghali 2012).

Nevertheless, the finite element method is still difficult to use in three-dimension cases (Wang and Xie 2009), (Lubin, Mezani and Rezzoug 2011), (Li, Ho and Fu 2012), (Mihai and Benelghali 2012). An important simplification, is to assume that the magnetic field behavior is the same across the axis of the machine or device (Arkkio 1987), (Bianchi 2005). Thus, it is necessary to perform some simplifications i.e. a plane symmetry or an axisymmetric assumption, to reduce the complexity of the problem, and being able to solve the field expressions, by using FEM matrix equations (Arkkio 1987), (Bianchi 2005), (Li, Ho and Fu 2012). The plane symmetry allows to model induction machines, while the axisymmetric symmetry permits to model transformers or components with round coils (Arkkio 1987), (Konrad, Chari and Csendes 1982), (Preiss 1983).

The FEM equations are derived by taking into account several assumptions on the electric

and magnetic fields. Because of this, it is very important that some basic concepts of magnetic and electric fields would be outlined. The aim is to furnish a good treatment and to derive a practical formulation. It is important to say that it is not an exhaustive treatment. There are other references that contain a precise exhaustive treatment of these electromagnetic concepts (Stratton 1941), (Bianchi 2005), (Cheng 1993), (Jianming 2002). The assumptions and considerations assumed for these variables, permits to derive a field equation of the device.

1.1.1 Variables of electric and magnetic fields

1.1.1.1 Current density field

The movement of the electric charges is described by means of the electric current density. Referring to a volume charge density ρ moving at a velocity v_ρ , the electric current density vector J can be defined as (Bianchi 2005), (Cheng 1993), (Jianming 2002),

$$J = \rho v_\rho \quad (1.1)$$

Whose reference positive direction is that of the positive charges. Its magnitude is measured in (A/m²). The vector J defines a vector field, called the current field. Let S_c be an open surface, then the current intensity I is given by (Bianchi 2005), (Cheng 1993), (Jianming 2002),

$$I = \int_{S_c} J dS \quad (1.2)$$

If the displacement current density vector is null ($\partial D/\partial t = 0$), it is possible to define the total current density vector as follows (Bianchi 2005), (Cheng 1993), (Jianming 2002),

$$J_{tot} = J \quad (1.3)$$

1.1.1.2 Magnetic flux density field

The movement of the electric charges causes effects in the points of the surrounding space, so that it is possible to define the magnetic flux density field B . Its magnitude is measured in Teslas (T). The fundamental property of the field B is this: the flux associated to this field, through any closed surface S_c is null. Thus the flux is given by (Bianchi 2005), (Cheng 1993), (Jianming 2002),

$$\oint_{S_c} B \cdot ndS = \int_V (\nabla \cdot B) dV = 0 \quad (1.4)$$

If (1.4) is expressed in a differential form, i.e.,

$$\nabla \cdot \mathbf{B} = 0 \quad (1.5)$$

1.1.1.3 Magnetic vector potential field

Observing (1.5) it can be seen that B is solenoidal in the whole space; thus, it is suitable to define a vector magnetic potential A . The vector B is solenoidal since its divergence is null in the domain defined by $\int_V dV$. The relationship between B and A is defined by (Bianchi 2005), (Cheng 1993), (Jianming 2002)

$$\mathbf{B} = \nabla \times \mathbf{A} \quad (1.6)$$

This relationship defines the field A apart from a generic irrotational field. A vector field is irrotational if its rotational is null in the domain defined by $\int_{S_c} ds$. The divergence of A can be defined in an arbitrary way; the positions that are commonly adopted for stationary and quasi-stationary magnetic fields are known as the *Coulomb's* position, (Bianchi 2005), (Cheng 1993), (Jianming 2002). It is defined by,

$$\nabla \cdot \mathbf{A} = 0 \quad (1.7)$$

1.1.1.4 Magnetic field strength

Together with the flux density vector B , the magnetic field strength vector H is introduced. The measure unit of its magnitude is A/m. The two vector fields are linked by the constitutive law defined by (Bianchi 2005), (Cheng 1993), (Jianming 2002),

$$\mathbf{B} = \mu \mathbf{H} \quad (1.8)$$

where μ (H/m) is the magnetic permeability of the medium. Within a *uniform medium*, the two fields B and H are *proportional* (i.e., they have same direction and proportional magnitude), while in an anisotropic medium their link exhibits a tensorial nature. In stationary or quasi-stationary magnetic condition, i.e. when the displacement current density is neglected, the fundamental property of the field H is defined by the Ampere's law (Bianchi 2005), (Cheng 1993), (Jianming 2002),

$$\nabla \times \mathbf{H} = \mathbf{J} \quad (1.9)$$

1.1.1.5 Electric fields

Forces of various natures can exist on the electric charges. Let δF_k be any force on a test positive charge δq , the specific electric field E_k is defined as (Bianchi 2005), (Stratton 1941), (Bianchi 2005), (Cheng 1993), (Jianming 2002)

$$E_k = \lim_{\delta q \rightarrow 0} \frac{\delta F_k}{\delta q} \quad (1.10)$$

Whose magnitude is measured in N/C. A useful classification of the specific electric field is given in Table 1.1

TABLE 1.1
CLASSIFICATION OF THE ELECTRICAL FIELDS

<i>Electric Field E_k</i>	Electromagnetic	<i>conservative</i>	E_c Coulomb	<i>E Electric Field</i>
		<i>Non-conservative</i>	E_i Induced	
			E_L Lorentz	
			E_m motional	
<i>Non-electromagnetic E_{ne}</i>				

1.1.1.5.1 Maxwell's electrical field

Since there is no constraint on the divergence of E_i , it is generally assumed that it is a solenoidal field. By means of this assumption, together with the Coulomb electrical field E_c shown in Table 1.1, the induced electric field E_i is given by (Bianchi 2005), (Cheng 1993), (Jianming 2002),

$$E_i = -\frac{\partial A}{\partial t} \quad (1.11)$$

This relationship is particularly useful in the computation of the induced currents in conductive media. The electric field E , also called Maxwell's electric field, corresponds to the sum of the Coulomb electric field E_c and the induced electric field E_i (Bianchi 2005), i.e.,

$$E = E_c + E_i = -\nabla V - \frac{\partial A}{\partial t} \quad (1.12)$$

1.1.1.5.2 Lorentz electrical field

The Lorentz specific electric force E_L acts on the electric charges moving in a magnetic flux density field B at a velocity v_q with respect to the adopted reference system. It is given by (Bianchi 2005), (Cheng 1993), (Jianming 2002),

$$E_L = v_q \times B \quad (1.13)$$

1.1.1.5.3 Motional electric field

The motion specific electric force E_m acts on the electric charges on a conductor moving at a velocity v_m with respect to the adopted reference system. It can be calculated using (Bianchi 2005), (Cheng 1993), (Jianming 2002),

$$E_m = v_m \times B \quad (1.14)$$

1.1.1.5.4 Total electric field

The total specific electric field E_t is the sum of the field E and the Lorentz's motion, and external specific forces. It gives (Bianchi 2005), (Cheng 1993), (Jianming 2002),

$$E_t = E + E_L + E_m + E_{ne} \quad (1.15)$$

In a conductive medium, characterized by the conductivity σ , the field E_t is linked to the current density vector field J by means of the constitutive relationship (Cheng 1993), (Bianchi 2005),

$$J = \sigma E_t \quad (1.16)$$

1.1.1.6 Total current density

If it is only considered a Maxwell's electric field, (1.16) can be defined by,

$$E_t = -\nabla V - \frac{\partial A}{\partial t} \quad (1.17)$$

If (1.17) is substituted in (1.16) gives (Bianchi 2005), (Cheng 1993), (Jianming 2002),

$$J = \sigma \left(-\nabla V - \frac{\partial A}{\partial t} \right) \quad (1.18)$$

1.1.2 Summary of main features of variables

After having explained all the variables, it is important to explain the main features that would lead to formulate a field equation. A brief summary of the most important features of these variables will be explained next. This summary contains the main field aspects considered in this investigation.

1.1.2.1 Coulomb's position

It is mainly used in stationary and quasi-stationary magnetic fields that correspond to a planar or an axisymmetric symmetry assumption. It is defined by,

$$\nabla \cdot \mathbf{A} = 0 \quad (1.19)$$

1.1.2.2 Displacement current neglected

If the displacement current is null, it is possible to formulate the next expression that relates the magnetic field strength and the current density,

$$\nabla \times \mathbf{H} = \mathbf{J} \quad (1.20)$$

1.1.2.3 Defining magnetic vector potential

The flux of a field density B , through any closed surface S_c is null. Thus it is possible to define a magnetic vector potential defined by,

$$\mathbf{B} = \nabla \times \mathbf{A} \quad (1.21)$$

1.1.2.4 Defining electric field

The electric field E , also called Maxwell's electric field, corresponds to,

$$\mathbf{E}_t = -\nabla V - \frac{\partial \mathbf{A}}{\partial t} \quad (1.22)$$

1.1.2.5 Defining total current density

Using (1.16) the total current density J is defined by,

$$J = \sigma \left(-\nabla V - \frac{\partial A}{\partial t} \right) \quad (1.23)$$

All the variables explained before, permit to derive a Helmholtz field equation, which consists on a partial differential equation with the current density J or the electrical field $-\nabla V$ as the forcing function. The magnetic vector potential is the variable to be solved. Laplace, Poisson and Helmholtz field equations will be discussed next.

1.1.3 Field equations

1.1.3.1 Laplace and Poisson field equations

Let us refer to a *magnetostatic* field, described by equations (1.19)-(1.23). The field problem is described by the quasi-harmonic equation defined by (Stratton 1941), (Arkkio 1987), (Cheng 1993), (Jianming 2002), (Bianchi 2005),

$$\nabla \times (\nu (\nabla \times A)) = J \quad (1.24)$$

If the materials are homogeneous, the reluctivity ν is constant, thus equation (1.24) is reduced to the Poisson equation. The Poisson equation is finally defined by (Stratton 1941), (Arkkio 1987), (Cheng 1993), (Jianming 2002), (Bianchi 2005),

$$-\nu (\nabla^2 A) = J \quad (1.25)$$

If the current density field J is null in the considered domain, the problem is described by the Laplace equation, defined by (Stratton 1941), (Arkkio 1987), (Cheng 1993), (Jianming 2002), (Bianchi 2005),

$$-\nu (\nabla^2 A) = 0 \quad (1.26)$$

1.1.3.2 Helmholtz field equation

The *Helmholtz* equation can be obtained if a uniform medium is considered. The first step consists on considering that the total current density J is defined by (Jianming 2002), (Bianchi 2005),

$$J = \sigma E_t \quad (1.27)$$

The total current density defined in (1.27) can be reformulated if the electrical field is taking into account. Thus (1.27) can be finally defined by (Jianming 2002), (Bianchi 2005),

$$J = \sigma(-\nabla V) - \sigma \frac{\partial A}{\partial t} \quad (1.28)$$

If (1.28) is substituted in (1.25) gives,

$$-v(\nabla^2 A) = \sigma(-\nabla V) - \sigma \frac{\partial A}{\partial t} \quad (1.29)$$

If the terms of (1.29) are rearranged, the Helmholtz equation can be finally obtained. It is defined by (Arkkio 1987), (Jianming 2002), (Bianchi 2005),

$$-v(\nabla^2 A) + \sigma \frac{\partial A}{\partial t} = \sigma(-\nabla V) \quad (1.30)$$

The Helmholtz and the Laplace field equations permits to model a device, using a magnetostatic formulation. If the magnetic fields are defined in two dimensions, it is assumed a planar and an axisymmetric symmetry and the conductor voltage is chosen as the forcing function; it is possible to formulate a transient FEM field equation which models the behavior of the conductor magnetic field (Arkkio 1987), (Chari and Sylvester 1980), (Jianming 2002). It is also possible to choose the conductor current as the forcing function, thus an alternative field FEM equation known as the *integro-differential* approach can be formulated (Arkkio 1987), (Konrad 1981), (Konrad 1982). Moreover, it is also possible to use the FEM field equation with the voltages as the forcing function to determine the magnetic vector potentials of the device when the conductors currents are known. This can be achieved by coupling the equation that relates the magnetic vector potentials with the conductors voltages and currents (Arkkio 1987), (Konrad 1981), (Konrad 1982), (Ho, Li and Fu 1999).

Nevertheless, the conductors currents or voltages of electrical machines or devices are not always known. Moreover, although the symmetry simplification of the field behavior reduces the complexity of the problem, it does not include some effects. For example, the end effects of the stator end windings or the end effects of the rotor end rings of an induction machine. If these effects are not included, the modeling of the field would not become accurate (Lubin, Mezani and Rezzoug 2011), (Li, Ho and Fu 2012). To tackle this problem it is necessary to couple external circuit equations which includes resistances and inductances, into the field FEM equation, in order to form a FEM-circuit coupled equation. Thus, electric parameters coupled with magnetic fields analysis using the finite element method have been widely used to simulate magnetic systems (Tsukerman et al. 1993), (Wang et al. 1985), (Arkkio 1987), (Wang and Xie 2009), (Ho, Li and Fu 1999), (Lubin, Mezani and Rezzoug 2011).

The FEM field and the FEM-circuit coupled expression derived by the finite element

method can be solved in the frequency domain (Shen et al. 1985) or in the time domain systems (Lubin, Mezani and Rezzoug 2011), (Wenliang et al. 2012), (Li, Ho and Fu 2012). The solution in the frequency domain is simple, since implies to calculate a simple matrix equation (Shen et al. 1985). For the specific case of a time domain solution, the most widely used method is the Backwards Euler (Arkkio 1987), (Okamoto, Fujiwara and Ishihara 2010). If the FEM-circuit coupled equation to be solved is nonlinear, the Newton Method can be used (Fu and Ho 2009), (Dlala and Arkkio 2010).

Nevertheless, the FEM equations may consist on matrices of larger order, may be difficult to obtain, or it may need of a considerable computation time. It is possible to overcome this situation, by using the parallel computing platform. Several methods have been developed for the finite element analysis based on the domain decomposition methods (Lavers, Boglaev y Sirotkin 1996). The finite element decomposition method is capable of solving a field problem by forming subdomains, it is an iterative process which coordinates the solution between adjacent subdomains by using their Neumann and boundary condition. The method permits that the problems on the subdomains are independent each other (Lavers, Boglaev y Sirotkin 1996), (Butrylo et al. 2003), (Mukades and Uragani 2008), (Wang et al. 2014). Parallel computing has been used this method, specifically it has been implemented on a distributed computing environment (Iwano et al. 1994), (Mukades and Uragani 2008); in the MPI platform (Butrylo et al. 2003) or in a Workstation Cluster (C. Fu 2008).

One tendency in the parallel computing is to establish a programming which executes the sequential parts of the algorithm in the CPU cores, while those steps that can be executed in a parallel way by using the GPUs (Kiss et al. 2012), (Luebke 2008), (Jalili-Marandi, Zhiyin and Dinavahi 2012). The NVIDIA CUDA (CUDA toolkit 5.0 2014) is a hardware-software platform that can be used to execute parallel algorithms using a program coded in C. Thus, there are several commands easy to implement which permit to conveniently use the GPU hardware. The sequential parts of an algorithm can be calculated in the CPU or host, while the parts that are mean to be calculated by a parallel way are executed by using kernels in the GPUs (NVIDIA 2012), (Luebke 2008). When a kernel is executed, blocks with an equal number of threads are created to execute the parallel function; blocks of thread form a grid (Owens , Houston and Luebke 2008), (Luebke 2008). Recently, the addition of the CUBLAS library in CUDA has become an excellent choice. This library is an equivalent computer parallel platform of the Basic Linear Algebra Subprograms (BLAS) library. These routines permits to easily implement a solution of a FEM equation using parallel computing (Barrachina et al. 2008).

1.2 Justification of the present research

In the actual times, it is very important to build electric machines optimized in their design, in order to get a high energy efficiency. Optimized designs permits to use a lesser amount of materials, and it requires less effort in the manufacturing and maintenance process. Moreover, it is very important to assure a reliable and secure operation. Because all these reasons, it is very important to have a reliable modelling of the electrical machines or devices (Brauer, Sadegui and Oerterlei 1999), (Manna and Marwaha 2008), (Bianchi 2005), (Wang and Xie 2009).

Maxwell equations allow an accurate modeling of electric and magnetic fields of electrical machines or devices. However the equation solution could be very difficult to obtain if conventional methods of solution are used. Computing technology development has allowed the development of several numerical method which allows an approximate solution of the Maxwell equations. Specifically, the Finite Element Method (FEM) has become a powerful tool to solve the field equation of electrical machines or devices (Arkkio 1987), (Ho, Fu and Wong 1997), (Jianming 2002). The FEM method is been extensively used in the design of several electrical machines: transformers, induction machines, synchronous machines, etc.

Although the FEM equations to be solved would be linear, and the planar and the axisymmetric symmetry assumptions would permit to simplify the finite element analysis; the matrix equations to be solved could be of large order, especially if it is required a details model of a device. For some cases, it is necessary to consider a large number of finite elements in order to know the behavior of the magnetic or electric field, in a specific region of a device (Arkkio 1987), (Bianchi 2005), (Jianming 2002). This could imply a frequency or time domain solution of a large order FEM equation, which could be very difficult to achieve.

Since the solution of some FEM equation can be difficult to obtain, it could be necessary to have optimized methods of solutions which allows deriving faster and accurate solutions in the frequency or the time domain. Moreover, these methods of solution can be implemented by using a parallel solution, since there are several actual computing platforms that allows, a fast and easy parallel implementation of an algorithm. One example is the NVIDIA CUDA-CUBLAS (CUDA toolkit 5.0 2014) (Barrachina et al. 2008), (Jalili-Marandi, Zhiyin and Dinavahi 2012).

1.3 Objectives

This investigation covers the solution of FEM field equations with voltages or currents known, and the solution of a FEM-circuit coupled equation. All these FEM expressions have been derived from a planar or an axisymmetric symmetry assumption. The main goal is to develop a methodology which permits to apply the Newton or other solution techniques, to obtain a faster and accurate solution of the FEM equations in the frequency and the time domain. The implementation by using modern sequential and parallel computing platforms is highly desirable. The specific objectives are:

- *Developing a methodology which permits to analyze and solve electrical machines of devices by using the finite element method.* The objective is to formulate an alternative method of solution, to derive a faster and accurate solution in the frequency and the time domain; by using the Newton method or other methods or solution forms.
- *Implementing the proposed methodology by using actual sequential and parallel computing platforms.* Conventional sequential platforms as *Matlab* or *GSL* will be used. The methodology will be also implemented in a parallel computing platform, i.e. CUBLAS- CUDA.
- *Testing the proposed method in several devices or electrical machine components.* Specifically, devices and tested which can be simplified by a planar or an axisymmetric symmetry assumptions will be analyzed. These symmetries can be used in a finite element analysis, in order to model a large number of electrical machines and devices.
- *Testing the results derived from the proposed method.* Since an alternative method of solution of FEM equations is proposed, it is extremely important to conduct a performance and results comparison, by analyzing and solving different devices or components. Thus, it is highly desirable to compare the results derived from the methodology with those results derived from a widely accepted FEM software, such as ANSYS, or those derived from another investigations.

1.4 Description of the Methodology

The developed a methodology that permits to solve FEM equations is based in the following methodology steps:

FEM field with voltage or current known, and a FEM-circuit coupled equation are solved. These FEM expressions are derived from a planar or an axisymmetric symmetry assumption of the field equations of a device. The methodology consists on performing several steps which leads to derive a reduced equivalent equation of a FEM equations of a device. The equation derived by the proposed method is expressed in terms of the time varying variables of the device.

The developed method consists on reordering the nodes of the FEM equation, performing an arrangement of the variables; and finally, performing some few simple matrix operations on the FEM equations. These actions allow getting a reduced equivalent equation, which is expressed in terms of time varying variables of the ordinary FEM expressions. The equation derived by the methodology can be solved in the frequency or the time domain. The solution in the frequency domain is similar to the solution of an ordinary FEM equation; since it only implies to calculate a simple matrix equation. For the specific case of a time domain solution, the equation can be solved by the Backwards Euler; but it can be obtained an approximate solution by using the Euler, the 4th order Runge Kutta and the Newton Methods.

Although the methodology permits to obtain a faster solution of the FEM equations, in some cases the proposed equation could be still difficult to solve, especially if a conventional sequential computing is used. Because of this, a parallel form of solution of the equation derived from the methodology, by using the LU method has been developed. The parallel LU method developed has been implemented in CUDA, since this computing platform already contains several standard matrix routines which can be easily used to perform several matrix-vector operations; and it can easily solved large scale matrix equations.

1.5 Thesis Content

The investigation has been organized as follows:

Chapter 1 explains how is organized the information contained in this thesis.

Chapter 2 explains the features of a 2D finite element analysis. The field equations, the basic principles of the finite element analysis, the FEM equation to be solved and their method of solution, the incorporation of parallel computing implementation of these equations by using CUDA are detailed.

Chapter 3 explains the proposed method of this investigation. How this method is able to get an equivalent equation from the FEM equations covered by this investigation is explained.

Chapter 4 explains several case studies in which the proposed methodology has been tested. Case studies are derived from a finite element analysis which considers a symmetry assumption.

Chapter 5 details how the proposed methodology and the ordinary FEM equations have been implemented in a sequential and a parallel computing platform, respectively.

Chapter 6 gives the main conclusions drawn from this investigation. Suggestions for future research work in the same field of knowledge are given.

And finally, Appendix A, B and C provide specific information about the finite element matrices and vectors; methods of solution of the FEM equations; and the programs used in study cases 3 and 5, respectively.

2 Finite element analysis and computational techniques

2.1 Introduction

The finite element analysis is a powerful tool that permits to solve the magnetic transient equation of an electrical machine or device. Although the equation derived can be difficult to solve when complex geometries or 3D analysis are used, the finite element analysis can be simplified by a symmetry simplification, i.e. a planar or an axisymmetric symmetry assumption.

Using this 2D simplification and other assumptions, the field equation complexity can be highly reduced. The use of this symmetry assumption, allows that simple but effective finite elements represent a good solution for the devices field equation.

The equation derived is named as FEM field equation. It is important that the FEM field equations are formulated in terms of the currents or voltages of the device. This is necessary since the primary FEM equation has the current density as the forcing function, and this parameter is not always known.

Nevertheless, the currents or voltages of the devices are not also always known. In some cases, it is necessary to add some parameters such as resistances or inductances, which are connected to the conductors to get a more precise model of the electrical machine or device. The electrical parameters mentioned before, can be taken into account by one or several voltage-current equations, thus the current-voltage and the FEM field equations can be coupled into a FEM-circuit coupled equation. The FEM-circuit coupled equation permits to accurately model a device.

The solution of the FEM field and FEM circuit coupled equations can be performed in the frequency or in the time domain. The solution of the frequency domain is very simple and easy to calculate, since it is considered that the state variables of the equation have a complex behavior in the time domain.

For the case of the time domain method, several methods can be used, i.e. the Euler, the Backwards Euler and the fourth order Runge Kutta methods. The solution in the time domain can be also achieved by the use of the Newton fast approach method, which can solve the periodic solution of a set of differential equation defined in the time domain.

The solution in the frequency and time domain can be also obtained in a faster way, if it is solved in a parallel computing platform. The recent technological advances in the parallel processing area, permits an easy and fast implementation of an equation parallel solution. Specifically the NVIDIA CUDA platform (CUDA toolkit 5.0 2014) allows the use of graphical processing units (GPUs) that can perform several computing calculations in a

parallel way (Luebke 2008), (Jalili-Marandi, Zhiyin and Dinavahi 2012). On this computing platform, a sequential processing can be performed in some stages, while other operations can be easily parallelized by using the GPUs as independent processing units. Since several matrix operations are continuously used in engineering problems, the CUBLAS library (Barrachina et al. 2008), (CUDA toolkit 5.0 2014) has been developed. This library contains routines that can perform basic matrix operations in a parallel way using the GPUs.

In this chapter the fundamentals of the finite element analysis based on a 2D symmetry simplification will be explained. The main assumptions and the main aspects of the Galerkin finite element analysis and the Galerkin *weak* FEM formulation will be detailed. These formulations permit to derive the FEM field and the FEM-circuit coupled equation covered in this investigation.

After that, the solution methods of these FEM equations, in the frequency domain and in the time domain will be discussed. Conventional methods in time domain, such as Euler, Backwards Euler, and fourth order Runge Kutta will be explained. A Newton method that allows a fast periodic solution of a set of equations in the time domain will be also explained.

After explaining the solution of the equation in the frequency and in the time domain, the main advantages of the CUBLAS and CUDA computing platforms will be described. They are a powerful computing platform that enables to perform an easy but powerful implementation of a parallel computing process, since several routines have been already implemented in the CUBLAS library.

2.2 The Galerkin finite element method

In this chapter the main fundamentals of the Galerkin finite element analysis will be explained. First, it will be covered the field equations that are being considered for this investigation. These equations assume a magnetostatic formulation, and it has been considered a magnetic field defined in two dimension. By taking into account these assumptions, the Helmholtz and the Laplace field equation permit to model an electrical machine or device (Bianchi 2005), (Arkkio 1987), (Konrad 1982), (Chari and Sylvester 1980), (Jianming 2002). The two dimensional fields can be defined in a planar and an axisymmetric symmetry. The finite element analysis that considers this symmetries and a two dimensional field will be explained next.

2.2.1 Application of finite element method in two-dimensional fields

In 2D field problems, the domain is considered to be a surface τ , and its boundary Γ is a curve. Let ϕ be the unknown function that it is to be determined. It is a scalar function of the space coordinates. There are two types of unknown function, a function which represents the solution of a field equation derived from a planar symmetry; and a function that represents the solution of a field equation derived from an axisymmetric symmetry. In this investigation two dimension fields based on these symmetry assumptions will be solved. The details of the two dimension fields will be explained next.

2.2.1.1 Two-Dimension Field defined by a planar symmetry

2.2.1.1.1 Poisson equation, current density as the forcing function

In the case of the planar symmetry, ϕ_z is a scalar function of the space coordinates x and y , i.e., $\phi_z = \phi_z(x, y)$. In a first stage, the time dependence is omitted. Let f_J be the forcing function, which is independent of time. The 2D field problem of a planar symmetry is defined for the next partial differential equation (Bianchi 2005), (Chari and Sylvester 1980),

$$-\frac{\partial}{\partial x} \left(\alpha_x \frac{\partial \phi_z}{\partial x} \right) - \frac{\partial}{\partial y} \left(\alpha_y \frac{\partial \phi_z}{\partial y} \right) + \beta \phi_z = f_J \quad (2.1)$$

Together with the boundary conditions that are imposed to the boundary Γ of the domain, there are Dirichlet boundary conditions on the portion Γ_1 of the boundary, and a Neumann boundary condition on the remaining portion Γ_2 of the boundary. They are defined by (2.2) and (2.3), respectively (Bianchi 2005), (Chari and Sylvester 1980),

$$\phi_z = \phi_k \text{ on } \Gamma_1 \quad (2.2)$$

$$\frac{\partial \phi_z}{\partial n} = \mathbf{0} \text{ on } \Gamma_2 \quad (2.3)$$

It is important to remark that the boundary Γ of the domain is defined by the next relationship between Γ_1 and Γ_2 ,

$$\Gamma_1 \cup \Gamma_2 = \Gamma \quad (2.4)$$

In the particular case of a Poisson equation and a homogeneous material, the parameters of (2.1) are given by (Bianchi 2005),

$$\phi_z = A_z ; f_J = J_z$$

$$\alpha_x = \alpha_y = v ; \beta = \mathbf{0} \quad (2.5)$$

The Poisson equation of a device with a planar symmetry can be defined by a simplified equation defined in (2.1) and the parameters defined in (2.5). It yields, (Chari and Sylvester 1980), (Sylvester and Ferrari 1983), (Bianchi 2005),

$$-\frac{\partial}{\partial x}\left(\mathbf{v}\frac{\partial A_z}{\partial x}\right) - \frac{\partial}{\partial y}\left(\mathbf{v}\frac{\partial A_z}{\partial y}\right) = J_z \quad (2.6)$$

2.2.1.1.2 Current density defined by an electrical field

The forcing function of (2.6) is the current density J_z . Nevertheless, the conductors of a device are not being supplied by a current density energy source, they are supplied by one or several voltage sources. Therefore, there is an electric field associated to such conductor voltage (Konrad 1982). In the conductors, the electrical field corresponds to the sum of the Coulomb electric field E_c and the induced electric field E_i *e.g.* (Bianchi 2005), (Konrad 1982),

$$\mathbf{E}_z = \mathbf{E}_c + \mathbf{E}_i = -\nabla V - \frac{\partial A_z}{\partial t} \quad (2.7)$$

The relationship between the electrical field and the current density in the conductors is given by (Bianchi 2005), (Konrad 1982),

$$\mathbf{J}_z = \sigma \mathbf{E}_z \quad (2.8)$$

If the electrical field E_c along the conductor length is constant along the axis z , the term $E_c = -\nabla V$ can be defined by the ratio of the voltage U_c applied along the conductor and the conductor's length l . Thus (2.8) can be redefined by (Bianchi 2005), (Konrad 1982),

$$\mathbf{J}_z = \sigma \frac{U_c}{l} - \sigma \frac{\partial A_z}{\partial t} \quad (2.9)$$

2.2.1.1.3 Poisson equation, voltage as the forcing function

Taking into account (2.9), if this expression is substituted in (2.6), it is possible to derive an equation in which the voltage applied to the conductors is the forcing function. The equation can be written by, (Silvester and Ferrari 1983), (Bianchi 2005),

$$-\frac{\partial}{\partial x}\left(\mathbf{v}\frac{\partial A_z}{\partial x}\right) - \frac{\partial}{\partial y}\left(\mathbf{v}\frac{\partial A_z}{\partial y}\right) = \sigma \frac{U_c}{l} - \sigma \frac{\partial A_z}{\partial t} \quad (2.10)$$

2.2.1.1.4 Defining the current as the forcing function

It is possible to define the current as the forcing function of (2.6). This can be achieved by obtaining the current I_z associated to the current density J_z defined in (2.9). If (2.9) is integrated through the region τ of the conductor, it yields (Konrad 1982),

$$(\mathbf{R}_c)^{-1} \mathbf{U}_c - \int_{\tau} \boldsymbol{\sigma} \frac{\partial A_z}{\partial t} d\boldsymbol{\tau} = \mathbf{I}_z \quad (2.11)$$

Where R_c is defined as the resistance of the conductors, and it can be calculated using (Konrad 1982), (Escarela-Perez, Melgoza and Alvarez-Ramirez 2009),

$$\mathbf{R}_c = \boldsymbol{\sigma} \frac{l}{\Delta} \quad (2.12)$$

Where Δ is the conductor's area, defined by its region τ . It can be seen that if the currents in the conductor are known; this can be defined as the forcing function. The equations involved are the expressions defined in (2.10) and (2.11), respectively. For the particular case of a planar symmetry, the region τ is given by (Konrad 1982),

$$\tau \rightarrow \int_{x_D} \int_{y_D} dx dy \quad (2.13)$$

2.2.1.2 Two-Dimension field defined by an axisymmetric symmetry

2.2.1.2.1 Poisson equation, current density as the forcing function

For the case of axisymmetric symmetry, ϕ_p is a scalar function of the space coordinates r and z , i.e., $\phi_p = \phi_p(r, z)$. In a first stage, the time dependence is omitted. Let f_p be the forcing function, which is independent of time. The 2D field problem of an axisymmetric symmetry is defined for the differential equation (Preiss 1983), (Jianming 2002),

$$-\frac{1}{r} \frac{\partial}{\partial r} \left(\alpha_r \frac{\partial \phi_p}{\partial r} \right) - \frac{1}{r} \frac{\partial}{\partial z} \left(\alpha_z \frac{\partial \phi_p}{\partial r} \right) + \beta \phi_p = f_p \quad (2.14)$$

Together with the boundary conditions that are imposed on the boundary Γ of the domain. There are a Dirichlet boundary conditions on the portion Γ_1 of the boundary, and a Neumann boundary condition on the remaining portion Γ_2 of the boundary. They are defined by (2.15) and (2.16), respectively.

$$\phi_p = \phi_k \text{ on } \Gamma_1 \quad (2.15)$$

$$\frac{\partial \phi_p}{\partial n} = \mathbf{0} \text{ on } \Gamma_2 \quad (2.16)$$

The relationship between the portions Γ_1 and Γ_2 , with the total boundary Γ was previously defined in (2.4) for the particular case of a homogeneous material, and an axisymmetric symmetry. The parameters of (2.14) are defined by,

$$\phi_\rho = A_\rho ; f_J = J_\rho$$

$$\alpha_r = \alpha_z = vr ; \beta = \frac{v}{r^2} \quad (2.17)$$

The Poisson equation of a device with an axisymmetric symmetry can be defined by the simplified equation (2.14) and the parameters given by (2.17). The Poisson equation expressed in a single expression is given by, (Konrad, Chari and Csendes 1982), (Preiss 1983), (Jianming 2002),

$$-\frac{1}{r} \frac{\partial}{\partial r} \left(vr \frac{\partial A_\rho}{\partial r} \right) - \frac{1}{r} \frac{\partial}{\partial z} \left(vr \frac{\partial A_\rho}{\partial z} \right) + v \frac{A_\rho}{r^2} = J_\rho \quad (2.18)$$

2.2.1.2.2 Current density defined by an electrical field

The forcing function of (2.18) is the current density. Nevertheless, the conductors of a device with an axisymmetric symmetry are not also being supplied by a current density energy source, they are supplied by one or several voltage sources. Therefore, there is also an electric field associated to such conductor voltage (Konrad 1982), (Konrad, Chari and Csendes 1982), (Preiss 1983). In the conductors exists an electric field that corresponds to the sum of the Coulomb electric field E_c and the induced electric field E_i (Konrad 1982), (Konrad, Chari and Csendes 1982), (Preiss 1983).

If E_c along the conductor length is constant along a specific value or the r -coordinate, the term $-\nabla V$ can be defined by the ratio of the voltage U_c applied along the conductor and the conductor's length along the r -coordinate ($2\pi r$). Thus, the current density J_ρ is defined by (Konrad 1982), (Konrad, Chari and Csendes 1982), (Preiss 1983),

$$J_\rho = \sigma \frac{U_c}{2\pi r} - \sigma \frac{\partial A_\rho}{\partial t} \quad (2.19)$$

2.2.1.2.3 Poisson equation, voltage as the forcing function

Taking into account (2.19), if this expression is substituted in (2.18), it is possible to derive an equation in which the voltage applied in the conductor is the forcing function. The equation can be written by (Konrad 1982), (Konrad, Chari and Csendes 1982), (Preiss 1983),

$$-\frac{1}{r} \frac{\partial}{\partial r} \left(vr \frac{\partial A_\rho}{\partial r} \right) - \frac{1}{r} \frac{\partial}{\partial z} \left(vr \frac{\partial A_\rho}{\partial z} \right) + v \frac{A_\rho}{r^2} = \sigma \frac{U_c}{2\pi r} - \sigma \frac{\partial A_\rho}{\partial t} \quad (2.20)$$

2.2.1.2.4 Defining the current as the forcing function

It is possible to define the current as the forcing function of (2.20). This can be achieved by obtaining the current I_ρ associated to the current density J_ρ defined in (2.19). If (2.19) is integrated through the region τ of the conductor results on (Konrad 1982), (Preiss 1983),

$$(\Delta_r)^{-1}(U_c) - \int_{\tau} \sigma \frac{\partial A_\rho}{\partial t} d\tau = I_\rho \quad (2.21)$$

Where Δ_r can be calculated using (Preiss 1983),

$$\Delta_r = \frac{2\pi}{\sigma} \left[\left(\int_{\tau_r} \frac{d\tau_r}{r} \right) \right]^{-1} \quad (2.22)$$

It can be seen that if the current in the conductor is known, this can be defined as the forcing function. The equations involved are the expressions defined in (2.20) and (2.21), respectively. For the particular case of an axisymmetric symmetry, the region τ is given by (Preiss 1983).

$$\tau_r \rightarrow 2\pi \int_{r_D} \int_{z_D} r dz dr \quad (2.23)$$

After having explained the two dimension field equations, derived from a planar or an axisymmetric symmetry, the basic principles of the finite element analysis will be explained in the next section.

2.2.2 Solution of field equations using Galerkin method

The requirement of more and more accuracy during the process of design and analysis of the electrical machine fostered the spreading of numerical models appropriate for computing electric and magnetic fields. These numerical methods are essentially based on the determination of the distribution of the electric and magnetic fields in the structures under study, based on the solution of the Maxwell's equations. An analytical solution is barely achieved, because of the complex geometrical machine structures and the nonlinear characteristics of the material. Then, in most cases, only a numerical solution is possible (Bianchi 2005), (Reece and Preston 2000). In this section will be explained the main features of the Galerkin method when it is used to solve field problems.

2.2.2.1 Field problems with boundary conditions

Generally, a vector field problem is described by a differential equation, defined in the domain D as, (Bianchi 2005),

$$L\phi(P, t) = f(P, t) \quad (2.24)$$

Together with the boundary conditions, the latter constrain in the fields along the boundary Γ of the domain under analysis. In equation (2.24), L is a differential operator, ϕ is the unknown function to be determined, and f is the forcing function. For the case of a planar symmetry (Bianchi 2005), equation (2.24) highlights that both ϕ and f are functions of the position in the space $P(x,y,z)$ and of the time t . For the case of an axisymmetric symmetry (Preiss 1983), equation (2.24) highlights that both ϕ and f are functions of the position in the space $P(r,z,\rho)$ and of the time t .

In general, L might be any differential operator. Usually represents a linear operator, satisfying the property of addition and the property of product by a constant. In the electromagnetic problems, (2.24) is given by the Poisson, Laplace or Helmholtz equation, in which ϕ is a scalar or vector field. As an example, for the case of the Poisson equation, ϕ indicates the magnetic vector potential A , the forcing function is the total current density J . Then (2.24) is rewritten as (Bianchi 2005),

$$L = -v(\nabla^2) \quad (2.25)$$

In which a homogenous medium is considered. The boundary conditions of the field equation shown in (2.24) will be explained next.

2.2.2.1.1 Boundary conditions of field equations

The field problem shown in (2.24) admits a solution not only if the differential equation that describes its distribution is known in all the points of the domain D , but also if the unknown function ϕ is given on the boundary Γ of the domain D itself (Bianchi 2005). In addition, it can be verified that once the solutions has been found, this solution is unique (this is the unicity theorem).

The conditions that express the behavior of the solution ϕ on the frontier Γ are called constraint, or boundary conditions. Among these conditions, one can assign a Dirichlet condition which is when a given constant value of ϕ is assigned to the boundary Γ , or a Neumann condition, when a value of the derivative of ϕ normal to the boundary Γ is assigned (Konrad 1982), (Reddy 1984), (Bianchi 2005). They will be explained next.

2.2.2.1.1.1 Dirichlet boundary condition

If we let Γ_1 be a portion of the boundary Γ , the Dirichlet condition is defined by (Bianchi 2005),

Homogeneous condition:

$$\phi = \mathbf{0} \text{ on } \Gamma_1 \quad (2.26)$$

Nonhomogeneous condition:

$$\phi = \phi_k \text{ on } \Gamma_1 \quad (2.27)$$

2.2.2.1.1.2 Neumann boundary condition

If we let Γ_2 be the remaining portion of the total boundary Γ , the Neumann's condition can be a *Homogeneous* condition which is defined by (Bianchi 2005),

$$\frac{\partial \phi}{\partial n} = \mathbf{0} \text{ on } \Gamma_2 \quad (2.28)$$

2.2.2.2 Solution of field problems using residual equation (Galerkin method)

Let the field problem be expressed by (2.24) and by suitable boundary conditions, as given in (2.26) and (2.28). The Galerkin method which permits to solve field problems is now illustrated. The method aims to define a function ϕ^* that approximates the unknown function ϕ as closely as possible. Specifically, it solves the field problem by reducing the residual of the differential equation (2.24); by using a function ϕ^* that better approaches the exact solution ϕ correspond to a residual (Bianchi 2005), (Jianming 2002),

$$\mathbf{r} = \mathbf{L}\phi^* - \mathbf{f} \quad (2.29)$$

Equation (2.29) equates to zero (or at least very low) in the whole analysis domain. Fixing some weight w_i , the residual method forces the integral of the residuals, weighed by w_i , to be zero over the domain volume τ_D . The following condition is forced, (Bianchi 2005), (Jianming 2002),

$$\mathbf{R} = \int_{\tau_D} \mathbf{w}(\mathbf{L}\phi^* - \mathbf{f})d\tau \quad (2.30)$$

The features of the function ϕ^* that approximates the unknown function ϕ will be explained in next Section; while the features of the weight function w_i will be explained in Section 2.2.2.2.2.

2.2.2.2.1 Defining an approximate solution of residual equation

It is defined a function ϕ^* that approximates the unknown function ϕ as closely as possible. Such a function is commonly expressed by a linear combination of a basic function, as (Bianchi 2005), (Jianming 2002), (Bastos 2003), (Reece and Preston 2000),

$$\phi^*(\mathbf{P}, t) = \sum_{j=1}^N N_j(\mathbf{P}, t)\phi_j \quad (2.31)$$

It is possible to express (2.31) in a matrix-vector form (Kwon and Bang 1997),

$$\phi^* = \{N_1 \ N_2 \ \dots \ N_i\}^T \{\phi_1 \ \phi_2 \ \dots \ \phi_i\} = \{N_j\} \{\phi_j\}^T \quad (2.32)$$

Where N_j are interpolating functions (that are also called expansion functions or base functions), while ϕ_j are unknown coefficients that have to be determined during the computation process. Such a combination has to be approximated to the exact solution, satisfying the differential operator and the boundary conditions at the same time (Arkkio 1987), (Kwon and Bang 1997), (Reece and Preston 2000).

2.2.2.2.2 Defining the weight functions of the residual equation

In the Galerkin method, the weight-base functions w_i are chosen equal to the interpolating function N_i ; it yields, (Arkkio 1987), (Kwon and Bang 1997), (Reece and Preston 2000),

$$w_i = N_i \quad i=1,2,3\dots m \quad (2.33)$$

If (2.33) is described in a matrix-vector form gives,

$$w = \{N_1 \ N_2 \ \dots \ N_i\}^T = \{N_i\}^T \quad (2.34)$$

2.2.2.2.3 Substitution of approximate solution and weight function in residual equation

Taking into account (2.32) and (2.34) and the operator defined in (2.24), the residual equation (2.30) can be defined by (Bianchi 2005).

$$\left[\int_{\tau_0} [\{N_i\}^T L \{N_j\}] d\tau \right] \{\phi_j\}^T = \left[\int_{\tau_0} \{N_i\}^T d\tau \right] f \quad (2.35)$$

2.2.2.2.4 Deriving matrix equation from residual expression

The development of (2.35) can lead to a system of equations that can be expressed as (Bianchi 2005), (Jianming 2002),

$$[S]\{\phi\} = \{F\} \quad (2.36)$$

Where $[S]$ is a matrix that depends on the interpolating functions, $\{\phi\}$ is the column vector of the unknown coefficients ϕ . If the left side of (2.36) is developed, their elements are defined by (Bianchi 2005), (Jianming 2002),

$$S_{ij}\phi_j = \left[\int_{\tau_0} (N_i L N_j) d\tau \right] \phi_j \quad (2.37)$$

Finally, $\{F\}$ in equation (2.36) is the column vector whose elements depend on the forcing function f . They are given by (Bianchi 2005), (Jianming 2002),

$$F_i = \left\{ \int_{\tau_0} N_i d\tau \right\} f \quad (2.38)$$

The Galerkin method permits to solve the field equations defined in (2.1) and (2.20). Nevertheless, the method requires interpolating functions N_j , and unknown coefficients ϕ_j that have to be determined during the computation process. Moreover, the functions N_j are defined in the whole domain. The a combination has to be approximated to the exact solution, satisfying the differential operator and the boundary conditions at the same time (Bianchi 2005), (Reece and Preston 2000).

Conversely, in the finite element method the whole domain is divided into subdomains, then the function ϕ^* is a combination of functions N_j that are defined in the subdomains. Consequently, since the subdomains are of reduced dimensions, the interpolating functions N_j can be very simple (Reddy 1984), (Bianchi 2005), (Reece and Preston 2000). The finite element method/analysis will be outlined next.

2.2.3 Solution of field equations using the finite element method/analysis

An analytical solution of field problems is barely achieved, because of the complex geometries on the electrical machines or devices. Then, in most cases, only a numerical solution is possible. The finite element method is a numerical technique that is suitable for this purpose. It allows a field solution to be obtained, even with time-variable fields and with materials that are nonhomogeneous, anisotropic, or nonlinear. Using the finite element method, the whole analysis domain is divided into elementary subdomains, which are called finite elements, and the field equation are applied to each of them (Bianchi 2005), (Reddy 1984), (Reece and Preston 2000), (Arkkio 1987).

The study of the field distributions, and in particular of electromagnetic field problems, exhibits the following advantages. It allows a meticulous local analysis to be carried out, highlighting dangerous field gradient, magnetic field strength, saturation and so on. It allows a good estimation of the performance of the electromagnetic devices under analysis. Finally, it permits one to reduce substantially the number of prototypes (Arkkio 1987), (Bianchi 2005).

However, the method has some drawbacks, too. Because of its numerical nature, the solution is necessarily approximate. Then, if the method is not correctly applied, it might generate inaccurate results. Finally, since the computed quantities are distributed in the space, the required computation time is generally long (Bianchi 2005), (Arkkio 1987), (Reddy 1984).

In order to reduce the computation time, and to improve the analysis at the same time, each symmetry (both geometric and electromagnetic symmetry) of the structures is used. The resulting accuracy is influenced by the dimensions of the finite element and by the uniformity of the subdivision. To increase the accuracy, a fine subdivision of the structure is carried out, adopting finite elements of smaller dimension (Bianchi 2005), (Arkkio 1987), (Reddy 1984). Nevertheless, an excessive subdivision of the analysis domain causes an aggravation of the computation time.

The finite element method is essentially based on the subdivision of the whole domain in a fixed number of subdomains. Despite of the classical methods described above, where the interpolating functions N_j are defined in the whole domain, in the finite element method they are defined only on each subdomain (Bianchi 2005). It follows that, because of the small dimensions of these subdomains, the function ϕ is approximated by simple interpolating functions whose coefficients are the unknown quantities. The finite element analysis is organized in the following steps (Bianchi 2005), (Arkkio 1987), (Reddy 1984), (Reece and Preston 2000),

1. *Partition of the domain.* The domain is divided into subdomains of reduced dimensions
2. *Choice of the interpolations functions:* the functions N_j are chosen. As said earlier, with the small dimensions of the subdomains, these functions can be very simple.
3. *Formulation of the system to solve the field problem:* The set of equations representing the field solution is developed by means of the Galerkin method.
4. *Solution of the problem.* The solution is obtained by solving the resulting set of equations. In this investigation, the FEM equations will be solved in the frequency and the time domain. Specific details about the FEM equation solution, can be consulted in Appendix B.

These steps will be outlined next.

2.2.3.1 Partition of the domain

The first step of the finite element method is to divide the domain. The whole domain is subdivided in N_m elements D_m ($m=1,2,3,\dots, N_m$). The way to achieve such subdivision greatly affects the solution accuracy. Moreover, it influences the memory space required by the computer (Bianchi 2005), (Reddy 1984), (Reece and Preston 2000).

In one-dimensional problems, the domain is a curve and such subdomains are segments. The connection of the different segments form the original curve. In two-dimensional problems, the domain is a surface and each subdomain is a polygon, usually a triangle or a rectangle. In three-dimensional problems, the domain is a volume and each subdomain is a tetrahedron, a triangular prism or a rectangular solid (Bianchi 2005). On this investigation, specifically one and two dimensional problems will be solved.

2.2.3.2 Choice of the interpolating function

The second step consists of the choice of the interpolating function to approximate the unknown function in each m -th element. If a first order polynomial is chosen, a *lineal interpolation* is achieved. With a second-order polynomial, a *quadratic interpolation* is achieved. Also a *high-order polynomial* can be chosen; however, although they yield to a higher accuracy in the interpolation, they require a more complex formulation and, thus, are barely adopted (Bianchi 2005), (Jianming 2002), (Reddy 1984), (Reece and Preston 2000). On this investigation linear interpolation functions will be solved, although for the specific case of a planar symmetry quadratic functions will be formulated. Once the order of the polynomial is chosen, the unknown solution for each m -th element is written as (Bianchi 2005), (Jianming 2002),

$$\phi_m^*(P, t) = \sum_{j=1}^N \phi_{mj} N_{mj}(P, t) \quad (2.39)$$

Where N is the number of the nodes of the element, ϕ_{mj} is the value of ϕ in the j -th node of the m -th element. Finally, N_{mj} is the interpolating function referred to the j -th node of the m -th element.

The function solution ϕ_m^* could correspond to the solution of a field equation derived from a planar symmetry assumption, thus $P=(x,y)$. For the case of a function solution ϕ_m^* of a field equation derived from a an axisymmetric symmetry, $P=(r,z)$. The highest order of the function defines also de order of the element. If equation (2.39) is expressed in a matrix way, results on (Kwon and Bang 1997), (Jianming 2002),

$$\phi_m^*(P, t) = \{N_{m1}(P, t) \quad N_{m2}(P, t) \quad \dots \quad N_{mj}(P, t)\} \{\phi_{m1} \quad \phi_{m2} \quad \dots \quad \phi_{mj}\}^T \quad (2.39a)$$

Finally, (2.39a) can be expressed in a reduced form given by (Kwon and Bang 1997), (Jianming 2002)

$$\phi_m^* = \{N_{mj}\} \{\phi_{mj}\}^T \quad (2.40)$$

Finite elements for a planar and axisymmetric symmetry are used in this thesis. Using these finite elements, it is possible to use the Galerkin method in order to solve field equations on each subdomain of reduced dimension. The different types of finite element used in this investigation for a planar symmetry will be explained next. Further details of these elements can be consulted in Appendix A.

2.2.3.2.1 Finite elements for a planar symmetry

It can be seen that the finite element analysis requires that the 2D domain of the device to be subdivided in a finite and sufficiently high number of elements. For the simplest case, they are elements of triangular form, not necessary equal, but not intersecting each other. Each vortex is called a *node*, and all of them set up the mesh (Bianchi 2005), (Silvester and Ferrari 1983), (Reece and Preston 2000). Let us assume that the structure has been divided into N_m finite elements, and the total number of nodes is N_n . Each of them assumes the value ϕ_i of the potential function ϕ . Thanks to the small dimensions of the elements, the interpolating functions $N_i(x,y)$ may be simple. Triangular finite elements were considered for a planar symmetry. They will be outlined next.

2.2.3.2.1.1 Triangular finite element in planar symmetry with three nodes

It is possible to define triangular elements, and define a linear interpolation of the function $\phi(x,y)$ assumed for each m -th triangular elements, given by (Bianchi 2005), (Kwon and Bang 1997), (Jianming 2002),

$$\phi_m(x, y) = a + bx + cy \quad (2.41)$$

In particular in the three nodes of the triangular, the three i -th values are given by,

$$\phi_1(x_1, y_1) = a + bx_1 + cy_1$$

$$\phi_2(x_2, y_2) = a + bx_2 + cy_2$$

$$\phi_3(x_3, y_3) = a + bx_3 + cy_3 \quad (2.42)$$

It can be observed that knowing the value of the function in the three nodes ϕ_1, ϕ_2, ϕ_3 ; by means of (2.42), it is possible to compute the scalar function at any point of the element. If the three values of the potentials are given in each node, it is possible to solve the system (2.41) in order to calculate the unknown parameters a, b, c , (Bianchi 2005), (Kwon and Bang 1997),

$$\begin{Bmatrix} a \\ b \\ c \end{Bmatrix} = \begin{pmatrix} 1 & x_1 & y_1 \\ 1 & x_2 & y_2 \\ 1 & x_3 & y_3 \end{pmatrix}^{-1} \begin{Bmatrix} \phi_1 \\ \phi_2 \\ \phi_3 \end{Bmatrix} \quad (2.43)$$

After several operations, the values a, b, c are defined as follows,

$$\begin{aligned}
\mathbf{a} &= \frac{1}{\Delta_d} [(x_2 y_3 - x_3 y_2) \phi_1 + (x_3 y_1 - x_1 y_3) \phi_2 + (x_1 y_2 - x_2 y_1) \phi_3] \\
\mathbf{b} &= \frac{1}{\Delta_d} [(y_2 - y_3) \phi_1 + (y_3 - y_1) \phi_2 + (y_1 - y_2) \phi_3] \\
\mathbf{c} &= \frac{1}{\Delta_d} [(x_3 - x_2) \phi_1 + (x_1 - x_3) \phi_2 + (x_2 - x_1) \phi_3]
\end{aligned} \tag{2.44}$$

The value of Δ_d is defined by (Kwon and Bang 1997), (Bianchi 2005),

$$\Delta_d = x_1 y_2 - x_2 y_1 + x_2 y_3 - x_3 y_2 + x_3 y_1 - x_1 y_3 \tag{2.45}$$

It is possible to express (2.41) taking into account the values a, b, c defined in (2.44) and the potentials defined in three nodes. The resultant equation can be expressed in a vector form by (Kwon and Bang 1997), (Jianming 2002),

$$\phi_m(x, y) = \{N_m\} \{\phi_m\} \tag{2.46}$$

Where the vectors of (2.46) can be defined by,

$$\begin{aligned}
\{N_m\} &= \{N_1 \quad N_2 \quad N_3\} \\
\{\phi_m\} &= \{\phi_1 \quad \phi_2 \quad \phi_3\}^T
\end{aligned} \tag{2.47}$$

The values of N_1, N_2, N_3 of (2.47) can be consulted in Appendix A. It can be seen that the three nodes of the triangular finite element can be defined by the values of ϕ_1, ϕ_2 and ϕ_3 at each node, and by the interpolating functions defined in (2.47). These functions depend on the nodes and their position along the x - y plane.

2.2.3.2.1.2 Triangular finite element in planar symmetry with six nodes

Another kind of linear interpolation of the function ϕ can be assumed for each m -th triangular elements of the structure. It is given by (Kwon and Bang 1997), (Bianchi 2005),

$$\phi_m(x, y) = a + bx + cy + dx^2 + exy + fy^2 \tag{2.48}$$

In particular in the six nodes of the triangular element, the six i -th values are given by (Kwon and Bang 1997), (Bianchi 2005),

$$\begin{aligned}
a + bx_1 + cy_1 + dx_1^2 + ex_1^2y_1^2 + fy_1^2 &= \phi_1 \\
a + bx_2 + cy_2 + dx_2^2 + ex_2^2y_2^2 + fy_2^2 &= \phi_2 \\
a + bx_3 + cy_3 + dx_3^2 + ex_3^2y_3^2 + fy_3^2 &= \phi_3 \\
a + bx_4 + cy_4 + dx_4^2 + ex_4^2y_4^2 + fy_4^2 &= \phi_4 \\
a + bx_5 + cy_5 + dx_5^2 + ex_5^2y_5^2 + fy_5^2 &= \phi_5 \\
a + bx_6 + cy_6 + dx_6^2 + ex_6^2y_6^2 + fy_6^2 &= \phi_6
\end{aligned} \tag{2.49}$$

If the six values of the potentials are given in each node, it is possible to solve the system (2.49) in order to calculate the unknown parameters a , b , c , d , e and f , (Kwon and Bang 1997), (Bianchi 2005),

$$\begin{Bmatrix} a \\ b \\ c \\ d \\ e \\ f \end{Bmatrix} = \begin{pmatrix} 1 & x_1 & y_1 & x_1^2 & x_1^2y_1^2 & y_1^2 \\ 1 & x_2 & y_2 & x_2^2 & x_2^2y_2^2 & y_2^2 \\ 1 & x_3 & y_3 & x_3^2 & x_3^2y_3^2 & y_3^2 \\ 1 & x_4 & y_4 & x_4^2 & x_4^2y_4^2 & y_4^2 \\ 1 & x_5 & y_5 & x_5^2 & x_5^2y_5^2 & y_5^2 \\ 1 & x_6 & y_6 & x_6^2 & x_6^2y_6^2 & y_6^2 \end{pmatrix}^{-1} \begin{Bmatrix} \phi_1 \\ \phi_2 \\ \phi_3 \\ \phi_4 \\ \phi_5 \\ \phi_6 \end{Bmatrix} \tag{2.50}$$

For this kind of finite element, it is also possible to express (2.48) taking into account the values a , b , c , d , e and f and the potentials defined in six nodes. The resultant equation can be expressed in a vector form by (Kwon and Bang 1997), (Bianchi 2005), (Jianming 2002),

$$\phi_m(x, y) = \{N_m\}\{\phi_m\} \tag{2.51}$$

Where the vectors of (2.51) can be defined by,

$$\{N_m\} = \{N_1 \quad N_2 \quad N_3 \quad N_4 \quad N_5 \quad N_6\}$$

$$\{\phi_m\} = \{\phi_1 \quad \phi_2 \quad \phi_3 \quad \phi_4 \quad \phi_5 \quad \phi_6\}^T \tag{2.52}$$

The values of N_1 , N_2 , N_3 , N_4 , N_5 and N_6 of (2.52) can be consulted in Appendix A. It can be seen that this six nodes triangular finite element can be defined by the values of ϕ_1 , ϕ_2 , ϕ_3 , ϕ_4 ,

ϕ_5 and ϕ_6 at each node, and by the interpolating functions defined in (2.52). These functions depend on the nodes and their position along the x - y plane.

2.2.3.2.2 Finite elements for an axisymmetric symmetry

For the case of an axisymmetric symmetry, the $2D$ domain is also subdivided in a finite high number of nodes. It also assumed that the structure is divided into N_m finite elements, and the total number of nodes is N_n . Each finite element assumes the value ϕ_i of the potential function ϕ .

2.2.3.2.2.1 Triangular finite element in an axisymmetric symmetry with three nodes

It is possible to define triangular elements, and define a linear interpolation of the function $\phi(r, z)$ assumed for each m -th triangular elements, given by (Preiss 1983), (Bianchi 2005),

$$\phi_m(\mathbf{r}, \mathbf{z}) = \mathbf{a} + \mathbf{br} + \mathbf{cz} \quad (2.53)$$

In particular, for the three nodes of the linear triangular element, the three i -th values are given by ϕ_1 , ϕ_2 and ϕ_3 . Taking these values into account, it is possible to compute the scalar function at any point of the element, thus, it is also possible to calculate the unknown parameters a , b , c , i.e.

$$\begin{Bmatrix} \mathbf{a} \\ \mathbf{b} \\ \mathbf{c} \end{Bmatrix} = \begin{pmatrix} \mathbf{1} & \mathbf{r}_1 & \mathbf{z}_1 \\ \mathbf{1} & \mathbf{r}_2 & \mathbf{z}_2 \\ \mathbf{1} & \mathbf{r}_3 & \mathbf{z}_3 \end{pmatrix}^{-1} \begin{Bmatrix} \phi_1 \\ \phi_2 \\ \phi_3 \end{Bmatrix} \quad (2.54)$$

After several operations, the values a , b , c are defined as follows (Preiss 1983), (Bianchi 2005),

$$\begin{aligned} \mathbf{a} &= \frac{1}{\Delta_r^d} [(\mathbf{r}_2\mathbf{z}_3 - \mathbf{r}_3\mathbf{z}_2)\phi_1 + (\mathbf{r}_3\mathbf{z}_1 - \mathbf{r}_1\mathbf{z}_3)\phi_2 + (\mathbf{r}_1\mathbf{z}_2 - \mathbf{r}_2\mathbf{z}_1)\phi_3] \\ \mathbf{b} &= \frac{1}{\Delta_r^d} [(\mathbf{z}_2 - \mathbf{z}_3)\phi_1 + (\mathbf{z}_3 - \mathbf{z}_1)\phi_2 + (\mathbf{z}_1 - \mathbf{z}_2)\phi_3] \\ \mathbf{c} &= \frac{1}{\Delta_r^d} [(\mathbf{r}_3 - \mathbf{r}_2)\phi_1 + (\mathbf{r}_1 - \mathbf{r}_3)\phi_2 + (\mathbf{r}_2 - \mathbf{r}_1)\phi_3] \end{aligned} \quad (2.55)$$

Where the value of Δ_r^d is defined by,

$$\Delta_r^d = \mathbf{r}_1\mathbf{z}_2 - \mathbf{r}_2\mathbf{z}_1 + \mathbf{r}_2\mathbf{z}_3 - \mathbf{r}_3\mathbf{z}_2 + \mathbf{r}_3\mathbf{z}_1 - \mathbf{r}_1\mathbf{z}_3 \quad (2.56)$$

It is possible to express (2.53) taking into account the values a, b, c defined in (2.55) and the potentials defined in the three nodes. The resultant equation can be expressed by (Preiss 1983), (Bianchi 2005), (Kwon and Bang 1997),

$$\phi_m(\mathbf{r}, \mathbf{z}) = \{N_m\}\{\phi_m\} \quad (2.57)$$

The values of N_1, N_2, N_3 can be consulted in Appendix A. The three nodes of the triangular finite element can be defined by the values of ϕ_1, ϕ_2 and ϕ_3 at each node, and by the interpolating functions defined in (2.57). These functions depend on the nodes and their position along the r - z plane.

After having explained the main features of the triangular finite elements for the planar and axisymmetric symmetry, it will be explained the use of an alternative system of coordinates, which permits to calculate the parameters of these finite elements in a simple way.

2.2.3.2.3 Using alternative systems of coordinates for finite element's calculation

The higher order (second or third order) triangular elements are also called high-precision elements. There are many other finite elements but the triangular element with three and six nodes will be used on this investigation. Although the square element is widely used, it can be easily obtained by splitting two triangular elements (Bastos 2003).

The finite element analysis requires to perform several operations in the interpolating functions, in order to generate the matrices and vector that are part of the FEM equations. This cannot be easily achieved by using the normal system of coordinates of a planar or an axisymmetric symmetry. It is necessary to switch, from a conventional system of coordinates, to other allowing an easy calculation. The change of the system of coordinates will be performed on the planar and the axisymmetric symmetry. This will be explained next.

2.2.3.2.3.1 Reference and local finite elements, planar symmetry

As a first step, the idea of a “reference” or “local” element and the reference or local system of coordinates or space is introduced. Figure 2.1 shows an example and the relationship between the local and global system of coordinates (Bastos 2003) in a planar symmetry.

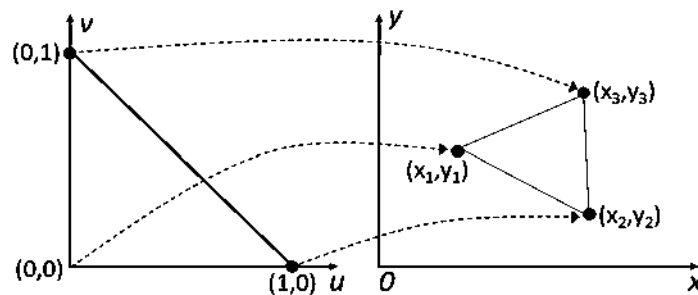


Figure 2.1. A finite element defined in a local system of coordinates (u, v) and mapping to a global system of coordinates (x, y)

The relation needed to define a finite element are generated in the *local* system of coordinates because it is easier to do so. Then, a unique transformation is established which transforms the element from the *local* coordinate system into the *global* coordinate system. This transformation is performed by the so-called “geometric transformation functions” or “mapping functions” which express the real coordinates (x,y) in terms of the local coordinates (u,v) , (Bastos 2003).

2.2.2.3.2.3.1.1 Triangular linear finite element with three nodes

In Figure 2.1 the triangle in local coordinates is defined as follows,

$$\mathbf{u} \geq \mathbf{0}$$

$$\mathbf{v} \geq \mathbf{0}$$

$$\mathbf{u} + \mathbf{v} \leq \mathbf{0} \tag{2.58}$$

The approximation within the triangle can be written in terms of the shape functions, $N(u,v)$, (Kwon and Bang 1997), (Bastos 2003),

$$\mathbf{x}(\mathbf{u}, \mathbf{v}) = \{N_1(\mathbf{u}, \mathbf{v}) \quad N_2(\mathbf{u}, \mathbf{v}) \quad N_3(\mathbf{u}, \mathbf{v})\} \{x_1 \quad x_2 \quad x_3\}^T \tag{2.59}$$

For a first order triangle, the shape functions in local coordinates are (Kwon and Bang 1997), (Bastos 2003),

$$N_1(\mathbf{u}, \mathbf{v}) = \mathbf{1} - \mathbf{u} - \mathbf{v} \tag{2.60}$$

$$N_2(\mathbf{u}, \mathbf{v}) = \mathbf{u} \tag{2.61}$$

$$N_3(\mathbf{u}, \mathbf{v}) = \mathbf{v} \tag{2.61a}$$

It is possible to replace (2.60), (2.61) and (2.61a) in (2.59), i.e. (Bastos 2003),

$$\mathbf{x}(\mathbf{u}, \mathbf{v}) = \{\mathbf{1} - \mathbf{u} - \mathbf{v} \quad \mathbf{u} \quad \mathbf{v}\} \{x_1 \quad x_2 \quad x_3\}^T \tag{2.62}$$

Identical transformations apply to the y coordinates, it yields

$$\mathbf{y}(\mathbf{u}, \mathbf{v}) = \{\mathbf{1} - \mathbf{u} - \mathbf{v} \quad \mathbf{u} \quad \mathbf{v}\} \{y_1 \quad y_2 \quad y_3\}^T \tag{2.63}$$

This means that the functions N_1 , N_2 and N_3 are valid for x and y . The net effect is that node ($u=0, v=0$) is mapped onto (x_1, y_1) . Node ($u=1, v=0$) is mapped onto (x_2, y_2) and the node at ($u=0, v=1$) is mapped onto (x_3, y_3) . Thus, for any point (u, v) , there corresponds a unique point (x, y) ; it is possible to establish a relation between the derivatives of N_i respect to u and v ; with the derivatives of N_i respect to x and y . The partial derivative of N_i respect to x or y are required to derive the matrices included in the Galerkin *weak* formulation in a planar symmetry. Further details about how the matrices of the Galerkin *weak* formulation are calculated, it can be seen in Section 2.2.3.3.1.1. The partial derivatives can be calculated by using the chain derivative rule (Bastos 2003),

$$\frac{\partial N_i}{\partial u} = \frac{\partial N_i}{\partial x} \frac{\partial x}{\partial u} + \frac{\partial N_i}{\partial y} \frac{\partial y}{\partial u} \quad (2.64)$$

$$\frac{\partial N_i}{\partial v} = \frac{\partial N_i}{\partial x} \frac{\partial x}{\partial v} + \frac{\partial N_i}{\partial y} \frac{\partial y}{\partial v} \quad (2.65)$$

If (2.64) and (2.65) are disposed in a matrix way, and the derivatives of x and y respect to u and v are performed yields (Bastos 2003),

$$\begin{Bmatrix} \frac{\partial N_i}{\partial x} \\ \frac{\partial N_i}{\partial y} \end{Bmatrix} = \begin{bmatrix} x_2 - x_1 & y_2 - y_1 \\ x_3 - x_1 & y_3 - y_1 \end{bmatrix}^{-1} \begin{Bmatrix} \frac{\partial N_i}{\partial u} \\ \frac{\partial N_i}{\partial v} \end{Bmatrix} \quad (2.66)$$

If the matrix inverse is developed, (2.66) can be written by,

$$\begin{Bmatrix} \frac{\partial N_i}{\partial x} \\ \frac{\partial N_i}{\partial y} \end{Bmatrix} = \frac{1}{\Delta_d} \begin{bmatrix} y_3 - y_1 & y_1 - y_2 \\ x_1 - x_3 & x_2 - x_1 \end{bmatrix} \begin{Bmatrix} \frac{\partial N_i}{\partial u} \\ \frac{\partial N_i}{\partial v} \end{Bmatrix} \quad (2.67)$$

All the weighting functions with derivative respect to x and y , can be calculated using (2.67). If the triangular finite element defined in 2.2.3.2.1.1 is used, we obtain (Bastos 2003),

$$\begin{Bmatrix} \frac{\partial N_1}{\partial x} & \frac{\partial N_2}{\partial x} & \frac{\partial N_3}{\partial x} \\ \frac{\partial N_1}{\partial y} & \frac{\partial N_2}{\partial y} & \frac{\partial N_3}{\partial y} \end{Bmatrix} = \frac{1}{\Delta_d} \begin{bmatrix} y_3 - y_1 & y_1 - y_2 \\ x_1 - x_3 & x_2 - x_1 \end{bmatrix} \begin{Bmatrix} \frac{\partial N_1}{\partial u} & \frac{\partial N_2}{\partial u} & \frac{\partial N_3}{\partial u} \\ \frac{\partial N_1}{\partial v} & \frac{\partial N_2}{\partial v} & \frac{\partial N_3}{\partial v} \end{Bmatrix} \quad (2.68)$$

The variable Δ_d was already defined in (2.45). The equation (2.68) permits to obtain the derivatives of any N_i that belong to the triangular finite element defined in 2.2.3.2.1.1 in an

easier way. Using (2.68), and by using the Galerkin *weak* formulation, the partial derivatives can be calculated and used to derive the FEM matrices.

2.2.2.3.2.3.1.2 Triangular quadratic finite element in planar symmetry with six nodes

In Figure 2.2 the triangle with six nodes in local coordinates is defined in the same way, as the three-node finite element does,

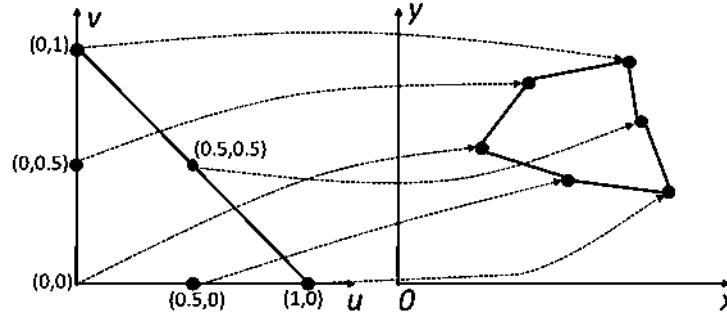


Figure 2.2. A finite element of six nodes defined in a local system of coordinates (u,v) and mapping to a global system of coordinates (x,y)

The approximation within the triangle can be written in terms of the shape functions, $N(u, v)$. It yields, (Bastos 2003),

$$x(\mathbf{u}, \mathbf{v}) = \{N_1 \ N_2 \ N_3 \ N_4 \ N_5 \ N_6\} \{x_1 \ x_2 \ x_3 \ x_4 \ x_5 \ x_6\}^T \quad (2.69)$$

For a first order triangle the shape functions in local coordinates are (Bastos 2003),

$$N_1(\mathbf{u}, \mathbf{v}) = (2\mathbf{u} + 2\mathbf{v} - 1)(\mathbf{u} + \mathbf{v} - 1)$$

$$N_2(\mathbf{u}, \mathbf{v}) = \mathbf{u}(2\mathbf{u} - 1)$$

$$N_3(\mathbf{u}, \mathbf{v}) = \mathbf{v}(2\mathbf{v} - 1)$$

$$N_4(\mathbf{u}, \mathbf{v}) = -\mathbf{u}(4\mathbf{u} + 4\mathbf{v} - 4)$$

$$N_5(\mathbf{u}, \mathbf{v}) = 4\mathbf{u}\mathbf{v}$$

$$N_6(\mathbf{u}, \mathbf{v}) = -\mathbf{v}(4\mathbf{u} + 4\mathbf{v} - 4) \quad (2.70)$$

This means that the functions N_1 , N_2 and N_3 are valid for x and y . The net effect is that node ($u=0, v=0$) is mapped onto (x_1, y_1) . The same effect can be observed in the last three nodes of the triangle. The partial derivative of N_i respect to x or y are also required to derive the matrices included in the Galerkin *weak* formulation in a planar symmetry. All the elements with derivative respect to x and y , can also be calculated using (2.71). It results on (Bastos 2003),

$$\begin{pmatrix} \frac{\partial N_1}{\partial x} & \frac{\partial N_2}{\partial x} & \frac{\partial N_3}{\partial x} & \frac{\partial N_4}{\partial x} & \frac{\partial N_5}{\partial x} & \frac{\partial N_6}{\partial x} \\ \frac{\partial N_1}{\partial y} & \frac{\partial N_2}{\partial y} & \frac{\partial N_3}{\partial y} & \frac{\partial N_4}{\partial y} & \frac{\partial N_5}{\partial y} & \frac{\partial N_6}{\partial y} \end{pmatrix} = \frac{1}{\Delta_d} \begin{bmatrix} y_3 - y_1 & y_1 - y_2 \\ x_1 - x_3 & x_2 - x_1 \end{bmatrix} \begin{pmatrix} \frac{\partial N_1}{\partial u} & \frac{\partial N_2}{\partial u} & \frac{\partial N_3}{\partial u} & \frac{\partial N_4}{\partial u} & \frac{\partial N_5}{\partial u} & \frac{\partial N_6}{\partial u} \\ \frac{\partial N_1}{\partial v} & \frac{\partial N_2}{\partial v} & \frac{\partial N_3}{\partial v} & \frac{\partial N_4}{\partial v} & \frac{\partial N_5}{\partial v} & \frac{\partial N_6}{\partial v} \end{pmatrix} \quad (2.71)$$

The variable Δ_d was already defined in (2.45). The equation (2.71) permits to obtain the derivatives of the quadratic triangular finite element defined in Section 2.2.3.2.1.2 in an easier way. Using (2.71) the partial derivatives can be calculated and used to derive the FEM matrices, by using the Galerkin *weak* formulation.

2.2.3.2.3.2 Reference and local finite elements, axisymmetric symmetry

For the case of a finite element defined for an axisymmetric symmetry, a unique transformation is also established which transforms the element from the *local* coordinate system into the *global* coordinate system. This transformation is accomplished by the so-called “mapping functions” which express the real coordinates (r, z) in terms of the local coordinates (u, v) (Bastos 2003).

2.2.3.2.3.2.1 Triangular linear finite element with three nodes

In Figure 2.3 shows a triangle in local coordinates r and z ,

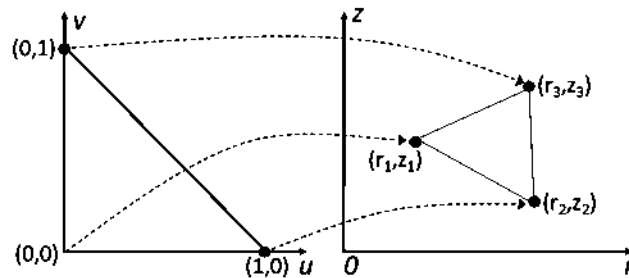


Figure 2.3. A finite element defined in a local system of coordinates (u, v) and mapping to a global system of coordinates (r, z)

The approximation within this triangle can be written in terms of the shape functions, $N(u, v)$, (Bastos 2003),

$$\mathbf{r}(\mathbf{u}, \mathbf{v}) = \{N_1(\mathbf{u}, \mathbf{v}) \quad N_2(\mathbf{u}, \mathbf{v}) \quad N_3(\mathbf{u}, \mathbf{v})\} \{\mathbf{r}_1 \quad \mathbf{r}_2 \quad \mathbf{r}_3\}^T \quad (2.72)$$

For a first order triangle the shape functions in local coordinates were defined in (2.60), (2.61) and (2.61a). If these shape function are substituted in (2.72) gives,

$$\mathbf{r}(\mathbf{u}, \mathbf{v}) = \{\mathbf{1} - \mathbf{u} - \mathbf{v} \quad \mathbf{u} \quad \mathbf{v}\} \{\mathbf{r}_1 \quad \mathbf{r}_2 \quad \mathbf{r}_3\}^T \quad (2.73)$$

If (2.73) is taken into account, an identical transformation apply to the z -coordinate,

$$\mathbf{z}(\mathbf{u}, \mathbf{v}) = \{\mathbf{1} - \mathbf{u} - \mathbf{v} \quad \mathbf{u} \quad \mathbf{v}\} \{\mathbf{z}_1 \quad \mathbf{z}_2 \quad \mathbf{z}_3\}^T \quad (2.74)$$

This means that the functions N_1 , N_2 and N_3 are valid for r and z . For any point (u, v) , there correspond a unique point (r, z) . It is possible to establish a relation between the derivatives of N_i respect to u and v ; with the derivatives of N_i respect to r and z . This is possible to achieve by using the chain derivative rule (Bastos 2003), i.e.

$$\frac{\partial N_i}{\partial u} = \frac{\partial N_i}{\partial r} \frac{\partial r}{\partial u} + \frac{\partial N_i}{\partial z} \frac{\partial z}{\partial u} \quad (2.75)$$

$$\frac{\partial N_i}{\partial v} = \frac{\partial N_i}{\partial r} \frac{\partial r}{\partial v} + \frac{\partial N_i}{\partial z} \frac{\partial z}{\partial v} \quad (2.76)$$

If (2.75) and (2.76) are disposed in a matrix way, and the derivatives of r and z respect to u and v are performed, it yields, (Bastos 2003),

$$\begin{Bmatrix} \frac{\partial N_i}{\partial r} \\ \frac{\partial N_i}{\partial z} \end{Bmatrix} = \begin{bmatrix} \mathbf{r}_2 - \mathbf{r}_1 & \mathbf{z}_2 - \mathbf{z}_1 \\ \mathbf{r}_3 - \mathbf{r}_1 & \mathbf{z}_3 - \mathbf{z}_1 \end{bmatrix}^{-1} \begin{Bmatrix} \frac{\partial N_i}{\partial u} \\ \frac{\partial N_i}{\partial v} \end{Bmatrix} \quad (2.77)$$

Taking into account the matrix inverse, (2.77) can be written by, (Bastos 2003),

$$\begin{Bmatrix} \frac{\partial N_i}{\partial r} \\ \frac{\partial N_i}{\partial z} \end{Bmatrix} = \frac{1}{\Delta'_d} \begin{bmatrix} \mathbf{z}_3 - \mathbf{z}_1 & \mathbf{z}_1 - \mathbf{z}_2 \\ \mathbf{r}_1 - \mathbf{r}_3 & \mathbf{r}_2 - \mathbf{r}_1 \end{bmatrix} \begin{Bmatrix} \frac{\partial N_i}{\partial u} \\ \frac{\partial N_i}{\partial v} \end{Bmatrix} \quad (2.78)$$

All the elements with derivative respect to r and z , can be calculated using (2.78). It results on, (Bastos 2003),

$$\left\{ \begin{array}{ccc} \frac{\partial N_1}{\partial r} & \frac{\partial N_2}{\partial r} & \frac{\partial N_3}{\partial r} \\ \frac{\partial N_1}{\partial z} & \frac{\partial N_2}{\partial z} & \frac{\partial N_3}{\partial z} \end{array} \right\} = \frac{1}{\Delta_d^r} \begin{bmatrix} \mathbf{z}_3 - \mathbf{z}_1 & \mathbf{z}_1 - \mathbf{z}_2 \\ \mathbf{r}_1 - \mathbf{r}_3 & \mathbf{r}_2 - \mathbf{r}_1 \end{bmatrix} \left\{ \begin{array}{ccc} \frac{\partial N_1}{\partial u} & \frac{\partial N_2}{\partial u} & \frac{\partial N_3}{\partial u} \\ \frac{\partial N_1}{\partial v} & \frac{\partial N_2}{\partial v} & \frac{\partial N_3}{\partial v} \end{array} \right\} \quad (2.79)$$

The variable Δ_d^r was already defined in (2.56). The equation (2.79) permits to obtain the derivatives of any N_i that belong to the triangular finite element defined in Section 2.2.3.2.2.1 in an easier way.

2.2.3.3 Formulation of the system to solve a field equation derived from a planar and axisymmetric symmetry assumptions

To solve the field problem, the values of ϕ_{mj} have to be computed in the nodes of each element. It is necessary to prepare a set of equations, whose solution correspond to the values of ϕ_{mj} . To develop this system, the residual method may be adopted. For the case of Galerkin equation explained in Section 2.2.2, this is applied to each finite element. Thus, the residual integral is set to zero. The residual integral of the m -th element is defined by (Bianchi 2005),

$$\mathbf{R}_{im} = \int_{\tau} \left[\{N_{mj}\} \mathbf{L} \left(\{N_{mj}\} \{ \phi_{mj} \}^T \right) \right] d\tau - \int_{\tau} \{N_{mj}\} \mathbf{f}_m d\tau \quad (2.80)$$

A set of n equations with the n unknown ϕ_{mj} is obtained. By applying the Galerkin method to all the N_m elements that form the domain, and considering the relationships that link the adjacent elements, a system of this kind is obtained as (Bianchi 2005);

$$[\mathbf{S}] \{ \phi \} - \{ \mathbf{F} \} = \mathbf{0} \quad (2.81)$$

The equation (2.81) is formed by N_n equations, with N_n unknown ϕ_j . The residual and the matrix equations (2.80) and (2.81) depends of the kind of symmetry assumption. The residual and the matrix equation for a planar and an axisymmetric symmetry will be explained next.

2.2.3.3.1 Formulation of the system to solve a field equation derived from a planar symmetry assumption

For the case of a device with a planar symmetry assumption, if the operator L defined in (2.25) along the interpolating and weigh functions defined in (2.32) and (2.34) are considered; and finally, a planar symmetry is considered on (2.80); it yields (Bianchi 2005),

$$\int_{\tau} \left[\{N_{mj}\} \mathbf{L} \left(\{N_{mj}\} \{ \phi_{mj} \}^T \right) \right] d\tau - \int_{\tau} \{N_{mj}\} \mathbf{f}_m d\tau = \left(\int_{\tau} N_i \left[-\frac{\partial}{\partial x} \left(\alpha_x \frac{\partial N_j}{\partial x} \right) - \frac{\partial}{\partial y} \left(\alpha_y \frac{\partial N_j}{\partial y} \right) \right] d\tau \right) \phi_j - \left(\int_{\tau} N_i d\tau \right) \mathbf{f} \quad (2.82)$$

If a Poisson equation is being formulated, the variable ϕ ; the forcing function F , and the parameters α_x and α_y of the right side of (2.82) are all defined by (Bianchi 2005),

$$\phi_j = A_z(x, y); f = J_z$$

$$\alpha_x = \alpha_y = \nu \quad (2.82a)$$

Where A_z is the magnetic vector potential defined along the z -axis. The region τ was previously defined in (2.13).

2.2.3.3.1.1 Solution of a field equation derived from a planar symmetry using the Galerkin weak formulation

The Galerkin *weak* formulation can be applied to the solution of partial differential equations derived from a planar symmetry assumption. In order to develop the Galerkin *weak* formulation of the first term of the right side of (2.82), integration by parts is applied to reduce the order of differentiation within the integral (Kwon and Bang 1997). The subsequent explanation shows the integration by parts. The next step consists on separating the first term of the right and left sides of (2.82). It yields,

$$\left[\int_{\tau_D} \left[\{N_i\}^T L \left(\{N_j\} \{ \phi_j \}^T \right) \right] d\tau \right] = \left(\int_{\tau_D} N_i \left[-\frac{\partial}{\partial x} \left(\alpha_x \frac{\partial N_j}{\partial x} \right) - \frac{\partial}{\partial y} \left(\alpha_y \frac{\partial N_j}{\partial y} \right) \right] d\tau \right) \phi_j \quad (2.83)$$

After that, it is possible to substitute the interpolating function (2.32) and the weigh functions (2.34) in the right side of (2.83). On the first step of the Galerkin *weak* formulation, the term with derivate respect to x can be separated from the term with derivate respect to y to develop them separately. Thus, the term with derivate respect to x can be evaluated first by performing an integration by parts respect to x (Kwon and Bang 1997), (Bianchi 2005). After that, an integration respect to y can be done. The result of these operations is given by (Arkkio 1987), (Kwon and Bang 1997), (Jianming 2002),

$$\left(\int_{\tau_D} \{N_i\}^T \left[-\frac{\partial}{\partial x} \left(\alpha_x \frac{\partial \{N_j\}}{\partial x} \right) \right] d\tau \right) \phi_j = - \left[\int_{y_i}^{y_f} \left(-\{N_i\}^T \alpha_x \frac{\partial \phi}{\partial x} \right)_{x_i}^{x_f} dy \right] + \left[\int_{y_i}^{y_f} \int_{x_i}^{x_f} \left(\alpha_x \frac{\partial \{N_i\}^T}{\partial x} \frac{\partial \{N_j\}}{\partial x} \right) dx dy \right] \{ \phi_j \}^T \quad (2.84)$$

Where x_i, x_f, y_i, y_f are limits of the integral area τ . The area τ is shown in Figure 2.4

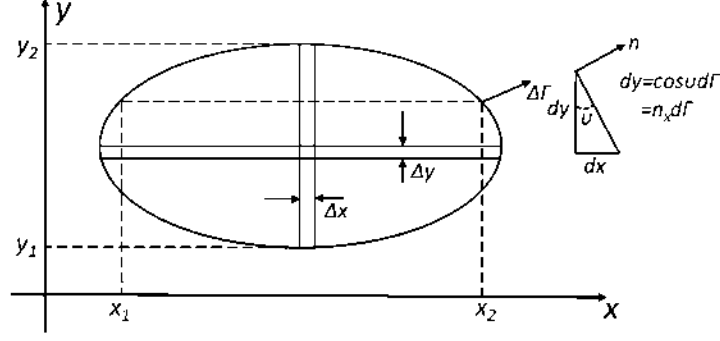


Figure 2.4. Two dimension domain of a planar symmetry assumption

It is possible to rewrite the boundary integration of (2.84), by defining it in terms of the boundary Γ , it yields (Kwon and Bang 1997), (Bianchi 2005),

$$\left[\int_{y_i}^{y_f} \left(-\{N_i\}^T \alpha_x \frac{\partial \phi}{\partial x} \right)_{x_i}^{x_f} dy \right] = - \left[\int_{\Gamma_2} \{N_i\}^T \alpha_x \frac{\partial \phi}{\partial x} n_x d\Gamma \right] + \left[\int_{\Gamma_1} \{N_i\}^T \alpha_x \frac{\partial \phi}{\partial x} n_x d\Gamma \right] \quad (2.85)$$

Where n_x is the unit normal vector, which is assumed to be positive in the outward direction as shown in Figure 2.4. Finally combining the two boundary integrals of (2.85) gives (Kwon and Bang 1997), (Bianchi 2005),

$$- \left[\int_{\Gamma_2} \{N_i\}^T \alpha_x \frac{\partial \phi}{\partial x} n_x d\Gamma \right] + \left[\int_{\Gamma_1} \{N_i\}^T \alpha_x \frac{\partial \phi}{\partial x} n_x d\Gamma \right] = \oint_{\Gamma_d} \left(-\{N_i\}^T \alpha_n \frac{\partial \phi}{\partial x} n_x \right) d\Gamma \quad (2.86)$$

If the right side of (2.86) is substituted in (2.84) it gives,

$$\left(\int_{\tau_d} \{N_i\}^T \left[-\frac{\partial}{\partial x} \left(\alpha_x \frac{\partial \{N_j\}}{\partial x} \right) \right] d\tau \right) \phi_j = \oint_{\Gamma_d} \left(-\{N_i\}^T \alpha_n \frac{\partial \phi}{\partial x} n_x \right) d\Gamma + \left[\int_{y_i}^{y_f} \int_{x_i}^{x_f} \left(\alpha_x \frac{\partial \{N_i\}^T}{\partial x} \frac{\partial \{N_j\}}{\partial x} \right) dx dy \right] \{ \phi_j \}^T \quad (2.87)$$

It is possible to perform the same integration in the term with derivate respect to y of (2.83). The boundary terms derived from this integration by parts can be modified according to (2.84), (2.85), (2.86) and (2.87). The result of these operations is given by (Kwon and Bang 1997), (Bianchi 2005),

$$\left(\int_{\tau_d} \{N_i\}^T \left[-\frac{\partial}{\partial y} \left(\alpha_y \frac{\partial \{N_j\}}{\partial y} \right) \right] d\tau \right) \phi_j = \oint_{\Gamma_d} \left(-\{N_i\}^T \alpha_y \frac{\partial \phi}{\partial y} n_y \right) d\Gamma + \left[\int_{x_i}^{x_f} \int_{y_i}^{y_f} \left(\alpha_y \frac{\partial \{N_i\}^T}{\partial y} \frac{\partial \{N_j\}}{\partial y} \right) dy dx \right] \{ \phi_j \}^T \quad (2.88)$$

Taking into account (2.87) and (2.88); (2.83) be written by (Kwon and Bang 1997), (Bianchi 2005),

$$\begin{aligned} \left[\int_{\tau_D} \left[\{N_i\}^T L \left(\{N_j\} \{ \phi_j \}^T \right) \right] d\tau \right] &= \oint_{\Gamma_d} \left(-\{N_i\}^T \alpha_x \frac{\partial \phi}{\partial x} n_x - \{N_i\}^T \alpha_y \frac{\partial \phi}{\partial y} n_y \right) d\Gamma \\ &+ \left[\int_{\tau_D} \left(\alpha_x \frac{\partial \{N_i\}^T}{\partial x} \frac{\partial \{N_j\}}{\partial x} + \alpha_y \frac{\partial \{N_i\}^T}{\partial y} \frac{\partial \{N_j\}}{\partial y} \right) d\tau \right] \{ \phi_j \}^T \end{aligned} \quad (2.89)$$

The boundary terms of (2.89) can be expressed in terms of the normal direction of the boundary (*Green's theorem*); thus (Kwon and Bang 1997), (Bianchi 2005), (Jianming 2002),

$$\begin{aligned} \left[\int_{\tau_D} \left[\{N_i\}^T L \left(\{N_j\} \{ \phi_j \}^T \right) \right] d\tau \right] &= \oint_{\Gamma_d} \left(-\{N_i\}^T \alpha_n \frac{\partial \{N_j\}}{\partial n} \right) d\Gamma \\ &+ \left[\int_{\tau_D} \left(\alpha_x \frac{\partial \{N_i\}^T}{\partial x} \frac{\partial \{N_j\}}{\partial x} + \alpha_y \frac{\partial \{N_i\}^T}{\partial y} \frac{\partial \{N_j\}}{\partial y} \right) d\tau \right] \{ \phi_j \}^T \end{aligned} \quad (2.90)$$

The first term of the right side of (2.90) contains the boundary conditions on the frontier Γ . This term contains the Neumann and the Dirichlet boundary conditions. It gives (Kwon and Bang 1997), (Bianchi 2005), (Jianming 2002),

$$\begin{aligned} \left[\int_{\tau_D} \left[\{N_i\}^T L \left(\{N_j\} \{ \phi_j \}^T \right) \right] d\tau \right] &= \left[\int_{\Gamma_d}^{(I)} \left(-\{N_i\}^T \alpha_n \frac{\partial \phi}{\partial n} \right) d\Gamma \right] + \left[\int_{\Gamma_d}^{(II)} \left(-\{N_i\}^T \alpha_n \frac{\partial \phi}{\partial n} \right) d\Gamma \right] + \\ &\left[\int_{\tau_D} \left(\alpha_x \frac{\partial \{N_i\}^T}{\partial x} \frac{\partial \{N_j\}}{\partial x} + \frac{\partial \{N_i\}^T}{\partial y} \frac{\partial \{N_j\}}{\partial y} \right) d\tau \right] \{ \phi_j \}^T \end{aligned} \quad (2.91)$$

The first and second terms at the left side of (2.91) represent the Neumann and Dirichlet boundary conditions, respectively.

2.2.3.3.2 Formulation of the system to solve a field equation derived from an axisymmetric symmetry assumption

For the case of a device with an axisymmetry assumption, if the operator L defined in (2.25) along the interpolating and weigh functions defined in (2.32) and (2.34) are considered; and finally, an axisymmetric symmetry is considered on (2.80); it yields (Bianchi 2005),

$$\begin{aligned} \int_{\tau_r} \left[\{N_{mj}\} L \left(\{N_{mj}\} \{ \phi_{mj} \}^T \right) \right] d\tau_r - \int_{\tau_r} \{N_{mj}\} f_m d\tau_r &= \\ \left(\int_{\tau_{rD}} N_i \left[-\frac{\partial}{\partial r} \left(\alpha_r \frac{\partial N_j}{\partial r} \right) - \frac{\partial}{\partial z} \left(\alpha_z \frac{\partial N_j}{\partial z} \right) + \beta N_j \right] d\tau_r \right) \phi_j - \left(\int_{\tau_{rD}} N_i d\tau_r \right) f \end{aligned} \quad (2.92)$$

If a Poisson equation is being formulated, the variable ϕ , the forcing function F , and the parameters β , α_r and α_z of (2.92) are defined by (Bianchi 2005), (Preiss 1983),

$$\phi_j = A_\rho(r, z) ; f = J_\rho$$

$$\alpha_r = \alpha_z = \frac{v}{r} ; \beta = \frac{v}{r} \quad (2.93)$$

Where A_ρ is the magnetic vector potential defined along the ρ -axis. The region τ_r was previously defined in (2.23).

2.2.3.3.2.1 Solution of a field equation derived from an axisymmetric symmetry using the Galerkin weak formulation

For an axisymmetric symmetry, the next steps consists on separating the first term of the right and left sides of (2.92). It yields,

$$\left[\int_{\tau_D} \left\{ N_i \right\}^T L \left(\left\{ N_j \right\} \left\{ \phi_j \right\}^T \right) d\tau_r \right] = \left(\int_{\tau_D} N_i \left[-\frac{\partial}{\partial r} \left(\alpha_r \frac{\partial N_j}{\partial r} \right) - \frac{\partial}{\partial z} \left(\alpha_z \frac{\partial N_j}{\partial z} \right) + \beta N_j \right] d\tau_r \right) \phi_j \quad (2.94)$$

After that, it is possible to substitute the interpolating function (2.32) and the weigh functions (2.34) in the right side of (2.94). At the same time, the term with derivate respect to r can be separated from the term with derivate respect to z , to develop them separately. Thus, the term with derivate respect to r can be evaluated by first performing an integration parts respect to r . After that, an integration respect to z can be done. The result of these operations is given by (Preiss 1983), (Kwon and Bang 1997), (Jianming 2002),

$$\left(\int_{\tau_D} \left\{ N_i \right\}^T \left[-\frac{\partial}{\partial r} \left(\alpha_r \frac{\partial N_j}{\partial r} \right) \right] d\tau_r \right) \phi_j = - \left[\int_{z_i}^{z_f} \left(-\left\{ N_i \right\}^T \alpha_r \frac{\partial \phi}{\partial r} \right)_{r_i}^{r_f} dz \right] + \left[\int_{z_i}^{z_f} \int_{r_i}^{r_f} \left(\alpha_r \frac{\partial \left\{ N_i \right\}^T}{\partial r} \frac{\partial \left\{ N_j \right\}}{\partial r} \right) dr dz \right] \left\{ \phi_j \right\}^T \quad (2.95)$$

Where r_i , r_f , z_i , z_f are limits of the integral area τ_r . The area τ_r can be seen in Figure 2.5

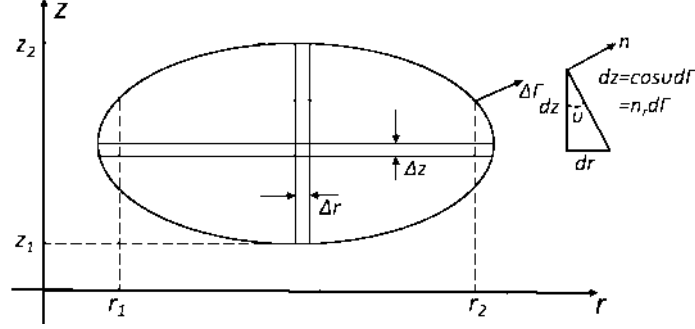


Figure 2.5 Two dimension domain of an axisymmetric symmetry assumption

It is possible to rewrite the boundary integration part of (2.95), by defining it in terms of the boundary Γ . It yields (Preiss 1983), (Kwon and Bang 1997),

$$\left[\int_{z_i}^{z_f} \left(-\{N_i\}^T \alpha_r \frac{\partial \phi}{\partial r} \right)_{r_i}^{r_f} dz \right] = - \left[\int_{\Gamma_2} \{N_i\}^T \alpha_r \frac{\partial \phi}{\partial r} n_r d\Gamma \right] + \left[\int_{\Gamma_1} \{N_i\}^T \alpha_r \frac{\partial \phi}{\partial r} n_r d\Gamma \right] \quad (2.96)$$

Where n_r is the unit normal vector, which is assumed to be positive in the outward direction as shown in Figure 2.5. Finally combining the two boundary integrals of (2.96) gives (Preiss 1983), (Kwon and Bang 1997),

$$- \left[\int_{\Gamma_2} \{N_i\}^T \alpha_r \frac{\partial \phi}{\partial r} n_r d\Gamma \right] + \left[\int_{\Gamma_1} \{N_i\}^T \alpha_r \frac{\partial \phi}{\partial r} n_r d\Gamma \right] = \oint_{\Gamma_d} \left(-\{N_i\}^T \alpha_n \frac{\partial \phi}{\partial r} n_r \right) d\Gamma \quad (2.97)$$

If the right side of (2.97) is substituted in (2.96) gives (Preiss 1983), (Kwon and Bang 1997),

$$\left(\int_{\tau_{rD}} \{N_i\}^T \left[-\frac{\partial}{\partial r} \left(\alpha_r \frac{\partial \{N_j\}}{\partial z} \right) \right] d\tau_r \right) \phi_j = \oint_{\Gamma_d} \left(-\{N_i\}^T \alpha_n \frac{\partial \phi}{\partial z} n_z \right) d\Gamma + \left[\int_{z_i}^{z_f} \int_{r_i}^{r_f} \left(\alpha_x \frac{\partial \{N_i\}^T}{\partial x} \frac{\partial \{N_j\}}{\partial x} \right) dr dz \right] \{ \phi_j \}^T \quad (2.98)$$

It is possible to perform the same integration of (2.94) in the terms with derivate respect to z . The boundary terms derived by this integration can be modified according to (2.96), (2.97) and (2.98). The result of these operations is given by (Preiss 1983), (Kwon and Bang 1997),

$$\left(\int_{\tau_{rD}} \{N_i\}^T \left[-\frac{\partial}{\partial z} \left(\alpha_z \frac{\partial \{N_j\}}{\partial z} \right) \right] d\tau_r \right) \phi_j = \oint_{\Gamma_d} \left(-\{N_i\}^T \alpha_z \frac{\partial \phi}{\partial z} n_z \right) d\Gamma + \left[\int_{r_i}^{r_f} \int_{z_i}^{z_f} \left(\alpha_z \frac{\partial \{N_i\}^T}{\partial z} \frac{\partial \{N_j\}}{\partial z} \right) dz dr \right] \{ \phi_j \}^T \quad (2.99)$$

Taking into account (2.98) and (2.99); (2.94) can be written by (Preiss 1983), (Kwon and Bang 1997),

$$\begin{aligned} \left[\int_{\tau_D} \left[\{N_i\}^T L \left(\{N_j\} \{ \phi_j \}^T \right) \right] d\tau_r \right] &= \oint_{\Gamma_d} \left(-\{N_i\}^T \alpha_r \frac{\partial \phi}{\partial r} n_r - \{N_i\}^T \alpha_z \frac{\partial \phi}{\partial z} n_z \right) d\Gamma \\ &+ \left[\int_{\tau_D} \left(\alpha_r \frac{\partial \{N_i\}^T}{\partial r} \frac{\partial \{N_j\}}{\partial r} + \alpha_z \frac{\partial \{N_i\}^T}{\partial z} \frac{\partial \{N_j\}}{\partial z} \right) d\tau_r \right] \{ \phi_j \}^T + \left[\int_{\tau_D} \{N_i\}^T \beta \{N_j\} d\tau_r \right] \{ \phi_j \} \end{aligned} \quad (2.100)$$

The boundary terms of (2.100) can be expressed in terms of the normal direction of the boundary (*Green's theorem* (Kwon and Bang 1997)), thus,

$$\begin{aligned} \left[\int_{\tau_D} \left[\{N_i\}^T L \left(\{N_j\} \{ \phi_j \}^T \right) \right] d\tau_r \right] &= \oint_{\Gamma_d} \left(-\{N_i\}^T \alpha_n \frac{\partial \{N_j\}}{\partial n} \right) d\Gamma \\ &+ \left[\int_{\tau_D} \left(\alpha_r \frac{\partial \{N_i\}^T}{\partial r} \frac{\partial \{N_j\}}{\partial r} + \alpha_z \frac{\partial \{N_i\}^T}{\partial z} \frac{\partial \{N_j\}}{\partial z} \right) d\tau_r \right] \{ \phi_j \}^T + \left[\int_{\tau_D} \{N_i\}^T \beta \{N_j\} d\tau_r \right] \{ \phi_j \} \end{aligned} \quad (2.101)$$

The first term of the right side of (2.101) contains the boundary conditions on the frontier Γ . This term contains the Neumann and the Dirichlet boundary conditions. It gives (Preiss 1983), (Kwon and Bang 1997),

$$\begin{aligned} \left[\int_{\tau_D} \left[\{N_i\}^T L \left(\{N_j\} \{ \phi_j \}^T \right) \right] d\tau_r \right] &= \left[\int_{\Gamma_d}^{(I)} \left(-\{N_i\}^T \alpha_n \frac{\partial \phi}{\partial n} \right) d\Gamma \right] + \left[\int_{\Gamma_d}^{(II)} \left(-\{N_i\}^T \alpha_n \frac{\partial \phi}{\partial n} \right) d\Gamma \right] + \\ &\left[\int_{\tau_D} \left(\alpha_r \frac{\partial \{N_i\}^T}{\partial r} \frac{\partial \{N_j\}}{\partial r} + \frac{\partial \{N_i\}^T}{\partial z} \frac{\partial \{N_j\}}{\partial z} \right) d\tau_r \right] \{ \phi_j \}^T + \left[\int_{\tau_D} \{N_i\}^T \beta \{N_j\} d\tau_r \right] \{ \phi_j \} \end{aligned} \quad (2.102)$$

The first and second terms of the right side of (2.102) represent the Neumann and Dirichlet boundary conditions, respectively.

2.2.3.4 Deriving final matrix equation that contains the solution of the problem

Equations (2.91) or (2.102) can be developed by performing the respective integration process, thus it is possible to compute the values $\{ \phi_j \}$ in the N_n nodes of the domain. At the same time, the second term of the right side of (2.82) and (2.92) can also be developed by perming an integrating process. It yields (Preiss 1983), (Kwon and Bang 1997),

$$\{ \mathbf{f}_b^{(I)} \} + \{ \mathbf{f}_b^{(II)} \} + [\mathbf{S}] \{ \phi_j \} = \{ \mathbf{f}_{gj} \} \mathbf{f} \quad (2.103)$$

The vector $\{f_b^{(I)}\}$ contains the Neumann boundary conditions; the Dirichlet boundary conditions are contained in the vector $\{f_b^{(II)}\}$; and the terms $[S]$ and $\{f_{gj}\}$ were derived by the Galerkin formulation. All these terms correspond either to the planar or the axisymmetric symmetry assumption. Further details about the matrices and vectors derived for the planar and axisymmetric symmetries can be consulted in Appendix A.

The set of equations (2.103) can be solved by means of common numerical algorithms, but it can be seen that have been considered field equations that do not have terms that depend in time. They will be derived next.

2.2.3.5 Deriving field equation with time varying terms

The inclusion of the time varying terms can be achieved, by redefining the current density of the Poisson equation, in order to include the electric field that considers the coulomb electrical field E_c and the induced electric field E_i . This action will be performed for the field equations of a planar and an axisymmetric symmetry assumption. This will be explained next.

2.2.3.5.1 Time varying terms of the planar symmetry, current and voltage as the forcing function

For the case of the planar symmetry, the electrical field included in (2.1) can substituted in the Poisson equation defined in (2.6). The resultant equation is shown in (2.10). It is possible to represent that equation in a general form defined by,

$$-\frac{\partial}{\partial x}\left(\alpha_x \frac{\partial \phi}{\partial x}\right) - \frac{\partial}{\partial y}\left(\alpha_y \frac{\partial \phi}{\partial y}\right) = f_U - \alpha_z \frac{\partial \phi}{\partial t} \quad (2.104)$$

The Galerkin method was already developed for the right side of (2.104), specifically the Galerkin *weak* formulation that can be seen in (2.91) was used. If the Galerkin method is applied to the right side of (2.104), and the equation is decomposed in two terms (Konrad 1982), (Arkkio 1987),

$$\int_{\tau_D} N_i \left(f_U - \alpha_z \frac{\partial \phi}{\partial t} \right) d\tau = \int_{\tau_D} N_i f_U d\tau - \int_{\tau_D} N_i \left(\alpha_z \frac{\partial \phi}{\partial t} \right) d\tau \quad (2.105)$$

According to the Galerkin method, the function N_i is defined by an interpolating function. Thus, (2.105) is given by,

$$\int_{\tau_D} N_i f d\tau \rightarrow \left[\int_{\tau_D} \{N_i\}^T d\tau \right] (f_U) \quad (2.106)$$

If the interpolation function defined in (2.34) is replaced in the second term of the right side of (2.106), and if at the same time the term N_i is modified according to the *Galerkin* method; it yields,

$$-\int_{\tau_D} N_i \left(\alpha_z \frac{\partial \phi}{\partial t} \right) d\tau \rightarrow - \left[\int_{\tau_D} \alpha_z \{N_i\}^T \{N_j\} d\tau \right] \frac{d\{\phi_j\}}{dt} \quad (2.107)$$

Finally, if the terms defined in (2.106) and (2.107) are substituted in (2.105) and the Galerkin *weak* formulation terms defined in (2.91) are included; it yields (Konrad 1982), (Arkkio 1987),

$$\begin{aligned} & \left[\int_{\Gamma_d}^{(I)} \left(-\{N_i\}^T \alpha_n \frac{\partial \phi}{\partial n} \right) d\Gamma \right] + \left[\int_{\Gamma_d}^{(II)} \left(-\{N_i\}^T \alpha_n \frac{\partial \phi}{\partial n} \right) d\Gamma \right] + \\ & \left[\int_{\tau_D} \left(\alpha_x \frac{\partial \{N_i\}^T \partial \{N_j\}}{\partial x} + \frac{\partial \{N_i\}^T \partial \{N_j\}}{\partial y} \right) d\tau \right] \{\phi_j\} \\ & + \left[\int_{\tau_D} \alpha_z \{N_i\}^T \{N_j\} d\tau \right] \frac{d\{\phi_j\}}{dt} = \left[\int_{\tau} \frac{\sigma \{N_i\}^T}{l} d\tau \right] (f_U) \end{aligned} \quad (2.108)$$

Equation (2.108) can be developed and will result on a matrix equation of the next form, (Konrad 1982), (Arkkio 1987), (Jianming 2002), (Reece and Preston 2000),

$$\{f_b^{(I)}\} + \{f_b^{(II)}\} + [S]\{\phi_j\} + [T] \frac{d}{dt} \{\phi_j\} = \{f_{gu}\} f_U \quad (2.109)$$

The vector $\{f_b^{(I)}\}$ contains the Neumann boundary conditions; the Dirichet boundary conditions are contained in the vector $\{f_b^{(II)}\}$; and the terms $[S]$ and $\{f_{gu}\}$ were derived by the *Galerkin* weak formulation. All these terms correspond to a planar symmetry assumption. Further details of the matrix $[T]$ and the vector $\{f_{gu}\}$ can be consulted in Appendix A. For the case of a Poisson equation, the variables ϕ_j and f_U are given by (Konrad 1982), (Arkkio 1987),

$$\phi_j = A_z; f_U = U_c \quad (2.110)$$

It is possible to define the current as a forcing function; this can be achieved by using the expression defined by (Konrad 1982), (Arkkio 1987),

$$(\mathbf{R}_c)^{-1} (f_U) - \int_{\tau} \sigma \frac{\partial \phi_j}{\partial t} d\tau = f_I \quad (2.111)$$

If the interpolation function defined in (2.34) is replaced in the second term of the left side of (2.111) yields, (Konrad 1982), (Arkkio 1987),

$$(\mathbf{R}_c)^{-1}(\mathbf{f}_U) - \left[\int_{\tau} \boldsymbol{\sigma}\{N_j\} d\boldsymbol{\tau} \right] \frac{d\{\phi_j\}}{dt} = \mathbf{f}_I \quad (2.112)$$

If (2.112) is represented in a matrix way (Konrad 1982), it takes the form,

$$(\mathbf{R}_c)^{-1}(\mathbf{f}_U) - \{\mathbf{f}_{ga}\} \frac{d\{\phi_j\}}{dt} = \mathbf{f}_I \quad (2.113)$$

For the case of a Poisson equation of a planar symmetry, the variables ϕ_j , f_U and f_I are substituted by,

$$\phi = A_z ; f_U = U_c ; f_I = I_z \quad (2.114)$$

Using (2.109) and (2.113), it is possible to formulate a coupled equation that has the conductors' current as the forcing function.

It is very important to mention that it is necessary to formulate a specific finite element in each subdomain, and apply the finite element analysis to derive the respective matrices and vector of it. The different types of finite element used in this investigation can be consulted in the Section 2.2.3.2. If these finite element are used, it is possible to derive the matrices and vector shown in (2.109) and (2.113). The matrices and vectors can be consulted in Appendix A of this thesis.

2.2.3.5.2 Time varying terms of the axisymmetric symmetry, current and voltage as the forcing function

For the case of axisymmetric symmetry, the current density included in (2.19) can substituted in the Poisson equation defined in (2.18). The resultant equation is shown in (2.20). It is possible to represent that equation in a general form defined by,

$$-\frac{1}{r} \frac{\partial}{\partial r} \left(\alpha_r \frac{\partial \phi}{\partial r} \right) - \frac{1}{r} \frac{\partial}{\partial z} \left(\alpha_z \frac{\partial \phi}{\partial z} \right) + \beta \phi = \sigma \frac{f_U}{2\pi r} - \alpha_z \frac{\partial \phi}{\partial t} \quad (2.115)$$

It is possible to apply the Galerkin *weak* formulation in the left side of (2.115). Moreover, if the Galerkin method is applied in the right side of (2.115), and the equation is decomposed in two terms yields,

$$\int_{\tau_D} N_i \left(\mathbf{f} - \alpha_z \frac{\partial \phi}{\partial t} \right) d\boldsymbol{\tau}_r = \int_{\tau_D} N_i \left(\sigma \frac{f_U}{2\pi r} \right) d\boldsymbol{\tau}_r - \int_{\tau_D} N_i \left(\alpha_z \frac{\partial \phi}{\partial t} \right) d\boldsymbol{\tau}_r \quad (2.116)$$

If the first term of the right side of (2.115) is modified, by replacing the weight function N_i , it gives,

$$\int_{\tau_D} N_i f d\tau_r \rightarrow \left[\int_{\tau_D} \sigma \frac{\{N_i\}^T}{(2\pi r)} d\tau_r \right] (f_U) \quad (2.117)$$

If the interpolation function defined in (2.34) is replaced in the second term of the right side of (2.117). It yields,

$$- \int_{\tau_D} N_i \left(\alpha_z \frac{\partial \phi}{\partial t} \right) d\tau \rightarrow - \left[\int_{\tau_D} \alpha_z \{N_i\}^T \{N_j\} d\tau_r \right] \frac{d\{\phi_j\}}{dt} \quad (2.118)$$

Finally, if the terms defined in (2.117) and (2.118) are substituted in (2.116) and the Galerkin *weak* formulation terms defined in (2.102) are included, results in (Preiss 1983), (Arkkio 1987),

$$\begin{aligned} & \left[\int_{\Gamma_a}^{(I)} \left(-\{N_i\}^T \alpha_n \frac{\partial \phi}{\partial n} \right) d\Gamma \right] + \left[\int_{\Gamma_a}^{(II)} \left(-\{N_i\}^T \alpha_n \frac{\partial \phi}{\partial n} \right) d\Gamma \right] + \\ & \left[\int_{\tau_D} \left(\alpha_r \frac{\partial \{N_i\}^T}{\partial r} \frac{\partial \{N_j\}}{\partial r} + \alpha_z \frac{\partial \{N_i\}^T}{\partial z} \frac{\partial \{N_j\}}{\partial z} \right) d\tau_r \right] \{\phi_j\} + \left[\int_{\tau_D} \{N_i\}^T \beta \{N_j\} d\tau_r \right] \{\phi_j\} \\ & + \left[\int_{\tau_D} \alpha_z \{N_i\}^T \{N_j\} d\tau_r \right] \frac{d\{\phi_j\}}{dt} = \left[\int_{\tau_D} \sigma \frac{\{N_i\}^T}{(2\pi r)} d\tau_r \right] (f_U) \quad (2.119) \end{aligned}$$

Equation (2.119) can be developed, resulting on a matrix equation defined by, (Preiss 1983), (Arkkio 1987), (Jianming 2002), (Reece and Preston 2000),

$$\{\mathbf{f}_b^{(I)}\} + \{\mathbf{f}_b^{(II)}\} + ([S] + [S_{II}])\{\phi_j\} + [T] \frac{d}{dt} \{\phi_j\} = \{\mathbf{f}_{gu}\} (f_U) \quad (2.120)$$

The terms $[S]$, $[S_{II}]$, $\{f_b^{(I)}\}$ and $\{f_b^{(II)}\}$ were derived using the Galerkin *weak* formulation. In the case of a Poisson equation, the variables ϕ and f_U are given by,

$$\phi = A_p ; f_U = U_c \quad (2.121)$$

It is possible to define the current as a forcing function, this can be achieved by using the expression defined by (Preiss 1983), (Arkkio 1987),

$$(\Delta_e)^{-1} (f_U) - \int_{\tau} \sigma \frac{\partial \phi}{\partial t} d\tau = f_I \quad (2.122)$$

If the interpolation function defined in (2.34) is replaced in the second term of the left side of (2.122), we obtain (Preiss 1983), (Arkkio 1987),

$$(\Delta_e)^{-1}(\mathbf{f}_U) - \left[\int_{\tau} \boldsymbol{\sigma}\{N_j\} d\tau \right] \frac{d\{\phi_j\}}{dt} = \mathbf{f}_I \quad (2.123)$$

If (2.123) is represented in a matrix way gives (Preiss 1983), (Arkkio 1987),

$$(\Delta_e)^{-1}(\mathbf{f}_U) - \{\mathbf{f}_{ga}\} \frac{d\{\phi_j\}}{dt} = \mathbf{f}_I \quad (2.124)$$

In the case of a Poisson equation and an axisymmetric symmetry, the variables ϕ , f_U and f_I , are substituted by (Preiss 1983), (Arkkio 1987),

$$\phi = A_\rho ; f_U = U_c ; f_I = I_\rho \quad (2.125)$$

Using (2.120) and (2.124), it is possible to formulate a coupled equation that has the conductors' current as the forcing function.

It is very important to mention that it is necessary to formulate a specific finite element on each subdomain, and apply the finite element analysis to derive the respective matrices and vector of that subdomain. The different types of finite element used in this investigation can be consulted in the Section 2.2.3.2. If these finite element are used, it is possible to derive the matrices and vector shown in (2.120) and (2.124). These matrices can be consulted in Appendix A of this thesis.

After having explained the finite element analysis, the main basic fundamentals of the three kind of FEM equations used will be explained in the next section.

2.3 FEM equations features

After having explained all the main features of the FEM equations, it is important to describe in an easier and faster way, the FEM equations that will be solved on this investigation. The FEM field equations (with voltages or currents known) and a FEM circuit coupled equation that could model an electrical machine or device will be solved. It is important to mention that specific details of the FEM field equations were extensively detailed in Section 2.2, but further details of the FEM-circuit coupled equation will be explained in this Section.

2.3.1. Assumptions of the FEM equations

1. Plane or axisymmetric symmetry on behavior of the magnetic field

For the case of the devices with a *planar symmetry assumption*, it is considered that the magnetic field behavior through the z -axis of the conductor is the same. Because of this assumption, the magnetic vector potential is only defined in the z -axis (Ho, Li and Fu 1999). For the case of the device with an *axisymmetric symmetry* assumption, it is considered that

the field behavior is the same along the ρ -axis. This allows assuming that the magnetic vector potentials is defined in the plane formed by the r and z axis (Preiss 1983).

2. Displacement current neglected

The frequency of the voltage sources is low enough, to neglect the displacement current in the Maxwell field equations (Arkkio 1987), (Ho, Li and Fu 1999).

3. Constant permeability and conductivity

The permeability over all the regions and the conductor conductivity are considered to be all constant.

4. Unique voltage applying though the conductor regions

It is assumed that there are no voltage differences at all points of conductor regions. The source current density of the conductors is constant over each cross-sectional surface (Konrad 1982), (Escarela-Perez, Melgoza and Alvarez-Ramirez 2009). After explaining the assumptions, the main features of the FEM equation field equations will explained next.

2.3.2 FEM field equation of a device with voltages known

It is important to correctly model the conductors' skin effects of the electrical machine or device; and it is also necessary to formulate the forcing function of the FEM field equation in terms of the voltages or currents of the conductor, since the electrical machines or devices are supplied by either voltage or current sources (Arkkio 1987). The FEM field equation that corresponds to planar and axisymmetric devices with the conductors' voltage known is given by,

$$[S_x]\{A_x\} + [T_x]\frac{d}{dt}\{A_x\} = \{f_x\}\{U_c\} \quad (2.126)$$

Where A_x represents the magnetic vector potentials. For the case of a device with a planar symmetry assumption, A_x is defined by A_z . On the other hand, for the case of a device with an axisymmetric symmetry assumption, A_x is defined by A_ρ . The matrices $[S_x]$, $[T_x]$ and the vector $\{f_x\}$ that correspond to a planar or an axisymmetric symmetry assumption can be consulted in Appendix A of this thesis.

2.3.3 FEM field equation of a device with currents known

A device with the conductors' currents known can be solved by the FEM field equation and by an expression that relates the voltage, the current and the magnetic vector potential of the conductors. This FEM equation is given by (Konrad 1982), (Preiss 1983), (Escarela-Perez, Melgoza and Alvarez-Ramirez 2009), (Ho, Li and Fu 1999),

$$[\Delta_x]^{-1}\{U_c\} - [M_c]\frac{dA_i}{dt} = \{I\} \quad (2.127)$$

The matrix $[M_c]$ that corresponds to a planar and an axisymmetric symmetry assumption can be consulted in the Appendix B of this thesis. Each element contained in the matrix $[\Delta_x]$, is defined by a planar or the axisymmetric symmetry of (2.128) and (2.129), respectively.

$$\Delta_x = R_c = \frac{l}{\sigma} \left(\iint_{S_c} dS \right)^{-1} \quad (2.128)$$

$$\Delta_x = \Delta_r = \frac{2\pi}{\sigma} \left(\iint_{S_c} \frac{dS}{r} \right)^{-1} \quad (2.129)$$

Where R_c is the conductor resistance. The FEM equations (2.126) and (2.127) can be coupled in a unique equation given by,

$$\begin{bmatrix} [S_x] & -\{f_x\} \\ \mathbf{0} & [\Delta_x]^{-1} \end{bmatrix} \begin{Bmatrix} \{A_x\} \\ \{U_c\} \end{Bmatrix} + \begin{bmatrix} [T_x] & \mathbf{0} \\ -[M_c] & \mathbf{0} \end{bmatrix} \frac{d}{dt} \begin{Bmatrix} \{A_x\} \\ \{U_c\} \end{Bmatrix} = \begin{Bmatrix} \mathbf{0} \\ \{I\} \end{Bmatrix} \quad (2.130)$$

It can be seen that (2.130) permits to calculate the magnetic vector potentials of $\{A_x\}$ and the conductor voltages of $\{U_c\}$. It is important to mention that it is also possible to directly calculate the magnetic vector potentials of $\{A_x\}$ using the *integro-differential* approach (Konrad 1982). The solution of the equations (2.126) and (2.130) can be seen in Appendix B of this thesis.

2.3.4 FEM-circuit coupled of a device

The FEM-circuit coupled equation permits to accurately model an electrical machine or device. A typical example is the magnetic model of an induction machine. The field equation of the machine is defined in two dimensions by a plane symmetry (Ho, Li and Fu 1999), or an axisymmetric symmetry assumption (Preiss 1983). Some effects as the stator end winding and the rotor end rings are taken into account by adding end-winding resistances and inductances. These parameters are included in the form of a voltage-current circuit equation, which can be coupled into the FEM field equation; in order to form a unique FEM-circuit coupled equation (Arkkio 1987), (Ho, Li and Fu 1999), (Ho, Shuangxia and Fu 2011).

As a first step the features of the voltage-current circuit equation that will be coupled to a FEM-circuit coupled equation will be explained.

2.3.4.1 Voltage-current circuit equation

In some cases, it could be proper to couple into the FEM field equations, a voltage-current circuit equation which contains several resistances and inductances that allow a more accurate model of the device (Arkkio 1987), (Ho, Li and Fu 1999), (Ho, Shuangxia and Fu 2011). Equation to be coupled can be defined by,

$$[R]\{I\} + [L] \frac{d\{I\}}{dt} + \{U_c\} = \{V\} \quad (2.131)$$

Where $[R]$ is the matrix resistance, $[L]$ is the inductance resistance and $\{V\}$ is a vector which contains each voltage source applied in the conductors of the device.

2.3.4.2 Deriving the FEM-circuit coupled equation

The FEM-circuit coupled equation results of coupling the equations (2.126) and (2.127), with the voltage-current circuit equation defined in (2.131). It yields (Tsukerman et al. 1993), (Arkkio 1987), (Ho, Li and Fu 1999), (Ho, Shuangxia and Fu 2011),

$$\begin{bmatrix} [S_x] & \mathbf{0} & -\{f_x\} \\ \mathbf{0} & [R] & \{1\} \\ \mathbf{0} & -\{1\} & [A_x]^{-1} \end{bmatrix} \begin{Bmatrix} \{A_x\} \\ \{I\} \\ \{U_c\} \end{Bmatrix} + \begin{bmatrix} [T_x] & \mathbf{0} & \mathbf{0} \\ \mathbf{0} & [L] & \mathbf{0} \\ -[M_c] & \mathbf{0} & \mathbf{0} \end{bmatrix} \frac{d}{dt} \begin{Bmatrix} \{A_x\} \\ \{I\} \\ \{U_c\} \end{Bmatrix} = \begin{Bmatrix} \mathbf{0} \\ \{V\} \\ \mathbf{0} \end{Bmatrix} \quad (2.132)$$

The solution of the FEM-circuit coupled equation in the frequency or in the time domain is explained in the Appendix B. The FEM field and the FEM-circuit coupled equations can be solved in the frequency and the time domain using the methods of solution explained in Appendix B. Nevertheless, the FEM equations may consist on matrices of larger order, may be difficult to obtain, or it may need of a considerable computation time. It is possible to overcome this situation, by using the parallel computing platform. The CUDA parallel computing platform enables to solve these equations in an easy and efficient way. This will be explained next.

2.4 Parallel processing

The Finite Element Method (FEM) is a very powerful tool to solve the electric and magnetic field equations of electrical machines or devices. The method has been widely used, since the computational technological advances have allowed the application of the method on the modeling and simulation of devices with complex geometries of configurations (Arkkio 1987), (Bianchi 2005) (Ho, Shuangxia and Fu 2011). The finite element analysis permits to derive a FEM matrix equation which can be solved in the frequency and in the time domain.

In this investigation, the equations are mainly solved in the frequency domain, since the proposed method can easily derive the voltage and currents of a device in a faster way, and the advantage of the proposed method is evident in a frequency analysis. Nevertheless, it is important to mention that it is possible to calculate the solution in the time domain in a shorter time. The parallel computing platform named CUDA (Compute Unified Device Architecture) (CUDA toolkit 5.0 2014) and several already-implemented library routines that access the graphical processing units (GPUs) (Luebke 2008), (Jalili-Marandi, Zhiyin and Dinavahi 2012) were used in this investigation. A brief explanation of the CUDA and

CUBLAS parallel computing platform is given next.

2.4.1 The CUDA platform

The NVIDIA CUDA (CUDA toolkit 5.0 2014) is a hardware-software platform that can be used to execute parallel algorithms using a program coded in C. The sequential parts of an algorithm can be calculated in the CPU or host, while the parts that are meant to be calculated by a parallel way are executed by using kernels in the GPUs (NVIDIA 2012). When a kernel is executed, blocks with an equal number of threads are created to execute the parallel function; blocks of thread form a grid (Owens, Houston and Luebke 2008).

The CUBLAS (CUDA Basic Linear Algebra Subprograms) library permits to easily calculate vector and matrix operations in the GPU device using the CUDA parallel computer platform (Barrachina et al. 2008), (CUDA toolkit 5.0 2014). These routines permit to easily implement a solution of a FEM equation using parallel computing.

Nevertheless, the parallel programming using CUDA requires a continuous exchange of information, between the CPU and the GPUs (Luebke 2008), (Cisneros-Magaña and Medina 2013). It is required to send information, from the CPU to the GPUs and backwards. Because of this, it can be seen that when the dimensions of the FEM matrix equations to be solved are large, a parallel computing of the algorithm can obtain the solution of the equation in a considerable shorter time, since the GPUs perform parallel computing that represents a significant saving in the total computing time (Luebke 2008), (Cisneros-Magaña and Medina 2013). This situation will be evident, when several study cases will be solved using the CUDA computing platform.

2.4.2 Using the CUDA platform to solve a FEM matrix equation

The FEM equation to be solved could correspond either to a planar or to an axisymmetric symmetry configuration. In order to recognize the kind of FEM equations to be solved, the ordinary FEM equation will be named as *conventional FEM equation*. On the other hand, the uncoupled equation derived from the proposed methodology explained in this investigation is named *reduced FEM equation*. The FEM equation may correspond either to a FEM field equations with voltages or currents known, or to a FEM field coupled equation. The features of these equations were previously defined in Section 2.3.

The solution of the *conventional FEM equation* in the frequency domain using parallel computing process will be explained next.

2.4.2.1. General form of the conventional FEM equation

It is possible to express in a general form, the equations that represent either FEM field equations of a FEM-circuit coupled equation. It yields,

$$[K]\{X\} + [G]\frac{d}{dt}\{X\} = \{F\} \quad (2.133)$$

The values of the matrices, vectors and elements of (2.133) depend on if they belong either to FEM field equations or to a FEM-circuit coupled equation. The equation defined in (2.133)

can also be solved in the frequency domain or in the time domain. The solution of (2.133) in the frequency domain is simple, since implies to calculate a simple expression given by (Bastos 2003),

$$([K] + j(2\pi f)[G])\{\tilde{X}\} = \{\tilde{F}\} \quad (2.134)$$

Where the variable $\{\tilde{X}\}$ and the voltage included in the vector $\{\tilde{F}\}$ defined in (2.134), are harmonic variables defined in a frequency f . Moreover, (2.134) can be represented in a simpler way, i.e.

$$[A_F]\{\tilde{X}_F\} = \{\tilde{b}_F\} \quad (2.135)$$

It can be recognized, two specific steps in the process of calculating (2.135) in the frequency domain, i.e. a *preprocessing* and a *calculating* steps. These stages will be explained next.

2.4.2.2. Preprocessing step of the FEM equation

The *preprocessing* step of the *conventional* FEM method consists on deriving the matrices $[K]$ and $[G]$ and the vector $\{F\}$ of the expression defined in (2.135). The process consists on first calculating the FEM matrices and vectors of one finite element, integrate them into the global matrices and vectors that model the device (Arkkio 1987), (Bianchi 2005), (Reddy 1984), (Reece and Preston 2000). After this, the required boundary conditions that permit to define a unique solution will be applied. This process has been discussed in Section 2.2.2. The *preprocessing* step of the *conventional* FEM equation is shown in Figure 2.6

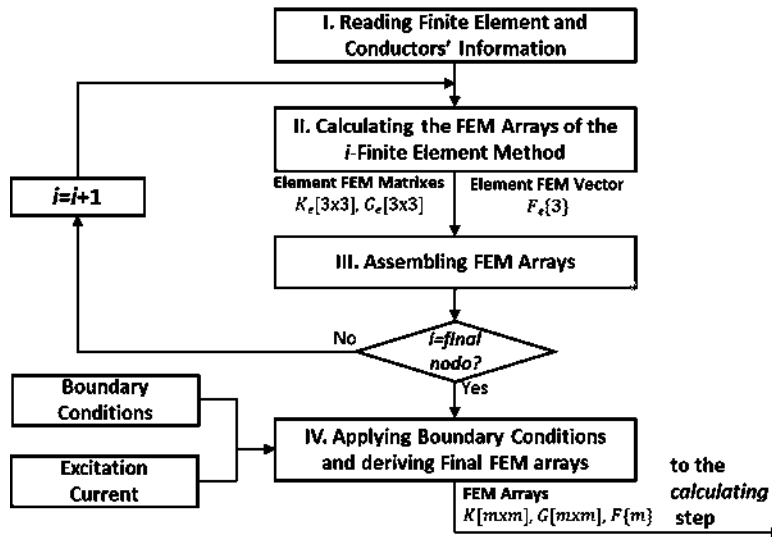


Figure 2.6. Preprocessing steps of the FEM equation

2.4.2.3. Calculating step of the FEM equation

Once the matrices and vector of the *conventional* FEM equation has been derived, it is possible to calculate their solution in the frequency domain. The *conventional* FEM equation has the form of the expression previously defined in (2.135). This matrix equation can be solved by using the *LU* method, thus, the *calculating process* of the equations is performed by the *LU* method. Thus, the first step consists on performing a decomposition of the matrix $[A_f]$ into two matrices $[L_f]$ and $[U_f]$, respectively. It yields,

$$[A_f] = [L_f][U_f] \quad (2.136)$$

Although this decomposition process have been not implemented in the CUBLAS library; if the matrices $[L_f]$ and $[U_f]$ were known, the solution of $[A_f]\{\tilde{x}_f\} = \{\tilde{b}_f\}$ could be easily achieved by a triangular decomposition *LU* using routines already implemented in the CUBLAS library. The decomposition process of the matrix $[A_f]$ will be discussed in the chapter 3. Having the matrices $[L_g]$ and $[U_g]$, the solution $\{\tilde{x}_g\}$ can be obtained by solving the next equations in the CUBLAS computing platform,

$$[L_g]\{\tilde{y}_g\} = \{\tilde{b}_g\} \quad (2.137)$$

$$[U_g]\{\tilde{x}_g\} = \{\tilde{y}_g\} \quad (2.138)$$

Equation (2.137) is solved in CUBLAS, specifying that the equation to be solved corresponds to a triangular matrix stored in lower mode (NVIDIA 2012); while (2.138) is also solved in CUBLAS, but specifying that the equation to be solved corresponds to a triangular matrix stored in upper mode (NVIDIA 2012). It can be seen that the solution of the complex equation $[A_g]\{\tilde{x}_g\} = \{\tilde{b}_g\}$ can be easily derived by implementing the *LU* method by a parallel computing in CUBLAS.

2.5 Conclusions

In this chapter has been covered the main characteristics of the finite element analysis: the main electric and magnetic variables, and the field equations that can be derived by a symmetry assumptions. These field equations permits to derive FEM equations using the finite element analysis. Specifically the Galerkin method and its *weak* formulation can be used to derive these FEM field equations. Specific details of the finite element analysis has been also analyzed on this chapter.

The FEM field equations derived have the voltage or the current of the device as a forcing function. Using these FEM equations, a FEM-circuit coupled equation can be derived. This equation permits to model a device in a more accurate way. In these chapter the FEM field

and the FEM circuit coupled equations have been described. At the same time, it has been discussed the main assumptions that allows their respective formulation.

If the FEM equations are formulated, they can be solved in the frequency and the time domain. The solution on both domains can be achieved by several methods. Most of the time, the solution can be easily obtained. Nevertheless, when the device to be modeled is complex or the number of finite element used is large, it could be necessary to formulate FEM matrices equations of a large order that cannot be easily solved.

In this chapter has been also described the use of the CUDA parallel computing platform. CUDA is an excellent choice, since permits to easily derive and implement the solution of a FEM equation using the parallel processing. Using the CUDA computing platform, the CUBLAS library which contains a collection of several matrices-vector common operations can be easily used. The CUBLAS library allows the solution of an equation using the LU decomposition.

Summarizing, in this chapter the main fundamentals of the FEM equations have been widely explained. It has been included an explanation of how the solution of the equation can be implemented in the parallel computing platform. The FEM equations to be solved, are conventional and can be derived using a standard finite element analysis.

This investigation proposes the use of a methodology that permits to derive an alternative FEM equation. This equation can directly solve the time varying variables of a FEM field and a FEM-circuit coupled equations. It is an equation of lesser order that can be solved in the frequency or the time domain. On the next chapter will be explained the proposed methodology of this investigation.

3 Proposed Methodology

3.1 Introduction

The Finite Element Method can solve the steady state and the transient field equations of electrical machines or devices (Ho, Li and Fu 1999), (Wang and Xie 2009), (Lubin, Mezani and Rezzoug 2011), (Li, Ho and Fu 2012), (Bianchi 2005), . In order to reduce the complexity of the finite element analysis, sometimes it is possible to perform a symmetry simplification, i.e. a planar or an axisymmetric symmetry (Arkkio 1987), (Bianchi 2005), (Bastos 2003). Along this symmetry assumption, it is important to correctly model the conductors' skin effect of the conductors of the device. Thus, it is necessary to formulate the forcing function of the FEM equations in terms of the voltages or currents of the conductors, since the electrical machines or devices are supplied by both kind of sources. These FEM field equations can be solved if the voltages or the currents in the conductors are known (Arkkio 1987), (Ho, Li and Fu 1999),(Bastos 2003).

Nevertheless, the conductors' currents or voltages are not always known. In some cases, it is necessary to add some parameters such as resistances or inductances, which are connected to the conductors to get a more precise model of the electrical machine or device, (Arkkio 1987), (Ho, Li and Fu 1999), (Fu and Ho 2009), (Ho, Shuangxia and Fu 2011). The electrical parameters mentioned before, can be taken into account by one or several voltage-current equations, thus the current-voltage and the FEM field equations can be coupled into a FEM-circuit coupled equation (Arkkio 1987), (Tsukerman et al. 1993), (Ho, Li and Fu 1999), (Ho, Li and Fu 1999), (Fu and Ho 2009), (Ho, Shuangxia and Fu 2011). Thus, a FEM-circuit coupled equation can accurately model an electrical machine or device.

In this investigation, FEM-field with currents or voltages known and a FEM-circuit coupled equations, in the frequency and the time domain will be solved. They will be solved using a methodology that allows deriving a reduced equation of lesser order; moreover, the time varying variables can be directly solved. The equation derived can be solved either in the frequency and the time domain.

In order to get a quick understanding of the FEM equations, the main features of them will be explained next. It is important to mention that further details of these FEM equations can be consulted in the Chapter 2 of this thesis.

3.1.1 Field equations

If a plane symmetry is considered, the magnetic vector potential is constant along the z -axis and varies in the x - y plane, then the magnetic vector potential is defined in two-dimensions (Bianchi 2005), (Arkkio 1987), (Ho, Li and Fu 1999). It is also assumed that the source electrical field along the z -axis of the conductors is also constant (Arkkio 1987), (Ho,

Li and Fu 1999). This assumption assumes that only exist one current associated to each voltage applied in a particular region of the device.

For the case of axisymmetric symmetry, this assumption permits to define a two-dimension magnetic field which is constant though the r -coordinate (Konrad 1982), (Preiss 1983), This consideration allows the magnetic vector potentials are to be dependent of the plane formed by the r and z axis. It is also assumed that the electrical field along a certain value of the r -axis is also constant (Konrad 1982), (Konrad, Chari and Csendes 1982), (Preiss 1983). This assumption also allows only one current and voltage associated to a particular region of the device.

Taking into account the symmetry assumptions, it is possible to derive two types of field equations,

- 1) Field equation with *voltage* as the forcing function
- 2) Field equation with *current* as the forcing function.

It is possible to derive a FEM field equation by applying the finite element analysis in these field equations. The FEM equations will be described next, while the features of the FEM-circuit coupled equation will be outlined in the Section 3.1.3. It is important to remark that boundaries conditions are necessary to be applied to the field equations; in order to properly define the model, and to have a unique solution for the finite element analysis. The considered boundaries are the Dirichlet and the Neumann boundary conditions. They were previously defined in Section 2.2.2.1.

3.1.2 FEM field equations

It is possible to perform a finite element analysis (Wang and Xie 2009), (Lubin, Mezani and Rezzoug 2011), (Preiss 1983) on the field equation defined in (2.10) and (2.20). The assumptions considered for these field equation can be seen in Section 2.3.1. At the same time, a Newton Cotes analysis (Konrad 1982), (Konrad 1981), (Reece and Preston 2000) can be performed on (2.11) and (2.21). Thus, it is possible to derive the FEM equations covered by this investigation. The FEM field equations will be outlined next.

3.1.2.1 FEM field equation with voltages known

If a finite element analysis is applied in field equation with voltages known results on,

$$[\mathbf{S}_x]\{\mathbf{A}_x\} + [\mathbf{G}_x] \frac{d}{dt} \{\mathbf{A}_x\} = \{\mathbf{f}_x\}\{\mathbf{U}_c\} \quad (3.1)$$

Where vectors $\{\mathbf{U}_c\}$ contain each voltage and to the conductors; it is defined by,

$$\{\mathbf{U}_c\} = \{\mathbf{U}_c^1 \quad \mathbf{U}_c^2 \quad \mathbf{U}_c^3.. \quad \mathbf{U}_c^{m-1} \quad \mathbf{U}_c^m\} \quad (3.2)$$

The matrices $[S_x]$, $[T_x]$ and the vector $\{f_x\}$ for a planar and an planar and an axisymmetric symmetry assumption were previously defined in Section 2.2.2.

3.1.2.2 FEM field equation with currents known

For the case where the conductors' currents are known, the FEM field equation is defined by, (Arkkio 1987), (Konrad 1981),

$$\begin{bmatrix} [S_x] & -\{f_x\} \\ \mathbf{0} & [\Delta_x]^{-1} \end{bmatrix} \begin{Bmatrix} \{A_x\} \\ \{U_c\} \end{Bmatrix} + \begin{bmatrix} [T_x] & \mathbf{0} \\ -[M_c] & \mathbf{0} \end{bmatrix} \frac{d}{dt} \begin{Bmatrix} \{A_x\} \\ \{U_c\} \end{Bmatrix} = \begin{Bmatrix} \mathbf{0} \\ \{I\} \end{Bmatrix} \quad (3.3)$$

Where vector $\{I\}$ contain each current applied to the conductors; it is defined by,

$$\{I\} = \{I_1 \quad I_2 \quad I_3 \dots I_{m-1} \quad I_m\} \quad (3.4)$$

The matrices $[\Delta_x]$, and $[M_c]$ for the planar and the axisymmetric symmetry were previously defined in (2.127). After having defined the FEM field equations (3.1) and (3.3), the features of a FEM-circuit coupled equation will be explained next.

3.1.3. FEM-circuit coupled equation

The FEM-circuit coupled equation permits to accurately model an electrical machine or device. Some effects as the stator end winding and the rotor end rings are taken into account by adding end-winding resistances and inductances. These parameters are included in the form of a voltage-current circuit equation, which can be coupled into the FEM field equation in order to form a unique FEM-circuit coupled equation (Arkkio 1987), (Tsukerman et al. 1993), (Ho, Li and Fu 1999), (Dlala and Arkkio 2010). Further details about this equation can be consulted in the Chapter 2. The FEM-circuit coupled equation is defined by,

$$\begin{bmatrix} [S_x] & \mathbf{0} & -\{f_x\} \\ \mathbf{0} & [R] & \{1\} \\ \mathbf{0} & -\{1\} & [\Delta_x]^{-1} \end{bmatrix} \begin{Bmatrix} \{A_x\} \\ \{I\} \\ \{U_c\} \end{Bmatrix} + \begin{bmatrix} [T_x] & \mathbf{0} & \mathbf{0} \\ \mathbf{0} & [L] & \mathbf{0} \\ -[M_c] & \mathbf{0} & \mathbf{0} \end{bmatrix} \frac{d}{dt} \begin{Bmatrix} \{A_x\} \\ \{I\} \\ \{U_c\} \end{Bmatrix} = \begin{Bmatrix} \mathbf{0} \\ \{V\} \\ \mathbf{0} \end{Bmatrix} \quad (3.5)$$

Until now, several FEM equations derived by the finite element analysis have been described. These equations can be solved in the frequency and the time domain, and they represent the solution of a field equation of an electrical machine or device.

In this investigation, these FEM equations can be solved with alternative method of solution in the frequency and the time domain. Specifically, a methodology that permits to derive an equation of a lesser order, to directly solve the time varying variables of the equations is proposed. Thus, it is possible to obtain a faster solution in the frequency and the

time domain. The details of the proposed methodology of this investigation will be explained next.

3.2 Proposed methodology

The methodology starts by identifying the *non-conductor* and the *conductor* region of the device. If the conductor voltage is chosen as the forcing function, it is possible to derive a field equation of the *non-conductor* and the *conductor* regions; and using the finite element analysis, it is possible to formulate a single FEM field equation (Arkkio 1987), (Ho, Li and Fu 1999), (Preiss 1983).

The FEM field equation will be modified by the proposed methodology. The main modification consists on using the difference of the *conductor* and the *non-conductor* regions, by identifying and associating the magnetic vector potentials of each region. This change permits to derive a completely new equation, in which the magnetic vector potentials of the *conductor* region are separated from those that correspond to the *non-conductor* region.

The next step of the methodology consists on using the FEM equation, derived through several and simple matrix operations. These steps permit to derive a reduced equation which has the following important features:

1) It can directly calculate the time varying variables, i.e. the magnetic vector potentials in the conductor regions and the conductor currents.

2) It is easy to calculate; it only requires of a nodal reordering of the equations and can be derived performing some simple matrix operations.

The methodology can also be applied to obtain reduced equations, from a FEM field equation with currents known, or from a FEM-circuit coupled equation. It is very important to mention that the equation derived by the methodology shares the same assumptions of these FEM equations. Further details about the assumption considered can be consulted in Chapter 2.

Although a brief summary of the methodology has been discussed, the main details will be covered next. The solution of the FEM equations in the frequency and the time domain can be consulted in the Appendix B.

3.2.1 Methodology applied on a FEM field equation with voltages known

3.2.1.1 Renumbering the nodes of the FEM field Equations

After taking into account the *conductor* and the *non-conductor* regions, the first step consists on renumbering the *conductor* and *non-conductor* region magnetic vector potentials of the FEM field equation previously defined in (3.1) in order to make them consecutive. It gives,

$$A_i = \{A_1 \quad A_2 \dots A_l\}^T \quad (3.6)$$

$$A_j = \{A_{l+1} \quad A_{l+2} \dots A_k\}^T \quad (3.7)$$

Where A_i and A_j are the vectors which contain the magnetic vector potentials of the *conductor* and the *non-conductor* regions, respectively; l and $k-l$ are the number of nodes of the *conductor* and *non-conductor* region, respectively; and k is the total number of nodes.

3.2.1.2. Deriving a new FEM field equation based on the nodal renumbering

If the FEM field equation defined in (3.1) is reformulated using the criterion of nodes renumbering used in the vectors shown in (3.6) and (3.7); it can be expressed by,

$$\begin{bmatrix} S_{ii} & S_{ij} \\ S_{ij}^T & S_{jj} \end{bmatrix} \begin{Bmatrix} A_i \\ A_j \end{Bmatrix} + \begin{bmatrix} T_{ii} & \mathbf{0} \\ \mathbf{0} & \mathbf{0} \end{bmatrix} \frac{d}{dt} \begin{Bmatrix} A_i \\ A_j \end{Bmatrix} = \begin{Bmatrix} \{f_i\} \\ \{U_c\} \end{Bmatrix} \quad (3.8)$$

Where the matrices S_{ii} , T_{ii} and the vector $\{f_i\}$ are associated with the vector A_i ; S_{jj} is related with A_j ; S_{ij} and S_{ji} are associated with common regions of the *conductor* and the *non-conductor* regions, respectively. Notice that in (3.8), the magnetic vector potentials of the *conductor* region have been associated and separated from the magnetic vector potentials of the *non-conductor* region.

3.2.1.3. Identifying submatrices and formulating matrix equations

The equation defined in (3.8) can be represented in a partitioned way by,

$$\begin{bmatrix} K_{11} & K_{12} \\ K_{21} & K_{22} \end{bmatrix} \begin{Bmatrix} x_1 \\ x_2 \end{Bmatrix} + \begin{bmatrix} G_{11} & \mathbf{0} \\ G_{21} & \mathbf{0} \end{bmatrix} \frac{d}{dt} \begin{Bmatrix} x_1 \\ x_2 \end{Bmatrix} = \begin{Bmatrix} f_1 \\ f_2 \end{Bmatrix} \quad (3.9)$$

Where the submatrices of (3.9) are defined by,

$$K_{11} = S_{ii} \quad (3.10)$$

$$K_{12} = S_{ij} \quad (3.11)$$

$$K_{21} = S_{ij}^T \quad (3.12)$$

$$K_{22} = S_{jj} \quad (3.13)$$

$$\mathbf{G}_{11} = \mathbf{T}_{ii} \quad (3.14a)$$

$$\mathbf{G}_{21} = \mathbf{0} \quad (3.14b)$$

Where the subvectors of (3.9) are defined by,

$$\mathbf{x}_1 = \mathbf{A}_i \quad (3.15)$$

$$\mathbf{x}_2 = \mathbf{A}_j \quad (3.16)$$

$$\mathbf{f}_1 = \{\mathbf{f}_i\}\{\mathbf{U}_c\} \quad (3.17a)$$

$$\mathbf{f}_2 = \mathbf{0} \quad (3.17b)$$

3.2.1.4. Deriving two matrix equations

It can be noticed that it is possible to generate two matrix equations from (3.9), i.e.

$$\mathbf{K}_{11}\mathbf{x}_1 + \mathbf{K}_{12}\mathbf{x}_2 + \mathbf{G}_{11}\frac{d}{dt}\mathbf{x}_1 = \mathbf{f}_1 \quad (3.18)$$

$$\mathbf{K}_{21}\mathbf{x}_1 + \mathbf{K}_{22}\mathbf{x}_2 + \mathbf{G}_{21}\frac{d}{dt}\mathbf{x}_1 = \mathbf{f}_2 \quad (3.19)$$

3.2.1.5. Calculating the reduced equation

After having obtained the two matrix equations (3.18) and (3.19) from the FEM field equation (3.9); it is possible to solve (3.19) in terms of \mathbf{x}_2 , and the result of such algebraic operation can be substituted into (3.18). Thus, a single equation can be derived. It gives,

$$\mathbf{K}_t\mathbf{x}_1 + \mathbf{G}_t\frac{d}{dt}\mathbf{x}_1 = \mathbf{f}_t \quad (3.20)$$

The matrices \mathbf{K}_t and \mathbf{G}_t and the vector \mathbf{f}_t are given by,

$$\mathbf{K}_t = \mathbf{K}_{11} - \mathbf{K}_{12}\mathbf{K}_{22}^{-1}\mathbf{K}_{21} \quad (3.21)$$

$$\mathbf{G}_t = \mathbf{G}_{11} - \mathbf{K}_{12}\mathbf{K}_{22}^{-1}\mathbf{G}_{21} \quad (3.22)$$

$$\mathbf{f}_t = \mathbf{f}_1 - \mathbf{K}_{12}\mathbf{K}_{22}^{-1}\mathbf{f}_2 \quad (3.23)$$

Once the vector A_i has been calculated, the vector A_j can be derived using,

$$\mathbf{S}_{ij}^T \mathbf{A}_i + \mathbf{S}_{jj} \mathbf{A}_j = \mathbf{0} \quad (3.24)$$

Please notice that (3.24) can be obtained from (3.8), which in turn was obtained from the renumbering of the magnetic vector potentials in the *conductor* and the *non-conductor* regions. Thus, the magnetic vector potentials of the *non-conductor* region can be derived using the potentials of the conductor regions as Dirichlet boundary conditions. After knowing the magnetic vector potentials defined in (3.8), the conductors' currents can be calculated using Equation (2.127).

3.2.2 Methodology applied on a FEM field equation with currents known

The proposed methodology also permits to derive a reduced equation from a FEM field equation with the currents known, using the same re-numbering criteria used on (3.6) and (3.7) for the magnetic vector potentials nodes of the *conductor* and the *non-conductor* region, respectively. The next steps will be explained next.

3.2.2.1. Deriving a new FEM field equation based on the nodal renumbering

The numbering criteria used on (3.6) and (3.7) permits to reformulate the equation that relates the magnetic vector potentials with the conductors voltages and currents. Thus, this equation can be only defined in terms of the magnetic vector potentials of the *conductor* region (A_i). It yields,

$$[\mathbf{A}_x]^{-1}\{\mathbf{U}_c\} - [\mathbf{M}_i] \frac{dA_i}{dt} = \{\mathbf{I}\} \quad (3.25)$$

3.2.2.2. Performing an arrangement of the time varying variables

It is possible to take the FEM equations (3.8) and (3.25) and combine them in order to form a coupled equation. At the same time, it is possible to perform a rearrangement of this new expression by grouping the time varying variables. For the case of the FEM field equation with currents known, their time varying variables are the magnetic vector potentials of the *conductor* region. It yields,

$$\begin{bmatrix} S_{ii} & -\{f_i\} & S_{ij} \\ \mathbf{0} & [\Delta_x]^{-1} & \mathbf{0} \\ S_{ij}^T & \mathbf{0} & S_{jj} \end{bmatrix} \begin{Bmatrix} A_i \\ \{U_c\} \\ A_j \end{Bmatrix} + \begin{bmatrix} T_{ii} & \mathbf{0} & \mathbf{0} \\ -[M_i] & \mathbf{0} & \mathbf{0} \\ \mathbf{0} & \mathbf{0} & \mathbf{0} \end{bmatrix} \frac{d}{dt} \begin{Bmatrix} A_i \\ \{U_c\} \\ A_j \end{Bmatrix} = \begin{Bmatrix} \mathbf{0} \\ \{I\} \\ \mathbf{0} \end{Bmatrix} \quad (3.26)$$

Please observe that (3.26) has been arranged to separate the time varying variables (A_i) from those variables which do not have time derivative terms (A_j and $\{U_c\}$). The next step consists on performing a partition matrix on (3.26).

3.2.2.3. Identifying submatrices and formulating matrix equations

The equation defined in (3.26) can be also represented in a partitioned way as,

$$\begin{bmatrix} K_{11} & K_{12} \\ K_{21} & K_{22} \end{bmatrix} \begin{Bmatrix} x_1 \\ x_2 \end{Bmatrix} + \begin{bmatrix} G_{11} & \mathbf{0} \\ G_{21} & \mathbf{0} \end{bmatrix} \frac{d}{dt} \begin{Bmatrix} x_1 \\ x_2 \end{Bmatrix} = \begin{Bmatrix} \mathbf{0} \\ f_2 \end{Bmatrix} \quad (3.27)$$

The matrices K_{11} and G_{11} have been defined in (3.10) and (3.14a), respectively. The matrices of (3.27) are defined by,

$$K_{12} = [-\{f_i\} \quad S_{ij}] \quad (3.28)$$

$$K_{21} = \begin{bmatrix} \mathbf{0} \\ S_{ij}^T \end{bmatrix} \quad (3.29)$$

$$K_{22} = \begin{bmatrix} [\Delta_x]^{-1} & \mathbf{0} \\ \mathbf{0} & S_{jj} \end{bmatrix} \quad (3.30)$$

$$G_{21} = \begin{bmatrix} -[M_i] \\ \mathbf{0} \end{bmatrix} \quad (3.31)$$

Where the subvectors of (3.27) are defined by,

$$x_1 = A_i \quad (3.32)$$

$$x_2 = \begin{bmatrix} \{U_c\} \\ A_j \end{bmatrix} \quad (3.33)$$

$$f_2 = \begin{bmatrix} \{I\} \\ \mathbf{0} \end{bmatrix} \quad (3.34)$$

Notice that the time varying variables of (3.26) have been associated and separated from those variables which do not have time derivative terms.

3.2.2.4. Deriving matrix equations

Two matrix equations can be obtained from (3.27). The equations were previously defined in (3.18) and (3.19).

3.2.2.5. Calculating the final reduced equation

It is also possible to derive a reduced equation of the expression shown in (3.27), using the two matrix equations (3.18) and (3.19). The reduced equation derived can be calculated using (3.20). The matrices K_t and G_t and the vector f_t can be calculated using,

$$K_t = K_{11} - K_{12}K_{22}^{-1}K_{21} \quad (3.35)$$

$$G_t = G_{11} \quad (3.36)$$

$$f_t = -K_{12}K_{22}^{-1}f_2 \quad (3.37)$$

Once the vector A_i is obtained, the vector A_j can be derived using (3.24), while the conductor voltages $\{U_c\}$ can be calculated using (3.25). The proposed method can be easily applied to calculate an equation of lesser dimension from a FEM field equation which has the voltage or current as the forcing function. Moreover, it can be applied to derive a similar expression from a FEM-circuit coupled equation. This will be discussed next.

3.2.3 Methodology applied on a FEM-circuit coupled equation

The proposed method also permits to derive a reduced expression from a FEM-circuit coupled equation. The process is the same to that applied in the FEM field equations mentioned earlier. The process will be explained next.

3.2.3.1. Performing an arrangement of the time varying variables

After performing a nodal renumbering in the magnetic vector potentials of the *conductor* and the *non-conductor* regions; it is also possible to derive a new equation. It is also possible to perform a rearrangement of the time varying variables, i.e. the magnetic vector potentials of the *conductor* region and the conductors' current. It yields,

$$\begin{bmatrix} S_{ii} & \mathbf{0} & -\{f_i\} & S_{ij} \\ \mathbf{0} & [R] & \{1\} & \mathbf{0} \\ \mathbf{0} & [\Delta_x]^{-1} & -\{1\} & \mathbf{0} \\ S_{ij}^T & \mathbf{0} & \mathbf{0} & S_{jj} \end{bmatrix} \begin{Bmatrix} A_i \\ \{I\} \\ \{U_c\} \\ A_j \end{Bmatrix} + \begin{bmatrix} T_{ii} & \mathbf{0} & \mathbf{0} & \mathbf{0} \\ \mathbf{0} & [L] & \mathbf{0} & \mathbf{0} \\ -[M_i] & \mathbf{0} & \mathbf{0} & \mathbf{0} \\ \mathbf{0} & \mathbf{0} & \mathbf{0} & \mathbf{0} \end{bmatrix} \frac{d}{dt} \begin{Bmatrix} A_i \\ \{I\} \\ \{U_c\} \\ A_j \end{Bmatrix} = \begin{Bmatrix} \mathbf{0} \\ \{V\} \\ \mathbf{0} \\ \mathbf{0} \end{Bmatrix} \quad (3.38)$$

Notice that (3.38) has been arranged to separate the time varying variables (A_i and $\{I\}$), from those variables which do not have time derivative terms (A_j and $\{U_c\}$). It is possible to perform a matrix partition in (3.38). This will be discussed next.

3.2.3.2. Identifying submatrices and formulating matrix equations

The equation defined in (3.38) can also be represented in a partitioned way as,

$$\begin{bmatrix} K_{11} & K_{12} \\ K_{21} & K_{22} \end{bmatrix} \begin{Bmatrix} x_1 \\ x_2 \end{Bmatrix} + \begin{bmatrix} G_{11} & \mathbf{0} \\ G_{21} & \mathbf{0} \end{bmatrix} \frac{d}{dt} \begin{Bmatrix} x_1 \\ x_2 \end{Bmatrix} = \begin{Bmatrix} f_1 \\ \mathbf{0} \end{Bmatrix} \quad (3.39)$$

Where the submatrices of (3.39) are defined by,

$$K_{11} = \begin{bmatrix} S_{ii} & \mathbf{0} \\ \mathbf{0} & [R] \end{bmatrix} \quad (3.40)$$

$$K_{12} = \begin{bmatrix} -\{f_i\} & S_{ij} \\ \{1\} & \mathbf{0} \end{bmatrix} \quad (3.41)$$

$$K_{21} = \begin{bmatrix} \mathbf{0} & [\Delta_x]^{-1} \\ S_{ij}^T & \mathbf{0} \end{bmatrix} \quad (3.42)$$

$$K_{22} = \begin{bmatrix} -\{1\} & \mathbf{0} \\ \mathbf{0} & S_{jj} \end{bmatrix} \quad (3.43)$$

$$G_{21} = \begin{bmatrix} T_{ii} & \mathbf{0} \\ \mathbf{0} & [L] \end{bmatrix} \quad (3.44)$$

$$G_{22} = \begin{bmatrix} -[M_c] & \mathbf{0} \\ \mathbf{0} & \mathbf{0} \end{bmatrix} \quad (3.45)$$

Where the subvectors of (3.39) are defined by,

$$x_1 = \begin{bmatrix} A_i \\ \{I\} \end{bmatrix} \quad (3.46)$$

$$x_2 = \begin{bmatrix} \{U_c\} \\ A_j \end{bmatrix} \quad (3.47)$$

$$f_1 = \begin{bmatrix} \mathbf{0} \\ \{V\} \end{bmatrix} \quad (3.48)$$

The time varying variables of (3.38) have been also associated and separated from those variables which do not have time derivative terms.

3.2.3.3. Calculating the matrix equations

It is possible to generate two matrix equations from (3.39). The equations were previously defined in (3.18) and (3.19).

3.2.3.4. Calculating the reduced equation

An uncoupled equation from the FEM-circuit coupled equation (3.38) can be obtained using (3.20). The matrices K_t and G_t and the vector f_t can be calculated using,

$$K_t = K_{11} - K_{12}K_{22}^{-1}K_{21} \quad (3.49)$$

$$G_t = G_{11} - K_{12}K_{22}^{-1}G_{21} \quad (3.50)$$

$$f_t = f_1 \quad (3.51)$$

Once the vector A_i is obtained, the vector A_j can be calculated from (3.24). The conductor voltages $\{U_c\}$ can be obtained using (3.25).

3.3 Solution of the equation derived by the methodology

The equation derived from the methodology can be expressed in a general form. All the reduced equations derived from the FEM equation have the form,

$$\begin{bmatrix} K_{11} & K_{12} \\ K_{21} & K_{22} \end{bmatrix} \begin{Bmatrix} x_1 \\ x_2 \end{Bmatrix} + \begin{bmatrix} G_{11} & \mathbf{0} \\ G_{21} & \mathbf{0} \end{bmatrix} \frac{d}{dt} \begin{Bmatrix} x_1 \\ x_2 \end{Bmatrix} = \begin{Bmatrix} f_1 \\ f_2 \end{Bmatrix} \quad (3.52)$$

The submatrices K_{11} , K_{12} , K_{21} , K_{22} , G_{11} , G_{21} , along the subvectors f_1 and f_2 depend on if the equation obtained by the methodology has been derived, either from a FEM field equation or from a FEM-circuit coupled equation. The expression defined in (3.52) can be written in a simplified form as,

$$[K_T]\{X_T\} + [G_T] \frac{d}{dt}\{X_T\} = \{F_T\} \quad (3.53)$$

Where the matrices $[K_T]$, $[G_T]$ and the vector $\{F_T\}$ can be calculated using,

$$[K_T] = K_{11} - K_{12}K_{22}^{-1}K_{21} \quad (3.54)$$

$$[G_T] = G_{11} - K_{12}K_{22}^{-1}G_{21} \quad (3.55)$$

$$\{F_T\} = f_1 - K_{12}K_{22}^{-1}f_2 \quad (3.56)$$

The equation defined in (3.53) can be solved in the frequency domain or in the time domain. The solution in the frequency domain is simple, since implies to calculate a simple matrix equation (Shen et al. 1985). For the specific case of a time domain solution, the most widely used method is the Backwards Euler method (Ho, Li and Fu 1999), (Arkkio 1987), (Kwon and Bang 1997), (Jianming 2002). The solution in both domains is discussed next.

3.3.1 Time domain solution

It is possible to calculate the periodic behavior of an electrical network or a FEM equation in the time domain by integrating the differential equation set that describes the dynamics of the system (Semlyen and Medina 1995). For the specific case of the expression shown in (3.53), the solution in the time domain can be obtained as,

$$\frac{d\{X_T\}}{dt} = [G_T]^{-1}(\{F_T\} - [K_T]\{X_T\}) \quad (3.57)$$

The numerical method for the solution of (3.57) in the time domain can be classified into explicit and implicit methods. They will be outlined next.

3.3.1.1 Explicit methods

In these methods, the solution depends on the solution of an earlier time step. There are several explicit methods but the most widely used are concisely described next.

3.3.1.1.1 Euler method (forward difference) (Jianming 2002)

The Euler method consists on dividing the time axis uniformly into a number of time intervals. A function $X_T(t+\Delta t)$ can be expanded into a Taylor series about t . Using this series expansion and neglecting some terms, it is possible to express the derivate respect the time as,

$$\frac{d\{X_T\}}{dt} \approx \frac{\{X_T\}_{(t+\Delta t)} - \{X_T\}_{(t)}}{\Delta t} \quad (3.58)$$

Further details about how (3.58) was calculated, can be consulted in Appendix B. Taking into account (3.58), the solution of (3.53) in the time domain with the Euler method is defined by,

$$\{X_T\}_{(t+\Delta t)} = (\Delta t)[G_T]^{-1}(\{F_T\}_{(t)} - [K_T]\{X_T\}_{(t)}) + \{X_T\}_{(t)} \quad (3.59)$$

The Euler method enables to obtain a solution of the equation derived from the proposed methodology. Nevertheless, the equation (3.59) cannot be solved in an accurate way because of this: the matrix inversion of $[G_T]$ cannot be achieved since this matrix has a bad conditioned number. The equation derived by the methodology is an equivalent equation and therefore cannot be accurately solved neither. The equation can be solved using an almost identical expression defined by,

$$\{\bar{X}_T\}_{(t+\Delta t)} = (\Delta t)[\bar{G}_T]^{-1}(\{F_T\}_{(t)} - [K_T]\{\bar{X}_T\}_{(t)}) + \{\bar{X}_T\}_{(t)} \quad (3.60)$$

Where the matrix $[\bar{G}_T]$ is calculated using,

$$[\bar{G}_T] = G_{11} - K_{12}K_{22}^{-1}\bar{G}_{21} \quad (3.61a)$$

$$\bar{G}_{21} \leq G_{21} \quad (3.61b)$$

In (3.61a) and (3.61b), the elements of \bar{G}_{21} are of lesser value than the elements of G_{21} . The approximate solution of (3.60) is defined by the vector $\{\bar{X}_T\}$.

3.3.1.1.2 Backwards Euler method (backward difference) (Jianming 2002)

The Backwards Euler method is an alternative to the Euler method. It consists on uniformly dividing the time axis into a number of time intervals. A function $X_T(t-\Delta t)$ can be expanded into a Taylor series about t , but for this case, a different expansion that the used for the Euler method will be used. The derivate respect the time is defined by,

$$\frac{dX_T}{dt} \approx \frac{X_{T(t)} - X_{T(t-\Delta t)}}{\Delta t} \quad (3.62)$$

Further details about how (3.62) was calculated can be consulted in Appendix B. Taking into account (3.62), the solution of (3.53) in the time domain is defined by,

$$\{X_T\}_{(t)} = \left([K_T] + \frac{[G_T]}{\Delta t} \right)^{-1} \left(\{F_T\}_{(t-\Delta t)} + \frac{[G_T]}{\Delta t} \{X_T\}_{(t-\Delta t)} \right) \quad (3.63)$$

The Backwards Euler method enables to obtain an accurate solution of the equation derived from the methodology. Specifically, it permits to accurately obtain the time varying variables of a FEM field or from a FEM-circuit coupled equation. This is possible to achieve, since the equation derived by the method is an equivalent expression of an equation that can be accurately solved using the Backwards Euler method.

3.3.1.1.3 Runge Kutta method (Jianming 2002)

Further details about the calculating process of this method can be consulted in Appendix B. The solution in the time domain of (3.53) using this method is given by,

$$\{X_T\}_{t+\Delta t} = \{X_T\}_t + \frac{1}{6} (\{k_{1,T}\} + 2\{k_{2,T}\} + 2\{k_{3,T}\} + \{k_{4,T}\}) \quad (3.64)$$

Where the values of $\{k_{1,T}\}$, $\{k_{2,T}\}$, $\{k_{3,T}\}$ and $\{k_{4,T}\}$ are defined by,

$$\{k_{1,T}\} = (\Delta t)[G]^{-1}(\{F_T\}_{(t)} - [K]\{X_T\}_{(t)}) \quad (3.65)$$

$$\{k_{2,T}\} = \left(t_n + \frac{\Delta t}{2} \right) [G]^{-1} \left(\{F_T\}_{(t)} - [K]\{X_T\}_{(t)} - \frac{1}{2}[K]\{k_{1,T}\} \right) \quad (3.66)$$

$$\{k_{3,T}\} = \left(t_n + \frac{\Delta t}{2} \right) [G]^{-1} \left(\{F_T\}_{(t)} - [K]\{X_T\}_{(t)} - \frac{1}{2}[K]\{k_{2,T}\} \right) \quad (3.67)$$

$$\{k_{4,T}\} = (t_n + \Delta t)[G]^{-1}(\{F_T\}_{(t)} - [K]\{X_T\}_{(t)} - [K]\{k_{3,T}\}) \quad (3.68)$$

Appendix B gives additional details about how (3.64) was calculated. After obtaining $\{X_T\}_{t+\Delta t}$, the rest of calculating process implies that the value of $\{X_T\}_{t+\Delta t}$ will be become the value $\{X_T\}_t$, necessary to derivate the value for the next step. The solution of the equation derived by the proposed methodology in the time domain using this method is not exact. Nevertheless, an approximate solution can be achieved using,

$$\{\bar{X}_T\}_{t+\Delta t} = \{\bar{X}_T\}_{(t)} + \frac{1}{6}(\{\bar{k}_{1,T}\} + 2\{\bar{k}_{2,T}\} + 2\{\bar{k}_{3,T}\} + \{\bar{k}_{4,T}\}) \quad (3.69)$$

Where the values of $\{\bar{k}_{1,T}\}$, $\{\bar{k}_{2,T}\}$, $\{\bar{k}_{3,T}\}$ and $\{\bar{k}_{4,T}\}$ are defined by,

$$\{\bar{k}_{1,T}\} = (\Delta t)[\bar{G}_T]^{-1}(\{F_T\}_{(t)} - [K_T]\{\bar{X}_T\}_{(t)}) \quad (3.70)$$

$$\{\bar{k}_{2,T}\} = \left(t_n + \frac{\Delta t}{2}\right)[\bar{G}_T]^{-1}\left(\{F_T\}_{(t)} - [K_T]\{\bar{X}_T\}_{(t)} - \frac{1}{2}[K_T]\{\bar{k}_{1,T}\}\right) \quad (3.71)$$

$$\{\bar{k}_{3,T}\} = \left(t_n + \frac{\Delta t}{2}\right)[\bar{G}_T]^{-1}\left(\{F_T\}_{(t)} - [K_T]\{\bar{X}_T\}_{(t)} - \frac{1}{2}[K_T]\{\bar{k}_{2,T}\}\right) \quad (3.72)$$

$$\{\bar{k}_{4,T}\} = (t_n + \Delta t)[\bar{G}_T]^{-1}(\{F_T\}_{(t)} - [K_T]\{\bar{X}_T\}_{(t)} - [K_T]\{\bar{k}_{3,T}\}) \quad (3.73)$$

The Runge Kutta method can be only used in an approximate way because of this: the matrix inversion of $[G_T]$ cannot be achieved due to the null elements along its main diagonal. The matrix can be calculated using the expressions defined in (3.61a) and (3.61b).

3.3.1.2 Implicit method: Newton method (Semlyen and Medina 1995)

The traditional method to determine the steady state of the equation (3.53); can be determined by integrating over a period of time, the differential equations that represent the dynamics of the system; by using the initial conditions. Equation (3.53) can be solved using the *brute force* method (Semlyen and Medina 1995).

The *brute force* method consists on first assuming initial conditions. After that, equation (3.53) is integrated along a time period. The results obtained at the end of such period are compared to the assumed initial conditions, in order to verify the maximum error or difference among them. If there is a significant difference, it is performed a second integrating process in an additional time period; by assuming as initial conditions, the results obtained by the first integrating process. The integrating process continues until there is no significant difference, between the results at the end of the integrating process with those at the beginning of such process (Semlyen and Medina 1995).

The equation derived in this thesis, contains voltage or current sources that have a periodic behavior. Because of this, the stable state solution of the proposed equation $\{X_T(t)\}$ is also periodic; and it can be represented as a limit cycle defined in terms of a periodic function (Semlyen and Medina 1995). All the maps near from the limit cycle are quasi-linear. This permits to use the Newton methods to estimate a point at the beginning of the limit cycle (Semlyen and Medina 1995); thus, this method can be used to determine a stable state solution of equation (3.53), by using the limit cycle. It yields,

$$\{\mathbf{X}_T\}_\infty = \{\mathbf{X}_T\}_0 + ([\mathbf{I}_T] - [\Phi_T])^{-1}(\{\mathbf{X}_T\}_T - \{\mathbf{X}_T\}_0) \quad (3.74)$$

Where $[\mathbf{I}_T]$ is an identity matrix; $[\Phi_T]$ is defined by,

$$[\Phi_T] = \exp\left(\int_{t_i}^{t_{i+T}} [\mathbf{J}(t)] dt\right) \{\Delta \mathbf{X}_T\}^i \quad (3.75)$$

In order to use the equation (3.74), it is necessary to calculate the elements of the matrix $[\Phi_T]$. The numerical difference approach (*ND*) permit to calculate these elements (Semlyen and Medina 1995). They can be derived by a calculating process which begins by defining an initial perturbation vector $\{\bar{\mathbf{X}}_T\}_i$, which is formed by perturbing just one element of $\{\mathbf{X}_T\}$ at a time. Specifically, if an i -element of $\{\mathbf{X}_T\}$ is affected by a factor ε , the perturbing vector $\{\bar{\mathbf{X}}_T\}_i$ is calculated by using,

$$\{\bar{\mathbf{X}}_T\}_i = \{\mathbf{X}_T\}_i + (\varepsilon)\{\mathbf{e}\} \quad (3.76)$$

The elements of the vector $\{\mathbf{e}\}$ of (3.76) are null, except the row that correspond to the i -element which has a value of 1.0. The variable ε is defined by a small value, i.e. 1×10^{-6} . The perturbation vector $\{\bar{\mathbf{X}}_T\}_i$ is used to perform an integrating process along a period, in order to derive a new vector defined by $\{\bar{\bar{\mathbf{X}}}_T\}_i$. After deriving the vector $\{\bar{\bar{\mathbf{X}}}_T\}_i$, the elements of the i -column of the matrix $[\Phi_T]$ can be calculated by using,

$$\{\Phi_T\}_i = \frac{1}{\varepsilon} \left(\{\bar{\bar{\mathbf{X}}}_T\}_i - \{\mathbf{X}_T\}_i \right) \quad (3.77)$$

The calculating process is repeated for all the variables contained in $\{\mathbf{X}_T\}$, in order to obtain all the columns of $[\Phi_T]$. The Figure 3.1 shows the calculating process of the *ND* method. It can be seen the details of how the columns of $[\Phi_T]$ are calculated.

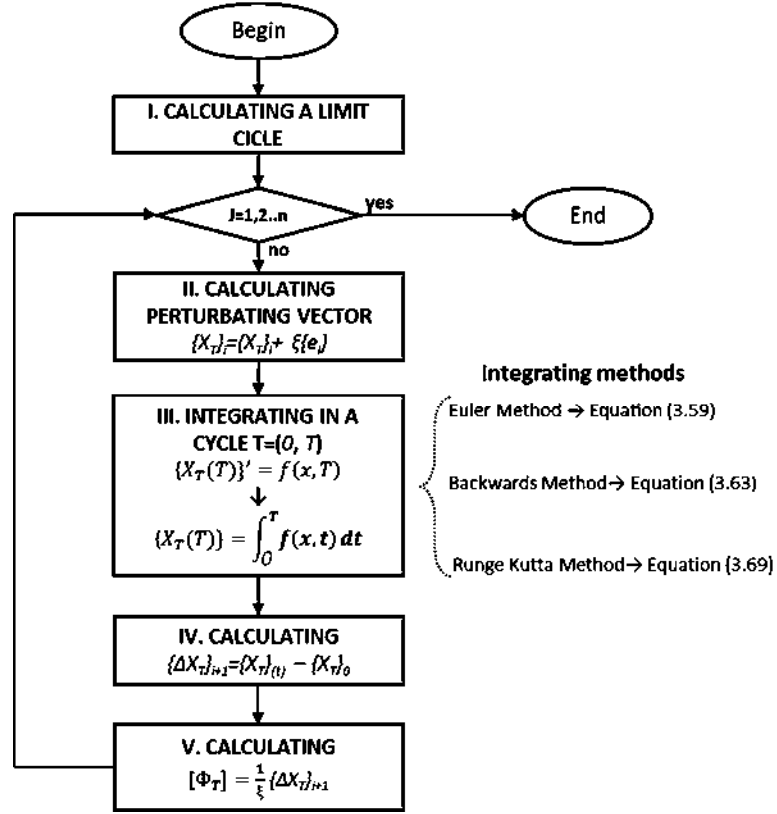


Figure 3.1. Calculating process of the Newton method using ND approach

Further details about the Newton and the *ND* method can be found in (Semlyen and Medina 1995). Summarizing, the expressions that permits to perform the integrating process, by using the Euler, Backwards Euler and the Runge Kutta method, can be seen in the expressions (3.78), (3.79) and (3.80), respectively.

$$\{\bar{X}_T\}_{(t+\Delta t)} = (\Delta t)[\bar{G}_T]^{-1}(\{F_T\}_{(t)} - [K_T]\{\bar{X}_T\}_{(t)}) + \{\bar{X}_T\}_{(t)} \quad (3.78)$$

$$\{X_T\}_{(t)} = \left([K_T] + \frac{[G_T]}{\Delta t}\right)^{-1} \left(\{F_T\}_{(t)} + \frac{[G_T]}{\Delta t}\{X_T\}_{(t-\Delta t)}\right) \quad (3.79)$$

$$\{\bar{X}_T\}_{t+\Delta t} = \{\bar{X}_T\}_{(t)} + \frac{1}{6}(\{\bar{k}_{1,T}\} + 2\{\bar{k}_{2,T}\} + 2\{\bar{k}_{3,T}\} + \{\bar{k}_{4,T}\}) \quad (3.80)$$

Further details about the main features of these methods are given in Appendix B of this thesis.

3.3.2 Frequency domain solution

The equation (3.53) can be solved in the frequency domain if it is considered that the source excitations contained in $\{F_T\}$ are sinusoidal and the materials are linear (Bastos 2003), (Shen et al. 1985),

$$\{\mathbf{F}_T(t)\} = \{\mathbf{F}_{si} \cos(\omega t + \beta_{si})\} \quad (3.81)$$

The vector $\{F_T(t)\}$ is formed by each current or voltage source F_{si} , and β_{si} represents the phase angle of each source. If the complex notation $j = \sqrt{-1}$ is used, (3.81) can be redefined by,

$$\{\mathbf{F}_T(t)\} = \mathbf{Re}\{\{\mathbf{F}_{si} e^{j(\omega t + \beta_{si})}\}\} \quad (3.82)$$

Where ω is the angular velocity; the system response to this excitation voltage is also in sinusoidal steady state and out of phase. With (3.53), the system response $\{X_T(t)\}$ is (Bastos 2003),

$$\{\mathbf{X}_T(t)\} = \mathbf{Re}\{\{\mathbf{X}_{si} e^{j(\omega t + \alpha_{si})}\}\} \quad (3.83)$$

Where α_{si} is the phase angle of each vector's component X_{si} . Taking into account (3.82) and (3.83), the solution of (3.53) can be defined by,

$$[\mathbf{K}_T]\{\mathbf{X}_{si} e^{j\omega t} e^{j\alpha_{si}}\} + [\mathbf{G}_T] \frac{d}{dt} \{\mathbf{X}_{si} e^{j\omega t} e^{j\alpha_{si}}\} = \{\mathbf{F}_{si} e^{j\omega t + j\beta_{si}}\} \quad (3.84)$$

If the term with derivative respect to t is developed in (3.84), it yields (Shen et al. 1985), (Bastos 2003),

$$[\mathbf{K}_T]\{\mathbf{X}_{si} e^{j\alpha_{si}}\} + j\omega[\mathbf{G}_T]\{\mathbf{X}_{si} e^{j\alpha_{si}}\} = \{\mathbf{F}_{si} e^{j\beta_{si}}\} \quad (3.85)$$

The equation (3.85) can be written using,

$$([\mathbf{K}_T] + j(2\pi f)[\mathbf{G}_T])\{\tilde{\mathbf{X}}_T\} = \{\tilde{\mathbf{F}}_T\} \quad (3.86)$$

Where the excitation vector $\{\tilde{\mathbf{F}}_T\}$ is defined by (Bastos 2003),

$$\{\tilde{\mathbf{F}}_T\} = \{\mathbf{F}_T(e^{j\beta_{si}})\} \quad (3.87)$$

After solving for $\{\tilde{\mathbf{X}}\}$, the components of this vector are,

$$\{\tilde{X}_T\} = \{X_{si}e^{j\alpha_{si}}\} \quad (3.88)$$

The vector $\{\tilde{X}_T\}$ contain each magnitude X_{si} and angle phase α_{si} . It is possible to express (3.86) in a simpler way using,

$$[A_T]\{X_T\} = \{b_T\} \quad (3.89)$$

The equation (3.89) will be named as *reduced* equation, since it is of lesser order than the original expression from which it was derived. The expression (3.86) has a *preprocessing* step, where their matrices are formed by a finite element analysis in order to get a FEM equation; and by a *calculating* step, in which the solution of (3.89) is obtained in the frequency domain using the *LU* method.

3.3.2.1 Preprocessing step

The *preprocessing* step consists on deriving submatrices and subvectors from the final matrices and vectors obtained from the *conventional* FEM equation, in order to calculate the matrices of the *reduced* equation. The *preprocessing* step of a *conventional* FEM equation was covered in Chapter 2; it is shown in flowchart of Figure 3.2.

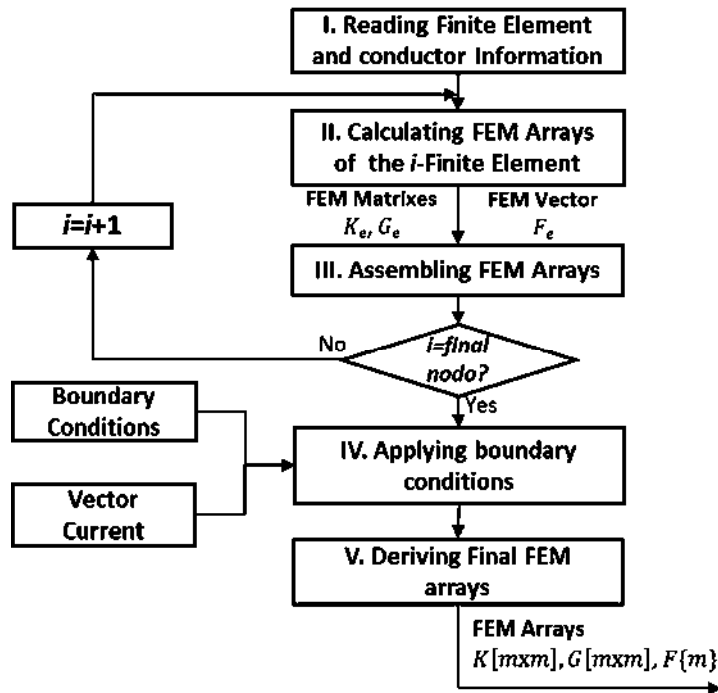


Figure 3.2. Preprocessing step of the *conventional* FEM equation

The *preprocessing step* of the *reduced* equation consists on performing the operations required to calculate the matrices and vectors of (3.89). The *preprocessing step* of the *reduced equation* can be seen in Figure 3.3.

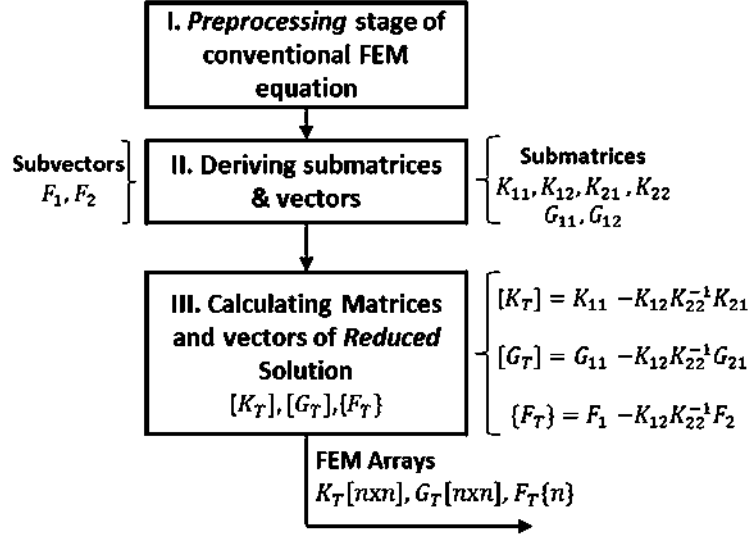


Figure 3.3. *Preprocessing step* of the *reduced* FEM equation

Further details about how the matrices K_T , G_T and the vector F_T were calculated can be consulted in the Section 3.2 of this thesis.

3.3.2.2 Calculating step

Once the matrices and the vector of the *reduced* equation are computed, it is possible to obtain its solution in the frequency domain. The process of calculating the solution of the equation is named *calculating step*. It can be seen that the *reduced* equation can be solved by using the *LU* method. The first step consists on performing a decomposition of the matrix $[A_T]$ into two matrices $[L_T]$ and $[U_T]$, respectively, i.e.

$$[A_T] = [L_T][U_T] \quad (3.90)$$

After having matrices $[L_T]$ and $[U_T]$, the solution of $[A_T]\{x_T\}=\{b_T\}$ can be achieved through triangular decomposition *LU*; and thus, the *reduced* FEM equation can be solved.

The *calculating process* of the *reduced* FEM matrix equations and some steps of the *preprocessing step* can be implemented by parallel computing. This will be explained next.

3.3.2.3 Parallel computing using the LU method

Although the reduced equation derived by the methodology can reduce the computation time since it is a lower order matrix equation; the solution in the frequency domain can be still difficult to obtain, since a large computing time to obtain the solution is still necessary.

It is possible to overcome this situation by using the CUDA parallel computing platform. This platform enables to solve the reduced equation in an easier way, using the routines already included in the CUBLAS library. Further details about the CUDA platform and the routines of the CUBLAS library can be consulted in (NVIDIA 2012), (CUDA toolkit 5.0 2014).

In this investigation, several stages of the preprocessing step were performed in the CUDA platform, using the routines of the CUBLAS library. Moreover, most of steps of the calculating step can be performed by parallel computing. These two actions permit to derive a significant time reduction of the computing time to solve the *reduced* equation in the frequency domain

3.3.2.3.1 Preprocessing steps implemented by a parallel computing

The *preprocessing* step can be implemented using parallel programming. Specifically, the matrix-matrix operations that calculate the matrices $[K_T]$, $[G_T]$ can be executed with parallel computing using the CUBLAS routine `cublasSgemm` (CUDA toolkit 5.0 2014). The matrix-vector operations that calculate the vector $\{F_T\}$ can be also performed with parallel computing using the CUBLAS routine `cublasSgemv` (CUDA toolkit 5.0 2014). The operations correspond to the stage III of the *preprocessing step* of the *reduced* equation. The *preprocessing* step of the *reduced* equation is shown in Figure 3.4.

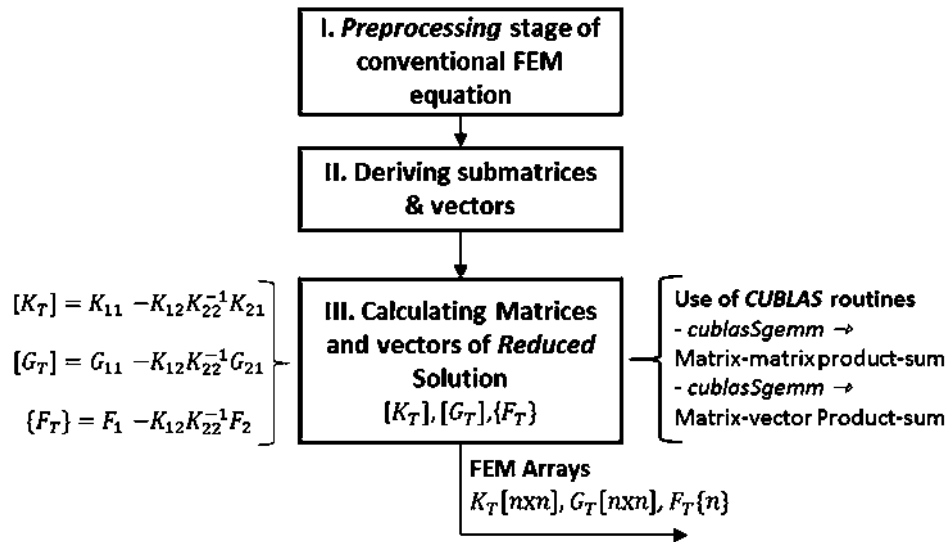


Figure 3.4 Preprocessing step of the proposed FEM equation

It is important to mention that stages I and II of the *preprocessing* step, which correspond to the determination of submatrices and vectors, are implemented using sequential computation. Parallel computing of stages I and II was implemented, however, no time reduction was achieved. It was not possible to get a time reduction, since the parallel computing of each finite element requires receiving and sending information to GPU's, which involved computing time. Because of this, the parallel computing of the stages I and II requires more time than the required for the sequential computing.

3.3.2.3.2 Calculating steps implemented by a parallel computing

Once the matrix $[A_T]$ and vector $\{b_T\}$ have been derived by the *preprocessing* step, the solution of $[A_T]\{X_T\}=\{b_T\}$ by the *calculating step* can be obtained. The *calculating step* consists on first performing a *LU* decomposition to obtain the matrices $[L_T]$ and $[U_T]$; after having these matrices the vector solution $\{X_T\}$ is calculated. Parallel processing is applied for the *LU* decomposition process.

3.3.2.3.2.1 CUBLAS decomposition LU

The decomposition process implies to calculate the pivot located in the main diagonal of $[A_T]$. This pivot is used to multiply the elements of the next rows, in order to form the triangular matrix $[L_T]$. Finally, a Gauss eliminating process to form the matrix $[U_T]$ will be performed. Figure 3.5 shows the decomposition process implemented by parallel computing in *CUBLAS*.

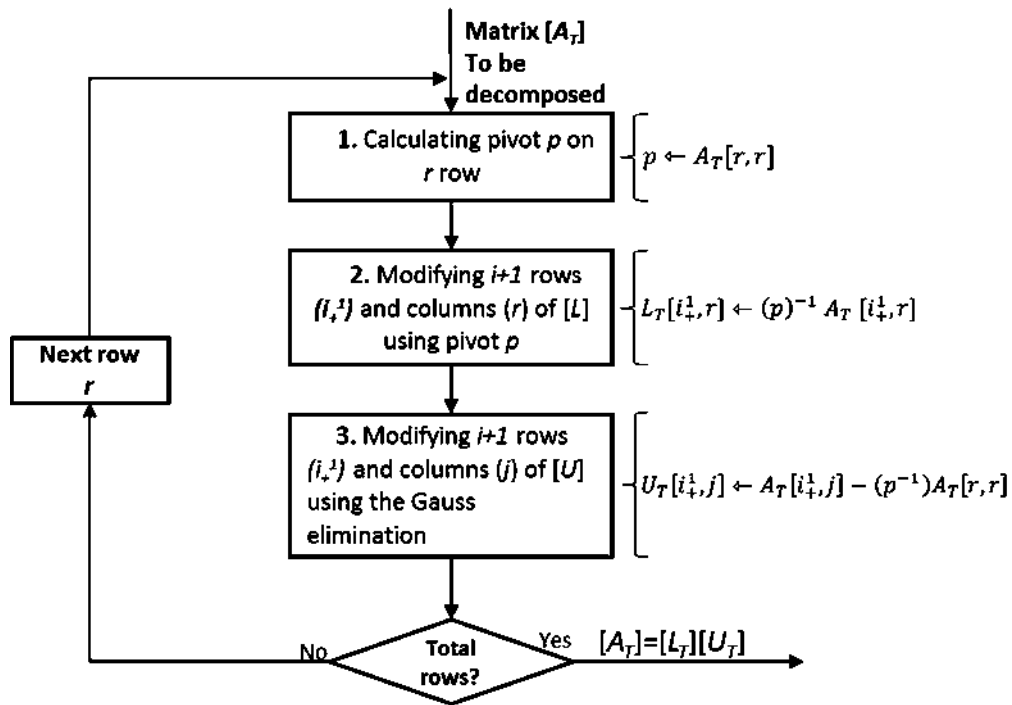


Figure 3.5 LU decomposition process implemented in *CUBLAS*

The *CUBLAS* routines used for the parallel computation of the *LU* decomposition correspond to matrices and vectors composed of single precision complex numbers (NVIDIA 2012). Once the matrix $[A_T]$ is decomposed into the matrices $[L_T]$ and $[U_T]$, the equation $[A_T]\{X_T\} = \{b_T\}$ can be solved.

3.3.2.3.2.2 Final solution of equation using CUBLAS

The vector solution $\{X_T\}$ can be calculated by solving the following equations using the *CUBLAS* computing platform,

$$[\mathbf{L}_T]\{\mathbf{Y}_T\} = \{\mathbf{b}_T\} \quad (3.91)$$

$$[\mathbf{U}_T]\{\mathbf{X}_T\} = \{\mathbf{Y}_T\} \quad (3.92)$$

The expression shown in (3.91) is solved by using the CUBLAS routine `cublasCstrv`, specifying that the equation to be solved corresponds to a triangular matrix stored in lower mode (NVIDIA 2012); while the expression (3.92) is also solved using the CUBLAS routine `cublasCstrv`, but specifying that the equation to be solved corresponds to a triangular matrix stored in upper mode (NVIDIA 2012).

It can be seen that the solution of the complex equation $[\mathbf{A}_T]\{x_T\} = \{b_T\}$ can be easily derived by implementing the *LU* method using parallel computing in CUBLAS. The results and the performance of this method of solution will be described in the next chapter.

3.4 Comparison between the conventional and the proposed method

The main characteristics of the FEM field equation and the FEM-circuit coupled equation have been explained in Section 3.2. The main features of the equation proposed by the methodology of Section 3.3 has been also covered. However, it is convenient to compare both approaches in order to discuss their main advantages and disadvantages. In this section a general comparison between the approaches will be explained; after that a comparison of their solution in the time domain and in the frequency domain will be explained.

3.4.1. General aspects

3.4.1.1 FEM field equation with voltages or currents known

For this case, the *conventional differential* equation permits to directly calculate the magnetic vector potentials of the *conductor* and the *non-conductor* regions, when the voltages or currents are known. After having the magnetic vector potentials, the equation (3.25) can be used to calculate the voltages or currents. However, it is necessary to calculate all the magnetic vector potentials, in order to derive the voltages or currents.

The equation derived from the methodology, permits to directly calculate the magnetic vector potentials of the *conductor* region using a lower order equation. Moreover, the same numbering criteria to reformulate the equation (3.25) that relates the magnetic vector potentials, the voltage and currents can be used; in order to get a reduced order expression to calculate the currents or voltages in a faster way. The magnetic vector potentials of the *non-conductor* regions can be calculated using (3.20).

3.4.1.2 FEM-circuit coupled equation

For this case, the FEM-circuit coupled equation permits to directly calculate the magnetic

vector potentials of the *conductor* and the *non-conductor* regions. Thus, the equation requires that all the time varying variables (magnetic vector potentials of the *conductor* region and currents) and the autonomous variables (magnetic vector potentials of the *non-conductor* region and voltages); need be calculated at the same time.

Moreover, the reduced equation permits to directly calculate the time varying variables, i.e. the magnetic vector potentials of the *conductor* region and the conductors' currents. Thus, it is not necessary to calculate the magnetic vector potentials of the *non-conductor* regions and the voltages. However, these variables can be calculated using (3.25) that relates the magnetic vector potentials with the conductors' voltages and currents. Nevertheless, in order to calculate the matrices and vectors of the equations, several matrix-vector operations are necessary to be performed and this can lead to a considerable computation effort.

A comparison between the solution in the time and the frequency domain of the conventional and the proposed approaches will be explained next.

3.4.2 Comparison in the time domain

Both the *conventional* and the *reduced* FEM equation, can be solved in the time domain, using the Euler, Backwards Euler, Runge Kutta and the Newton methods. This will be discussed next.

3.4.2.1 Euler method

The solution in the time domain of the original FEM equation, using the Euler method is given by,

$$\{\mathbf{X}\}_{(t+\Delta t)} = (\Delta t)[\mathbf{G}]^{-1}(\{\mathbf{F}\}_{(t)} - [\mathbf{K}]\{\mathbf{X}\}_{(t)}) + \{\mathbf{X}\}_{(t)} \quad (3.93)$$

The equation (3.93) cannot be solved in an accurate way because the matrix inversion of $[\mathbf{G}]$ cannot be achieved since the matrix has null elements along the main diagonal. Thus, it is not possible to get an accurate solution using (3.93).

For the case of the reduced equation, an accurate solution using the Euler method cannot also be obtained, but an approximate solution can be derived using,

$$\{\bar{\mathbf{X}}_T\}_{(t+\Delta t)} = (\Delta t)[\bar{\mathbf{G}}_T]^{-1}(\{\mathbf{F}_T\}_{(t)} - [\mathbf{K}_T]\{\bar{\mathbf{X}}_T\}_{(t)}) + \{\bar{\mathbf{X}}_T\}_{(t)} \quad (3.94)$$

The Euler method can be only used in an approximate way in the reduced equation, since this expression has been derived from an equation that cannot be accurately solved by the Euler method. Nevertheless, the reduced equation is of lower order and can directly solve the time varying variables included in (3.93).

3.4.2.2 Backwards Euler method

The solution in the time domain of the original FEM equation, using the Backwards Euler method is given by,

$$\{\mathbf{X}\}_{(t)} = \left([\mathbf{K}] + \frac{[\mathbf{G}]}{\Delta t} \right)^{-1} \left(\{\mathbf{F}\}_{(t)} + \frac{[\mathbf{G}]}{\Delta t} \{\mathbf{X}\}_{(t-\Delta t)} \right) \quad (3.95)$$

While the solution of the reduced equation by the Backwards Euler method is defined by

$$\{\mathbf{X}_T\}_{(t)} = \left([\mathbf{K}_T] + \frac{[\mathbf{G}_T]}{\Delta t} \right)^{-1} \left(\{\mathbf{F}_T\}_{(t)} + \frac{[\mathbf{G}_T]}{\Delta t} \{\mathbf{X}_T\}_{(t-\Delta t)} \right) \quad (3.96)$$

Equations (3.95) and (3.96) are almost identical. The solution obtained in the time domain is accurate, since an approximate equation to get a solution has not been used. The matrix to be inverted for the case of the conventional expression is defined by the sum of $[\mathbf{K}]$ and $(\Delta T^{-1})[\mathbf{G}]$; and for the case of the reduced equation by the sum of matrices $[\mathbf{K}_T]$ and $(\Delta T^{-1})[\mathbf{G}_T]$. The main difference between the conventional and the reduced expression is the order of the matrix equation to be solved.

3.4.2.3 Runge Kutta method

The solution in the time domain of the original FEM equation using the Runge-Kutta method is obtained as,

$$\{\mathbf{X}\}_{(t+\Delta t)} = \{\mathbf{X}\}_{(t)} + \frac{1}{6} (\{\mathbf{k}_1\} + 2\{\mathbf{k}_2\} + 2\{\mathbf{k}_3\} + \{\mathbf{k}_4\}) \quad (3.97)$$

Equation (3.97) cannot be accurately solved in an accurate, since the matrix inversion of $[\mathbf{G}]$ involves the inversion of an ill-conditioned matrix. Although it is possible to use an approximation of (3.97), it is also still necessary to derive all the magnetic vector potentials at the same time.

For the case of the reduced order equation, its approximate solution in the time domain using the Runge Kutta method is quite similar to (3.97), i.e.

$$\{\bar{\mathbf{X}}_T\}_{(t+\Delta t)} = \{\bar{\mathbf{X}}_T\}_{(t)} + \frac{1}{6} (\{\bar{\mathbf{k}}_{1,T}\} + 2\{\bar{\mathbf{k}}_{2,T}\} + 2\{\bar{\mathbf{k}}_{3,T}\} + \{\bar{\mathbf{k}}_{4,T}\}) \quad (3.98)$$

The equation (3.97) and (3.98) are almost identical. However, the method can be only used in an approximate way in the *reduced* equation, since this one has been derived from an expression that cannot be accurately solved by the Runge Kutta method. Nevertheless, the

equation derived by the methodology is of lesser order and its solution in the time domain can be rapidly achieved.

3.4.2.4 Newton method based on Poincaré map and extrapolation to the limit cycle

The solution in the time domain of the original FEM equation using the Newton method based on Poincaré map and extrapolation to the limit cycle is defined by,

$$\{\mathbf{X}\}_\infty = \{\mathbf{X}\}_t + (\mathbf{I} - \boldsymbol{\Phi})^{-1}(\{\mathbf{X}\}_{t+\Delta t} - \{\mathbf{X}\}_{t+\Delta t}) \quad (3.99)$$

While the solution of the reduced equation using the Newton method is given by,

$$\{\mathbf{X}_T\}_\infty = \{\mathbf{X}_T\}_t + (\mathbf{I}_T - \boldsymbol{\Phi}_T)^{-1}(\{\mathbf{X}_T\}_{t+\Delta t} - \{\mathbf{X}_T\}_{t+\Delta t}) \quad (3.100)$$

The difference between (3.99) and (3.100) relies on the order of the matrix equation to be solved. The Newton method used in this investigation, consider that the matrix $\boldsymbol{\Phi}$ will be calculated using the *ND* method (Semlyen and Medina 1995). The *ND* method requires to integrate along a period of time, or Base Cycle, using the Euler, Backwards Euler or the Runge Kutta method. The precision of the Newton methods would depend of the accuracy of these methods and the step size selected. While the Backwards Euler provides an excellent solution, the Euler and the Runge Kutta provide an approximate solution in the time domain.

3.4.2.5 Summary of the time domain comparison

The *reduced* equation can be solved in the time domain using several methods. The equation can provide a good solution when the Backwards Euler is used. On the other hand, the Euler and the Runge Kutta can be used to get an approximate solution. The equation can be also solved using the Newton method described in the previous section. The solution of the time domain can be easily achieved using the equation derived by the methodology, although it is necessary to perform several matrix operation in order to derive it; these matrices and vector are required to be calculated only once, therefore, it can be provide a faster time domain solution.

3.4.3 Comparison in the frequency domain

The solution of a conventional FEM equation in the frequency domain is defined by,

$$([\mathbf{K}] + j(2\pi f)[\mathbf{G}])\{\tilde{\mathbf{X}}\} = \{\tilde{\mathbf{F}}\} \quad (3.101)$$

While the solution of the equation derived by the methodology is given by,

$$([K_T] + j(2\pi f)[G_T])\{\tilde{X}_T\} = \{\tilde{F}_T\} \quad (3.102)$$

The equations (3.101) and (3.102) are quite similar. The main difference between them is the order of the matrix equation to be solved. The solution of both equation requires of solving an equation of the form $Ax=b$. Although the *reduced* equation is of lower order, it is necessary to perform additional matrix operations in order to obtain its matrices and vectors.

3.4.3.1 Summary of the frequency domain comparison

The equation derived by the proposed methodology requires of several matrix operations in order to obtain the respective matrices and vectors. This calculating process requires of an additional computing time. Because of this, the reduced equation cannot always represent a better method of solution in the frequency domain. However if an analysis is performed which involves several calculations in the frequency domain, the method can represent an excellent way of solution. This will be shown in the case studies discussed in the next chapter of this thesis.

3.5 Conclusions

In this chapter, a methodology, which permits to derive a *reduced* equation expressed in terms of time varying variables of a FEM field or a FEM-circuit coupled equation has been presented.

Although these FEM equations were widely covered in Chapter 2, a summary of the most important features of these equations has been included, in order to get a quick understanding of them.

The proposed methodology consists on perform a renumbering of the magnetic vector potentials of the FEM equation; this permits to derive an equivalent expression. Using this equation and performing a rearrangement of its variables along several matrix-vector operations; permits to get a reduced equation of lower order, which can be solved in the frequency and the time domain.

The solution in the time domain can be performed using several methods, i.e. Euler, Backwards Euler and the Runge Kutta method. The Newton method based on Poincaré map and extrapolation to the limit cycle can be used. These methods have their own advantages or disadvantages when they are used to get a solution in the time domain.

Moreover, the equation derived can be solved in the frequency domain. Although the solution of the frequency domain can be easy to derive, it can involve the solution of a large matrix equation. This can be overcome by using a *LU* method, implemented in a parallel computing platform. The use of the CUDA and the routines used in the CUBLAS library were covered and performed in this investigation. They offer an excellent choice of

implementing the *LU* method. The use of a *LU* decomposition method implemented in CUBLAS, which permits to solve an equation in the frequency domain using parallel computing has been proposed.

Although the reduced equation is of lower order, it is necessary to perform several matrix operations in order to derive the components which form the expression. Because of this, the solution in the frequency or the time domain may require of additional computing time. This will depend of the problem to be solved. This will be discussed in the Chapter 5, where several case studies will be presented.

4 Proposed sequential and parallel routines used in the methodology

4.1 Introduction

In this chapter, how the FEM equations of this investigation were performed using sequential and the parallel computing platforms will be detailed. The FEM equations are derived from finite element analysis which can be simplified by a planar or an axisymmetric symmetry assumption. As a first step, how the *conventional* FEM equations were solved using sequential computing will be explained. Besides, the solution of these equations using the *CUBLAS* parallel computing platform will be explained. After that, how the equations derived from the proposed methodology are solved using the sequential and parallel computing platforms will be described. Three stages in the implementation of conventional and the equation derived from the methodology can be recognized:

1. *Preprocessing FEM Stage*. All the devices are modeled using the FEM software ANSYS. Thus, this stage consists on modeling the geometry of the device, by entering the magnetic and electric properties, by assigning the boundary conditions; and finally, by performing the geometry meshing. After doing all this, it is possible to generate the information of the finite elements, specifically, the element numbers, the nodes and the electric and magnetic properties.
2. *Preprocessing Stage*. This stage consists on deriving the FEM matrices and vectors by performing a finite element analysis. The information provided by the *Preprocessing FEM Stage* will be used. The final goal of this stage is to generate the FEM matrix equation.
3. *Calculating process*. This stage consists on solving the FEM equation, either in the frequency or in the time domain.

The stages that correspond to *conventional* FEM equations and to equations derived from the proposed methodology will be detailed next.

4.2 Conventional FEM equations

4.2.1 Preprocessing FEM stage

The preprocessing FEM stage consists on first modeling the geometry of the device, i.e. the keypoints, elements and areas. Then, the magnetic and electric properties of the different sections will be set up. With the geometry model finished, it is possible to perform a meshing

to perform a partition of the device domain in small finite elements. For the case of conventional FEM equations, the automatic meshing functions of ANSYS are used. The next step consists on introducing the boundary conditions; since 2D finite element analysis is considered, it is only necessary to set the Dirichlet boundary conditions. With all this information, it is possible to generate three data file: the *Element* Data File that contains the elements, their nodes and the electric and magnetic properties; the *Nodes* Data File that contains the coordinates of each node the geometry modeled; and finally, the *Boundary Conditions* Data File that contains the boundary conditions. The *Preprocessing FEM* stage is shown in Figure 4.1

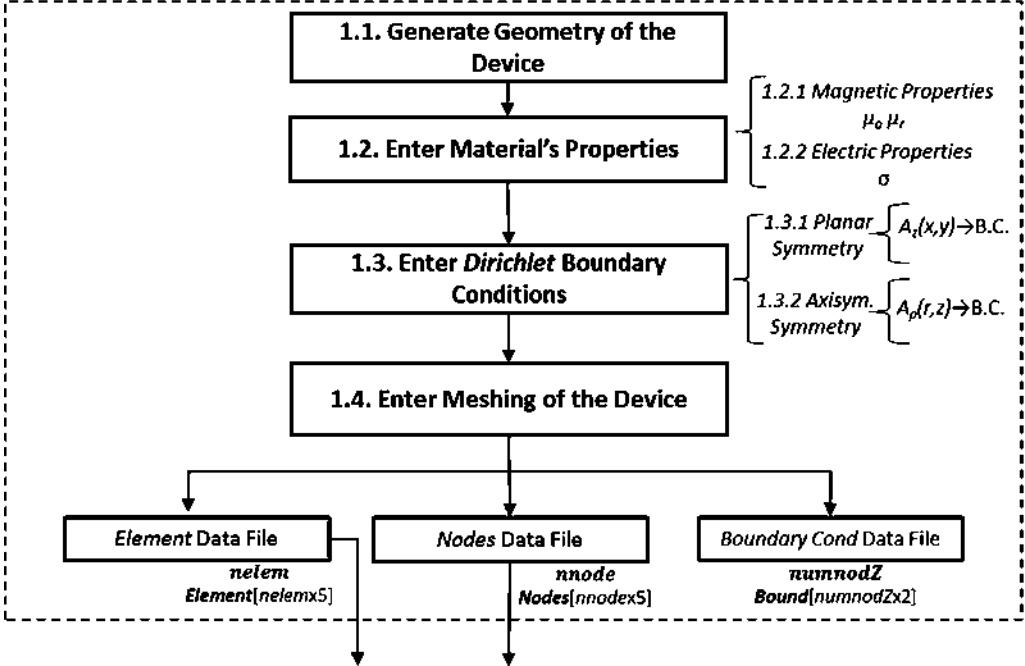


Figure 4.1 *Preprocessing FEM* stage of a conventional FEM equation performed by ANSYS

With the information of elements and nodes contained in the data files derived from the *Preprocessing FEM* stage; it is possible to derive the FEM matrices and vectors of each finite element. These will correspond to three specific FEM expressions: a FEM field equation with voltages or currents known, and a FEM-circuit coupled equation.

4.2.1.1 FEM field equation with voltages known

If a device with voltages known is modeled, it is possible to derive the FEM matrices and vectors using the element and node information included in the data files of the *preprocessing FEM* stage. The matrices and vectors can be calculated using a finite element analysis which considers a planar or an axisymmetric symmetry. The different steps that lead to derive a FEM field equation with voltages known is shown in Figure 4.2. The platforms that allow to derive each specific step shown in Figure 2 are indicated in Table 4.1.

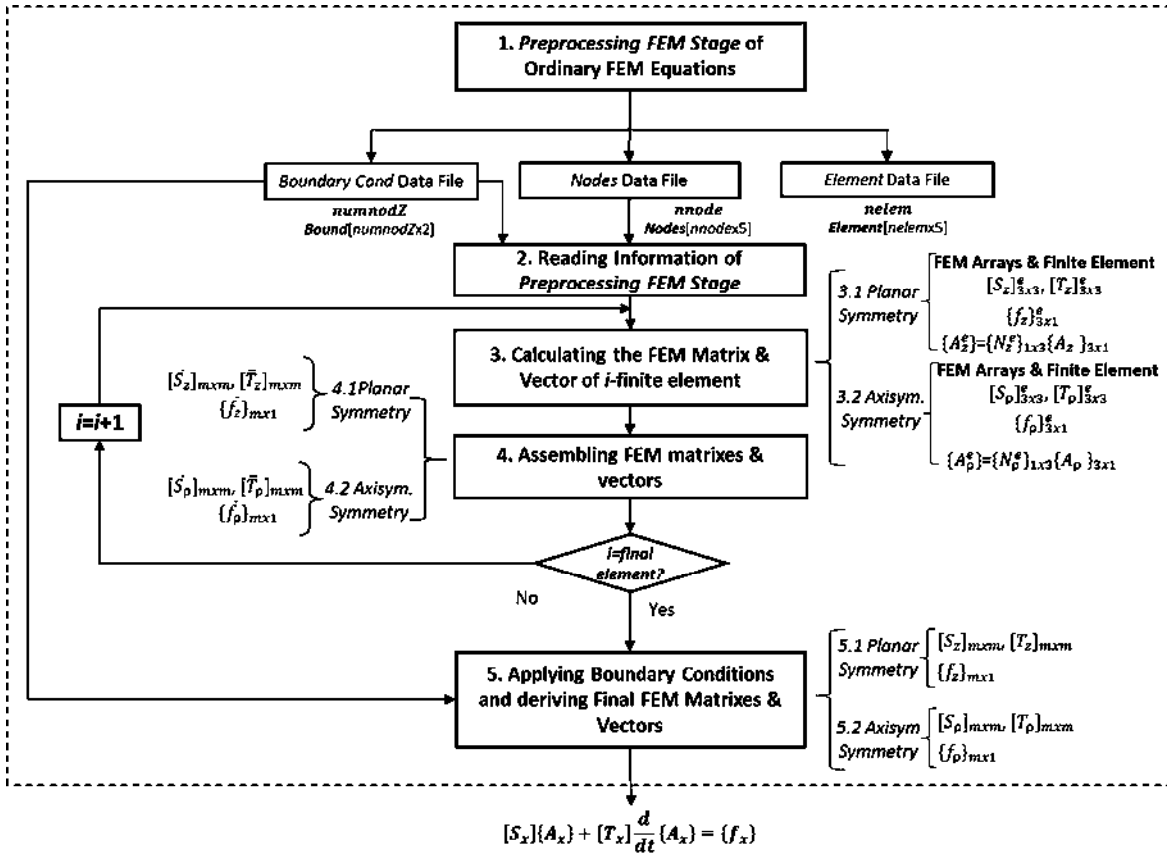


Figure 4.2. Preprocessing stage of a FEM field equation with voltages known

TABLE 4.1. ROUTINES AND PLATFORMS USED IN THE PREPROCESSING STAGE OF A FEM FIELD EQUATION WITH VOLTAGES KNOWN

Operation Performed	MATLAB Platform	GSL Platform
1. Preprocessing FEM Stage	ANSYS	
2. Reading information of preprocessing FEM stage	ANSYS/Windows XP	
3. Calculating the FEM matrix & vector of the i-finite element	Matlab own-routines	C own-routines
4. Assembling FEM matrixes & vectors		gsl_matrix_set gsl_vector_set
5. Applying boundary conditions and deriving final matrixes and vectors of the FEM expression		

4.2.1.2 FEM field equation with currents known

The preprocessing FEM stage explained in the Section 4.2.1, also permit to derive the FEM matrices and vectors of a device with currents known. For this case, it has also been used a finite element analysis which considers a planar or an axisymmetric symmetry assumption. The matrices and vectors are also obtained, by considering the node and element information; but this preprocessing FEM stage is different. It consists on deriving the matrices and vectors of a FEM coupled equation, which models a device with currents

known. The FEM coupled equation is formed by a FEM field expression with voltage as the forcing function; and by the FEM expression that relates the voltage, current and magnetic vector potentials of the device. Thus, on this *preprocessing stage*, the matrices and vectors of these two FEM expressions are calculated; and finally, they are used to derive the matrices and vector of the FEM coupled equation.

Figure 4.3 shows the different steps that lead to derive a FEM equation with currents known, while the platforms and routines that allow each specific step of Figure 4.3 are shown in Table 4.2. It can be seen that it is necessary to use the preprocessing stage shown in Figure 4.2.

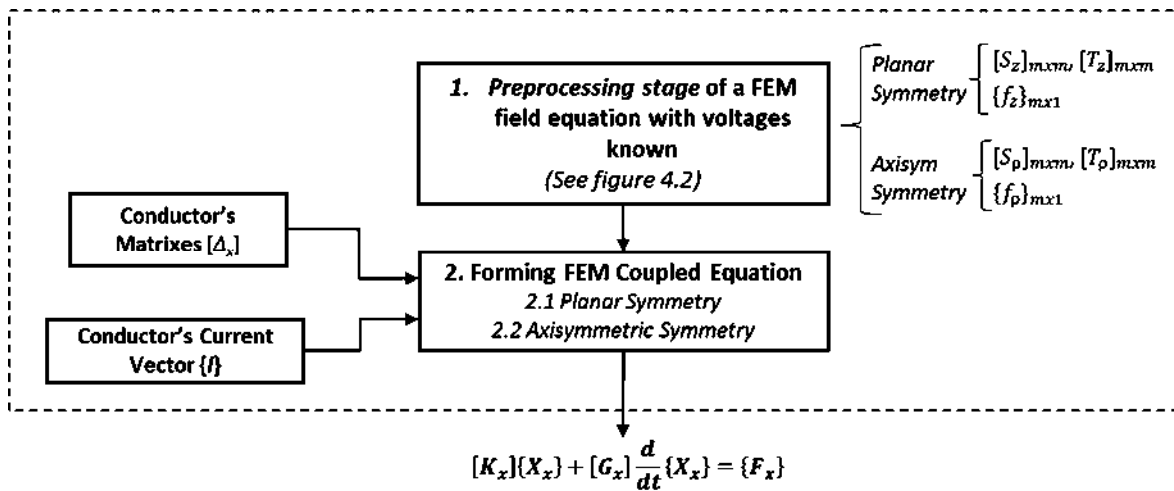


Figure 4.3. *Preprocessing stage of a FEM field equation with currents known*

TABLE 4.2. ROUTINES AND PLATFORMS USED IN THE *PREPROCESSING STAGE OF A FEM FIELD EQUATION WITH CURRENTS KNOWN*

Operation Performed	<i>MATLAB</i> Platform	<i>GSL</i> Platform
1. <i>Preprocessing FEM stage of a FEM equation with voltages known</i>	<i>See Table 4.1</i>	<i>See Table 4.1</i>
2. Forming FEM coupled equation	<i>Matlab own-routines</i>	<i>C own-routines</i>

4.2.1.3 *FEM circuit coupled equation*

If a device using a FEM-circuit coupled equation is modeled, the *preprocessing FEM stage* covered in Section 4.2.1, also permits to derive the FEM matrices and vectors. These matrices and vectors are also derived by a finite element analysis, which considers a planar or axisymmetric symmetry assumption.

The FEM-circuit coupled expression is formed by a FEM-field equation with voltages as the forcing function; by the FEM equation that relates voltage and currents with the magnetic vector potentials; and finally, by a voltage-current equation. On this *preprocessing stage*, the matrices and vectors of these three expressions are calculated in order to derive the FEM-circuit coupled equation. The different steps that lead to derive the *preprocessing stage* of a

FEM-circuit coupled equation are shown in Figure 4.4, while the platforms and routines that allow each specific step are given in Table 4.3. It can be seen that it is necessary to use the preprocessing stage shown in Figure 4.3.

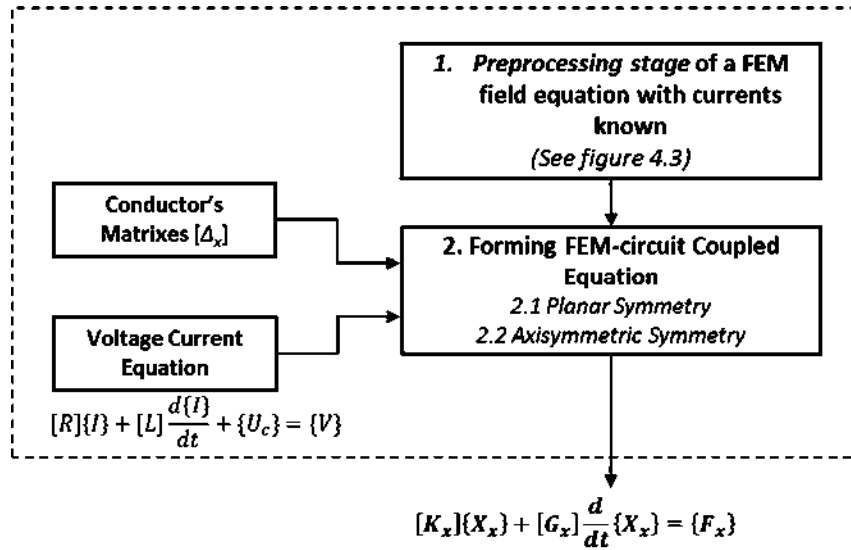


Figure 4.4. Preprocessing stage of a FEM-circuit coupled equation

TABLE 4.3. ROUTINES AND PLATFORMS USED IN THE *PREPROCESSING* STAGE OF FEM-CIRCUIT COUPLED EQUATION

Operation Performed	<i>MATLAB</i> Platform	<i>GSL</i> Platform
1. <i>Preprocessing FEM Stage</i> of a FEM equation with currents known	See Table 4.2	See Table 4.2
2. Forming the FEM-circuit coupled Equation	<i>Matlab own-routines</i>	<i>C own-routines</i>

Summarizing, the *preprocessing stage* permits to derive all the FEM equations described in the Sections 4.2.1.1, 4.2.1.2 and 4.2.1.3. The FEM equations can be solved either in the frequency and the time domain. The process of solving the FEM equation is named *calculating stage* and will be explained next.

4.2.2. Calculating stage

The *preprocessing stage* permits to obtain a FEM field equation with voltages or currents known, and a FEM-circuit coupled equation. These equations can be represented in a general form as,

$$[K]\{X\} + \frac{d}{dt}[G]\{X\} = \{f\} \tag{4.1}$$

The expression (4.1) can be solved in the frequency and in the time domain. Specific details on the solution methods can be consulted in Appendix B.

4.2.2.1 Solution in the frequency domain

If (4.1) is solved in the frequency domain, it has the form,

$$([K] + j(2\pi f)[G])\{\tilde{X}\} = \{\tilde{f}\} \quad (4.2)$$

Moreover, (4.2) can be represented in a simpler way using,

$$[A]\{\tilde{X}\} = \{\tilde{b}\} \quad (4.3)$$

The Equation (4.3) can be solved in the frequency domain using the *LU* decomposition method. The *LU* method can be solved using sequential and parallel computing platforms. For the case of a sequential solution, the Matlab (MATLAB 2010) and the GSL (GNU Scientific Library 2013) platforms were used. For the case of a parallel solution, the CUBLAS platform was used (NVIDIA 2012), (Barrachina et al. 2008), (CUDA toolkit 5.0 2014). The method is concisely illustrated by Figure 4.5. Further details of the parallel and the sequential implementation of the *LU* method can be consulted in Chapter 3. All the routines used by each platform are given in Table 4.4.

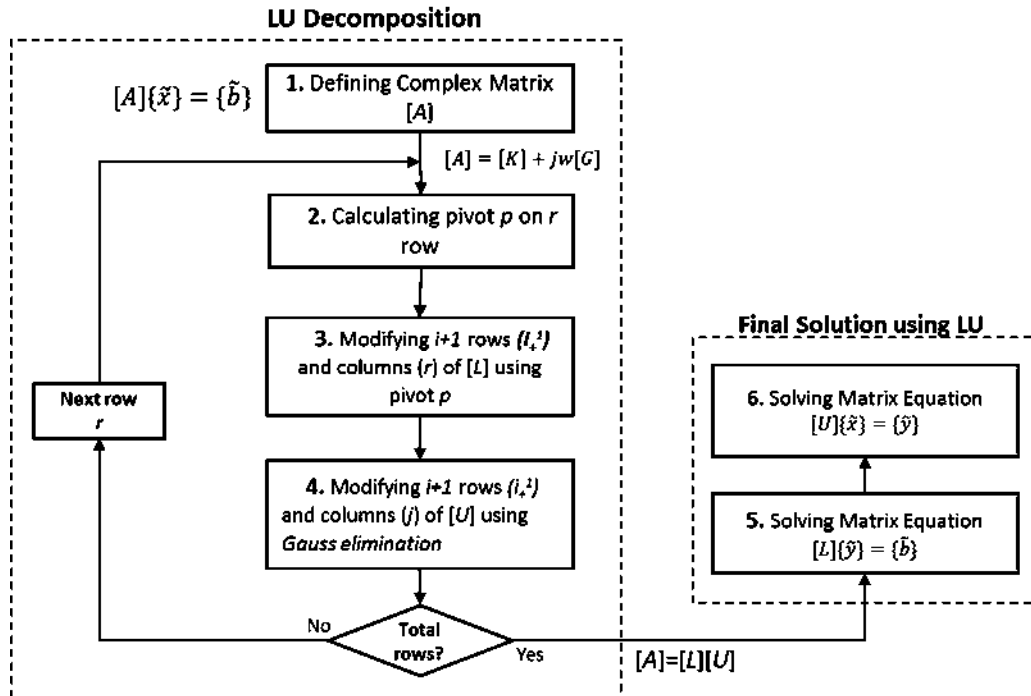


Figure 4.5 Calculating process for the conventional FEM equations in the frequency domain

TABLE 4.4. ROUTINES AND PLATFORMS USED IN THE FREQUENCY DOMAIN SOLUTION OF A CONVENTIONAL FEM EQUATION

Method	Operation Performed	MATLAB Platform	GSL Platform	CUBLAS Platform
		Routine used	Routine used	Routine used
LU decomp. [A]= [L][U]	1. Defining matrix complex [A]	MatLab Routine	<i>gsl_matrix_set</i>	Cublas Routine
	2. Calculating pivot <i>p</i> on r-row	NA	<i>gsl_linalg_complex_LU_decomp</i>	<i>cuCdivf</i>
	3. Modifying rows & columns of [L] using pivot <i>p</i>			<i>cublasCscal</i>
	4. Modifying rows & columns of [U] using Gauss Elimination			<i>cublasCgeru</i>
Final solution [A]{ \tilde{X} } = { \tilde{b} }	5. Solving the 1 st Matrix equation [L]{ \tilde{Y} } = { \tilde{b} }	<i>linsolve</i>	<i>gsl_linalg_complex_LU_solve</i>	<i>cublasCtsv</i>
	6. Solving the 2 nd matrix equation [U]{ \tilde{X} } = { \tilde{Y} }			<i>cublasCtsv</i>

4.2.2.2 Solution in the time domain

The equation shown in (4.1) can be represented in a different way using,

$$[G] \frac{d}{dt} \{X\} = \{f\} - [K] \{X\} \quad (4.4)$$

It is possible to solve the expression shown in (4.4) in time domain, using the Backwards Euler method. It gives,

$$\left([K] + \frac{[G]}{\Delta t} \right) \{X\}_{(t)} = \{F\}_{(t-\Delta t)} + (\Delta t)^{-1} [G] \{X\}_{(t-\Delta t)} \quad (4.5)$$

Moreover, (4.5) can be represented in a general form, i.e.

$$[A]_{(t)} \{X\}_{(t)} = \{b\}_{(t-\Delta t)} \quad (4.6)$$

Where the matrix $[A]_{(t)}$ and the vector $\{b\}_{(t-\Delta t)}$ are given by,

$$[A]_{(t)} = \left([K] + \frac{[G]}{\Delta t} \right) \quad (4.7)$$

$$\{b\}_{(t-\Delta t)} = \{F\}_{(t-\Delta t)} + (\Delta t)^{-1} [G] \{X\}_{(t-\Delta t)} \quad (4.8)$$

It is possible to solve (4.6) using the *LU* decomposition method. For the particular case of the time domain solution, a sequential computing platform will be used. Specifically, the Matlab (MATLAB 2010) and the GSL (GNU Scientific Library 2013) platforms were used. The routines used by these platforms are listed in Table 4.5.

TABLE 4.5. ROUTINES AND PLATFORMS USED IN THE TIME DOMAIN SOLUTION OF A CONVENTIONAL FEM EQUATION USING THE BACKWARDS EULER METHOD

Method	Operation performed	MATLAB platform	GSL platform
		Routine used	Routine used
<i>LU Decomposition</i> $[A]_{(t)} = [L]_{(t)}[U]_{(t)}$	1. Defining matrix complex $[A]_{(t)}$	<i>MatLab Routine</i>	<i>gsl_matrix_set</i>
	2. Calculating pivot p on r-row	NA	<i>gsl_linalg_complex_LU_decomp</i>
	3. Modifying rows & columns of $[L]_{(t)}$ using pivot p		
	4. Modifying rows & columns of $[U]_{(t)}$ using <i>Gauss elimination</i>		
Final Solution $[A]_{(t)}\{X\}_{(t)} = \{b\}_{(t-\Delta t)}$	5. Solving the 1 st Matrix Equation $[L]_{(t)}\{Y\}_{(t-\Delta t)} = \{b\}_{(t-\Delta t)}$	<i>linsolve</i>	<i>gsl_linalg_complex_LU_solve</i>
	6. Solving the 2 nd Matrix Equation $[U]_{(t)}\{X\}_{(t-\Delta t)} = \{Y\}_{(t-\Delta t)}$		

4.3 Proposed methodology

4.3.1 Preprocessing FEM Stage

The *preprocessing FEM stage* of the methodology consists on first modeling the geometry of the device. Specifically, it models the keypoints, elements and areas that form the geometry of the device. After that, the magnetic and electric properties are set up. With the geometry modeled, it is possible to perform a meshing, that allows a partition of the domain in small finite elements.

For the specific case of the proposed methodology, it is necessary to perform the meshing in the conductors of the device first. Thus, each conductor will be consecutively meshed. After having meshed the conductors, this process is performed for the other parts of the geometry. It is important to take into account the number of nodes that correspond to the *conductor region*, and the number of nodes that correspond to the *non-conductor region*. The number of nodes of the *conductor region* is $nnodeC$, while the number of nodes of the *non-conductor region* is $nnode - nnodeC$, where $nnode$ is the total node numbers of the geometry. Using these node numbers, it is possible to perform the proposed methodology, which consists on deriving a *reduced FEM equation*.

After having performed the meshing process, the boundary conditions of the device is set up. Since a 2D finite element analysis is considered, it is only necessary to set the Dirichlet boundary conditions. With all this information, it is also possible to generate three data file: the *Element Data File* that contains the elements, their nodes and the electric and magnetic properties; the *Nodes Data File* that contains the coordinates of each node of the device; and

finally, the *Boundary Conditions Data File* that contains the Dirichlet boundary conditions. The *Preprocessing FEM* stage of the proposed methodology is shown in Figure 6.

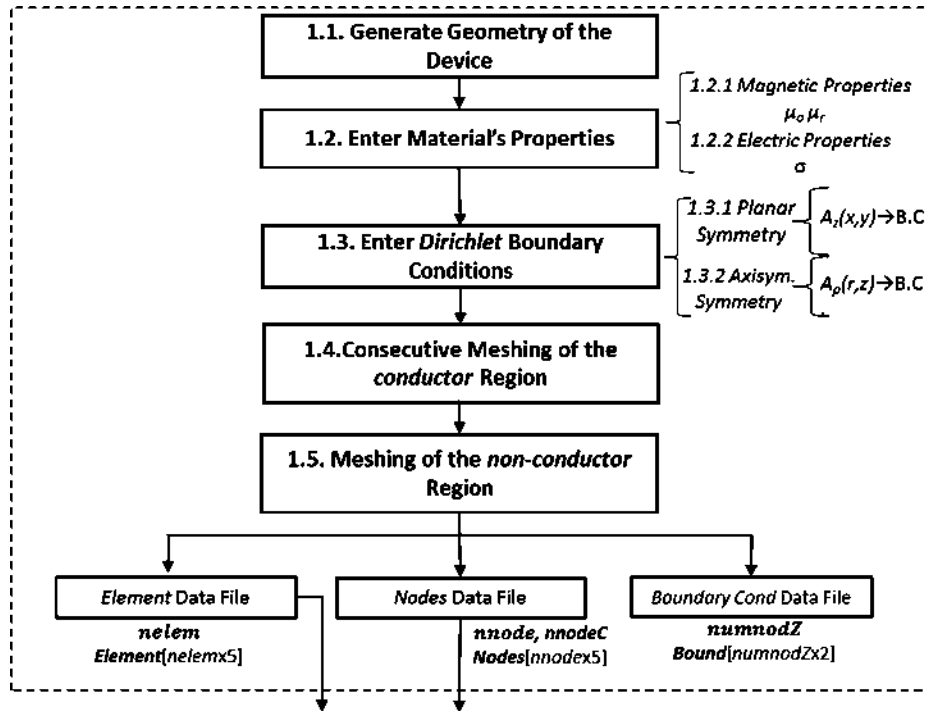


Figure 4.6. *Preprocessing FEM* stage of the proposed methodology using ANSYS

4.3.1.1 FEM field equation with voltages known

The proposed methodology permit to derive a *reduced* FEM equation, from a FEM field equation with voltages known. The *preprocessing FEM* stage which permit to derive the matrices and vector of the FEM field equation with voltages known, was previously covered in Section 4.2.1.1.

The *preprocessing stage* of the *reduced* equation, consists on deriving its FEM matrices and vectors; specifically it is used a calculating process, which takes into account the node number of the *conductor* and the *non-conductor* regions of the FEM field equation. The different necessary steps to perform the *preprocessing stage* of the proposed methodology, in a FEM field equation with voltages known; are shown in Figure 4.7. The platforms to derive each specific step shown in Figure 4.7 are listed in Table 4.6.

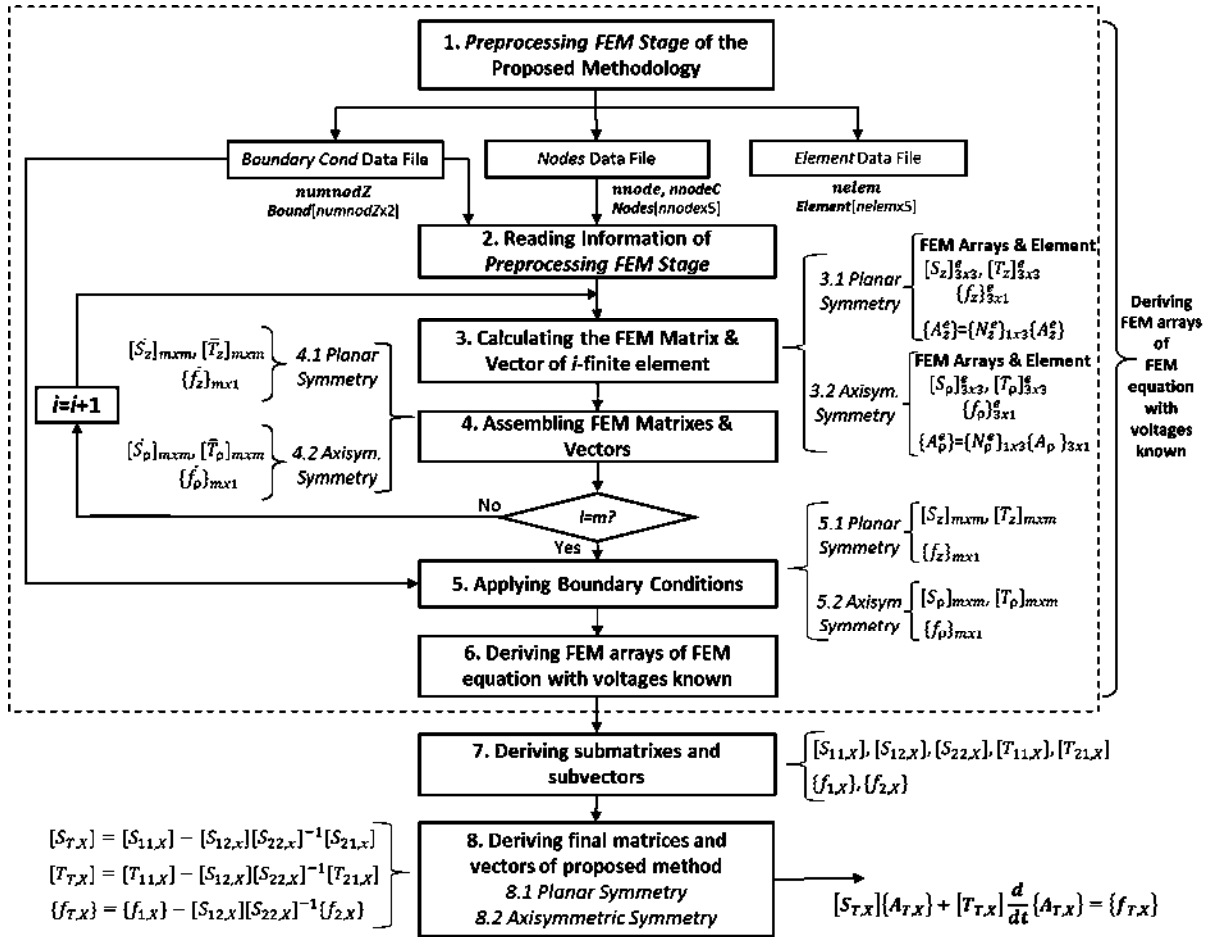


Figure 4.7. Preprocessing stage of the methodology applied to a FEM-field equation with voltages known

TABLE 4.6. ROUTINES AND PLATFORMS USED IN THE PREPROCESSING STAGE OF THE PROPOSED METHOD FOR A FEM-FIELD EQUATION WITH VOLTAGES KNOWN

Operation Performed	MATLAB platform	GSL platform	CUBLAS platform
1. Preprocessing FEM Stage	ANSYS		
2. Reading information of preprocessing FEM stage	Matlab own-routines	C own-routines	
3. Calculating the FEM matrix & vector of the i-finite element			
4. Assembling FEM matrixes & vectors			
5. Applying boundary conditions		gsl_matrix_set gsl_vector_set	
6. Deriving FEM arrays of the FEM field equation with voltages known			
7. Deriving submatrixes & subvectors		gsl_matrix_get, gsl_vector_get gsl_matrix_set, gsl_vector_set	
8. Deriving final matrices & vectors of the proposed method	Matlab standard matrix routines	gsl_blas_dgemm gsl_blas_dgmev gsl_linalg_LU_solve ₁	cublasSgemm, cublasSgemv cublasSger ¹ cublasStrsm ¹

¹ These routines are used to calculate the matrix inversion shown in Figure 4.7.

4.3.1.2 FEM field equation with currents known

It is also possible to use the proposed methodology, to derive a *reduced* equation from a FEM field equation with currents known. The *preprocessing FEM stage* of this FEM field equation was covered in Section 4.2.1.2.

For this case, the *preprocessing FEM stage* of the *reduced* equation can also be derived by the calculating process, which takes into account the nodes of the *conductor* and the *non-conductor* regions of the FEM coupled equation. The different necessary steps to perform the proposed methodology in a FEM field equation with currents known, are shown in Figure 4.8. The platforms to derive each specific step shown in Figure 4.8 are listed in Table 4.7. It can be seen that it is necessary to use the preprocessing stage shown in Figure 4.7.

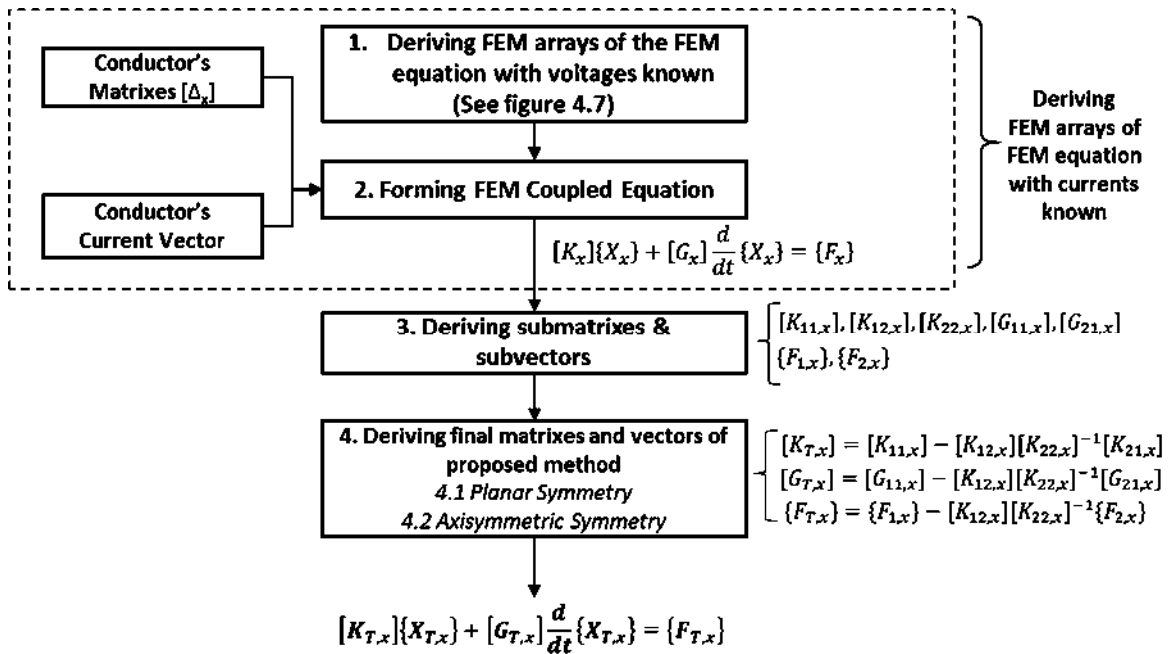


Figure 4.8. *Preprocessing stage* of the methodology applied to a FEM-field equation with currents known

TABLE 4.7. ROUTINES AND PLATFORMS USED IN THE *PREPROCESSING STAGE* OF THE PROPOSED METHOD FOR A FEM-FIELD EQUATION WITH CURRENTS KNOWN

Operation performed	MATLAB platform	GSL platform	CUBLAS platform
1. Deriving FEM arrays of the FEM field equation with voltages known	See Table 4.6	See Table 4.6	
2. Forming FEM coupled equation	Matlab own-routines	<i>gsl_matrix_get, gsl_vector_get</i>	
3. Deriving submatrices & subvectors		<i>gsl_matrix_set, gsl_vector_set</i>	
4. Deriving final matrices & vectors of the proposed method	Matlab standard matrix routines	<i>gsl_blas_dgemm</i> <i>gsl_blas_dgmev</i> <i>gsl_linal_LU_solve</i> ¹	<i>cublasSgemm,</i> <i>cublasSgemv</i> <i>cublasSger</i> ¹ <i>cublasStrsm</i> ¹

Note. ¹ These routines are used to calculate the matrix inversion shown in Figure 4.8.

4.3.1.3 FEM circuit coupled equation

For a device modeled using a FEM-circuit coupled equation, the FEM matrices and vectors can be obtained using the element and node information provided by ANSYS. The FEM-circuit coupled equation consists on a FEM field equation with voltages as the forcing function; the FEM expression that relates the voltage, current and magnetic vector potentials; and finally, a voltage-current equation.

The proposed methodology can be applied in order to get a *reduced* equation from a FEM-circuit coupled equation. The *preprocessing FEM stage* of the reduced equation, uses the calculating process based on the node numbers of the *conductor* and the *non-conductor* regions. The different steps in which is based the proposed methodology is shown in Figure 4.9. Table 4.8 shown the platforms and routines used.

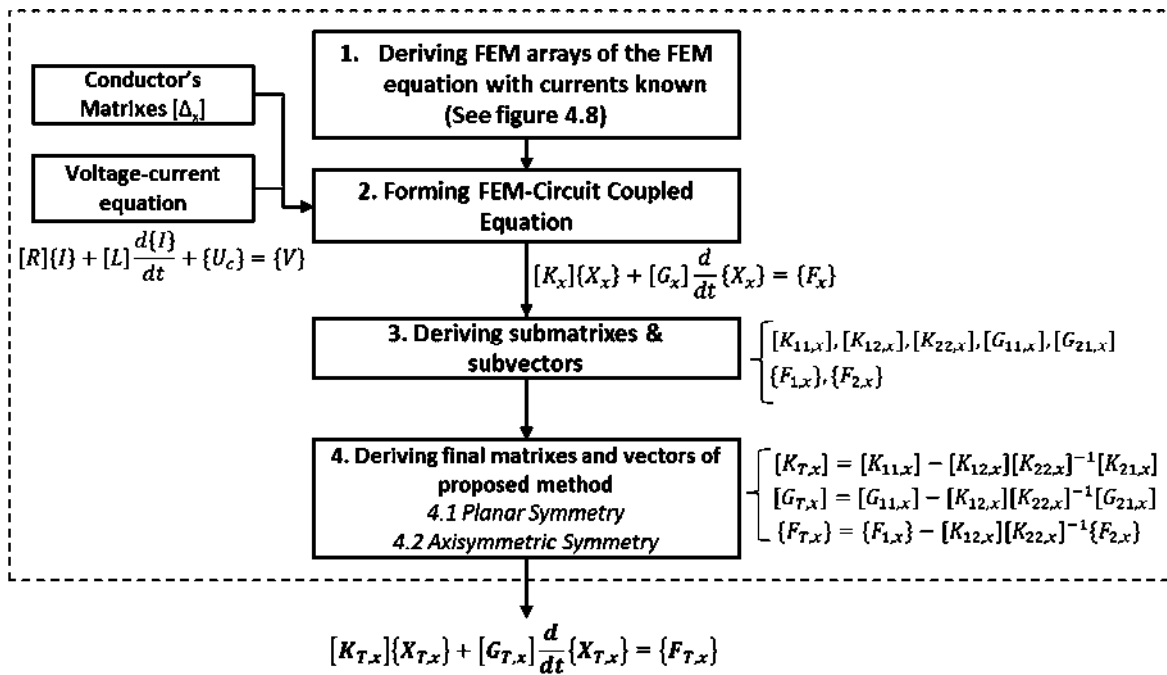


Figure 4.9. *Preprocessing stage* of the methodology applied to a FEM-circuit coupled equation

TABLE 4.8. ROUTINES AND PLATFORMS USED IN THE *PREPROCESSING STAGE* OF THE PROPOSED METHOD FOR A FEM-CIRCUIT COUPLED EQUATION

Operation performed	MATLAB platform	GSL platform	CUBLAS platform
1. Deriving FEM arrays of the FEM field equation with currents known	See Table 4.6	See Table 4.6	
2. Forming FEM coupled equation	Matlab own-routines	<i>gsl_matrix_get</i> , <i>gsl_vector_get</i>	
3. Deriving submatrixes & subvectors		<i>gsl_matrix_set</i> , <i>gsl_vector_set</i>	
4. Deriving final matrices & vectors of the proposed method	Matlab standard matrix routines	<i>gsl_blas_dgemm</i> <i>gsl_blas_dgmev</i> <i>gsl_linal_LU_solve</i> ¹	<i>cublasSgemm</i> , <i>cublasSgemv</i> <i>cublasSgerl</i> <i>cublasStrsm</i> ¹

Note. ¹ These routines are used to calculate the matrix inversion shown in Figure 4.8.

4.3.2. Calculating Stage

The proposed methodology represents an alternative of solution to a FEM field equation with voltages or currents known, and a FEM-circuit coupled equation. Reduced expressions from these FEM equations can be obtained, which can be represented in a general form defined by,

$$[\mathbf{K}_T]\{\mathbf{X}_T\} + \frac{d}{dt}[\mathbf{G}_T]\{\mathbf{X}_T\} = \{\mathbf{f}_T\} \quad (4.9)$$

The Equation (4.9) can be solved in the frequency and in the time domain. Specific details on the solution methods can be consulted in Appendix B of this thesis.

4.3.2.1 Solution in the frequency domain

If (4.9) is solved in the frequency domain, it yields,

$$([\mathbf{K}_T] + j(2\pi f)[\mathbf{G}_T])\{\tilde{\mathbf{X}}_T\} = \{\tilde{\mathbf{f}}_T\} \quad (4.10)$$

Moreover, (4.10) can be represented in a simpler way using,

$$[\mathbf{A}_T]\{\tilde{\mathbf{X}}_T\} = \{\tilde{\mathbf{b}}_T\} \quad (4.11)$$

The reduced equation (4.11) can also be solved in the frequency domain using the *LU* decomposition method. The *LU* method can be solved using sequential and parallel computing platforms. For the case of a sequential solution, the Matlab (MATLAB 2010) and the GSL (GNU Scientific Library 2013) platforms were used. For the case of a parallel solution, the CUBLAS platform was used (NVIDIA 2012), (Barrachina et al. 2008), (CUDA toolkit 5.0 2014). The method is briefly shown in Figure 4.10. Further details of the parallel and the sequential implementation of the *LU* method are given in Chapter 3. All the routines used by each platform are indicated in Table 4.9.

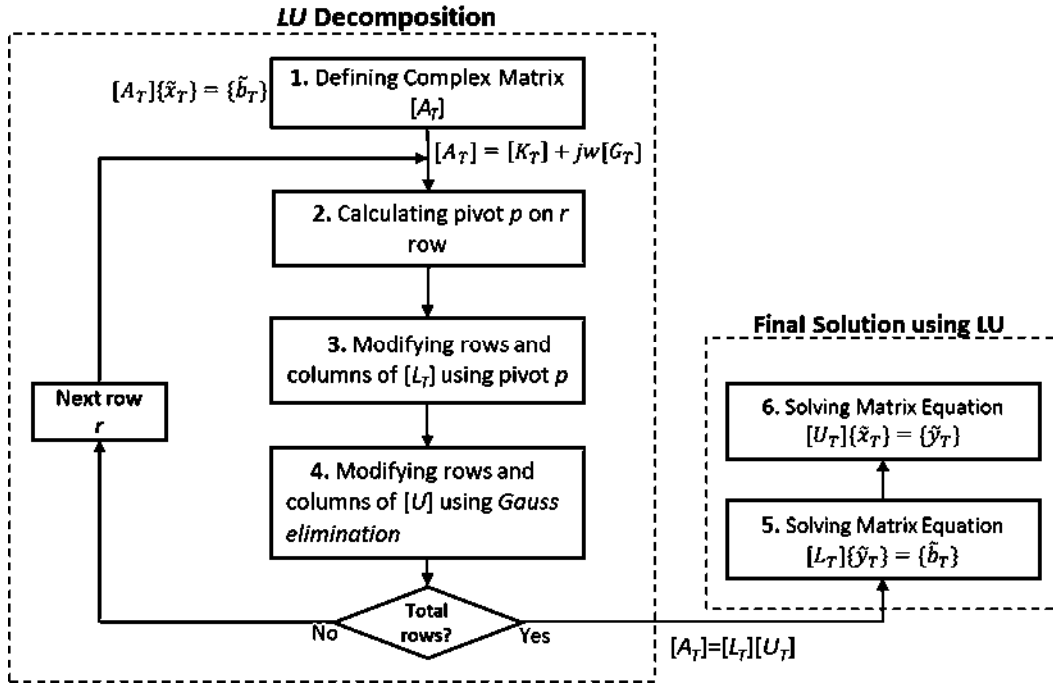


Figure 4.10. Calculating process of the proposed method in the frequency domain

TABLE 4.9. ROUTINES USED IN THE FREQUENCY DOMAIN SOLUTION OF THE REDUCED EQUATION DERIVED FROM THE PROPOSED METHOD

Method	Operation performed	MATLAB Platform	GSL Platform	CUBLAS Platform
		Routine used	Routine used	Routine used
LU decomp. [A _T]= [L _T][U _T]	1. Defining matrix complex [A _T]	MatLab Routine	<i>gsl_matrix_set</i>	Cublas Routine
	2. Calculating pivot <i>p</i> on r-row	NA	<i>gsl_linalg_comple x_LU_decomp</i>	<i>cuCdivf</i>
	3. Modifying rows & columns of [L _T] using pivot <i>p</i>			<i>cublasCscal</i>
	3. Modifying rows & columns of [U _T] using Gauss Elimination			<i>cublasCgeru</i>
Final solution [A _T]{x _T } = {b _T }	5. Solving the 1 st matrix equation [L _T]{y _T } = {b _T }	<i>linsolve</i>	<i>gsl_linalg_comple x_LU_solve</i>	<i>cublasCtsv</i>
	6. Solving the 2 nd matrix equation [U _T]{x _T } = {y _T }			<i>cublasCtsv</i>

4.3.2.2 Solution in the time domain

The Equation (4.9) can be represented in a different way using,

$$[G_T] \frac{d}{dt} \{X_T\} = \{f_T\} - [K_T] \{X_T\} \quad (4.12)$$

It is possible to solve the expression shown in (4.12) in time domain, using the Backwards Euler and the Euler methods. It yields,

$$\left([K_T]_{(t)} + \frac{[G_T]_{(t)}}{\Delta t}\right)\{X_T\}_{(t)} = \{F_T\}_{(t-\Delta t)} + (\Delta t)^{-1}[G_T]_{(t-\Delta t)}\{X_T\}_{(t-\Delta t)} \quad (4.13)$$

$$[\tilde{G}_T]_{(t)}(\Delta t)\{X_T\}_{(t+\Delta t)} = \{F_T\}_{(t)} + \left([\tilde{G}_T]_{(T)}(\Delta t) - [K_T]_{(t)}\right)\{X_T\}_{(t)} \quad (4.14)$$

Where matrix $[A]_{(t)}$ and vector $\{b\}_{(t)}$ for the Backwards Euler method are given by,

$$[A_T]_{(t)} = \left([K_T]_{(t)} + \frac{[G_T]_{(t)}}{\Delta t}\right) \quad (4.15)$$

$$\{b_T\}_{(t)} = \{F_T\}_{(t-\Delta t)} + (\Delta t)^{-1}[G_T]_{(t)}\{X_T\}_{(t-\Delta t)} \quad (4.16)$$

Where the matrix $[A]_{(t)}$ and the vector $\{b\}_{(t)}$ for the Euler method are given by,

$$[A_T]_{(t)} = [\tilde{G}_T]_{(t)}(\Delta t) \quad (4.17)$$

$$\{b_T\}_{(t)} = \{F_T\}_{(t)} + \left([\tilde{G}_T]_{(t)}(\Delta t) - [K_T]_{(t)}\right)\{X_T\}_{(t)} \quad (4.18)$$

The expression (4.14) can be also solved by using the 4th order Runge Kutta method, yielding,

$$\{X_T\}_{(t+\Delta t)} = \{X_T\}_{(t)} + \frac{1}{6}(\{\tilde{k}_{1T}\}_{(t)} + 2\{\tilde{k}_{2T}\}_{(t)} + 2\{\tilde{k}_{3T}\}_{(t)} + \{\tilde{k}_{4T}\}_{(t)}) \quad (4.19)$$

Where the vectors $\{\tilde{k}_{1T}\}_{(t)}$, $\{\tilde{k}_{2T}\}_{(t)}$, $\{\tilde{k}_{3T}\}_{(t)}$, and $\{\tilde{k}_{4T}\}_{(t)}$ are calculated by solving the next four equations,

$$\left((\Delta t)^{-1}[\tilde{G}_T]_{(t)}\right)\{\tilde{k}_{1T}\}_{(t)} = \{F_T\}_{(t)} - [K_T]_{(t)}\{X_T\}_{(t)} \quad (4.20)$$

$$\left[\left(t_n + \frac{\Delta t}{2}\right)^{-1}[\tilde{G}_T]_{(t)}\right]\{\tilde{k}_{2T}\}_{(t)} = \{F_T\}_{(t)} - [K_T]_{(t)}\{X_T\}_{(t)} - \frac{1}{2}[K_T]\{\tilde{k}_{1T}\}_{(t)} \quad (4.21)$$

$$\left[\left(t_n + \frac{\Delta t}{2}\right)^{-1}[\tilde{G}_T]_{(t)}\right]\{\tilde{k}_{3T}\}_{(t)} = \{F_T\}_{(t)} - [K_T]_{(t)}\{X_T\}_{(t)} - \frac{1}{2}[K_T]\{\tilde{k}_{2T}\}_{(t)} \quad (4.22)$$

$$\left[(\mathbf{t}_n + \Delta \mathbf{t})^{-1} [\tilde{\mathbf{G}}_T]_{(t)} \right] \{ \tilde{\mathbf{k}}_{4T} \}_{(t)} = \{ \mathbf{F}_T \}_{(t)} - [\mathbf{K}_T]_{(t)} \{ \mathbf{X}_T \}_{(t)} - [\mathbf{K}_T] \{ \tilde{\mathbf{k}}_{3T} \}_{(t)} \quad (4.23)$$

Observing the equations derived from the Backwards Euler, Euler and 4th order Runge Kutta methods, it can be seen that can also be represented in a general form defined by,

$$[\mathbf{A}]_{(t)} \{ \mathbf{X} \}_{(t)} = \{ \mathbf{b} \}_{(t)} \quad (4.24)$$

It is possible to solve (4.24) using the *LU* decomposition method. For the particular case of the time domain solution, a sequential computing platform will be used. Specifically, the Matlab (MATLAB 2010) and GSL (GNU Scientific Library 2013) platforms were used. Table 4.10 gives the routines used by these platforms. The solution of the reduced equation derived from the methodology is quite similar to the solution of the *conventional* FEM equation.

TABLE 4.10. ROUTINES USED IN THE TIME DOMAIN SOLUTION OF AN CONVENTIONAL FEM EQUATION USING THE BACKWARDS EULER, EULER AND THE 4TH ORDER RUNGE KUTTA METHODS

Method	Operation Performed	MATLAB Platform	GSL Platform
		Routine used	Routine used
<i>LU Decomposition</i> [A] _(t) = [L] _(t) [U] _(t)	1. Defining matrix complex [A] _(t)	<i>MatLab Routine</i>	<i>gsl_matrix_set</i>
	2. Calculating pivot <i>p</i> on r-row	NA	<i>gsl_linalg_LU_decomp</i>
	3. Modifying rows & columns of [L] _(t) using pivot <i>p</i>		
	4. Modifying rows & columns of [U] _(t) using Gauss Elimination		
Final Solution [A] _(t) {X} _(t) = {b} _(t)	5. Solving the 1 st matrix equation [L] _(t) {Y} _(t) = {b} _(t)	<i>linsolve</i>	<i>gsl_linalg_LU_solve</i>
	6. Solving the 2 nd matrix equation [U] _(t) {X} _(t) = {Y} _(t)		

4.4 Conclusions

In this chapter the different routines and platforms used, to solve the conventional FEM expression and the equations derived from the proposed methodology have been discussed. For both cases, three specific type of FEM equations have been solved, i.e. a FEM field equation with voltages known, a FEM field equation with currents known; and finally, a FEM-circuit coupled equation. These FEM expressions are formed by matrices and vectors which are calculated by a *preprocessing stage*.

The different computing platforms and routines that allow defining the *processing stage* of the *conventional* and the *proposed* FEM equation have been explained. For the case of the

conventional FEM equations, the sequential computing platforms Matlab and GSL have been used. Besides, for the case of the proposed methodology, the sequential computing platforms Matlab and GSL have been used; as well as the parallel computing platform CUBLAS.

It is important to mention, that the ANSYS FEM software has been used. This software can model the geometry of the device using the finite element analysis; thus, it is possible to generate the information of the finite element and the nodes used in the modeling of the device. Using this information the matrices and vectors that form the FEM equations can be calculated. The process of forming the finite elements in the modeling of the device using ANSYS has been identified as the *processing FEM stage*. The *preprocessing FEM stage* of the proposed method is slightly different, since it requires the consecutive meshing of the *conductor region*.

Finally in this chapter has been shown, the platforms and routines used in the frequency and the time domain solution of the FEM equations. The process of solving the *conventional* FEM and the equation derived by the methodology, is named as *calculating stage*. The solution of the *conventional* FEM equations and those equations derived from the proposed methodology are quite similar. The difference relies on the order of the matrix equation to be solved.

5 Case studies

5.1 Introduction

In this chapter, several case studies of devices whose field equation have been simplified either by a planar or an axisymmetric symmetry assumption will be presented. Using the finite element analysis, it is possible to solve these field equations in an easier way, since the symmetry assumption simplifies the complexity of the analysis. The finite element analysis permits to derive a FEM field or a FEM-circuit coupled equation, which can be solved in the frequency and the time domain. However, these equations may be difficult to solve because their matrix order can be of large dimensions.

This investigation proposes a methodology which allows to simplify the FEM equations in order to solve them in the time or in the frequency domain. Although the time domain solution was a priority of this investigation, the advantages of applying the methodology in the frequency domain was evident during the development of this investigation.

Further details about the methodology are given in Chapter 3. However, a brief summary is as follows: it consists on performing a renumbering of the magnetic vector potentials of the conductor regions. Using this new criterion and performing a reordering of the variables with non-null derivative respect the time, it is possible to derive a new FEM equation. Using this equation and performing several matrix operations, it is possible to derive a completely new FEM expression. This equation is of lower order and is defined in terms of the time varying variables.

Although the proposed methodology has been widely explained in Chapter 3, in this chapter this methodology will be applied to the solution of several devices. These devices will be analyzed by conventional finite element analysis, but they will be also analyzed using the proposed methodology. It is important to mention, the assumptions made in the finite element analysis:

1. Plane or axisymmetric symmetry on behavior of the magnetic field

For the case of the devices with a *planar symmetry* assumption, it is considered that the magnetic field behavior through the z -axis of the conductor is the same. Because of this assumption, the magnetic vector potential is only defined in the z -axis (Ho, Li and Fu 1999), (Arkkio 1987), (Bianchi 2005). For the case of device with an *axisymmetric symmetry* assumption, it is considered that the field behavior is the same through the ρ -axis. This allows assuming that the magnetic vector potentials is defined by the plane formed by the r and z axis (Preiss 1983), (Konrad, Chari and Csendes 1982).

2. Displacement current neglected

The frequency of the voltage sources is low enough, to neglect the displacement current in the Maxwell field equations (Ho, Li and Fu 1999), (Arkio 1987), (Bianchi 2005).

3. Constant permeability and conductivity

The permeability over all the regions and the conductor conductivity are considered to be all constant.

4. Unique voltage applied through the conductor regions

It is assumed that there are no voltage differences at all points of conductor regions. The source current density in the conductors is constant over each cross-sectional surface (Preiss 1983), (Konrad 1982).

After explaining the main assumptions made for the analysis of the devices, the study cases related to devices modelled by a planar or an axisymmetric symmetry assumption will be explained and the main conclusions drawn.

5.2 Planar symmetry assumption cases

5.2.1 Case study 1. Slot embedded conductors modeled by a one-dimension finite element analysis and by a FEM-circuit coupled equation

5.2.1.1 Introduction

The example to be analyzed consists on solving a FEM-circuit coupled equation that models three identical slot conductors, coupled with a two loop circuit that contains several resistances and inductances. A Finite Element Analysis can be performed in the three conductors. It is considered that the conductors have a Neumann boundary along their vertical walls. This assumption permits to consider the conductors independent from each other. Further details about the conductors' dimension and their characteristics can be consulted in (Konrad 1981), (Konrad 1982), (Jafari-Shapoorabadi, Konrad and Sinclair 2002), (ANSYS 2010). The conductors are shown in Figure 5.1, the two-loop circuit in Figure 5.2.

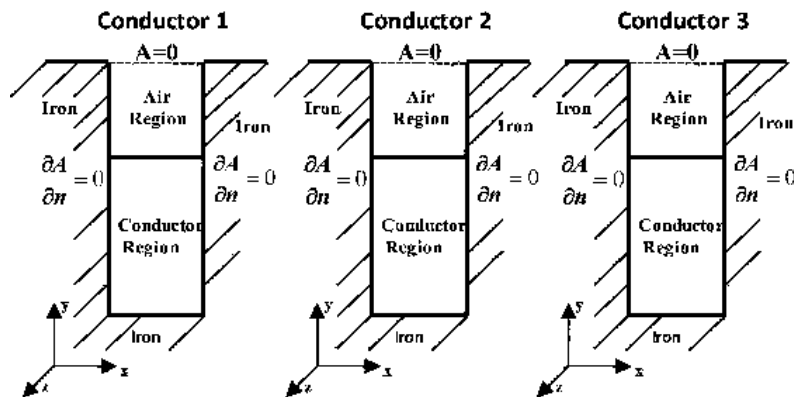


Figure 5.1. Scheme of the three slot embedded conductors.

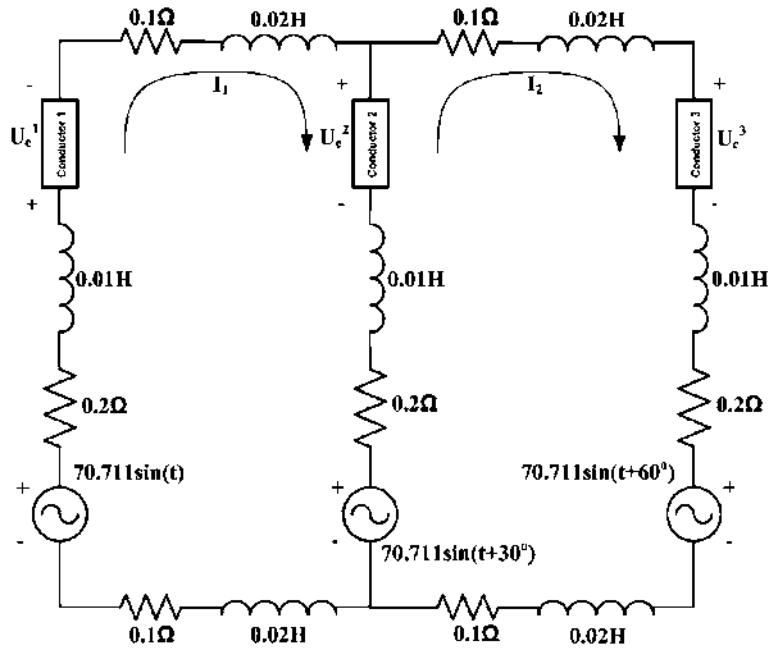


Figure 5.2. Two loop circuit used for the Example.

It is assumed that the embedded conductors can be modeled through plane symmetry, to allow a one dimension finite element analysis. The one dimension FEM discretization considered for the conductors is shown in Figure 5.3. Further details about the conductors' one dimension finite element model are given in (Konrad 1981), (Konrad 1982), (Jafari-Shapoorabadi, Konrad and Sinclair 2002), (ANSYS 2010). The electrical and magnetic parameters of the conductors are listed in Table 5.1.

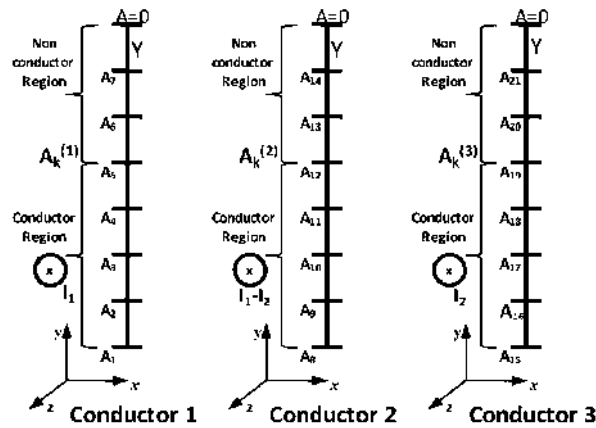


Figure 5.3. FEM discretization of the conductors

TABLE 5.1
PARAMETERS OF THE CONDUCTORS AND THE VOLTAGE-CURRENT EQUATION

	Parameter	Symbol	Value
Voltage-Current Equation's Parameters	Voltage vector, {V}	V_1	36.6sin(t-75°) V
		V_2	36.6sin(t-45°) V
	Voltage angular speed	w	1 rad/s
	Elements of $[R_{ij}]$	R_{11}, R_{22}	0.60 Ω
		R_{12}, R_{21}	-0.20 Ω
	Elements of $[L_{ij}]$	L_{11}, L_{22}	0.06 H
L_{12}, L_{21}		-0.01 H	
Conductors Parameters	Resistance	$R_c^{(1)}, R_c^{(2)}, R_c^{(3)}$	0.25 Ω
	Length	l	1 m
	Area	S_c	4 m ²
	Conductivity	σ	1.0 Ω ⁻¹ ·m ⁻¹

5.2.1.2 Two-loop circuit voltage-current equation

If a circuit voltage-loop analysis is performed for the two loop circuit, a voltage-current equation can be obtained, i.e.

$$[R_{ij}]\{I\} + [L_{ij}] \frac{d}{dt} \{I\} + [b]\{U_c\} = \{V\} \quad (5.1)$$

Where $[b]$ is given by,

$$[b] = \begin{bmatrix} 1 & 1 & 0 \\ 0 & -1 & 1 \end{bmatrix} \quad (5.2)$$

And $\{I\}$ and $\{U_c\}$ are the unknown currents and voltages; $[R_{ij}]$ and $[L_{ij}]$ are the resistance and inductance matrices; $\{V\}$ is the voltage vector, all defined in Table 5.1. The components of these matrices and vectors are in Table 5.1.

5.2.1.3 Field equations of the device

If the assumptions mentioned at the beginning of this chapter are considered in the conductor modelling; two regions can be identified: a *non-conductor* region, where there is no voltage excitation; and a *conductor* region, which is supplied with a voltage source and includes the skin effect (Escarela-Perez, Melgoza and Alvarez-Ramirez 2009). The field equations of these regions is defined by the field equation shown in (2.10).

5.2.1.4 Finite Element Analysis

It is possible to perform a finite element on the field (2.10), in order to derive a FEM equation, with the conductor voltage as the forcing function. At the same time, a Newton Cotes Analysis can be performed on (2.11) in order to derive another FEM equation. Details about the finite element equations can be consulted in Chapter 2. The FEM expressions

derived from these analysis are defined by,

$$[S_{11}^G]\{A_k\} + [T_{11}^G] \frac{d}{dt} \{A_k\} = -(R_c^{-1})\{T_{31}^G\}\{U_c\} \quad (5.3)$$

$$(R_c)[b]^T\{I\} + \{T_{31}^G\} \frac{d\{A\}}{dt} = \{U_c\} \quad (5.4)$$

The vectors A_k and $\{U_c\}$ of (5.3) and (5.4) are defined by the magnetic vector potentials and the voltages applied on terminals of each conductor,

$$A_k = \{A_k^{(1)} \quad A_k^{(2)} \quad A_k^{(3)}\}^T \quad (5.5)$$

$$\{U_c\} = \{U_c^{(1)} \quad U_c^{(2)} \quad U_c^{(3)}\}^T \quad (5.6)$$

The matrices $[S_{11}^G]$, $[T_{11}^G]$ and $[T_{31}^G]$ of (5.3) and (5.4) are defined by,

$$S_{11}^G = [S_{kk}^{(1)} \quad S_{kk}^{(2)} \quad S_{kk}^{(3)}]_{3 \times 3}^{diag} \quad (5.7)$$

$$T_{11}^G = [T_{kk}^{(1)} \quad T_{kk}^{(2)} \quad T_{kk}^{(3)}]_{3 \times 3}^{diag} \quad (5.8)$$

$$T_{31}^G = (R_c)[\{M\}_k^{(1)} \quad \{M\}_k^{(2)} \quad \{M\}_k^{(3)}]_{3 \times 3}^{diag} \quad (5.9)$$

The notation $[]^{(n)}$ and $\{ \}^{(n)}$ indicates that the matrix $[]$ and the vector $\{ \}$ respectively; are associated to the conductor n , where $n=1,2,3$. The matrices $S_{kk}^{(i)}$, $T_{kk}^{(i)}$ and $\{M\}_k^{(i)}$ are obtained from applying the finite element and the Newton Cotes analysis on each i -embedded conductor. The FEM discretization shown in Figure 5.3 has been considered. The matrices $S_{kk}^{(n)}$, $T_{kk}^{(n)}$ $\{M\}_k^{(n)}$ of conductors can be consulted in (Konrad 1981).

5.2.1.5 FEM-circuit coupled equation

It is possible to obtain the FEM-circuit coupled equation of the two-loop circuit and the embedded conductors. This can be achieved by coupling the FEM equations (5.3) and (5.4) with the voltage-current equation defined in (5.1). It yields,

$$\begin{bmatrix} S_{11}^G & \mathbf{0} & -(R_c^{-1}T_{31}^G)^T \\ \mathbf{0} & [R_{ij}] & [b] \\ \mathbf{0} & (R_c)[b]^T & -\{1\} \end{bmatrix} \begin{Bmatrix} A_k \\ \{I\} \\ \{U_c\} \end{Bmatrix} + \begin{bmatrix} T_{11}^G & \mathbf{0} & \mathbf{0} \\ \mathbf{0} & [L_{ij}] & \mathbf{0} \\ T_{31}^G & \mathbf{0} & \mathbf{0} \end{bmatrix} \frac{d}{dt} \begin{Bmatrix} A_k \\ \{I\} \\ \{U_c\} \end{Bmatrix} = \begin{Bmatrix} \mathbf{0} \\ \{V\} \\ \mathbf{0} \end{Bmatrix} \quad (5.10)$$

5.2.1.6 Solution derived by the proposed methodology

It is possible to use the method explained in Chapter 3 to obtain the vector of magnetic potentials and currents of conductors. As a first step, it is necessary to perform a nodal renumbering in the vector of magnetic potentials of the *conductor* region and the *non-conductor* region of conductors. The proposed FEM discretization for the conductors is shown in Figure 5.4. Please notice that nodes have been renumbered in the *conductor* and the *non-conductor* regions, to make them consecutive.

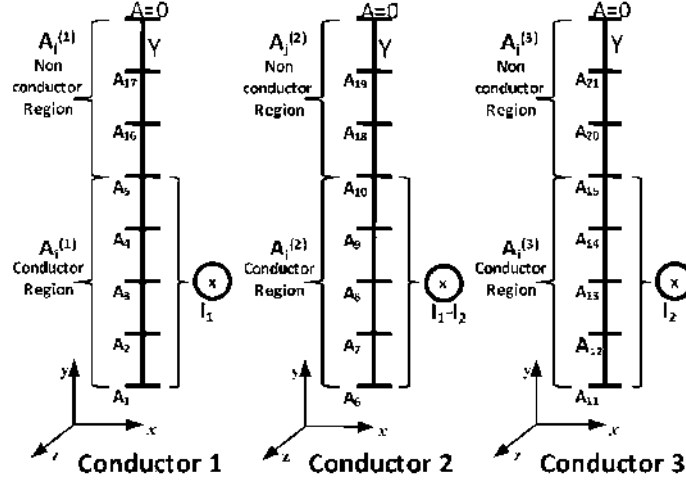


Figure 5.4. Proposed FEM discretization of the conductors.

Taking into account the FEM discretization shown in Figure 5.4, it is possible to obtain a new FEM circuit-coupled equation, by deriving new FEM field equations for each conductor and by coupling them with the voltage-current equation defined in (5.1). It is also possible to redefine (5.4). The new FEM equations are now defined by,

$$\begin{bmatrix} S_{ii} & S_{ij} \\ S_{ij}^T & S_{jj} \end{bmatrix} \begin{Bmatrix} A_i \\ A_j \end{Bmatrix} + \begin{bmatrix} T_{ii} & \mathbf{0} \\ \mathbf{0} & \mathbf{0} \end{bmatrix} \frac{d}{dt} \begin{Bmatrix} A_i \\ A_j \end{Bmatrix} = \{ (R_c^{-1}T_{31})^T \} \{U_c\} \quad (5.11)$$

$$(R_c)[b]^T \{I\} + \{T_{31}\} \frac{dA_i}{dt} = \{U_c\} \quad (5.12)$$

Where the vectors A_i and A_j of (5.11) and (5.12) are defined by,

$$A_i = \{A_i^{(1)} \quad A_i^{(2)} \quad A_i^{(3)}\}^T \quad (5.13)$$

$$A_j = \{A_j^{(1)} \quad A_j^{(2)} \quad A_j^{(3)}\}^T \quad (5.14)$$

And the matrices of (5.11) and (5.12) are given by,

$$S_{ii} = [S_{11}^{(1)} \quad S_{11}^{(2)} \quad S_{11}^{(3)}]_{3 \times 3}^{diag} \quad (5.15)$$

$$S_{ij} = [S_{12}^{(1)} \quad S_{12}^{(2)} \quad S_{12}^{(3)}]_{3 \times 3}^{diag} \quad (5.16)$$

$$S_{jj} = [S_{22}^{(1)} \quad S_{22}^{(2)} \quad S_{22}^{(3)}]_{3 \times 3}^{diag} \quad (5.17)$$

$$T_{ii} = [G_{ii}^{(1)} \quad G_{ii}^{(2)} \quad G_{ii}^{(3)}]_{3 \times 3}^{diag} \quad (5.18)$$

$$T_{31} = (R_c)[\{M_i\}^{(1)} \quad \{M_i\}^{(2)} \quad \{M_i\}^{(3)}]_{3 \times 3}^{diag} \quad (5.19)$$

If the equations (5.11) and (5.12) are coupled to the voltage-current equation (5.1), a new FEM-circuit coupled equation can be obtained. Besides, time varying variables can be reordered, in order to separate them from the variables whose derivative respect the time is zero. It yields,

$$\begin{bmatrix} S_{ii} & \mathbf{0} & (-R_c^{-1}T_{31})^T & S_{ij} \\ \mathbf{0} & [R_{ij}] & [b] & \mathbf{0} \\ \mathbf{0} & (R_c)[b]^T & -\{1\} & \mathbf{0} \\ S_{ij}^T & \mathbf{0} & \mathbf{0} & S_{jj} \end{bmatrix} \begin{Bmatrix} A_i \\ \{I\} \\ \{U_c\} \\ A_j \end{Bmatrix} + \begin{bmatrix} T_{ii} & \mathbf{0} & \mathbf{0} & \mathbf{0} \\ \mathbf{0} & \mathbf{0} & \mathbf{0} & \mathbf{0} \\ T_{31} & \mathbf{0} & \mathbf{0} & \mathbf{0} \\ \mathbf{0} & \mathbf{0} & \mathbf{0} & \mathbf{0} \end{bmatrix} \frac{d}{dt} \begin{Bmatrix} A_i \\ \{I\} \\ \{U_c\} \\ A_j \end{Bmatrix} = \begin{Bmatrix} \mathbf{0} \\ \{V\} \\ \mathbf{0} \\ \mathbf{0} \end{Bmatrix} \quad (5.20)$$

It is possible to perform a matrix partition on (5.20), i.e.

$$\begin{bmatrix} K_{11} & K_{11} \\ K_{11} & K_{22} \end{bmatrix} \begin{Bmatrix} x_1 \\ x_2 \end{Bmatrix} + \begin{bmatrix} G_{11} & \mathbf{0} \\ G_{21} & \mathbf{0} \end{bmatrix} \frac{d}{dt} \begin{Bmatrix} x_1 \\ x_2 \end{Bmatrix} = \begin{Bmatrix} f_1 \\ f_2 \end{Bmatrix} \quad (5.21)$$

The submatrices and subvectors of (5.21) have been previously defined in (3.40)-(3.45) and (3.46)-(3.48), respectively. It is possible to derive the reduced equation from (5.21). It yields,

$$K_T x_1 + G_T \frac{d}{dt} x_1 = f_T \quad (5.22)$$

Where the matrices K_T and G_T and the vector f_T of (5.22) can be calculated using (3.49), (3.50) and (3.51), respectively.

The time varying variables of (5.10) are the vectors A_i and $\{I\}$. These variables can be directly calculated using (5.22). Once the FEM-circuit coupled and the equation derived by the method are obtained, both approaches can be solved in the frequency and the time domain. Thus, a comparison results can be made on both approaches. These results can be compared with those derived by a FEM simulation performed in ANSYS, as explained next.

5.2.1.7 Comparison results in frequency domain

A first comparison of results is performed in the frequency domain. Details about how a FEM equation is solved in the frequency domain are given in Appendix B. In order to know if the magnetic potentials and currents calculated with (5.10), and those calculated with the proposed methodology are correct; a FEM simulation was performed in ANSYS. Some of the results of conductors magnetic potentials and currents, obtained with the FEM-circuit coupled equation that assumes the FEM discretization shown in Figure 5.4 are included in Table 5.2. Table 5.2 also included the results obtained with proposed equation which assumes the same FEM discretization.

TABLE 5.2
MAGNETIC VECTOR POTENTIALS (MVP) AND CURRENTS IN THE FREQUENCY DOMAIN

MVP (Wb/m) Currents (A)	ANSYS	Conv. FEM-circ. coupled Equation	% Error	Proposed Method	% Error
A_1	25.090	24.888	-0.805	24.888	-0.805
A_2	25.196	24.992	-0.809	24.992	-0.809
A_3	25.113	24.928	-0.737	24.928	-0.737
A_4	23.677	23.576	-0.427	23.576	-0.427
A_6	4.550	4.512	-0.835	4.512	-0.835
A_7	4.570	4.531	-0.833	4.531	-0.833
A_8	4.554	4.519	-0.769	4.519	-0.769
A_9	4.294	4.274	-0.466	4.274	-0.466
A_{11}	25.231	25.028	-0.804	25.028	-0.804
A_{12}	25.338	25.132	-0.813	25.132	-0.813
A_{13}	25.254	25.068	-0.737	25.068	-0.737
I_1	6.411	6.412	0.015	6.412	0.015
I_2	6.447	6.448	0.015	6.448	0.015

An error percentage (*%Error*), for each magnetic vector potential or current included in Table 5.2 was calculated using,

$$\%Error = \frac{X_{norm} - X_{prop}}{X_{norm}} (100\%) \quad (5.23)$$

Where X_{norm} is the magnetic vector potential or current derived by ANSYS in the frequency domain; X_{prop} is the magnetic vector potential or current calculated by (5.22) or conventional FEM equation (5.10). Comparing the results, it can be observed that the proposed method permits to get an accurate solution in the frequency domain. Additionally, it was measured the computing time of solving the proposed equation. It was obtained a time

reduction of 5.0%, compared to time required for solving the conventional FEM equation (5.10). A more detailed performance comparison was performed in the time domain solution that will be outlined next.

5.2.1.8 Comparison results in time domain

A second comparison is now performed in the time domain using the Backwards Euler method. Details of solution of the FEM equation in time domain using the Backwards Euler method are given in Appendix B. The results are given in Table 5.3.

TABLE 5.3
MAGNETIC VECTOR POTENTIALS (MVP) AND CURRENTS IN THE TIME DOMAIN USING THE
BACKWARDS-EULER METHOD

MVP (Wb/m) Currents (A)	ANSYS	Conv. FEM-circ. coupled Eq.	% Error	Proposed Method	% Error
A_1	25.090	24.888	-0.805	24.888	-0.805
A_2	25.196	24.992	-0.809	24.992	-0.809
A_3	25.113	24.928	-0.737	24.928	-0.737
A_4	23.677	23.576	-0.427	23.576	-0.427
A_6	4.550	4.512	-0.835	4.512	-0.835
A_7	4.570	4.531	-0.833	4.531	-0.833
A_8	4.554	4.519	-0.769	4.519	-0.769
A_9	4.294	4.274	-0.466	4.274	-0.466
A_{11}	25.231	25.028	-0.804	25.028	-0.804
A_{12}	25.338	25.132	-0.813	25.132	-0.813
A_{13}	25.254	25.068	-0.737	25.068	-0.737
I_1	6.411	6.412	0.015	6.412	0.015
I_2	6.447	6.448	0.015	6.448	0.015

The solution in the time domain considers that $\Delta t=0.001$ s. *Rms* values of the variables are shown

An excellent agreement was achieved with the results derived from the Backwards Euler method, a maximum error of 0.8% was obtained. The error percentage (*%Error*), for each magnetic vector potential or current calculated with the proposed methodology and with (5.10) has been included in Table 5.3. The variable X_{norm} is the magnetic vector potential or current obtained with ANSYS; while X_{prop} is the magnetic vector potential or current obtained by solving the proposed equation (5.22) and the conventional equation (5.10) in the time domain. It has been obtained accurate results with lesser computer effort. A performance comparison was made between the conventional and the proposed method, and it will be covered in the next Section.

The 4th order Runge Kutta and the Euler methods are also used to perform a comparison in the time domain. These methods can be used to derive an approximate solution of the proposed equation, given as,

$$K_T x_1 + \bar{G}_T \frac{d}{dt} x_1 = f_T \quad (5.24)$$

Where the matrix \bar{G}_t shown in (5.24) is calculated using,

$$\bar{G}_T = G_{11} - K_{12}K_{22}^{-1}\bar{G}_{21} \quad (5.25)$$

$$\bar{G}_{21} = [\bar{T}_{31} \quad \mathbf{0}]_{2 \times 2}^{diag} \quad (5.26)$$

$$\bar{\bar{T}}_{31} \cong T_{31} \quad (5.27)$$

The Euler and the 4th order Runge Kutta method consider a matrix $\bar{\bar{T}}_{31}$ defined by (5.28) and (5.29), respectively.

$$\bar{\bar{T}}_{31} = 0.9945 T_{31} \quad (5.28)$$

$$\bar{\bar{T}}_{31} = 0.9960 T_{31} \quad (5.29)$$

The results obtained from solving the conventional and the proposed equation are given in Table 5.4. The error (*%Error*) shown in Table 5.4 was calculated using (5.23). X_{norm} is the vector of magnetic potentials or currents obtained by solving (5.10) using the Backwards Euler method; X_{prop} is obtained by solving (5.22), using the Euler and the 4th order Runge Kutta methods.

TABLE 5.4
MAGNETIC VECTOR POTENTIALS (MVP) AND CURRENTS IN THE TIME DOMAIN USING THE BACKWARDS EULER AND THE RUNGE KUTTA METHODS

MVP (Wb/m) Current (A)	Back-Euler Conv. FEM-Circ. Equation	Euler Proposed Method	% Error	Runge K. Proposed Method	% Error
A ₁	25.090	24.887	-0.809	24.887	-0.809
A ₂	25.196	24.991	-0.814	24.991	-0.814
A ₃	25.113	24.927	-0.741	24.927	-0.741
A ₄	23.677	23.574	-0.435	23.574	-0.435
A ₆	4.550	4.517	-0.725	4.517	-0.725
A ₇	4.570	4.535	-0.744	4.535	-0.744
A ₈	4.554	4.523	-0.681	4.523	-0.681
A ₉	4.294	4.278	-0.373	4.278	-0.373
A ₁₁	25.231	25.031	-0.793	25.031	-0.793
A ₁₂	25.338	25.136	-0.797	25.136	-0.797
A ₁₃	25.254	25.071	-0.725	25.071	-0.725
A ₁₄	23.811	23.710	-0.424	23.710	-0.424
I ₁	6.411	6.412	0.015	6.412	0.015
I ₂	6.447	6.449	0.015	6.449	0.015

The solution in the time domain considers that $\Delta t=0.001s$. *Rms* values of the variables are shown

Although the Euler and the 4th order Runge Kutta methods derive an approximate solution of (5.22) in the time domain, it can be seen that an excellent agreement was achieved when

they are used. An error of almost 0.8% was obtained when the 4th order Runge Kutta method was used. The Euler method allows a solution with a maximum error of almost 0.6%.

It is important to mention that the time-domain solution of the equation derived by the methodology, requires lesser computer effort than the required for solving the conventional FEM equation (5.10). A performance comparison of the time domain solution will be outlined next.

5.2.1.9 Performance comparison

The proposed method allows to directly calculate the time varying variables. For the case of the example analyzed, the proposed equation is of 15 order; while the original FEM circuit coupled matrix is of 26 order. The derived equation by the proposed method is easier to solve either in the frequency or in the time domain. It is significantly faster, as will be demonstrated next.

In order to quantify the performance of the equation derived by the proposed method, the simulation time was measured. The simulation time needed to solve a conventional FEM-circuit coupled equation was measured in order to make a comparison. Both equations were solved with separate Matlab programs; a PC with 1GB RAM, AMD Turion-two cores 1.90GHz processor, Windows®-XP 32 bit platform was used.

The equations were solved in the time domain using the Backwards Euler method; a total simulation time of 63s and $\Delta T=0.001s$ were chosen. The proposed equation (5.22) and the conventional FEM-circuit coupled equation (5.10) were solved seven times in order to quantify the required solution time. The simulation time was obtained using the Matlab *cputime* function. The results are listed in Table 5.5. It can be observed that the equation derived by the proposed method, allows a faster solution that the conventional equation (5.10). For the case study, it is more than 5% faster.

The time varying variables can be calculated without knowing the magnetic vector potentials of the *non-conductor* region. It is also possible to calculate the conductors' voltage since the magnetic vector potentials of the *conductor* region are already known.

TABLE 5.5
COMPUTING TIME TO SOLVE THE EQUATIONS IN THE TIME DOMAIN

Simulation Number	FEM-Circuit Coupled Equation	Proposed Methodology	% Diff
1	284.97s	271.31s	-4.79
2	288.30s	269.78s	-6.42
3	286.52s	256.33s	-10.53
4	284.33s	263.20s	-7.43
5	274.97s	266.06s	-3.24
6	274.10s	270.30s	-1.38
7	290.48s	270.11s	-7.01
Average	283.38s	266.72s	-5.87

5.2.2 Case study 2. Slot embedded conductors modeled by a two-dimension finite element analysis, and by a FEM-circuit coupled equation

5.2.2.1 Introduction

The example to be analyzed consists on solving the same FEM-circuit coupled equation that models three identical and independent slot embedded conductors. In the last case study, a one-dimension Finite Element Analysis was considered; but now, a two-dimension finite element analysis will be used (Konrad 1981), (Konrad 1982), (ANSYS 2010). Moreover, the same boundary conditions and the two-loop circuit will be considered. It is assumed that the conductors can be modeled by a plane symmetry, which allows to perform a two dimension finite element analysis (Konrad 1982), (Escarela-Perez, Melgoza and Alvarez-Ramirez 2009). The parameters of the conductors can be shown in Table 5.1. The two-dimension FEM discretization of the three slot embedded conductors is shown in Figure 5.5.

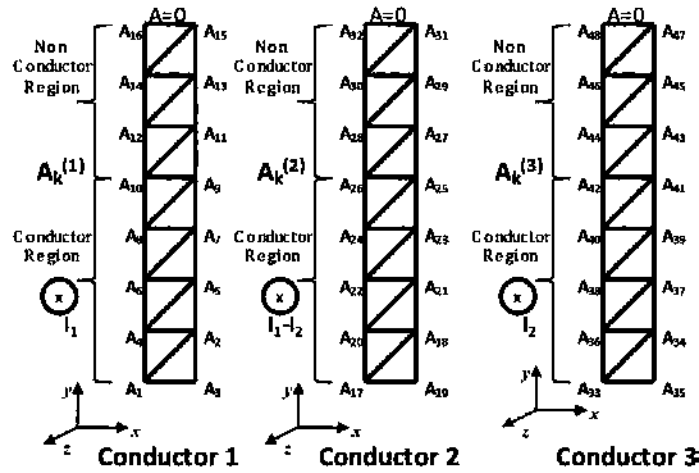


Figure 5.5. FEM discretization of the three slot conductors.

5.2.2.2 Two-loop circuit voltage-current equation

The same voltage-current equation for the two-loop circuit is considered. The equation was already defined in (5.1).

5.2.2.3 Field equations of the device

It is considered the same field equations for the *conductor* and the *non-conductor* region of the embedded conductors. The same expression that relates the magnetic vector potentials, voltages and currents of the conductors is also considered.

5.2.2.4 Finite element analysis

It is possible to perform a two dimension finite element analysis in the field equation, in order to derive a unique FEM equation. At the same time, a Newton Cotes analysis can be performed in the field equation that relates the magnetic vector potentials with the conductors

voltages and currents. Further details about the Finite Element analysis can be consulted in Chapter 2. The FEM expressions has the same form of (5.3) and (5.4), respectively. However, it is important to remark that they correspond now to a two-dimension finite element analysis.

5.2.2.5 FEM-circuit coupled equation

The FEM-circuit coupled equation of the example, results from coupling the FEM equations with the voltage-current equation of the two-loop circuit. Although the FEM expression is the same as that used for the case study 1 (Section 5.2.1), it will be shown again,

$$\begin{bmatrix} S_{11}^G & \mathbf{0} & -(R_c^{-1}T_{31}^G)^T \\ \mathbf{0} & [R_{ij}] & [b] \\ \mathbf{0} & -[b]^T & [R_c]^{-1} \end{bmatrix} \begin{Bmatrix} A_k \\ \{I\} \\ \{U_c\} \end{Bmatrix} + \begin{bmatrix} T_{11}^G & \mathbf{0} & \mathbf{0} \\ \mathbf{0} & [L_{ij}] & \mathbf{0} \\ T_{31}^G & \mathbf{0} & \mathbf{0} \end{bmatrix} \frac{d}{dt} \begin{Bmatrix} A_k \\ \{I\} \\ \{U_c\} \end{Bmatrix} = \begin{Bmatrix} \mathbf{0} \\ \{V\} \\ \mathbf{0} \end{Bmatrix} \quad (5.30)$$

The vectors A_k and $\{U_c\}$ of (5.30) were previously defined in (5.5) and (5.6), while the matrices were defined in (5.7), (5.8), and (5.9).

5.2.2.6 Solution derived by the proposed methodology

It is possible to use the method explained in Chapter 3, in order to solve the vector of conductor magnetic potentials and currents of this case study. As a first step, it is necessary to perform a nodal renumbering on the magnetic vector potentials of the *conductor* region and the *non-conductor* regions of the three embedded conductors. The proposed FEM discretization for the conductors is illustrated in Figure 5.6. Please notice that the nodes have been renumbered in the *conductor* and the *non-conductor* regions, in order to make them consecutive.

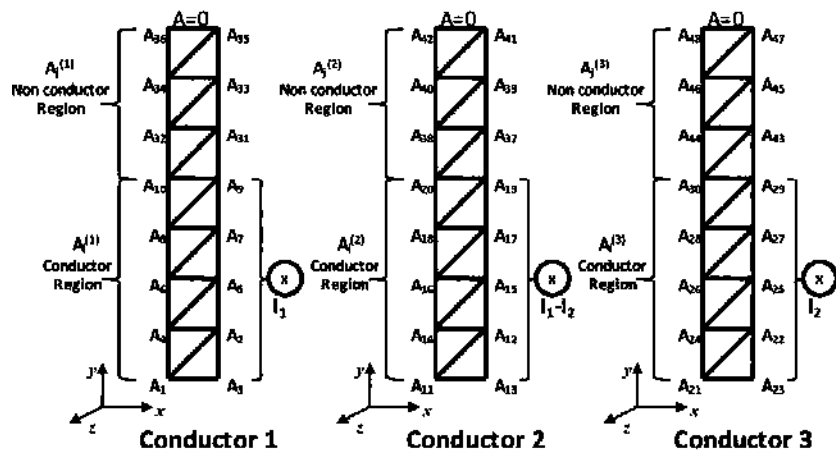


Figure 5.6. Proposed FEM discretization of the three slot conductors.

Taking into account the FEM discretization shown in Figure 5.6, it is possible to get a new FEM circuit-coupled equation, by obtaining new FEM field equations on each conductor,

and coupling them with the voltage-current equation defined in (5.1). It is also possible to re-define the expression defined in (5.8) using the FEM discretization shown in Figure 5.6. The new FEM equations are now,

$$\begin{bmatrix} S_{ii} & S_{ij} \\ S_{ij}^T & S_{jj} \end{bmatrix} \begin{Bmatrix} A_i \\ A_j \end{Bmatrix} + \begin{bmatrix} T_{ii} & \mathbf{0} \\ \mathbf{0} & \mathbf{0} \end{bmatrix} \frac{d}{dt} \begin{Bmatrix} A_i \\ A_j \end{Bmatrix} = \{((R_c^{-1})T_{31})^T\} \{U_c\} \quad (5.31)$$

$$(R_c)[b]^T \{I\} + [T_{31}] \frac{dA_i}{dt} = \{U_c\} \quad (5.32)$$

If the expressions (5.31) and (5.32) are coupled to the voltage-current equation defined in (5.1), it is possible to get a new FEM-circuit coupled equation. Moreover, the time varying variables can be reordered, in order separate them from the variables whose derivative respect the time is zero, i.e.

$$\begin{bmatrix} S_{ii} & \mathbf{0} & (-R_c^{-1})T_{31})^T & S_{ij} \\ \mathbf{0} & [R_{ij}] & [b] & \mathbf{0} \\ \mathbf{0} & -(R_c)[b]^T & -\mathbf{1} & \mathbf{0} \\ S_{ij}^T & \mathbf{0} & \mathbf{0} & S_{jj} \end{bmatrix} \begin{Bmatrix} A_i \\ \{I\} \\ \{U_c\} \\ A_j \end{Bmatrix} + \begin{bmatrix} T_{ii} & \mathbf{0} & \mathbf{0} & \mathbf{0} \\ \mathbf{0} & \mathbf{0} & \mathbf{0} & \mathbf{0} \\ T_{31} & \mathbf{0} & \mathbf{0} & \mathbf{0} \\ \mathbf{0} & \mathbf{0} & \mathbf{0} & \mathbf{0} \end{bmatrix} \frac{d}{dt} \begin{Bmatrix} A_i \\ \{I\} \\ \{U_c\} \\ A_j \end{Bmatrix} = \begin{Bmatrix} \mathbf{0} \\ \{V\} \\ \mathbf{0} \\ \mathbf{0} \end{Bmatrix} \quad (5.33)$$

It is possible to perform a matrix partition on (5.33), i.e.

$$\begin{bmatrix} K_{11} & K_{11} \\ K_{11} & K_{22} \end{bmatrix} \begin{Bmatrix} x_1 \\ x_2 \end{Bmatrix} + \begin{bmatrix} G_{11} & \mathbf{0} \\ G_{21} & \mathbf{0} \end{bmatrix} \frac{d}{dt} \begin{Bmatrix} x_1 \\ x_2 \end{Bmatrix} = \begin{Bmatrix} f_1 \\ f_2 \end{Bmatrix} \quad (5.34)$$

Please observe that (5.34) has the same form of (5.21). Because of this it is possible to directly calculate the time varying variables using this equation. For this particular case, the vector x_i is defined by,

$$x_1 = (A_i \quad \{I\})^T \quad (5.35)$$

It can be seen that the magnetic vector potentials A_i and the current vectors $\{I\}$ can be directly calculated using (5.22). Once the FEM-circuit coupled and the equation derived by the methodology are obtained, both approaches can be solved in the frequency and the time domain. Thus, a comparison results can be performed on both approaches. Additionally these results can be compared with those derived by a FEM simulation performed in ANSYS. This will be explained next.

5.2.2.7 Comparison results in frequency domain

A first comparison of results is performed by solving the equations in the frequency domain. In order to know if the magnetic potentials calculated with (5.30) and those calculated by the proposed method are correct; a simulation was performed with the FEM software ANSYS. Some of the conductors magnetic potentials and the circuit currents results, obtained with the FEM-circuit coupled equation that assumes the FEM discretization shown in Figure 5.5, are included in Table 5.6. Table 5.6 include the results obtained with the proposed equation, which assumes the FEM discretization shown in Figure 5.6. An error percentage (*%Error*), for the magnetic potentials or currents, obtained with the proposed equation, has been calculated using the equation defined in (5.23).

By comparing the results, it can be observed that the methodology permits to obtain an accurate solution in the frequency domain.

TABLE 5.6
MAGNETIC VECTOR POTENTIALS (MVP) AND CURRENTS IN THE FREQUENCY DOMAIN

MVP (Wb/m) Currents (A)	ANSYS	Conventional FEM-Circuit Coupled Equation	% Error	Proposed Method	% Error
A_1	25.101	24.891	-0.844	24.891	-0.844
A_2	25.123	24.959	-0.657	24.959	-0.657
A_3	25.060	24.888	-0.691	24.888	-0.691
A_{11}	4.542	4.513	-0.643	4.513	-0.643
A_{12}	4.550	4.525	-0.552	4.525	-0.552
A_{13}	4.539	4.512	-0.598	4.512	-0.598
A_{21}	25.222	25.031	-0.763	25.031	-0.763
A_{22}	25.267	25.100	-0.665	25.100	-0.665
A_{23}	25.203	25.028	-0.699	25.028	-0.699
I_1	6.411	6.412	0.015	6.412	0.015
I_2	6.447	6.448	0.016	6.448	0.016

5.2.2.8 Comparison results in time domain

A second comparison is now performed in the time domain. The Backwards Euler method was used, the results are given in Table 5.7. The error percentage (*%Error*) shown in this Table was calculated using (5.23). For this case X_{ord} is the magnetic vector potential or current derived by ANSYS in the frequency domain; X_{prop} is the magnetic vector potential or current obtained, by solving in the time domain the proposed equation, or using (5.30). The results obtained from both approaches are practically identical. The maximum percentage of error is 0.8%.

TABLE 5.7
MAGNETIC VECTOR POTENTIALS (MVP) AND CURRENTS IN THE TIME DOMAIN USING THE
BACKWARDS EULER METHOD

MVP (Wb/m) Currents (A)	ANSYS	Conventional FEM-Circuit Coupled Equation	% Error	Proposed Method	% Error
$ A_1 $	25.101	24.889	-0.852	24.889	-0.852
$ A_2 $	25.123	24.957	-0.665	24.957	-0.665
$ A_3 $	25.060	24.886	-0.699	24.886	-0.699
$ A_{11} $	4.542	4.513	-0.643	4.513	-0.643
$ A_{12} $	4.550	4.524	-0.575	4.524	-0.575
$ A_{13} $	4.539	4.511	-0.621	4.511	-0.621
$ A_{21} $	25.222	25.030	-0.767	25.030	-0.767
$ A_{22} $	25.267	25.099	-0.669	25.099	-0.669
$ A_{23} $	25.203	25.028	-0.699	25.028	-0.699
$ I_1 $	6.411	6.411	0.000	6.411	0.000
$ I_2 $	6.447	6.447	0.000	6.447	0.000

Rms values of the variables are shown, the solution in the time domain considers that $\Delta t=0.001s$.

The 4th order *Runge Kutta* and the Euler method were also used to perform a comparison in the time domain. The results can be seen in Table 5.8. It is important to mention that these methods allow an approximate solution of the proposed equation to be obtained. Equations (5.24)-(5.27) were used. For this case, the *Euler* and the 4th order *Runge Kutta* method consider a matrix $\bar{\bar{T}}_{31}$ defined by (5.36) and (5.37), respectively.

$$\bar{\bar{T}}_{31} = 0.97 T_{31} \quad (5.36)$$

$$\bar{\bar{T}}_{31} = 0.98 T_{31} \quad (5.37)$$

The results obtained from solving the conventional and the proposed equations can be seen in Table 5.8. It can be observed that the *Euler* method allows a solution to be obtained with a maximum error of almost 9%. A maximum error of almost 5.0% is obtained with the 4th order *Runge Kutta* method.

TABLE 5.8
MAGNETIC VECTOR POTENTIALS (MVP) AND CURRENTS IN THE TIME DOMAIN USING THE EULER
AND THE 4TH ORDER RUNGE KUTTA METHODS

MVP (Wb/m) Currents (A)	Backwards Euler Ord. FEM-Circuit Coupled Equation	Euler Proposed Method	% Error	4 th Runge Kutta Proposed Method	% Error
$ A_1 $	24.889	23.852	-4.348	24.188	-2.898
$ A_2 $	24.957	24.255	-2.894	24.255	-2.894
$ A_3 $	24.886	24.185	-2.898	24.185	-2.898
$ A_{11} $	4.513	4.381	-3.013	4.424	-2.012
$ A_{12} $	4.524	4.436	-1.984	4.436	-1.984
$ A_{13} $	4.511	4.423	-1.990	4.424	-1.967
$ A_{21} $	25.030	24.308	-2.970	24.308	-2.970
$ A_{22} $	25.099	24.375	-2.970	24.375	-2.970
$ A_{23} $	25.028	24.306	-2.970	23.306	-2.970
$ I_1 $	6.411	7.046	9.012	6.728	4.712
$ I_2 $	6.447	7.079	8.928	6.762	4.658

RMS values of variables are shown in Table 5.8, the solution in the time domain was obtained with $\Delta t=0.001s$.

5.2.2.9 Performance comparison

The proposed equation defined in terms of the time varying variables, is significantly lower order than the FEM circuit coupled equation (5.30). In the tested example, the proposed matrix equation is of order 32, while the original FEM circuit coupled matrix equation is of order 53. As it will be shown, the equation derived with the proposed method, is faster and easier to solve either in the frequency or in the time domain.

In order to quantify the performance of the proposed matrix equation, the simulation time was measured. The simulation time needed to solve an conventional FEM-circuit coupled equation, was in addition measured in order to make a comparison. Both equations were solved with separate Matlab® programs; it was used the same computing platform and operative system of the case study 1 (Section 5.2.1).

The equations were solved in the time domain, using the Backwards Euler method. A total time simulation of 75s and a value of $\Delta T=0.001s$ were chosen. The proposed equation along with the expression (5.22), and the conventional FEM-circuit coupled equation (5.30) were solved seven times in order to quantify the required time to solve all the equations. The equation (5.32) is considered, since allows the derivation of the conductor voltages, which are not being calculated by the proposed equation.

The simulation time was obtained using the Matlab® *cputime* function. The results are listed in Table 5.9. It can be observed than the proposed matrix equation (5.22), allow a faster solution than the original FEM-circuit coupled equation (5.30) to be obtained. For instance, for the case study, it is more than 12 % faster.

It can be observed that the time varying variables can be directly calculated without knowing the magnetic potentials of the *non-conductor* region. Moreover, it is possible to calculate the conductor voltages, since the magnetic vector potentials of the *conductor region*, and the conductor currents are already known.

TABLE 5.9
COMPUTING TIME TO SOLVE THE EQUATIONS IN THE TIME DOMAIN

Simulation Number	Conventional FEM-circuit Coupled Equation (5.30)	Proposed Method Equation (5.22)	%Diff
1	471.33s	457.08s	-3.024
2	465.83s	432.63s	-7.130
3	471.33s	422.38s	-10.390
4	464.03s	445.44s	-4.006
5	459.67s	403.48s	-12.224
6	461.30s	453.09s	-1.778
7	488.16s	450.72s	-7.669
Average	467.80s	437.83s	-6.602

5.2.3 Case study 3. T slot-embedded conductor modeled by a two-dimension finite element analysis

5.2.3.1 Introduction

The case to be analyzed consists on a reverse “T” slot-embedded conductor with a copper conductor region and an air region (Konrad 1981), (Konrad 1982), (ANSYS 2010). In the conductor, the magnetic flux is normal to its vertical walls. The conductor has a zone of zero magnetic vector potential in the air region. In order to solve in an easier way the field equation, a planar symmetry is assumed. This symmetry allows considering that the magnetic field only has a component in the z -axis. It is assumed that the electric field has two components: one constant along the z -axis, and the second one varies with the frequency and produces eddy current losses (Konrad 1981), (Konrad 1982).

The cross section of the single “T” conductor is supplied with a *rms* sinusoidal current of 4A. As a result of the circulation of current, magnetic potentials will be present in the conductor and in the air regions. The sinusoidal current mentioned above is supplied in a range of frequency of 0.001Hz to 60Hz. The objective of the case study is to analyze how the total source current density of the conductor varies in this range of frequencies (Konrad 1981), (Konrad 1982), (ANSYS 2010).

The sketch of the conductor cross sections is shown in Figure 5.7. The physical dimensions of the conductor are given in Table 5.10.

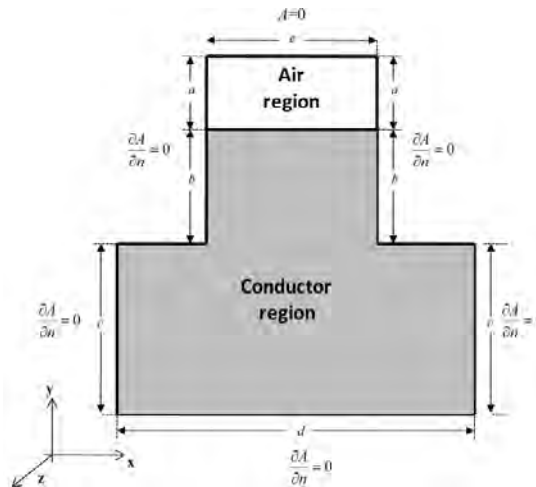


Figure 5.7. “T” slot-embedded conductor

TABLE 5.10
REVERSE “T” SLOT-EMBEDDED CONDUCTOR PHYSICAL DIMENSIONS

Parameter	Symbol	Value
Conductor Geometric Parameters	a	$6.450 \times 10^{-3} \text{ m}$
	b	$8.550 \times 10^{-3} \text{ m}$
	c	$8.450 \times 10^{-3} \text{ m}$
	d	$18.850 \times 10^{-3} \text{ m}$
	e	$8.950 \times 10^{-3} \text{ m}$
Conductor Area	Δ	$2.358 \times 10^{-4} \text{ m}^2$

Since the magnetic lines located in the vertical lines of the conductor are normal to them, these walls will be considered boundary conditions for the magnetic model. There is a zone of zero magnetic potential in the air region. The magnetic model of the conductor and its boundary conditions; the type of the finite elements used, the number of nodes and the FEM meshing, are all shown in Figure 5.8. The conductors' magnetic and electric properties are all shown in Table 5.11.

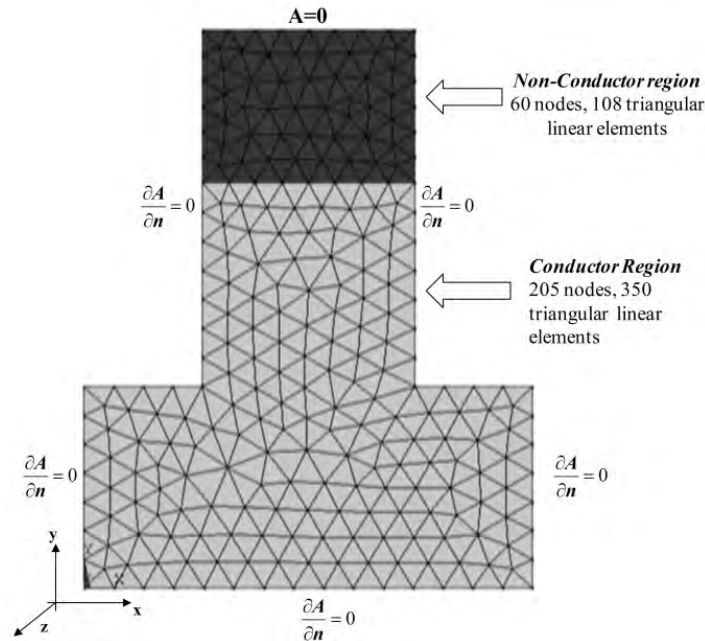


Figure 5.8. Magnetic model of the conductor, its boundary conditions and the FEM meshing.

TABLE 5.11
ELECTRIC AND MAGNETIC PROPERTIES OF THE “T” SLOT EMBEDDED CONDUCTOR

Parameters of the Conductor	Symbol	Value
Vacuum Permeability	μ_0	$4\pi \times 10^{-7}$ H/m
Relative Permeability in the Air and Conductor Regions	μ_r	1.0
Conductor Conductivity	σ	$58 \times 10^6 \Omega^{-1} \text{ m}^{-1}$
Conductor length	l	1.0m

In order to validate the results obtained with the proposed method, these will be compared against those calculated with the integro-differential finite element formulation (Konrad 1981), (Konrad 1982).

5.2.3.2 Field equation of the device

The proposed example will be solved using the Finite Element Integro-differential approach, thus the field equation to be solved is given by (Arkkio 1987), (Konrad 1981), (Konrad 1982),

$$-\nabla \cdot (\nu(\nabla A)) + \sigma \frac{\partial A}{\partial t} - \frac{1}{\Delta} \iint_{S_c} \sigma \frac{\partial A}{\partial t} dS = \frac{I_c}{\Delta} \quad (5.38)$$

Where S_c is the conductor area, I_c is the current passing through the conductor.

It is possible to add a field equation for the device, specifically, the expression which relates its voltage, current and the magnetic vector potentials. This equation was previously defined in (2.13)

5.2.3.3 Finite element analysis

If the field equation defined in (5.38) is solved in the frequency domain using FEM, it gives (Arkkio 1987), (Konrad 1982),

$$\left([S] + j(2\pi f)[T] - j(2\pi f) \frac{1}{\Delta} [G][D] \right) \{\tilde{A}\} = [T] \frac{I_c}{\Delta} \quad (5.39)$$

Where the matrices $[S]$ and $[T]$ are matrices derived by FEM analysis; the discretization is shown in Figure 5.8. Further details about Equation (5.39) can be consulted in (Konrad 1981), (Konrad 1982). The equation (5.39) can solve all the magnetic vector potentials in the conductor for a frequency f . If it is considered the field equation defined on (2.13), and if a Newton Cotes analysis is performed on it; it yields,

$$R_c \tilde{I}_c + j(2\pi f)(R_c) \{M_c\} \{\tilde{A}\} = \tilde{U}_c \quad (5.40)$$

After having calculated the conductor voltage \tilde{U}_c , the source current density is calculated as,

$$\tilde{J}_s = \sigma \frac{\tilde{U}_c}{l} \quad (5.41)$$

There will be a specific source current density \tilde{J}_s for a frequency f . The objective of this case study consists on calculating this source current density for a specific frequency range.

5.2.3.4 Solution obtained with the proposed methodology

It is possible to use the method explained in Chapter 3, to solve the magnetic vector potentials of the *conductor* region of the slot conductor. After having these magnetic potentials, (5.40) and (5.41) can be used to calculate the conductor voltage \tilde{U}_c and the source current density \tilde{J}_s .

The first step of the methodology requires to perform a nodal renumbering on the magnetic vector potentials, of the *conductor* region and the *non-conductor* regions of the

conductors. Thus, it is possible to derive FEM equations that takes into account this nodal renumbering. It yields,

$$\begin{bmatrix} \mathbf{S}_{ii} & \mathbf{S}_{ij} \\ \mathbf{S}_{ij}^T & \mathbf{S}_{jj} \end{bmatrix} \begin{Bmatrix} \mathbf{A}_i \\ \mathbf{A}_j \end{Bmatrix} + \begin{bmatrix} \mathbf{T}_{ii} & \mathbf{0} \\ \mathbf{0} & \mathbf{0} \end{bmatrix} \frac{d}{dt} \begin{Bmatrix} \mathbf{A}_i \\ \mathbf{A}_j \end{Bmatrix} = \{\mathbf{f}_i\}(\mathbf{U}_c) \quad (5.42)$$

$$\mathbf{R}_c^{-1} \mathbf{U}_c - \{\mathbf{M}\}_i \frac{d\mathbf{A}_i}{dt} = \mathbf{I}_c \quad (5.43)$$

Where the magnetic vector potentials of the *conductor* and *non-conductor* regions of (5.42) and (5.43) are given by,

$$\mathbf{A}_i = \{\mathbf{A}_1 \quad \mathbf{A}_2 \dots \mathbf{A}_{205}\} \quad (5.44)$$

$$\mathbf{A}_j = \{\mathbf{A}_{206} \quad \mathbf{A}_{207} \dots \mathbf{A}_{265}\} \quad (5.45)$$

If the equations (5.42) and (5.43) are combined in order to form a unique FEM equation, it yields,

$$\begin{bmatrix} \mathbf{S}_{ii} & -\{\mathbf{f}_i\} & \mathbf{S}_{ij} \\ \mathbf{0} & \mathbf{R}_c^{-1} & \mathbf{0} \\ \mathbf{S}_{ij}^T & \mathbf{0} & \mathbf{S}_{jj} \end{bmatrix} \begin{Bmatrix} \mathbf{A}_i \\ \mathbf{U}_c \\ \mathbf{A}_j \end{Bmatrix} + \frac{d}{dt} \begin{bmatrix} \mathbf{T}_{ii} & \mathbf{0} & \mathbf{0} \\ -\{\mathbf{M}\}_i & \mathbf{0} & \mathbf{0} \\ \mathbf{0} & \mathbf{0} & \mathbf{0} \end{bmatrix} \begin{Bmatrix} \mathbf{A}_i \\ \mathbf{U}_c \\ \mathbf{A}_j \end{Bmatrix} = \begin{Bmatrix} \mathbf{0} \\ \mathbf{I}_c \\ \mathbf{0} \end{Bmatrix} \quad (5.46)$$

If (5.46) is partitioned and a frequency domain solution is considered; it gives,

$$\begin{bmatrix} \mathbf{K}_{11} & \mathbf{K}_{12} \\ \mathbf{K}_{21} & \mathbf{K}_{22} \end{bmatrix} \begin{Bmatrix} \tilde{\mathbf{x}}_1 \\ \tilde{\mathbf{x}}_2 \end{Bmatrix} + j\omega \begin{bmatrix} \mathbf{G}_{11} & \mathbf{0} \\ \mathbf{G}_{21} & \mathbf{0} \end{bmatrix} \frac{d}{dt} \begin{Bmatrix} \tilde{\mathbf{x}}_1 \\ \tilde{\mathbf{x}}_2 \end{Bmatrix} = \begin{Bmatrix} \mathbf{0} \\ \tilde{\mathbf{f}}_2 \end{Bmatrix} \quad (5.47)$$

Please notice that (5.47) has the same form of (5.22), if solved in the frequency domain, i.e.

$$(\mathbf{K}_T + j\omega \mathbf{G}_T) \tilde{\mathbf{x}}_T = \tilde{\mathbf{f}}_T \quad (5.48)$$

The matrices \mathbf{K}_T , \mathbf{G}_T , and the vector $\tilde{\mathbf{f}}_T$ of this reduced equation are derived using (3.49), (3.50) and (3.51), respectively. These matrices are calculated by considering the matrices and vectors \mathbf{K}_{11} , \mathbf{K}_{12} , \mathbf{K}_{21} , \mathbf{K}_{22} , \mathbf{G}_{21} , \mathbf{G}_{22} and \mathbf{F}_2 all shown in (5.47). The vectors $\tilde{\mathbf{x}}_1$, $\tilde{\mathbf{x}}_2$ and $\tilde{\mathbf{f}}_2$ of (5.47) are defined by,

$$\tilde{\mathbf{x}}_1 = \tilde{\mathbf{A}}_i \quad (5.49)$$

$$\tilde{\mathbf{x}}_2 = \{\tilde{\mathbf{U}}_c \quad \tilde{\mathbf{A}}_j\}^T \quad (5.50)$$

$$\tilde{\mathbf{f}}_2 = \{\tilde{\mathbf{I}}_c \quad \mathbf{0}\}^T \quad (5.51)$$

After calculating the magnetic vector potentials $\tilde{\mathbf{A}}_i$, the voltage $\tilde{\mathbf{U}}_c$ can be calculated using (5.43). If the conductor voltage $\tilde{\mathbf{U}}_c$ is known, the source current density of the conductor $\tilde{\mathbf{J}}_s$ can be calculated using (5.41). Once the FEM equation and the expression derived by the methodology are used to calculate the conductor source density, a comparison of the results obtained from both approaches can be performed. Additionally these results were compared with those derived by an ANSYS FEM simulation (ANSYS 2010). The results derived by ANSYS are almost identical to the results obtained with the integro-differential approach. The results derived by the integro-differential and the proposed method will explained next.

5.2.3.5 Comparison results

The results obtained from the integro-differential approach, and those derived from the proposed methodology are given in Table 5.12.

TABLE 5.12
SOURCE CURRENT DENSITY IN THE FREQUENCY DOMAIN

Frequency	Integro-differential approach	Proposed method	%Error
0.001 Hz	4,241+j0.700	4,241+j0.700	0.000%
1.00 Hz	4,245+j701.0	4,245+j698.0	-0.023%
5.00 Hz	4,352+j3,495	4,350+j3,483	-0.161%
10.0 Hz	4,676+j6,937	4,668+j6,916	-0.263%
15.0 Hz	5,190+j10,283	5,175+j10,255	-0.286%
20.0 Hz	5,858+j13,498	5,832+j13,467	-0.258%
25.0 Hz	6,641+j16,562	6,605+j16,553	-0.123%
30.0 Hz	7,495+j19,469	7,455+j19,445	-0.177%
35.0 Hz	8,391+j22,224	8,344+j22,206	-0.139%
40.0 Hz	9,294+j24,832	9,245+j24,828	-0.079%
45.0 Hz	10,183+j27,328	10,135+j27,325	-0.068%
50.0 Hz	11,042+j29,710	10,998+j29,715	-0.030%
55.0 Hz	11,863+j32,003	11,825+j32,015	-0.020%
60.0 Hz	12,640+j34,224	12,609+j34,240	0.010%

The results show the conductor source current density J_s , if a sinusoidal current of 4A in a range of frequencies of 0.001Hz to 60Hz is supplied.

The percentage of error between the results derived from the two approaches can be calculated using,

$$\%Error = \frac{J_{sinteg} - J_{sprop}}{J_{sinteg}} (100\%) \quad (5.52)$$

Where J_{sinteg} is magnitude of the source current density when the integro-differential approach is used; J_{sprop} is the one obtained with the equivalent equation. The results obtained with the proposed method are in excellent agreement with those obtained with the integro-differential approach. The maximum absolute error is clearly negligible, almost 0.286%

5.2.3.6 Performance comparison

The proposed method allows to directly calculate the time varying variables. For the case of the “T” planar conductor, the equation derived from the methodology is of order 205; while the original FEM field equation is of order 266. The proposed equation is easier to solver either in the frequency or in the time domain.

In order to quantify the performance of the equation derived by the proposed method, the simulation time was measured. The simulation time needed to solve a conventional FEM-circuit coupled equation, was measured in order to make a comparison. Both equations were solved with separate GSL-based program (GNU Scientific Library 2013). The programs were implemented in the same computer and operative system. A Dell Precision R5500 Rack Workstation, GPU NVIDIA® Quadro® 600, 1 GB RAM and an Ubuntu Operative System were used.

The results of solving the conventional FEM equation and the expression derived by the methodology, in a sequential computing with GSL are shown in Figure 5.9.

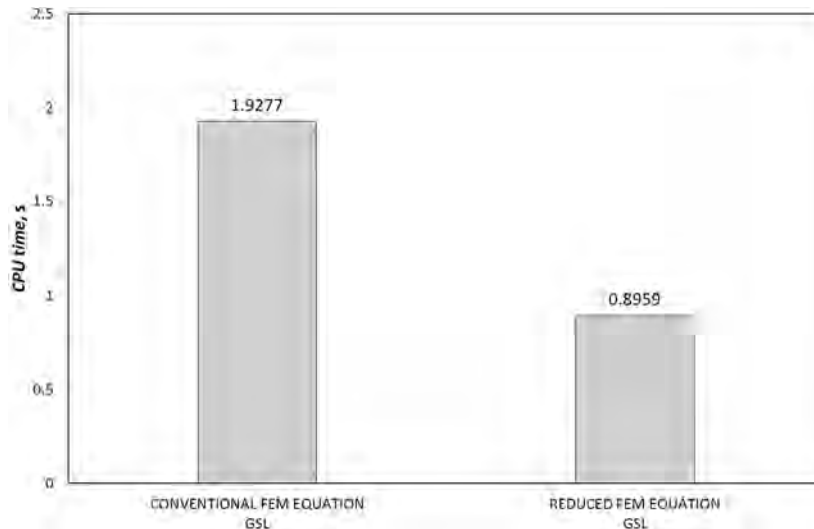


Figure 5.9. CPU times derived for the FEM equations solutions

It can be observed that the proposed equation permits to derive a faster solution compared to the conventional FEM equation solution. Specifically, the CPU time of the conventional and the proposed equation are 1.9277sec and 0.8959sec, respectively. The difference between these CPU times is significant, nearly 217%. It is possible to perform a comparison

between the conventional and the proposed equation using a parallel computing with CUBLAS. This will be explained next.

5.2.3.7 Parallel solution using CUBLAS

The conventional FEM equation derived from the proposed methodology can be solved by a parallel solution of CUBLAS (CUDA toolkit 5.0 2014). For the particular case of the conventional FEM equation, it is possible to use other computing platform to calculate the conductor voltage and the source current density defined in (5.41). This can be achieved by using the FEM expressions,

$$([S] + j(2\pi f)[T])\{\tilde{A}\} = \{f\}(\tilde{U}_c) \quad (5.53)$$

$$(\mathbf{R}_c)^{-1}(\tilde{U}_c) - j(2\pi f)[M_c]\{\tilde{A}\} = \tilde{I}_c \quad (5.54)$$

Equation (5.53) is quite similar to (5.39), the difference relies in the forcing function used. Equations (5.53) and (5.54) can be coupled into a unique expression defined by,

$$\begin{bmatrix} [S] & -\{f\} \\ \mathbf{0} & (\mathbf{R}_c)^{-1} \end{bmatrix} \begin{Bmatrix} \{\tilde{A}\} \\ \tilde{U}_c \end{Bmatrix} + j(2\pi f) \begin{bmatrix} [T] & \mathbf{0} \\ -[M_c] & \mathbf{0} \end{bmatrix} \begin{Bmatrix} \{\tilde{A}\} \\ \tilde{U}_c \end{Bmatrix} = \begin{Bmatrix} \mathbf{0} \\ \tilde{I}_c \end{Bmatrix} \quad (5.55)$$

Equation (5.55) can be represented by,

$$[K]\{\tilde{X}\} + j(2\pi f)[G]\{\tilde{X}\} = \tilde{f} \quad (5.56)$$

Moreover, (5.56) can be expressed by,

$$[A]\{\tilde{X}\} = \{\tilde{b}\} \quad (5.57)$$

For the case of the proposed equation (5.48), it can be represented by,

$$[A_T]\{\tilde{X}_T\} = \{\tilde{b}_T\} \quad (5.58)$$

The FEM equation (5.57) is named as *conventional* FEM equation, while the expression shown in (5.58) is named as *reduced* FEM equation. The features of these FEM equations can be seen in Table 5.13. Please notice that these equations are required to be solved several

times for the respective frequency range, to obtain the source current density of the conductor.

TABLE 5.13
FEM EQUATIONS TO BE SOLVED IN A FREQUENCY RANGE

Device to be analyzed	Conventional FEM equation	Reduced FEM equation	Number of FEM equations to be solved
“T” Planar conductor	$[A_{266 \times 266}]\{\tilde{X}_{266}\} = \{\tilde{b}_{266}\}$	$[A_{T,205 \times 205}]\{\tilde{X}_{T,205}\} = \{\tilde{b}_{T,205}\}$	14

Two specific steps in the process of calculating the solution in the frequency domain of FEM equations (5.57) and (5.58) can be identified, i.e. a *preprocessing* and a *calculating* step. The *preprocessing* step of the *conventional* FEM method consists on deriving the matrices and vectors $[K]$, $[G]$ and $\{f\}$ that form (5.57); while the *preprocessing* step of the *reduced* FEM method consists on deriving submatrices and subvectors that form (5.58). The *calculating process* of the *conventional* and the *reduced* FEM equations consists on solving both equations using the *LU* method. The *preprocessing* and the *calculating* steps of the *conventional* and a *reduced* FEM equations were covered in Chapter 3.

5.2.3.7.1 Performance comparison between the sequential and the parallel solutions

In order to measure the performance of the method implemented in CUBLAS, the *conventional* and the *reduced* FEM equations were also solved in a sequential computing platform. The *preprocessing* and the *calculating* steps were entirely implemented in the sequential GSL platform (GNU Scientific Library 2013).

For the parallel solution, some stages of the *preprocessing* step were calculated by a sequential computing in GSL (GNU Scientific Library 2013), while the *calculating* steps were completely implemented in the CUBLAS computing platform (Barrachina et al. 2008), (CUDA toolkit 5.0 2014). On the other hand, the *calculating* step of the *conventional* and the *reduced* FEM equation will be solved for each frequency by the *LU* method implemented in CUBLAS. Specific details of the sequential and the parallel computing of the *preprocessing* and *calculating* steps can be consulted in Chapter 3.

The *conventional* and the *reduced* FEM equations were solved in the computing platforms GSL and CUBLAS. The programs were implemented in the same computer and operative system. A Dell Precision R5500 Rack Workstation, GPU NVIDIA® Quadro® 600 with 96 cores, 1 GB RAM and an Ubuntu Operative System were used. Specific details about the parallel and the sequential solution of this case study, can be found in Appendix C.

The total computation time (*CPU time*) required to solve the planar “T” conductor in the correspondent frequency range was measured. Figure 5.10 shows the *CPU times* needed to solve these equations using the sequential and the parallel computing platforms.

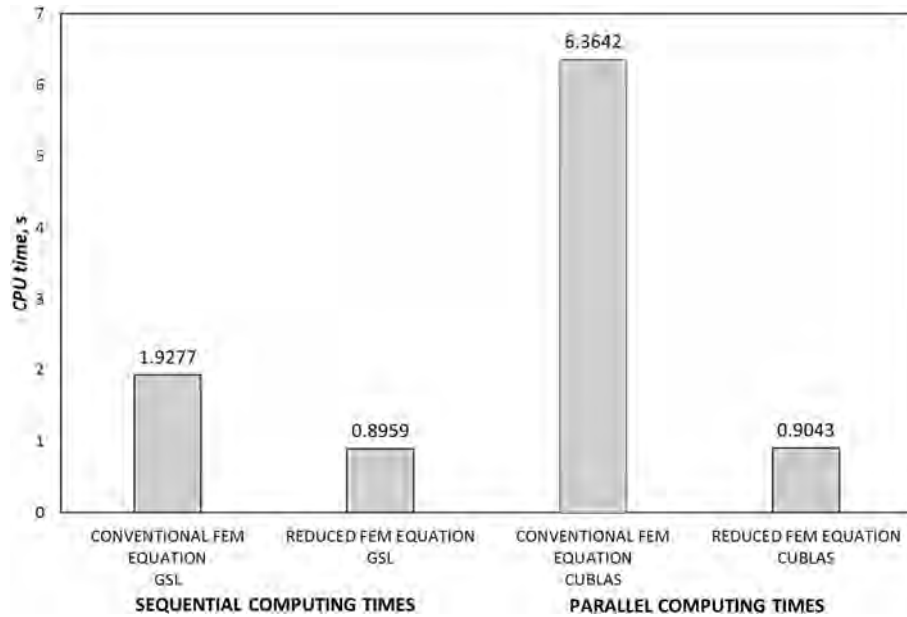


Figure 5.10. *CPU times* derived for solving the “T” planar conductor

It can be observed that the *reduced* FEM equation allows a faster solution compared to the *conventional* FEM equation. Specifically, when the sequential computing was used, the *CPU time* of the *conventional* and the *reduced* equation are 1.92sec and 0.89sec, respectively. Moreover, when the parallel computing was used, the *CPU time* for the *conventional* and the *reduced* equation are 6.36sec and 0.90sec, respectively. Although the *reduced* FEM equation allows a faster solution with both computing platforms, a reduction of *CPU time* was not obtained when parallel computing with CUBLAS was used. The reason is that the *reduced* and the *conventional* equations of the planar device are of low order, i.e. 205 and 266, respectively. A *CPU time* reduction cannot be achieved, since the advantage of using the parallel platform is only evident when the order of system equations to be solved is of considerably larger scale. The ratio of sequential (t_s) and parallel (t_p) *cputime* of conventional and reduced equation confirms this situation. It can be seen in Figure 5.10a.

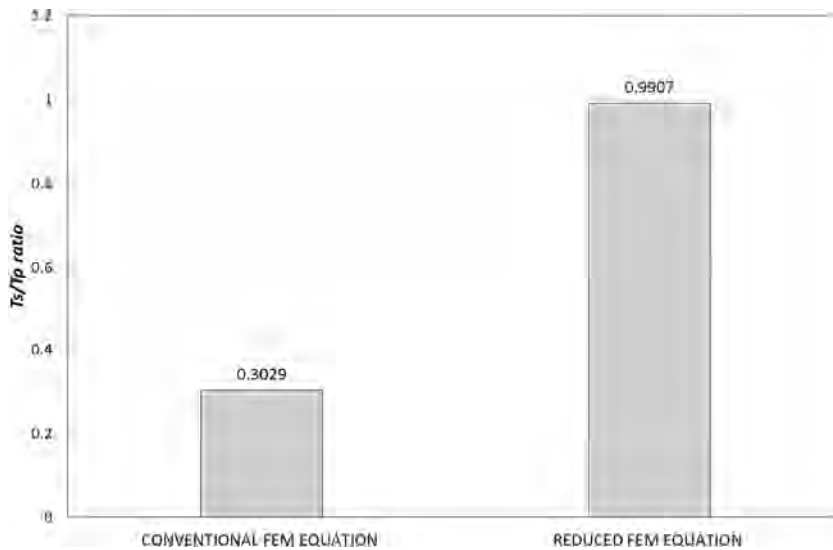


Figure 5.10a. *Ratio t_s/t_p* derived for solving the “T” planar conductor

5.3 Axisymmetric symmetry assumption cases

5.3.1. Case study 4. Air series reactor modeled by a two-dimension finite element analysis

5.3.1.1 Introduction

It consists on analyzing in the frequency domain two small air-cored reactors with specific turn configuration. The example consists on analyzing how the reactors inductance ratio L_{ca}/L_{cd} varies within a frequency range, defined from 0.15915Hz to 1000Hz. The original case study can be consulted in (Preiss 1983).

The inductance ratio L_{ca}/L_{cd} of reactors 1 and 2 can be derived by providing a *rms* sinusoidal current of 1.0A at a frequency range of 0.15915Hz to 1000Hz on both reactors. As a result of applying that current, a voltage appears at each turn i of both reactors.

The voltage at turn i can be calculated by finite element analysis, since the current is known. It is assumed that all the points in each reactor turn has the same voltage. Once the voltage at each turn is known, it is possible to calculate the total voltage in both reactors, by adding all the voltage turns. Having the total voltage, and since the current is also known, it is possible to calculate the impedance and therefore, the inductance L_{ca} at a frequency f . The inductance L_{cd} is calculated by injecting a current of 1.0 at a frequency of 0.15915Hz ($\omega=1.0$ rad/s).

The reactor to be analyzed are labeled as 1, and 2. The turns number i and the dimension of each reactor are all shown in Figure 5.11. The boundary conditions and the symmetry plane and symmetry axis are also shown in Figure 5.11, while the dimensions of both reactors can be consulted in Table 5.14.

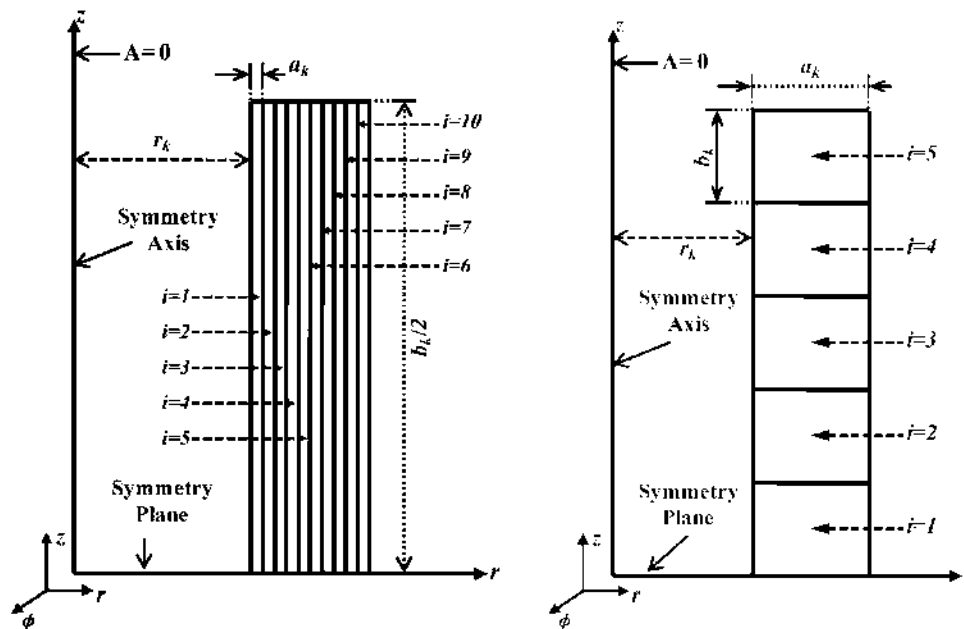


Figure 5.11. Air reactors to be analyzed.
A) Reactor 1. B) Reactor 2.

TABLE 5.14
DIMENSIONS AND PROPERTIES OF AIR REACTORS 1 AND 2

	Parameter	Reactor 1 ($k=1$)	Reactor 2 ($k=2$)
Dimension Parameters	Number of turns	10	5
	a_k	1.0mm	10mm
	b_k	200mm	20mm
	r_k	100mm	
Electric and Magnetic Properties	Permeability relative μ_r	1.0	
	Conductivity σ	$\sigma^{(1)} = \sigma^{(2)} = 3 \times 10^7 \Omega^{-1} \text{m}^{-1}$	

The air series reactor 1 is an aluminum sheet-wound winding with 10 series turns; while the air series reactor 2 consists of 5 series turns of aluminum conductors. Since the exact dimensions of the reactors are not mentioned in the original study case (Preiss 1983), the dimensions shown in Figure 5.12 are assumed for the finite element analysis performed on both reactors. The electric and magnetic properties of reactors can be consulted in Table 5.14.

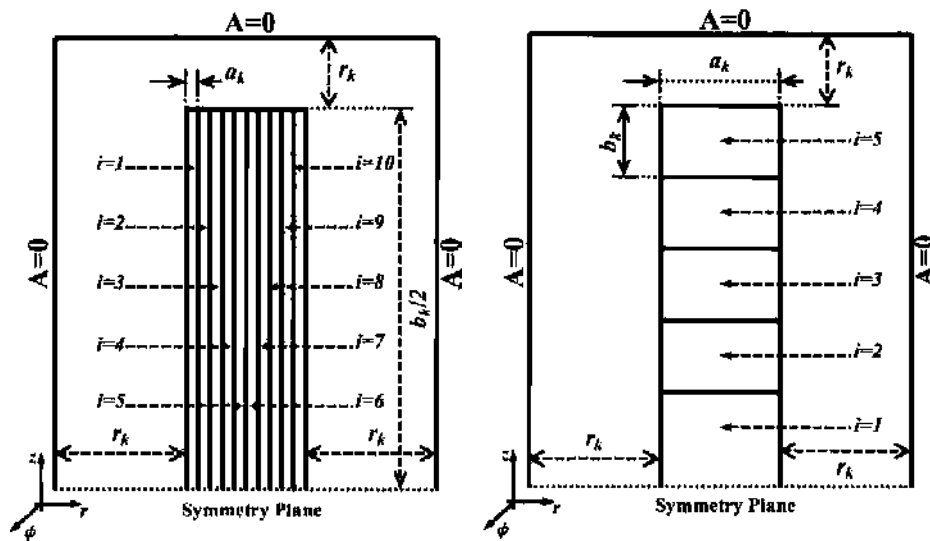


Figure 5.12. Geometry of air reactors
A) Air Series Reactor 1. B) Air Series Reactor 2.

After defining the characteristics of the air series reactors, the field equations, the finite element model used and the finite element analysis will be defined.

5.3.1.2 Field equations

If the assumptions mentioned in the beginning of this chapter are considered for the modelling of the air series reactor; two regions can be identified: a *non-conductor* region, where there is no voltage excitation; and a *conductor* region, supplied with a voltage source and includes the skin effect (Escarela-Perez, Melgoza and Alvarez-Ramirez 2009), (Ho, Li and Fu 1999). The field equation can be consulted in Chapter 2.

5.3.1.3 Finite element analysis

An axisymmetric behavior of the magnetic field can be assumed by neglecting the pith of the turns of both reactors (Preiss 1983). It is also assumed that the reactors walls have a zero magnetic potential. A linear triangular finite element with three nodes has been considered. The number of finite elements for each turn of the air series reactors 1 and 2 are 126 and 44, respectively. The finite element number of the air zone of reactors 1 and 2, are 5658 and 2990, respectively. The number of nodes for each turn of reactors 1 and 2, are 126 and 36 respectively; the nodes used in the air zone of reactors 1 and 2, are 2250 and 1488, respectively. The finite elements and their nodes, along the boundary conditions for the center region of air series reactors 1 and 2 are all shown in Figure 5.13.

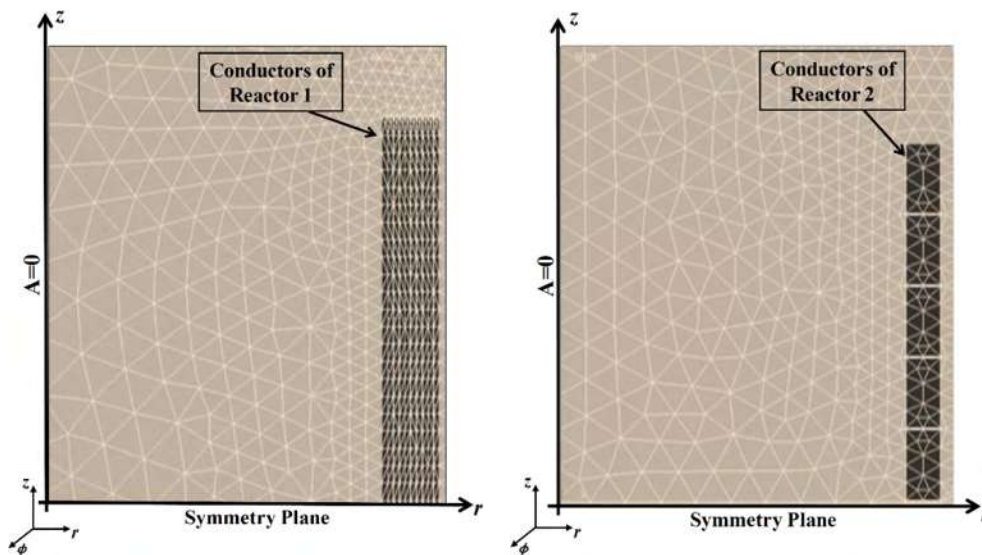


Figure 5.13. Finite element model of air reactors.
A) Air Series Reactor 1. B) Air Series Reactor 2.

It is assumed that there are no voltage differences at different turns of reactors, therefore, all points in a reactor turn have the same voltage. It is also assumed that the source current density is constant along the coordinate r (Preiss 1983), (Konrad 1981), (Konrad 1982), (Escarela-Perez, Melgoza and Alvarez-Ramirez 2009).

It is important to mention that in order to perform a valid comparison, a finite element analysis will be performed between ANSYS, the conventional FEM equation, and by the equation derived from the proposed methodology. All these approaches consider the FEM model mentioned earlier. The finite element analysis derived from these approaches will be discussed next.

5.3.1.3.1 Conventional Finite Element Analysis

It is possible to perform a finite element analysis on the field equation (2.20), to derive a FEM equation with the voltage as the forcing function. Besides, a Newton Cotes analysis can be performed on (2.21) in order to derive an alternative expression. Details about the Finite Element are given in Chapter 2. The FEM expressions derived from these analysis are defined by,

$$[S]\{A_\phi\} + [T] \frac{d\{A_\phi\}}{dt} = \{f\}\{U_c\}_{(k)} \quad (5.59)$$

$$[\Delta_r]_{(k)}^{-1}\{U_c\}_{(k)} - [M_c] \frac{d\{A_\phi\}}{dt} = \{I\} \quad (5.60)$$

The matrices $[\Delta_r]_{(k)}$ of the air series reactor 1 and 2 are,

$$[\Delta_r]_{(1)} = [\Delta_{r1}^{(1)} \quad \Delta_{r2}^{(1)} \quad \Delta_{r3}^{(1)} \quad \Delta_{r4}^{(1)} \quad \Delta_{r5}^{(1)}]_{5 \times 5}^{diag} \quad (5.61)$$

$$[\Delta_r]_{(2)} = [\Delta_{r1}^{(2)} \quad \Delta_{r2}^{(2)} \quad \Delta_{r3}^{(2)} \quad \dots \quad \Delta_{r9}^{(2)} \quad \Delta_{r10}^{(2)}]_{10 \times 10}^{diag} \quad (5.62)$$

The vector voltage for the reactor 1 and 2 are defined by $\{U_c\}_{(1)}$ and $\{U_c\}_{(2)}$, respectively, as

$$\{U_c\}_{(1)} = [U_{c1}^{(1)} \quad U_{c2}^{(1)} \quad U_{c3}^{(1)} \quad U_{c4}^{(1)} \quad U_{c5}^{(1)}]_{5 \times 5}^{diag} \quad (5.63)$$

$$\{U_c\}_{(2)} = [U_{c1}^{(2)} \quad U_{c2}^{(2)} \quad U_{c4}^{(2)} \quad \dots \quad U_{c9}^{(2)} \quad U_{c10}^{(2)}]_{10 \times 10}^{diag} \quad (5.64)$$

The vector value $U_{ci}^{(k)}$ corresponds to the voltage in the turn i of the reactor k ; while the vector value $\Delta_{ri}^{(k)}$ is the Δ_r value on the turn i of the reactor k . The variable $\Delta_{ri}^{(k)}$ contained in vectors (5.61) and (5.62) is given in Table 5.15.

TABLE 5.15
PARAMETERS OF AIR REACTORS 1 AND 2

	Reactor 1 (k=1)	Reactor 2 (k=2)
$\Delta_{r1}^{(k)}$	0.00031673m ⁻¹	0.00030340m ⁻¹
$\Delta_{r2}^{(k)}$	0.00031323m ⁻¹	
$\Delta_{r3}^{(k)}$	0.00030994m ⁻¹	
$\Delta_{r4}^{(k)}$	0.00030666m ⁻¹	
$\Delta_{r5}^{(k)}$	0.00030344m ⁻¹	
$\Delta_{r6}^{(k)}$	0.00030300m ⁻¹	It does not apply
$\Delta_{r7}^{(k)}$	0.00029721m ⁻¹	
$\Delta_{r8}^{(k)}$	0.00029419m ⁻¹	
$\Delta_{r9}^{(k)}$	0.00029123m ⁻¹	
$\Delta_{r10}^{(k)}$	0.00028833m ⁻¹	

Equations (5.59) and (5.60) can be combined to form a unique FEM equation, which can be solved in the frequency domain as,

$$\begin{bmatrix} [\mathbf{S}] & -\{\mathbf{f}\} \\ \mathbf{0} & [\mathbf{A}_r]_{(k)}^{-1} \end{bmatrix} \begin{Bmatrix} \{\tilde{\mathbf{A}}_\phi\} \\ \{\tilde{\mathbf{U}}_c\}_{(k)} \end{Bmatrix} + \frac{d}{dt} \begin{bmatrix} [\mathbf{T}] & \mathbf{0} \\ -[\mathbf{M}_c] & \mathbf{0} \end{bmatrix} \begin{Bmatrix} \{\tilde{\mathbf{A}}_\phi\} \\ \{\tilde{\mathbf{U}}_c\}_{(k)} \end{Bmatrix} = \begin{Bmatrix} \mathbf{0} \\ \{\tilde{\mathbf{I}}\} \end{Bmatrix} \quad (5.65)$$

Equation (5.65) permits to obtain the voltage vector $\{U_c\}_{(k)}$ in the frequency domain. The voltage vector contains the voltages at each turn of each reactor k . After explaining how the turn voltages of the reactors are obtained using the conventional equation shown in (5.65); how the proposed method can derive the voltage vectors on reactors will be now explained.

5.3.1.3.2 Finite Element Analysis using the proposed methodology

To perform a finite element analysis using the equation derived by the proposed methodology. This equation can directly calculate the magnetic potentials conductors at each reactor, since the current of both reactors is known. If the magnetic potentials are known, it is possible to calculate the turn voltages of reactors using as a base (5.59). The proposed methodology can derive alternative equations to (5.59) and (5.60), i.e.

$$\begin{bmatrix} \mathbf{S}_{ii} & \mathbf{S}_{ij} \\ \mathbf{S}_{ij}^T & \mathbf{S}_{jj} \end{bmatrix} \begin{Bmatrix} \mathbf{A}_i \\ \mathbf{A}_j \end{Bmatrix} + \begin{bmatrix} \mathbf{T}_{ii} & \mathbf{0} \\ \mathbf{0} & \mathbf{0} \end{bmatrix} \frac{d}{dt} \begin{Bmatrix} \mathbf{A}_i \\ \mathbf{A}_j \end{Bmatrix} = \begin{Bmatrix} \{\mathbf{f}_i\} \{\mathbf{U}_c\}_{(k)} \\ \mathbf{0} \end{Bmatrix} \quad (5.66)$$

$$[\mathbf{A}_r]_{(k)}^{-1} \{\mathbf{U}_c\}_{(k)} - [\mathbf{M}_i] \frac{d\mathbf{A}_i}{dt} = \{\mathbf{I}\} \quad (5.67)$$

By combining (5.66) and (5.67) into a unique FEM equation and associating the time varying variables, results in,

$$\begin{bmatrix} \mathbf{S}_{ii} & -\{\mathbf{f}_i\} & \mathbf{S}_{ij} \\ \mathbf{0} & [\mathbf{A}_r]_{(k)}^{-1} & \mathbf{0} \\ \mathbf{S}_{ij}^T & \mathbf{0} & \mathbf{S}_{jj} \end{bmatrix} \begin{Bmatrix} \mathbf{A}_i \\ \{\mathbf{U}_c\}_{(k)} \\ \mathbf{A}_j \end{Bmatrix} + \frac{d}{dt} \begin{bmatrix} \mathbf{T}_{ii} & \mathbf{0} & \mathbf{0} \\ -[\mathbf{M}_i] & \mathbf{0} & \mathbf{0} \\ \mathbf{0} & \mathbf{0} & \mathbf{0} \end{bmatrix} \begin{Bmatrix} \mathbf{A}_i \\ \{\mathbf{U}_c\}_{(k)} \\ \mathbf{A}_j \end{Bmatrix} = \begin{Bmatrix} \mathbf{0} \\ \{\mathbf{I}\} \\ \mathbf{0} \end{Bmatrix} \quad (5.68)$$

By performing a matrix partition of (5.68), and considering a frequency domain solution yields,

$$\begin{bmatrix} \mathbf{K}_{11} & \mathbf{K}_{12} \\ \mathbf{K}_{21} & \mathbf{K}_{22} \end{bmatrix} \begin{Bmatrix} \tilde{\mathbf{x}}_1 \\ \tilde{\mathbf{x}}_2 \end{Bmatrix} + j(2\pi f) \begin{bmatrix} \mathbf{G}_{11} & \mathbf{0} \\ \mathbf{G}_{21} & \mathbf{0} \end{bmatrix} \begin{Bmatrix} \tilde{\mathbf{x}}_1 \\ \tilde{\mathbf{x}}_2 \end{Bmatrix} = \begin{Bmatrix} \mathbf{0} \\ \tilde{\mathbf{f}}_2 \end{Bmatrix} \quad (5.69)$$

Notice that two matrix equation can be derived from (5.69). Using these two matrix equation, it is possible to obtain the equation proposed in this investigation. Further details of this expression can be consulted in Chapter 3. If this expression is solved in the frequency domain yields,

$$(\mathbf{K}_T + j\omega\mathbf{G}_T)\tilde{\mathbf{x}}_T = \tilde{\mathbf{f}}_T \quad (5.70)$$

Matrices \mathbf{K}_T , \mathbf{G}_T , and the vector \mathbf{f}_T of (5.70) are derived using (3.35), (3.36) and (3.37); and considering the matrices and vectors K_{11} , K_{12} , K_{21} , K_{22} , G_{21} , G_{22} , F_1 and F_2 all shown in (5.69). The vectors $\tilde{\mathbf{x}}_1$, $\tilde{\mathbf{x}}_2$ and $\tilde{\mathbf{f}}_2$ of (5.69) are defined by,

$$\tilde{\mathbf{x}}_i = \tilde{\mathbf{A}}_i \quad (5.71)$$

$$\tilde{\mathbf{x}}_2 = \{\{\mathbf{U}_c\}_{(k)} \quad \tilde{\mathbf{A}}_j\}^T \quad (5.72)$$

$$\tilde{\mathbf{f}}_2 = \{\tilde{\mathbf{I}} \quad \mathbf{0}\}^T \quad (5.73)$$

After calculating the magnetic vector potentials $\tilde{\mathbf{A}}_i$ on each reactor, the voltage vector $\{\mathbf{U}_c\}_{(k)}$ of both reactors can be calculated using (5.67).

5.3.1.3.3 Finite Element Analysis using ANSYS

The finite element model explained earlier is simulated with the FEM software to obtain the turn voltages when a *rms* sinusoidal current of 1.0A is injected in both reactors. The voltage $\{\tilde{\mathbf{U}}_c\}_{(k)}$ is directly determined from the FEM software. The voltages which cannot be directly obtained with the software are calculated with (5.67), since the magnetic vector potential $\tilde{\mathbf{A}}_i$ can be easily determined with ANSYS.

5.3.1.4 Calculating the Inductances of the reactors 1 and 2

After calculating the voltage vector $\{\tilde{\mathbf{U}}_c\}_{(k)}$ by using finite element analysis, the total voltage at each reactor is calculated by adding the voltage on each turn. The total voltage of reactors 1 and 2 is calculated with (5.74) and (5.75), respectively.

$$\tilde{\mathbf{U}}_{CT@f}^{(1)} = \sum_{i=1}^{i=5} \tilde{\mathbf{U}}_{ci}^{(1)} \quad (5.74)$$

$$\tilde{\mathbf{U}}_{CT@f}^{(2)} = \sum_{i=1}^{i=10} \tilde{\mathbf{U}}_{ci}^{(2)} \quad (5.75)$$

Where $\tilde{\mathbf{U}}_{CT@f}^{(1)}$ and $\tilde{\mathbf{U}}_{CT@f}^{(2)}$ are the total voltage at terminals of reactors 1 and 2. Since a *rms* current of 1A has been injected and since the reactors total voltage at frequency f on each reactor is known; it is possible to calculate the inductance of both reactors at each frequency f using,

$$L_{ca@f}^{(1)} = \frac{imag(\tilde{U}_{CT@f}^{(1)})}{2\pi f} \quad (5.76)$$

$$L_{ca@f}^{(2)} = \frac{imag(\tilde{U}_{CT@f}^{(2)})}{2\pi f} \quad (5.77)$$

Where $L_{ca@f}^{(1)}$ and $L_{ca@f}^{(2)}$ are inductances at frequency f of reactors 1 and 2, respectively. The dc inductance for both reactors is calculated at frequency 0.1591Hz. It yields,

$$L_{cd}^{(1)} = imag(\tilde{U}_{CT@0.1591}^{(1)}) \quad (5.78)$$

$$L_{cd}^{(2)} = imag(\tilde{U}_{CT@0.1591}^{(k)}) \quad (5.79)$$

Where $L_{cd}^{(1)}$ and $L_{cd}^{(2)}$ are the dc inductance of the reactors 1 and 2, respectively.

5.3.1.5 Calculating the inductance Ratio

Once the inductance for each reactor is known, the inductance ratio is calculated as,

$$r^{(1)} = \frac{L_{ca@f}^{(1)}}{L_{cd}^{(1)}} \quad (5.80)$$

$$r^{(2)} = \frac{L_{ca@f}^{(2)}}{L_{cd}^{(2)}} \quad (5.81)$$

Where $r^{(1)}$ and $r^{(2)}$ are the inductance of reactors 1 and 2, respectively. The inductance ratio for both reactors will be determined for a frequency range from 0.15915Hz to 1000Hz. This parameter can be calculated with the conventional FEM equation (5.65), the proposed equation (5.70) and by the FEM software ANSYS. A comparison of results is discussed next.

5.3.1.6 Comparison results

In order to perform a first comparison, the voltages at some turns of the reactors 1 and 2 were calculated using ANSYS and the proposed equation (5.70) along (5.65) at frequencies of 0.15915Hz, 500Hz and 1000 Hz, respectively. The voltage at turns of the reactor 1 is given in Table 5.16.

TABLE 5.16
VOLTAGES AT EACH TURN OF REACTOR 1

Frequency	Voltage at turn i , U_{ci}	Proposed Method	ANSYS	%Error
0.15915Hz	U_{c1}	0.1099mV	0.1099mV	0.0000%
	U_{c2}	0.1099mV	0.1099mV	0.0000%
	U_{c3}	0.1099mV	0.1099mV	0.0000%
	U_{c4}	0.1099mV	0.1099mV	0.0000%
	U_{c5}	0.1099mV	0.1099mV	0.0000%
500Hz	U_{c1}	3.9159mV	3.9175mV	-0.0408%
	U_{c2}	3.8359mV	3.8374mV	-0.0391%
	U_{c3}	3.6448mV	3.6463mV	-0.0411%
	U_{c4}	3.3169mV	3.3182mV	-0.0392%
	U_{c5}	2.8155mV	2.8167mV	-0.0426%
1000Hz	U_{c1}	7.6282mV	7.6315mV	-0.0432%
	U_{c2}	7.4744mV	7.4775mV	-0.0414%
	U_{c3}	7.1223mV	7.1252mV	-0.0407%
	U_{c4}	6.5406mV	6.5433mV	-0.0413%
	U_{c5}	5.6975mV	5.7002mV	-0.0474%

The same comparison is given in Table 5.17, but applied to the voltage at turns of reactor 2.

TABLE 5.17
VOLTAGES AT EACH TURN OF REACTOR 2

Frequency	Voltage at turn i , U_{ci}	Proposed Method	ANSYS	%Error
0.15915Hz	U_{c1}	0.1053mV	0.1053mV	0.0000%
	U_{c3}	0.1076mV	0.1076mV	0.0000%
	U_{c5}	0.1099mV	0.1099mV	0.0000%
	U_{c7}	0.1122mV	0.1122mV	0.0000%
	U_{c9}	0.1145mV	0.1145mV	0.0000%
500Hz	U_{c1}	3.3309mV	3.3331mV	-0.0660%
	U_{c3}	3.4662mV	3.4664mV	-0.0635%
	U_{c5}	3.5503mV	3.5523mV	-0.0563%
	U_{c7}	3.5872mV	3.5895mV	-0.0641%
	U_{c9}	3.5729mV	3.5748mV	-0.0532%
1000Hz	U_{c1}	6.6171mV	6.6215mV	-0.0802%
	U_{c3}	6.8813mV	6.8856mV	-0.0713%
	U_{c5}	7.0519mV	7.0560mV	-0.0709%
	U_{c7}	7.1254mV	7.1296mV	-0.1558%
	U_{c9}	7.0973mV	7.1074mV	-0.1479%

By observing Tables 5.16 and 5.17, it can be noticed that the voltages obtained with (5.65) and (5.70), are very close to those obtained with the FEM software ANSYS. A voltage

percentage error (*%error*) was calculated. This error was obtained by using as a base the voltages obtained with ANSYS, i.e.

$$\%Error = \frac{U_{ci,FEM}^{(k)} - U_{ci,Prop}^{(k)}}{U_{ci,FEM}^{(k)}} (100\%) \tag{5.82}$$

Where $U_{ci,FEM}^{(k)}$ is the voltage at turn i of reactor k , obtained with ANSYS; $U_{ci,Prop}^{(k)}$ is the voltage at turn i of reactor k , obtained with (5.65) and (5.70). It can be observed that the voltage percentage error, obtained with these equations is almost negligible, i.e. around 0.2%. It can be concluded that (5.65) and (5.70) allow to calculate in an accurate way all the turn voltages of both reactors at frequencies 0.15915Hz, 500Hz, and 1000 Hz, respectively. It is clear that they can be confidently used to calculate the inductance ratio defined in (5.80) and (5.81). The chart of the inductance ratio L_{cd}/L_{cd} for that frequency range for reactors 1 and 2 is shown in Fig 5.14 and 5.15, respectively. The inductance ratio was calculated on frequency steps of 20Hz. *PropEq* was obtained using (5.70) and (5.65) for each frequency.

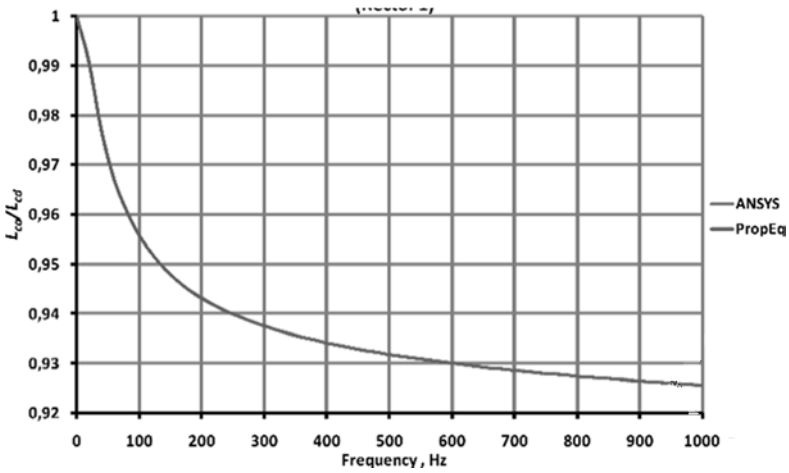


Figure 5.14. Inductances ratio of air reactor 1

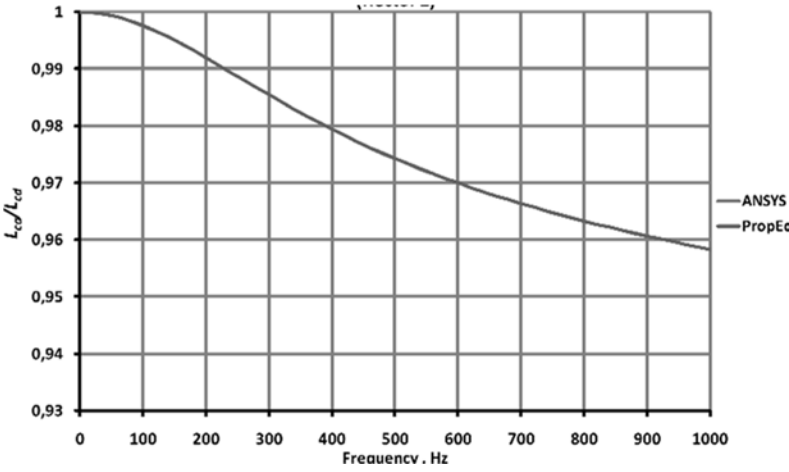


Figure 5.15. Inductances ratio of air reactor 2

It can be observed that the charts obtained by ANSYS and by the proposed equation (5.70) along (5.65), are almost identical for both reactors. These charts can be consulted in the original case study (Preiss 1983). It can be concluded that the magnetic vector potentials \tilde{A}_i have been calculated in an accurate way, by using the equation derived by the proposed methodology.

5.3.1.7 Performance comparison

A finite element analysis using a conventional approach and the proposed equation is now performed. Equations (5.70) and (5.65) are compared: for the case of reactor 1, the conventional equation is of order 3520×3520 ; while the conventional equation of reactor 2 of 1668×1668 . For the case of reactor 1, the proposed equation is of order 1260×1260 ; and for reactor 2 of 220×220 . The matrix equation derived from the proposed methodology can obtain these voltages more efficiently, since their matrix equations are of smaller order.

In order to quantify the performance efficiency of the proposed equation for reactors 1 and 2, the computation time (*CPU time*) was measured. The conventional and the proposed equations were solved in the frequency domain, in separated MATLAB programs. The inductance ratio of reactors 1 and 2 are shown in Figure 5.14. A frequency range from 0.15915Hz to 1000Hz was considered, with a frequency step of 20Hz.

The CPU time of the programs was obtained using the MATLAB *cputime* function. A PC with 1GB RAM, Windows®-XP 32 bits platform, and an AMD® Turion 1.90GHz processor was used. The results of the total CPU time to determine the results shown in Figure 5.14 are given in Tables 5.18 and 5.19, respectively. In order to quantify the CPU time (*Comp. time*) in a more accurate way, the programs were run six times (*#Sim*). *Time_{ind}* is the average CPU time to obtain the inductance ratio for one frequency, and it is given in both tables. The difference, in percentage (*%diff*) between the CPU time needed to solve the equations of the two approaches for reactors 1 and 2 are given in Tables 5.18 and 5.19, respectively. The *CPU time* required to solve the conventional FEM equation was used as a reference. An average of all the variables mentioned before has been included in both tables.

TABLE 5.18
SIMULATION TIME TO SOLVE THE CONVENTIONAL AND THE PROPOSED EQUATION FOR REACTOR 1

#Sim	Proposed Equation		Conventional Equation		%diff
	<i>Time_{ind}</i>	<i>CPU Time</i>	<i>Time_{ind}</i>	<i>CPU Time</i>	
1	22.2616s	1135.34s	51.4062s	2622.72s	-56.71%
2	23.1298s	1179.63s	51.3900s	2620.89s	-54.99%
3	25.6179s	1306.52s	53.2755s	2716.95s	-51.91%
4	22.9566s	1170.79s	53.7079s	2743.65s	-57.32%
5	23.5788s	1202.52s	51.4975s	2626.37s	-54.21%
6	23.4688s	1196.91s	53.0837s	2707.27s	-55.79%
Average	23.5023s	1198.62s	52.3934s	2672.98s	-55.15%

TABLE 5.19

SIMULATION TIME TO SOLVE THE CONVENTIONAL AND THE PROPOSED EQUATION FOR REACTOR 2

#Sim	Proposed Equation		Conventional FEM Equation		%diff
	<i>Time_{ind}</i>	<i>CPU Time</i>	<i>Time_{ind}</i>	<i>CPU Time</i>	
1	1.5134s	72.00s	5.9063s	301.22s	-76.10%
2	1.5592s	74.35s	6.1979s	316.09s	-76.48%
3	1.4505s	69.27s	5.9818s	305.07s	-77.29%
4	1.5698s	75.00s	6.2057s	316.49s	-76.30%
5	1.5705s	74.87s	6.1953s	315.96s	-76.30%
6	1.6043s	76.56s	6.2377s	318.08s	-75.93%
Average	1.5446s	73.68s	6.1207s	312.15s	-76.40%

By observing the Table 5.18 and 5.19, it can be seen than the proposed equation permits to obtain a faster solution for reactor 1, i.e. it requires 44.8% of the time needed by the conventional equation to obtain Figure 5.14. On the other hand, it can be observed from Table 5.19, that the proposed equation also allows the determination of a faster solution for the reactor 2, i.e. it only requires 23.6% of the time taken by the conventional equation obtain the solution shown in Figure 5.14. It can be concluded that the equation derived from the methodology allows the determination of a significantly faster solution for both reactors.

5.3.2. Case study 5. Parallel solution of the air series reactors

5.3.2.1 Introduction

It consists on analyzing the air series reactors in the frequency domain, but using parallel computing with CUBLAS. For the case of the conductor analyzed in 5.2.3, it was not possible to get a faster solution using parallel computing. The reason is that the *reduced* and the *conventional* equations of this conductor are of low order, i.e. 205 and 266, respectively. A *CPU time* reduction cannot be achieved, since the advantage of using the parallel platform is only evident when the size of the equations to be solved is considerable.

The FEM equations derived from the finite element analysis of the air series reactors of the study case 4 (Section 5.3.1) are of large dimension. Because of this, it should be possible to obtain a time reduction using parallel computing if the parallel solution using the LU method is used. This solution will be implemented in this study case.

5.3.2.2 Parallel calculating process

The *conventional* FEM equation shown in (5.65) and the *reduced* equation (5.70) can be solved by a parallel solution of CUBLAS. The conventional expression (5.65) can be also solved in the frequency domain as,

$$[\mathbf{K}]\{\tilde{\mathbf{X}}\} + j(2\pi f)[\mathbf{G}]\{\tilde{\mathbf{X}}\} = \tilde{\mathbf{f}} \quad (5.83)$$

Moreover, (5.83) can be also expressed by,

$$[A]\{\tilde{X}\} = \{\tilde{b}\} \quad (5.84)$$

For the case of the equation derived from the proposed method and defined in (5.70), it can also be solved in the frequency domain and represented by,

$$[A_T]\{\tilde{X}_T\} = \{\tilde{b}_T\} \quad (5.85)$$

The FEM equation (5.84) will be named *conventional* FEM equation, while the expression shown in (5.85) will be named *reduced* FEM equation. The main characteristics of these FEM equations are summarized in Table 5.20. Please notice that these equations are required to be solved several times for the respective frequency range, in order to obtain the respective inductance ratio for both reactors.

TABLE 5.20
FEM EQUATIONS TO BE SOLVED IN A FREQUENCY RANGE

Device to be analyzed	<i>Conventional</i> FEM equation	<i>Reduced</i> FEM equation	Number of FEM equations to be solved
Air -cored Reactor 1	$[A_{3520 \times 3520}]\{\tilde{x}_{3520}\} = \{\tilde{b}_{3520}\}$	$[A_{T,12705 \times 1270}]\{\tilde{x}_{T,1270}\} = \{\tilde{b}_{T,1270}\}$	51
Air-cored Reactor 2	$[A_{1673 \times 1673}]\{\tilde{x}_{1673}\} = \{\tilde{b}_{1673}\}$	$[A_{T,185 \times 185}]\{\tilde{x}_{T,185}\} = \{\tilde{b}_{T,185}\}$	

Two specific steps in the process of calculating the solution in the frequency domain of the equations (5.84) and (5.85) can be identified, i.e. a *preprocessing* and a *calculating* step. The *preprocessing* step of the *conventional* FEM method consists on deriving the matrices and vectors $[K]$, $[G]$ and $\{f\}$ that form the equation shown in (5.84); while the *preprocessing* step of the *reduced* FEM method consists on deriving sub-matrices and sub-vectors that form the expression shown in (5.85). The *calculating process* of the *conventional* and the *reduced* FEM equations, consists on solving both equations using the *LU* method. The *preprocessing* and the *calculating* steps of the *conventional* and a *reduced* FEM equations were previously covered in Chapter 3.

5.3.2.3 Performance comparison between the sequential and the parallel solutions

In order to measure the performance of the method implemented in CUBLAS, the *conventional* and the *reduced* FEM equations were also solved in a sequential computing platform. The *preprocessing* and the *calculating* steps were entirely implemented in the sequential GSL platform (GNU Scientific Library 2013).

For the parallel solution, some stages of the *preprocessing* step were calculated by a sequential computing in GSL (GNU Scientific Library 2013), while the *calculating* steps were completely implemented in the CUBLAS computing platform (Barrachina et al. 2008), (CUDA toolkit 5.0 2014). On the other hand, the *calculating* step of the *conventional* and the

reduced FEM equation will be solved for each frequency by the *LU* method implemented in CUBLAS. Specific details of the sequential and the parallel computing of the *preprocessing* and *calculating* steps are described in Chapter 3.

Conventional and *reduced* FEM equations were also solved in the computing platforms GSL and CUBLAS. The programs were implemented in the same computer and operative system. A Dell Precision R5500 Rack Workstation, GPU NVIDIA® Quadro® 600 with 96 cores, 1 GB RAM and an Ubuntu Operative System were used.

The total computation time (*CPU time*) required to solve air core reactors in the correspondent frequency range was measured. Figs. 5.16 and 5.17 show the *CPU times* needed to solve the equations of the air core reactors 1 and 2, using the sequential and the parallel computing platforms.

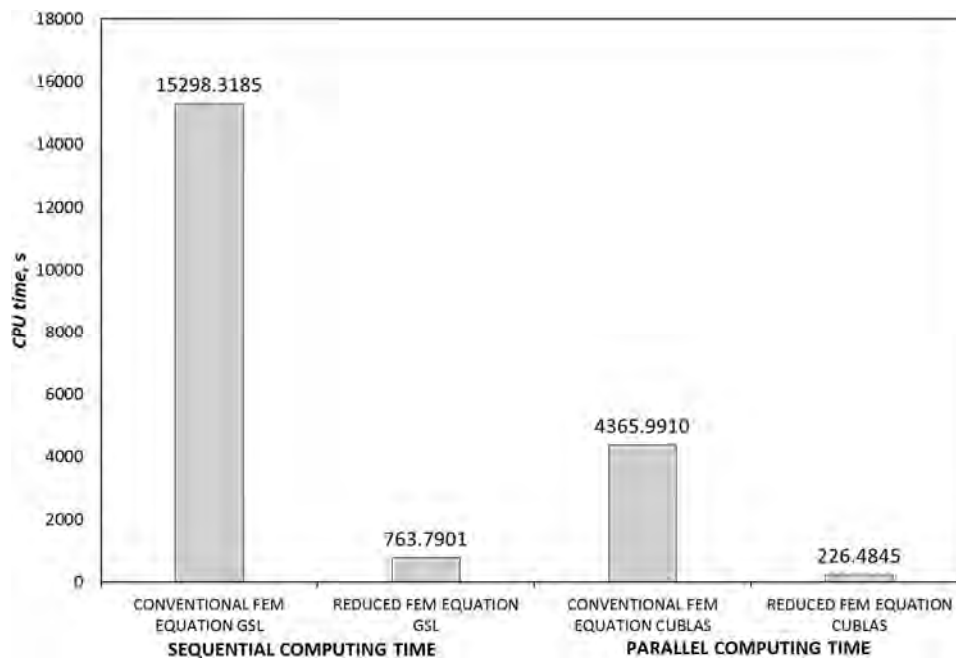


Figure 5.16. *CPU time* derived for reactor 1

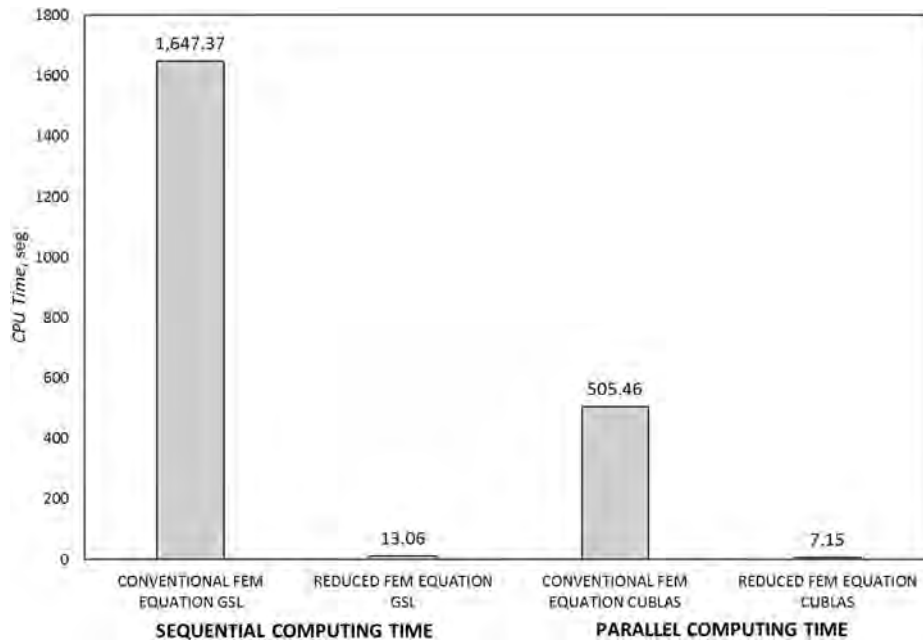


Figure 5.17. CPU time derived for reactor 2

It can be observed that the *reduced* FEM equation allows to derive a faster solution compared to the *conventional* FEM equation solution. For the case of the reactor 1, when the sequential computing was used; the *CPU time* of the *conventional* and the *reduced* equation are 15298sec and 763sec, respectively. There is a large difference between these times. Moreover, when the parallel computing was used for reactor 1, the *CPU time* of the *conventional* and the *reduced* equation are 4365sec and 227sec, respectively. The proposed equation implemented in a parallel computing, can be solved in 227sec, while the sequential solution of the conventional equation requires of 15298sec, or almost 67 times more.

For the specific case of the reactor 2, when the sequential computing was used; the *CPU time* of the *conventional* and the *reduced* equation are 1647sec and 13sec, respectively. There is also a big difference between this times, i.e. nearly 127 times. When the parallel computing was used for reactor 2, the *CPU time* of the *conventional* and the *reduced* equation are 505sec and 7.15sec, respectively, or less than 4 and 2 times. Besides, the proposed equation implemented by parallel computing, can be derived in only 7.15sec, compared to the sequential solution of the conventional equation that requires 1647sec; the difference is really huge.

For both reactors the parallel solution can provide a reduction of nearly one third of the *CPU time* needed by the conventional FEM equation; and of almost one half of the time required by the proposed equation. It can be concluded that the proposed equation can be used in a parallel platform to obtain significantly faster solutions in the frequency domain.

The developed parallel form of solution can be verified by the ratio of sequential (t_s) and parallel *cpu time* (t_p), for the conventional and the proposed method. Ratio t_s/t_p for reactors 1 and 2 can be seen in Figure 5.18 and 5.19, respectively.

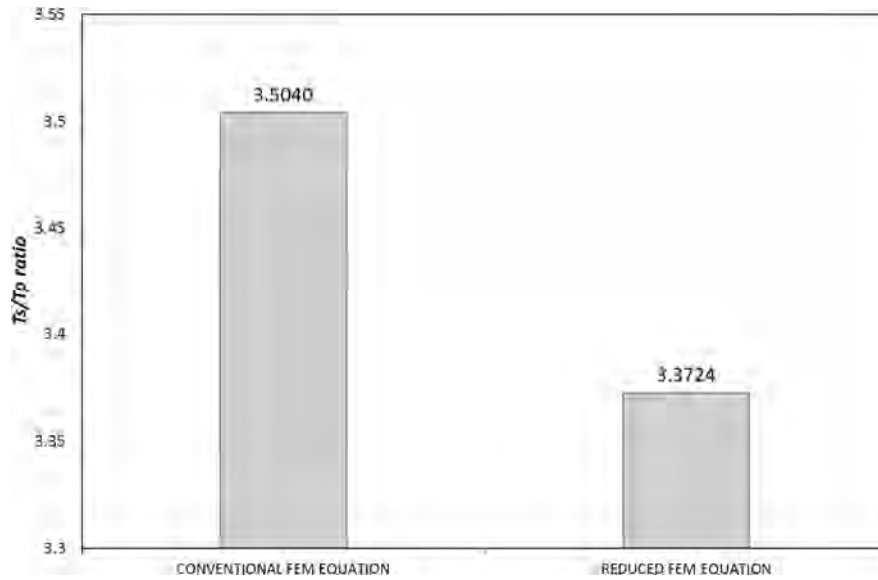


Figure 5.18. Ratio t_s/t_p derived for reactor 1

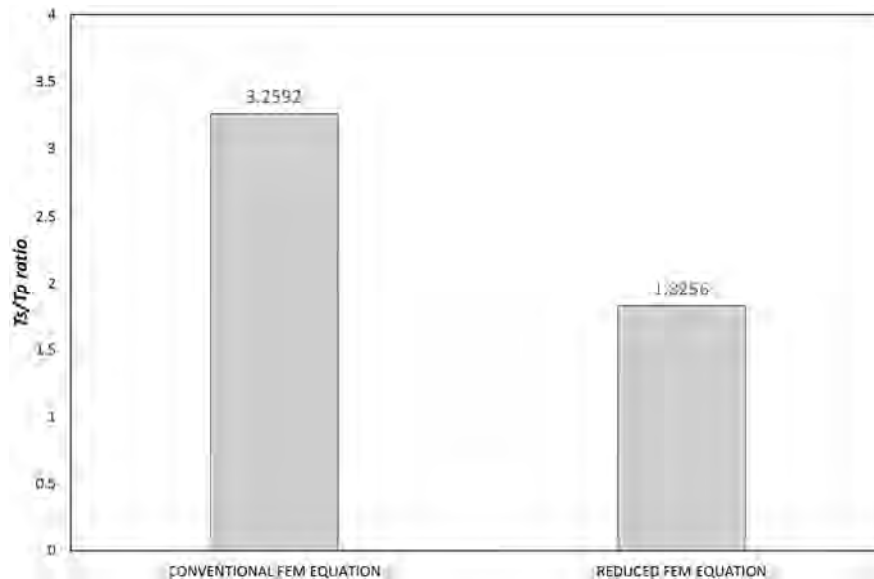


Figure 5.19. Ratio t_s/t_p derived for reactor 2

It can be seen that the ratio t_s/t_p indicates that the proposed parallel form of solution is slightly more efficient for the conventional FEM equation. Nevertheless, the use of the proposed methodology permits to use a lesser order equation, which permits to derive the solution in a faster way than the conventional FEM equation. Specific details about the parallel and the sequential solution of the reactors 1 and of this case study, can be found in Appendix C.2.

5.4 Conclusions

The resulted matrix equation from the proposed methodology for FEM analysis has been tested with several case studies. Three devices modelled by a finite element analysis derived

from a planar symmetry assumption and two by an axisymmetric symmetry were analyzed. The devices have been solved in the frequency and the time domain. A sequential and a parallel solution has been considered.

The parallel solution was implemented using the CUBLAS platform. This platform permits a fast implementation of parallel computing. Although several routines already implemented in the platform were used, it was necessary to define a *LU* decomposition. Thus, it was possible to perform a parallel computing in some of the case studies. The advantage of using the parallel computing solution is evident when large equations are solved.

All the devices can be modeled by a conventional finite element analysis, but they can also be analyzed by using the proposed methodology. This methodology permits to derive a reduced equation that can be solved in the frequency and the time domain. The proposed methodology consists on performing a renumbering of the magnetic vector potentials. Using this reordering it is possible to associate the time varying variables, and after performing some simple matrix operations, to obtain an equation that has several advantages, i.e.

- It can be applied to FEM-field equations and FEM-circuit coupled equations.
- It can directly calculate the time varying variables, i.e. the magnetic vector potentials in the *conductor* regions and the conductor currents.
- It can be solved by parallel computing, such as the *CUBLAS* platform.

Nevertheless, it is important to mention that several matrix operations are necessary to derive the equation. In the analyzed cases, the advantage of using the methodology was evident in the more complex problems

Finally, it is important to mention, that an excellent agreement between the results derived with a conventional approach and the proposed method has been obtained. For all the case studies, the FEM software ANSYS has been used, in order to validate the reported results.

6 Conclusions

6.1 Summary of results

This investigation has covered the solution of a field equation by using FEM matrix equations, derived from a finite element analysis; which has been simplified by a planar or an axisymmetric symmetry assumption. A new form of solution of FEM field and a FEM-circuit coupled equations has been proposed and solved. The fundamentals and basic principles of these equations have been widely explained in this investigation, along their respective method of solution in the frequency and in the time domain.

In this investigation a new methodology, which consists on performing several steps that lead to derive an alternative expression of a FEM field or a FEM-circuit coupled equation has been proposed. The equation derived by the proposed method has the important feature of being only defined in terms of the time varying variables; thus, these variables can be directly calculated. The equation derived is of lower order than the conventional and can be easier to solve in the frequency and in the time domain. For the case of the time domain solution, several methods have been used in the solution of the proposed equation i.e., the Euler, Backwards Euler, 4th order Runge Kutta and the ND Newton method. An effective form for the solution of the FEM equations has been obtained.

Although the proposed method provides a faster solution of the FEM equations, it may still require of considerable computation effort, especially if large equations need to be solved. Because of this, it a parallel solution in CUBLAS has been implemented. The CUBLAS-CUDA is a powerful platform that allows a fast and powerful parallel computing, since it already contains several matrix routines that are very useful and efficient to derive faster solutions from the conventional and the proposed equation. After having explained the methodology, and after solving several case studies consisting on solving the ordinary FEM equation, along the expression derived by the proposed methodology; it can be concluded that the proposed method developed through this investigation has the following advantages:

- 1) It permits to directly calculate in an easier and faster way, the time varying variables of a FEM field and a FEM-circuit coupled equations; by deriving a unique equation. Thus, it is possible to calculate these variables in the frequency or the time domain, by using a lower order matrix expression. For the specific case of the air series reactor 1 and 2 covered in Section 5.3.2, the use of the proposed methodology requires 45% and 24% of the computing time required for the conventional FEM equation solution. Moreover, a computing time reduction has been also obtained for the T-slot conductor covered in Section 5.2.3, for this case the proposed methodology requires 45% of the computing time of the conventional FEM expression. It can be seen the proposed method allows a computing time reduction, even performing a sequential computing.

- 2) It consists on a simple calculating process, i.e. it requires of a nodal renumbering of the FEM field matrices equations in order to get a new FEM field equation; associating the time varying variables; and finally, on performing some simple matrix operations. These matrix operation requires computing time, but they are necessary to perform only time in order to derive the matrices of the equation derived by the explained methodology.
- 3) It allows the solution in the time domain by using the Euler, the Newton and the 4th order Runge Kutta methods. Nevertheless, it is important to remark that an approximate solution is achieved. Moreover, an accurate solution in the time domain can be achieved, if the Backwards Euler method is used.
- 4) It has been implemented on a parallel form of solution by using the CUDA platform. The CUDA platform was created as a computing platform for the videogames industry. Nevertheless, it has been extensively used in parallel computing, since it allows a faster implementation using a known computing platform (CUDA C).
- 5) Since the proposed method requires of standard matrix-vectors operations; it has been easily implemented in CUBLAS-CUDA. This parallel computing platform already contains several tested routines, which have been used to derive the equations covered by this investigation. For the air series reactor 1 and 2 covered in Section 5.3.2, the use of the proposed methodology along the developed parallel solution, permit to get a faster solution, it requires 1.48% and 0.5% of the computing time required for the GSL sequential solution of the conventional FEM equation.
- 6) It allows a significant time reduction when a parallel computing with CUBLAS is used. A significant reduction of CPU time to solve larger order FEM equations in the frequency domain has been obtained. The CPU time for solving the equation derived from the methodology by using CUBLAS it is several times smaller than the time required for solving the *normal* FEM equation with GSL. Parallel computing permit to get a computing time reduction, when the dimension of the FEM matrix involved are large, i.e., the air reactor 1 and 2 are modeled by FEM matrix of order 3520 and 1673, respectively

An excellent agreement between the results derived with a conventional approach and the proposal method has been obtained. Moreover, several study cases has been also simulated by ANSYS. The FEM simulation helped to prove the accuracy of the proposed method. The obtained results have been successfully validated.

6.2 Recommendations for Further Developments

- 1) Although the method developed by this investigations provides a good alternative in the solution of the FEM equations, the method has some disadvantages. For example, it requires of performing several matrix operations. These operations could require of additional computing time, which could eliminate the advantage of having to solve a lower order matrix equation. Moreover, it could be proper to enhance the calculating process of the methodology, in order to require of lesser computing times.
- 2) Another aspect to remark is that the non-linear properties of the materials have not been considered. For example, the permeability of the magnetic materials of the electrical machines or devices is clearly non-linear; and therefore, the FEM matrix equations are non-linear too. In the final stages of the investigation, the FEM equations of devices with non-linear parameters by using the Newton Method were solved; an interesting challenge could be exploring the possibility of solving a non-linear time-varying equation. The developed method of solution can be compared with others methods or forms of solution, i.e. those results obtained with ANSYS. In theory, the solution of the non-linear time-varying equation can be obtained, since the methodology permits to derive a recursive equation which can be solved with the ND method. In theory this approach can be implemented, since the Backwards Euler method can be used as an integrating method.
- 3) Another subject of possible future work is the possibility of analyzing other electric or magnetic devices. Specifically, those devices with more complex geometry or configuration. There are several elements that can be analyzed, such as induction rotating machines, synchronous machines, some components of the transformers, etc.
- 4) A parallel form of solution of a matrix equation by using CUDA-CUBLAS has been also developed. If the solution of non-linear equations is performed, it can be implemented, by using a new parallel method of solution. Moreover, it can be possible to engage the developed method in other sequential computing platform such as Matlab or GSL. Thus, a performance comparison can be performed.

Bibliography

- (ANSYS 2010) ANSYS. "Low-Frequency Electromagnetic Analysis Guide." ANSYS Inc. , 2010
- (Arkkio 1987) Arkkio, A. . "Analysis of induction motors based on the numerical solution of the magnetic field and circuit equations." *Docthoral thesis, Acta Polytechnica Scandinavica Electrical Engineering Series No. 59.* Helsiki University of Technology, 1987.
- (Bastos 2003) Bastos, J.A. . *Electromagnetic Modeling by Finite Element Method.* Mercel Dekker, 2003.
- (Bianchi 2005) Bianchi, N. *Electrical Machine Analysis Using Finite Element Method.* Francis Group, 2005.
- (Brauer, Sadegui and Oerterlei 1999) Brauer, J., H. Sadegui, and R. Oerterlei. "Polyphase Induction Motor Performance Computed Directly by Finite Elements." *IEEE Transaction on Energy Conversion* 14, no. 3 (September 1999): 583-584.
- (Butrylo et al. 2003) Butrylo, F. , F. Musy, L. Nicolas , E. Perrusel , R. Scorreti, and C. Vollaie. "A survey of parallel solvers for the Finite Element Method in Computation Electromagnetics." *COMPEL The International Journal for Computation and Mathematics in Electric and Electronic Engineering* 23, no. 2 (2003): 531-546.
- (Chari and Sylvester 1980) Chari, M.V.K., and P.P. Sylvester. *Finite Elements in Electrical and Magnetic Field Problem.* New York: John Wiley & Sons , 1980.
- (Cheng 1993) Cheng, D.K. . *Fundamentals of Engineering Electromagnetics.* Reading MA: Addison-Wesley, 1993.
- (Cisneros-Magaña and Medina 2013) Cisneros-Magaña, R. , and A. Medina. "Parallel Kalman Filter Based Time-Domain Harmonic State Stimulation." *Proceedings of the North American Power Symposium (NAPS).* 2013. 1-6.
- (CUDA toolkit 5.0 2014) CUDA toolkit 5.0. *CUBLAS Library.* 2701 San Tomas Express Way Santa Clara CA: NVIDIA Corporation, 2014.
- (Dlala and Arkkio 2010) Dlala, E. , and A. Arkkio. "General Formulation for the Newton-Raphson Method and the Fixed-Point Method in Finite Element Programs." *Proceedings of the 2010 XIXth International Conference on Electrical Machines (ICEM).* Rome, 2010. 1-14.

- (Engleman and Middendorf 1995) Engleman, R.H., and W.H. Middendorf. *Handbook of Electrical Motors*. Mercel & Dekker Inc., 1995.
- (Escarela-Perez, Melgoza and Alvarez-Ramirez 2009) Escarela-Perez, E., E. Melgoza, and J. Alvarez-Ramirez. "A 2-D Time-Harmonic Modified Nodal Analysis Framework." *IEEE Transaction on Magnetics* 45, no. 3 (February 2009): 707-709.
- (C. Fu 2008) Fu, Chaojiang. «Parallel Computing for Finite Element Structural Analysis on Workstation Cluster.» *International Conference on Computer Science and Software Engineering*. Wuhan, Hubei, 2008. 291-294.
- (Fu and Ho 2009) Fu, W.N., and S.L. Ho. "Matrix Analysis of 2-D Eddy-Current Magnetic Fields." *IEEE Transaction on Magnetics* 45, no. 9 (September 2009): 3343-3344.
- (GNU Scientific Library 2013) GNU Scientific Library. "GNU Scientific Library." GNU Project, 2013.
- (Ho, Shuangxia and Fu 2011) Ho, S.L. , N. Shuangxia, and W.N. Fu. "An Equivalent Parameter Extraction Method of Transient Electric Circuit and Magnetic Field Coupled Problems Based on Sensitivity Computation of System Equations." *IEEE Transactions on Magnetics* 47, no. 8 (August 2011): 4218-4219.
- ((Ho, Li and Fu 1999) Ho, S.L., H.L. Li, and W.N. Fu. "Inclusion of Interbar Currents in a Network-Field Coupled Time-Stepping Finite-Element Model of Skewed-Rotor Induction Motors." *IEEE Transaction on Magnetics* 35, no. 5 (September 1999): 4218-4219.
- (Ho, Fu and Wong 1997) Ho, S.L., W.N. Fu, and H.C. Wong . "Application of Automatic Choice of Step Size for Time Stepping Finite Element Method to Induction Motors." *IEEE Transaction on Magnetics* 45, no. 9 (March 1997): 1370-1371.
- (Iwano et al. 1994) Iwano, K. , V. Cingoski, K. Kaneda, and H. Yamashita. "A parallel processing method in Finite Element Analysis using domain division." *IEEE Transaction on Magnetics* 30, no. 5 (September 1994): 3598-3601.
- (Jafari-Shapoorabadi, Konrad and Sinclair 2002) Jafari-Shapoorabadi, R. , A. Konrad , and A.N. Sinclair. "Comparison of Three Formulation for Eddy-Current and Skin Effect Problems." *IEEE Transaction on Magnetics*, March 2002: 617-620.
- (Jalili-Marandi, Zhiyin and Dinavahi 2012) Jalili-Marandi, V. , Z. Zhiyin , and V. Dinavahi. "Large-Scale Transient Stability Simulation of Electrical Power Systems on Parallel GPUs." *IEEE Transaction on Parallel and Distributed Systems* 23, no. 7 (August 2012): 1255-1266.

- (Jianming 2002) Jianming, J. . *The Finite Element Method in Electromagnetics*. John Wiley & sons, 2002.
- (Kiss et al. 2012) Kiss, I., Badics, Z., Gyimoth, S., & Pavo, J. (2012). High locality and increased intra-node parallelism for solving finite element models by novel element-by-element implementation. *IEEE Conference on High Performance Extreme Computing (HPEC)*, (pp. 1-5). Waltham MA.
- (Konrad 1982) Konrad, A. . "Integrodifferential Finite Element Formulation of Two-Dimensional Steady-State Skin Effect Problems." *IEEE Transaction on Magnetics* 18, no. 1 (January 1982): 284-286.
- (Konrad 1981) Konrad, A. . "The Numerical Solution of Steady-State Skin Effect Problems -An Integrodifferential Approach." *IEEE Transaction on Magnetics* 175, no. 1 (January 1981): 1149-1150.
- (Konrad, Chari and Csendes 1982) Konrad, A. , M.V.K. Chari, and Z.J. Csendes. "New Finite Element Techniques for Skin Effect Problems." *IEEE Transactions on Magnetics* 18, no. 2 (March 1982): 450-455.
- (Kwon and Bang 1997) Kwon, K. , and H. Bang. *The Finite Element Method using MATLAB*. CRC Press, 1997.
- (Lavers, Boglaev y Sirotkin 1996) Lavers, D. , I. Boglaev , y V. Sirotkin. «Numerical Solution of Transient 2-D Eddy Current Problem by Domain Decomposition Algorithm.» *IEEE Transaction on Magnetics* 32, n° 3 (May 1996): 1413-1416.
- (Li, Ho and Fu 2012) Li, H.L. , S.L. Ho, and W.N. Fu. "Application of Multi-Stage Diagonally-Implicit Runge-Kutta Algorithm to Transient Magnetic Field Computation using Finite Element Method." *IEEE Transaction on Magnetics* 48, no. 2 (February 2012): 279-280.
- (Lubin, Mezani and Rezzoug 2011) Lubin, T. , S. Mezani, and A. Rezzoug. "Analytic Calculation of Eddy Currents in the Slots of Electrical Machines: Application to Cage Rotor Induction Motors." *IEEE Transaction on Magnetics* 47, no. 11 (November 2011): 4650-4651.
- (Manna and Marwaha 2008) Manna, M.S., and A. Marwaha. "Eddy Current Analysis on Induction Machine by 3D Finite Element Method." *IEEE Power India Conference*. 2008. 1-3.
- (MATLAB 2010) MATLAB. "MATLAB." Matworks Inc., 2010.
- (Mihai and Benelghali 2012) Mihai, A.M. , and S. Benelghali. "Design and FEM Analysis of Five-Phase Permanent Magnet Generators of Gearless Small-Scale Wind Turbines." *Proceedings of the XXth International Conference on Electrical Machines (ICEM)*. Marseille, 2012. 150-156.

- (Mukades and Uragani 2008) Mukades , A.M.M. , and A. Uragani . "Parallel performance of domain decomposition method on distributed computing environment." *11th International Conference on Computer and Information Technology*. Khulna, 2008. 617-622.
- (NVIDIA 2012) NVIDIA. *NVIDIA CUDA API reference manual Version 5.0*. NVIDIA Inc., 2012.
- (Okamoto, Fujiwara and Ishihara 2010) Okamoto, Y. , K. Fujiwara, and Y. Ishihara . "Effectiveness of Higher Order Time Integration in Time-Domain Finite-Element Analysis." *IEEE Transaction on Magnetics* 46, no. 8 (August 2010): 3321-3322.
- (Owens , Houston and Luebke 2008) Owens , J.D. , M. Houston , and D. Luebke. "GPU Computing." *Proceedings of the IEEE* 96, no. 5 (May 2008): 879-899.
- (Preiss 1983) Preiss , K. . "A Contribution to Eddy Current Calculation in Plane and Axisymmetric Multiconductor Systems." *IEEE Transaction on Magnetics* 19, no. 6 (November 1983): 2397-2399.
- (Reddy 1984) Reddy, J.N. . *An Introduction to Finite Element Method*. New York: McGraw-Hill, 1984.
- (Reece and Preston 2000) Reece, A. , and T. Preston. *Finite Element Method in Electric Power Engineering*. UK: Oxford University Press, 2000.
- (Semlyen and Medina 1995) Semlyen, A., and J. Medina. "Computation of the Periodic Steady State in Systems with Nonlinear Components Using a Hybrid Time and Frequency Domain Methodology." *IEEE Transaction on Power Systems* 10, no. 3 (August 1995): 1498-1501.
- (Shen et al. 1985) Shen, D. , G. Meunier, J.L. Coulomb, and J.C. Sabonnadiere. "Solution of Magnetic Fields and Electrical Circuits Combined Problems." *IEEE Transaction on Magnetics* 21, no. 6 (November 1985): 2288-2289.
- (Silvester and Ferrari 1983) Silvester, P.P., and R.L. Ferrari. *Finite Element Analysis and Design of Electromagnetic Devices*. Cambridge, England: Cambridge University Press, 1983.
- (Stratton 1941) Stratton, J.A. . *Electromagnetic Theory*. New York: McGraw-Hill, 1941.
- (Tsukerman et al. 1993) Tsukerman, I.A. , A. Konrad , G. Meunier, and J.C. Sabonnadiere. "Coupled field-circuit problems: trends and accomplishments." *IEEE Transactions on Magnetics* 20, no. 2 (March 1993): 1701-1704.
- (Wang and Xie 2009) Wang, X. , and D. Xie. "Analysis of Induction Motor Using Field-Circuit Coupled Time-Periodic Finite Element Method Taking Account of Hysteresis." *IEEE Transaction on Magnetics* 45, no. 3 (March 2009): 1740-1741.

(Wang, et al.
2014)

Wang, Y., J. Jiaming, T. Krein, and P. Magill. "A Finite Element-Based Domain Decomposition Method for Efficient Simulation of Non-Linear Electromechanical Problems." *IEEE Transaction on Energy Conversion* 29, no. 2 (June 2014): 309-317.

(Wenliang et al.
2012)

Wenliang, C. , L. Yujing , J. Islam, and D. Svechkarenko. "Strand-Level Finite Element Model of Stator AC Copper Losses in the High Speed Machines ." *Proceedings of the 2012 XXth International on Electrical Machines (ICEM)*. Marseille, 2012. 477-482

Appendix A FEM matrices and vectors derived by Finite Element Analysis

A.1 Planar symmetry's FEM matrices and vectors

A.1.1 Finite elements

A.1.1.1 Triangular linear finite element with three nodes

$$A_{zj}(x, y) = \{N_1 \ N_2 \ N_3\} \{A_{z1} \ A_{z2} \ A_{z3}\}^T \quad (\text{A.1})$$

The values of N_1, N_2, N_3 of (A.1) are defined by,

$$N_1 = \frac{x_2y_3 - x_3y_2}{\Delta_d} + \frac{y_2 - y_3}{\Delta_d} x + \frac{x_3 - x_2}{\Delta_d} y \quad (\text{A.2})$$

$$N_2 = \frac{x_3y_1 - x_1y_3}{\Delta_d} + \frac{y_3 - y_1}{\Delta_d} x + \frac{x_1 - x_3}{\Delta_d} y \quad (\text{A.3})$$

$$N_3 = \frac{x_1y_2 - x_2y_1}{\Delta_d} + \frac{y_1 - y_2}{\Delta_d} x + \frac{x_2 - x_1}{\Delta_d} y \quad (\text{A.4})$$

The variable Δ_d is calculated using,

$$\Delta_d = x_1y_2 - x_2y_1 + x_2y_3 - x_3y_2 + x_3y_1 - x_1y_3 \quad (\text{A.5})$$

A.1.1.2 Triangular linear finite element with six nodes

$$A_{zj}(x, y) = \{N_1 \ N_2 \ N_3 \ N_4 \ N_5 \ N_6\} \{A_{z1} \ A_{z2} \ A_{z3} \ A_{z4} \ A_{z5} \ A_{z6}\}^T \quad (\text{A.6})$$

The values of L_1, L_2 and L_3 of (A.6) are defined by N_1, N_2 and N_3 , respectively. N_1, N_2 and N_3 are defined in (A.2), (A.3) and (A.4), respectively. N_4, N_5 and N_6 are given by,

$$N_4 = 4L_1L_2 \quad (\text{A.7})$$

$$N_5 = 4L_2L_3 \quad (\text{A.8})$$

$$N_6 = 4L_3L_1 \quad (\text{A.9})$$

A.1.2 Field equation with current density as the forcing function

$$-\frac{\partial}{\partial x} \left(\nu \frac{\partial A_z}{\partial x} \right) - \frac{\partial}{\partial y} \left(\nu \frac{\partial A_z}{\partial y} \right) = J_z \quad (\text{A.10})$$

A.1.2.1 Matrices and vectors derived from applying FEA

$$[\text{Dirichlet B.C.}] + [S]\{A_{zj}\} = \{f_{gj}\}(J_z) \quad (\text{A.11})$$

The matrices and vectors of (A.11) are defined by,

$$[S] = \left[\int_{\tau} \nu \left(\frac{\partial \{N_i\}^T}{\partial x} \frac{\partial \{N_j\}}{\partial x} + \frac{\partial \{N_i\}^T}{\partial y} \frac{\partial \{N_j\}}{\partial y} \right) d\tau \right] \quad (\text{A.12})$$

$$\{f_{gj}\} = \left[\int_{\tau} (\{N_i\}^T) d\tau \right] \quad (\text{A.13})$$

A.1.1.2.1 Matrices and vectors for finite element of three nodes

$$[S]_{3 \times 3} = \frac{\nu}{4d} \begin{bmatrix} (y_2 - y_3)^2 + (x_3 - x_2)^2 & (y_2 - y_3)(y_3 - y_1) + (x_3 - x_2)(x_1 - x_3) & (y_2 - y_3)(y_1 - y_2) + (x_3 - x_2)(x_2 - x_1) \\ \text{sym} & (y_3 - y_1)^2 + (x_1 - x_3)^2 & (y_3 - y_1)(y_1 - y_2) + (x_3 - x_1)(x_2 - x_1) \\ \text{sym} & \text{sym} & (y_1 - y_2)^2 + (x_2 - x_1)^2 \end{bmatrix} \quad (\text{A.14})$$

$$\{f_{gj}\}_{1 \times 3} = \frac{4d}{6} \{1 \quad 1 \quad 1\}^T \quad (\text{A.15})$$

A.1.1.2.2 Matrices and vectors derived for finite element of six nodes

$$[S]_{6 \times 6} = \nu \begin{bmatrix} S_{11} & S_{12} & S_{13} & S_{14} & S_{15} & S_{16} \\ S_{21} & S_{22} & S_{23} & S_{24} & S_{25} & S_{26} \\ S_{31} & S_{32} & S_{33} & S_{34} & S_{35} & S_{36} \\ S_{41} & S_{42} & S_{43} & S_{44} & S_{45} & S_{46} \\ S_{51} & S_{52} & S_{53} & S_{54} & S_{55} & S_{56} \\ S_{61} & S_{62} & S_{63} & S_{64} & S_{65} & S_{66} \end{bmatrix} \quad (\text{A.16})$$

$$\{f_g\}_{1 \times 6} = \frac{\Delta_d}{6} \{0 \ 0 \ 0 \ 1 \ 1 \ 1\}^T \quad (\text{A.17})$$

The elements of (A.16) are defined by,

$$\begin{aligned} S_{11} &= [(a_{11})^2 + (a_{12})^2 + (a_{21})^2 + (a_{22})^2 + 2a_{11}a_{12} + 2a_{21}a_{22}]/(2\Delta_d) \\ S_{12} &= S_{21} = [(a_{11})^2 + (a_{21})^2 + a_{11}a_{12} + a_{21}a_{22}]/(6\Delta_d) \\ S_{13} &= S_{31} = [(a_{12})^2 + (a_{22})^2 + a_{11}a_{12} + a_{21}a_{22}]/(6\Delta_d) \\ S_{14} &= S_{41} = -4S_{12}; \quad S_{15} = S_{51} = 0; \quad S_{16} = S_{61} = -4S_{13}; \quad S_{22} = [(a_{11})^2 + (a_{21})^2]/(2\Delta_d) \\ S_{23} &= S_{32} = -[a_{11}a_{12} + a_{21}a_{22}]/(6\Delta_d); \quad S_{24} = S_{42} = -4S_{12}; \quad S_{25} = S_{52} = -4S_{23}; \quad S_{26} = S_{62} = 0 \\ S_{33} &= [(a_{12})^2 + (a_{22})^2]/(2\Delta_d); \quad S_{34} = S_{43} = 0; \quad S_{35} = S_{53} = -4S_{23}; \quad S_{36} = S_{63} = -4S_{13} \\ S_{44} &= 4[(a_{11})^2 + (a_{12})^2 + (a_{21})^2 + (a_{22})^2 + a_{11}a_{12} + a_{21}a_{22}]/(3\Delta_d); \quad S_{45} = S_{54} = -4S_{13} \\ S_{46} &= S_{64} = -4S_{23}; \quad S_{55} = S_{44}; \quad S_{56} = S_{65} = -4S_{12}; \quad S_{66} = S_{44} \end{aligned}$$

The variables a_{11} , a_{12} , a_{21} , a_{22} are defined by,

$$a_{11} = y_3 - y_1; \quad a_{12} = y_1 - y_2$$

$$a_{21} = x_1 - x_3; \quad a_{22} = x_2 - x_1 \quad (\text{A.18})$$

A.1.3 Field equation with voltages as the forcing function

$$-\frac{\partial}{\partial x}\left(\nu \frac{\partial A_z}{\partial x}\right) - \frac{\partial}{\partial y}\left(\nu \frac{\partial A_z}{\partial y}\right) + \sigma \frac{\partial A_z}{\partial t} = \sigma \frac{U_c}{l} \quad (\text{A.19})$$

A.1.3.1 Matrices and vectors derived from applying FEA

$$[\text{Dirichlet B.C.}] + [S]\{A_{zj}\} + [T] \frac{d}{dt}\{A_{zj}\} = \{f_{gu}\}(U_c) \quad (\text{A.20})$$

The matrix $[S]$ was defined in (A.12). Matrices $[T]$ and the vector $\{f_{gu}\}$ of (A.20) are defined by,

$$[T] = \left[\int_{\tau_0} \sigma \{N_i\}^T \{N_j\} d\tau \right] \quad (\text{A.21})$$

$$\{f_{gu}\} = \left[\int_{\tau_0} \frac{\sigma}{l} \{N_i\}^T d\tau \right] \quad (\text{A.22})$$

A.1.3.1.1 Matrices and vectors for finite element of three nodes

The matrix $[S]_{3 \times 3}$ was defined in (A.14). Matrix $[T]_{3 \times 3}$ and vector $\{f_{gu}\}_{3 \times 1}$ are defined by,

$$[T]_{3 \times 3} = \sigma \frac{\Delta d}{24} \begin{bmatrix} 2 & 1 & 1 \\ 1 & 2 & 1 \\ 1 & 1 & 2 \end{bmatrix} \quad (\text{A.23})$$

$$\{f_{gu}\}_{1 \times 3} = \frac{\sigma \Delta d}{l \cdot 6} \{1 \quad 1 \quad 1\}^T \quad (\text{A.24})$$

A.1.3.1.2 Matrices and vectors for finite element of six nodes

The matrix $[S]_{6 \times 6}$ was defined in (A.16). The matrix $[T]_{6 \times 6}$ and the vector $\{f_{gu}\}_{1 \times 6}$ are defined by,

$$[T]_{6 \times 6} = \sigma \frac{\Delta d}{360} \begin{bmatrix} 6 & -1 & -1 & 0 & -4 & 0 \\ -1 & 6 & -1 & 0 & 0 & -4 \\ -1 & -1 & 6 & -4 & 0 & 0 \\ 0 & 0 & -4 & 32 & 16 & 16 \\ -4 & 0 & 0 & 16 & 32 & 16 \\ 0 & -4 & 0 & 16 & 16 & 32 \end{bmatrix} \quad (\text{A.25})$$

$$\{f_{gu}\}_{1 \times 6} = \frac{\sigma \Delta d}{l \cdot 6} \{0 \quad 0 \quad 0 \quad 1 \quad 1 \quad 1\}^T \quad (\text{A.26})$$

A.1.4 Field equation with currents as the forcing function

$$-\frac{\partial}{\partial x}\left(v\frac{\partial A_z}{\partial x}\right) - \frac{\partial}{\partial y}\left(v\frac{\partial A_z}{\partial y}\right) + \sigma\frac{\partial A_z}{\partial t} = \sigma\frac{U_c}{l} \quad (\text{A.27})$$

$$(\mathbf{R}_c)^{-1}\mathbf{U}_c - \int_{\tau} \sigma\frac{\partial A_z}{\partial t} d\tau = I_z \quad (\text{A.28})$$

A.1.4.1 Matrices derived from applying FEA and the Newton Cotes

$$[\text{Dirichlet B. C.}] + [\mathbf{S}]\{\mathbf{A}_{zj}\} + [\mathbf{T}]\frac{d}{dt}\{\mathbf{A}_{zj}\} = \{\mathbf{f}_{ga}\}(\mathbf{U}_c) \quad (\text{A.29})$$

$$(\mathbf{R}_c)^{-1}(\mathbf{U}_c) - \{\mathbf{f}_{ga}\}\frac{d\{\mathbf{A}_{zj}\}}{dt} = I_z \quad (\text{A.30})$$

The matrices $[\mathbf{S}]$ and $[\mathbf{T}]$ of (A.29) were previously defined in (A.12) and (A.21). The vector $\{\mathbf{f}_{ga}\}$ is defined by,

$$\{\mathbf{f}_{ga}\} = \left[\int_{\mathbf{v}_p} \sigma\{\mathbf{N}_i\}^T d\tau \right] \quad (\text{A.31})$$

A.1.4.1.1 Vectors for finite element of three nodes

$$\{\mathbf{f}_{ga}\}_{1 \times 3} = \sigma\frac{A_d}{6}\{\mathbf{1} \quad \mathbf{1} \quad \mathbf{1}\} \quad (\text{A.32})$$

A.1.4.1.2. Vectors for finite element of six nodes

$$\{\mathbf{f}_{ga}\}_{1 \times 6} = \sigma\frac{A_d}{6}\{\mathbf{0} \quad \mathbf{0} \quad \mathbf{0} \quad \mathbf{1} \quad \mathbf{1} \quad \mathbf{1}\} \quad (\text{A.33})$$

A.2 Axisymmetric symmetry's FEM matrices and vectors

A.2.1 Finite elements

A.2.1.1 Triangular linear finite element method with three nodes

$$A_{\rho j}(\mathbf{r}, z) = \{N_1 \quad N_2 \quad N_3\} \{A_{\rho 1} \quad A_{\rho 2} \quad A_{\rho 3}\}^T \quad (\text{A.34})$$

The values of N_1, N_2, N_3 of (A.34) are defined by,

$$N_1 = \frac{r_2 z_3 - r_3 z_2}{\Delta_d^r} + \frac{z_2 - z_3}{\Delta_d^r} \mathbf{r} + \frac{r_3 - r_2}{\Delta_d^r} z \quad (\text{A.35})$$

$$N_2 = \frac{r_3 z_1 - r_1 z_3}{\Delta_d^r} + \frac{z_3 - z_1}{\Delta_d^r} \mathbf{r} + \frac{r_1 - r_3}{\Delta_d^r} z \quad (\text{A.36})$$

$$N_3 = \frac{r_1 z_2 - r_2 z_1}{\Delta_d^r} + \frac{z_1 - z_2}{\Delta_d^r} \mathbf{r} + \frac{r_2 - r_1}{\Delta_d^r} z \quad (\text{A.37})$$

A.2.2 Field equation with current density as the forcing function

$$-\frac{1}{r} \frac{\partial}{\partial r} \left(v r \frac{\partial A_\rho}{\partial r} \right) - \frac{1}{r} \frac{\partial}{\partial z} \left(v r \frac{\partial A_\rho}{\partial z} \right) + v \frac{A_\rho}{r^2} = J_\rho \quad (\text{A.38})$$

A.2.2.1 Matrices derived from applying FEA

$$[\text{Dirichlet B. C.}] + [\mathbf{S}]\{A_{\rho j}\} + [\mathbf{S}_{II}]\{A_{\rho j}\} = \{f_j\}(J_\rho) \quad (\text{A.39})$$

Where the matrices of (A.39) are defined by,

$$[\mathbf{S}] = \left[\int_{\tau_D} \left(v \frac{\partial \{N_i\}^T}{\partial r} \frac{\partial \{N_j\}}{\partial r} + v \frac{\partial \{N_i\}^T}{\partial z} \frac{\partial \{N_j\}}{\partial z} \right) d\tau_r \right] \quad (\text{A.40})$$

$$[\mathbf{S}_{II}] = \left[\int_{\tau_D} v \{N_i\}^T \{N_j\} d\tau_r \right] \quad (\text{A.41})$$

$$\{f_j\} = \left[\int_{\tau_D} \{N_i\}^T d\tau_r \right] \quad (\text{A.42})$$

A.2.2.1.1 Matrices and vectors derived for finite element of three nodes

$$[S]_{3 \times 3} = \frac{v \pi R_c}{\Delta_r^d} \begin{bmatrix} (r_3 - r_2)^2 + (z_2 - z_3)^2 & (r_3 - r_2)(r_1 - r_3) + (z_2 - z_3)(z_3 - z_1) & (r_3 - r_2)(r_2 - r_1) + (z_2 - z_3)(z_1 - z_2) \\ \text{sym} & (r_1 - r_3)^2 + (z_3 - z_1)^2 & (r_1 - r_3)(r_2 - r_1) + (z_3 - z_1)(z_1 - z_2) \\ \text{sym} & \text{sym} & (r_2 - r_1)^2 + (z_1 - z_2)^2 \end{bmatrix} \quad (\text{A.43})$$

$$[S_{II}]_{3 \times 3} = \frac{\pi v}{12(r_c)} \begin{bmatrix} 2 & 1 & 1 \\ 1 & 2 & 1 \\ 1 & 1 & 2 \end{bmatrix} \quad (\text{A.44})$$

$$\{f_j\}_{1 \times 3} = \frac{\Delta_r^d}{12} \{(2\mathbf{r}_1 + \mathbf{r}_2 + \mathbf{r}_3) \quad (\mathbf{r}_1 + 2\mathbf{r}_2 + \mathbf{r}_3) \quad (\mathbf{r}_1 + \mathbf{r}_2 + 2\mathbf{r}_3)\}^T \quad (\text{A.45})$$

The variable Δ_r^d of (A.43) and (A.45) is calculated using,

$$\Delta_r^d = r_1 z_2 - r_2 z_1 + r_2 z_3 - r_3 z_2 + r_3 z_1 - r_1 z_3 \quad (\text{A.46})$$

A.2.3 Field equation with voltages as the forcing function

$$-\frac{1}{r} \frac{\partial}{\partial r} \left(v r \frac{\partial A_\rho}{\partial r} \right) - \frac{1}{r} \frac{\partial}{\partial z} \left(v r \frac{\partial A_\rho}{\partial z} \right) + v \frac{A_\rho}{r^2} + \sigma \frac{\partial A_\rho}{\partial t} = \sigma \frac{U_c}{2\pi r} \quad (\text{A.47})$$

A.2.3.1 Matrices derived from applying FEA to the partial differential equation

$$[\text{Dirichlet B.C.}] + [S]\{A_{\rho j}\} + [S_{II}]\{A_{\rho j}\} + [T] \frac{d}{dt} \{A_{\rho j}\} = \{f_{gu}\} U_c \quad (\text{A.48})$$

Where the matrix $[S]$ and $[S_{II}]$ were defined in (A.43) and (A.44). Matrix $[T]$ and vector $\{f_{gu}\}$ are defined by,

$$[T] = \left[\int_{\tau_D} \sigma \{N_i\}^T \{N_j\} \, d\tau_r \right] \quad (\text{A.49})$$

$$\{f_{gu}\} = \left[\int_{\tau_D} \sigma \frac{\{N_i\}^T}{(2\pi r)} \, d\tau_r \right] \quad (\text{A.50})$$

A.2.3.1.1 Matrices and vectors derived for finite element of three nodes

The matrix $[S]_{3 \times 3}$ and $[S_{II}]_{3 \times 3}$ were defined in (A.14). The matrix $[T]_{3 \times 3}$ and the vector $\{f_{gu}\}_{1 \times 3}$ are given by,

$$[T]_{3 \times 3} = \sigma \frac{\Delta r}{24} \begin{bmatrix} 2 & 1 & 1 \\ 1 & 2 & 1 \\ 1 & 1 & 2 \end{bmatrix} \quad (\text{A.51})$$

$$\{f_{gu}\}_{1 \times 3} = \sigma \frac{\Delta r}{6} \{1 \quad 1 \quad 1\}^T \quad (\text{A.52})$$

A.2.4. Field equations with currents as the forcing function

$$-\frac{1}{r} \frac{\partial}{\partial r} \left(\nu r \frac{\partial A_\rho}{\partial r} \right) - \frac{1}{r} \frac{\partial}{\partial z} \left(\nu r \frac{\partial A_\rho}{\partial z} \right) + \nu \frac{A_\rho}{r^2} + \sigma \frac{\partial A_\rho}{\partial t} = \sigma \frac{U_c}{2\pi r} \quad (\text{A.53})$$

$$(\Delta_r)^{-1}(U_c) - \int_{\tau} \sigma \frac{\partial A_\rho}{\partial t} d\tau = I_\rho \quad (\text{A.54})$$

A.2.4.1. Matrices and vectors derived from applying FEA

$$[\text{Dirichlet B.C.}] + [S]\{A_{\rho j}\} + [S_{(l)}]\{A_{\rho j}\} + [T] \frac{d}{dt} \{A_{\rho j}\} = \{f_{gu}\}(U_c) \quad (\text{A.55})$$

$$(\Delta_r)^{-1}(U_c) - \{f_{ga}\} \frac{d\{A_{\rho j}\}}{dt} = I_\rho \quad (\text{A.56})$$

Where the matrix [S] and [S_{ll}] were defined in (A.43) and (A.44). Matrix [T] and vector {f_{gu}} were defined in (A.49) and (A.50), respectively. The vector {f_{ga}} is defined by,

$$\{f_{ga}\} = \left[\int_{\tau_D} \frac{\sigma \{N_i\}^T}{2\pi r} d\tau \right] \quad (\text{A.57})$$

A.2.4.1.1. Vectors for finite element of three nodes

$$\{f_{ga}\}_{1 \times 3} = \sigma \frac{\Delta r}{6} \{1 \quad 1 \quad 1\} \quad (\text{A.58})$$

Appendix B Solution of FEM equations in the frequency and time domain

The FEM equation to be solved could correspond to a FEM field equation with voltage or currents known, or to a FEM-circuit coupled equation. These equations can be represented in a general form given by,

$$[K]\{X\} + [G]\frac{d}{dt}\{X\} = \{F\} \quad (B.1)$$

For the case of the expression which corresponds to a *FEM field equation where the voltages are known*, the variables of (B.1) will be defined by,

$$\{X\} = \{A_x\}$$

$$\{F\} = \{f_x\}\{U_c\}$$

$$[K] = [S_x]$$

$$[G] = [T_x] \quad (B.2)$$

For the case of the expression that corresponds to a *FEM field equation where the currents are known*, the variables of (B.1) are defined by,

$$\{X\} = \{\{A_x\} \quad \{U_c\}\}^T$$

$$\{F\} = \{\mathbf{0} \quad \{I\}\}^T$$

$$[K] = \begin{bmatrix} [S_x] & -\{f_x\} \\ \mathbf{0} & [\Delta_x]^{-1} \end{bmatrix}$$

$$[G] = \begin{bmatrix} [T_x] & \mathbf{0} \\ -[M_c] & \mathbf{0} \end{bmatrix} \quad (B.3)$$

For the case of a *FEM-circuit coupled equation*, the variables of (B.1) are defined by,

$$\{X\} = \{\{A_x\} \quad \{I\} \quad \{U_c\}\}^T$$

$$\{F\} = \{\mathbf{0} \quad \{V\} \quad \mathbf{0}\}^T$$

$$[K] = \begin{bmatrix} [S_x] & \mathbf{0} & -\{f_x\} \\ \mathbf{0} & [R] & \{1\} \\ \mathbf{0} & -\{1\} & [\Delta_x]^{-1} \end{bmatrix}$$

$$[G] = \begin{bmatrix} [T_x] & \mathbf{0} & \mathbf{0} \\ \mathbf{0} & [L] & \mathbf{0} \\ -[M_c] & \mathbf{0} & \mathbf{0} \end{bmatrix} \quad (\text{B.4})$$

The equation defined in (B.1) can be solved in the frequency domain or in the time domain. The solution in the frequency domain is simple, since implies to calculate a simple matrix equation (Bastos 2005). For the specific case of a time domain solution, the mostly used method is the Backwards Euler method (Arkkio 1987), (Ho, Li and Fu 1999), (Ho, Shuangxia, and Fu 2011). If the equation to be solved is non-linear, the Newton Method can be used (Okamoto, Fujiwara and Ishihara 2010). The solution on both domains will be discussed next.

B.1 Frequency domain solution

The purpose of this section is to explain how is solved the FEM equation (B.1) in the frequency domain. The equation to be solved is defined by,

$$[K]\{X\} + [G] \frac{d}{dt} \{X\} = \{F\} \quad (\text{B.5})$$

However, if the excitation contained in $\{F\}$ is sinusoidal and the materials are linear, we can use complex variables in $\{X\}$. On the FEM equations used in this investigation, $\{X\}$ could contains complex magnetic vector potentials or complex currents or voltages. The excitation $\{F\}$ could have current or voltages sources, thus this vector can be defined by (Bastos 2003), (Shen, et al. 1985),

$$\{F(t)\} = \{F_s \cos(\omega t + \beta_i)\} \quad (\text{B.6})$$

Where β_i represents the phase angle known of each excitation source contained in $\{F\}$. If the complex notation $j = \sqrt{-1}$ is used, (B.6) can be redefined by (Bastos 2003), (Shen, et al. 1985),

$$\{F(t)\} = \text{Re}(\{F_s e^{j(\omega t + \beta_i)}\}) \quad (\text{B.7})$$

Where w is the angular velocity. The system's response to this excitation is also at steady state sinusoidal and out of phase, therefore,

$$\{\mathbf{X}(t)\} = \mathbf{Re}(\{\mathbf{X}_s e^{j(\omega t + \alpha_i)}\}) \quad (\text{B.8})$$

Where $\{\mathbf{X}_s e^{j\alpha_i}\}$ is the solution of (B.4) and α_i is the phase angle of $\{\mathbf{X}(t)\}$. Thus, (B.5) can be written as (Bastos 2003), (Shen, et al. 1985),

$$[\mathbf{K}]\{\mathbf{X}_s e^{j\omega t} e^{j\alpha_i}\} + [\mathbf{G}] \frac{d}{dt} \{\mathbf{X}_s e^{j\omega t} e^{j\alpha_i}\} = \{\mathbf{F}_s e^{j\omega t + j\beta_i}\} \quad (\text{B.9})$$

If the term with derivative respect to t is developed on (B.9), yields, (Bastos 2003), (Shen, et al. 1985),

$$[\mathbf{K}]\{\mathbf{X}_s e^{j\alpha_i}\} + j\omega[\mathbf{G}]\{\mathbf{X}_s e^{j\alpha_i}\} = \{\mathbf{F}_s e^{j\beta_i}\} \quad (\text{B.10})$$

The equation (B.10) can be written as (Bastos 2003),

$$[\mathbf{K}]\{\mathbf{X}_s e^{j\alpha_i}\} + j\omega[\mathbf{G}]\{\mathbf{X}_s e^{j\alpha_i}\} = \{\mathbf{F}_s e^{j\beta_i}\} \quad (\text{B.11})$$

The vector $\{\mathbf{X}_s e^{j\alpha_i}\}$ contains complex variables denoted as $\{\tilde{\mathbf{X}}\}$. The excitation vector $\{\mathbf{F}_s e^{j\beta_i}\}$ also contains complex variables $\{\tilde{\mathbf{F}}\}$. It can be seen that the equation (B.11) can be written as,

$$([\mathbf{K}] + j\omega[\mathbf{G}])\{\tilde{\mathbf{X}}\} = \{\tilde{\mathbf{F}}\} \quad (\text{B.12})$$

Where the excitation vector $\{\tilde{\mathbf{F}}\}$ is defined by,

$$\{\tilde{\mathbf{F}}\} = \{\mathbf{F}_s e^{j\beta_i}\} \quad (\text{B.13})$$

After solving $\{\tilde{\mathbf{X}}\}$, it can be seen that the components of this vector are defined by,

$$\{\mathbf{X}_s e^{j\alpha_i}\} = \{\tilde{\mathbf{X}}\} \quad (\text{B.14})$$

The vector $\{\mathbf{X}_s e^{j\alpha_i}\}$ contains each magnitude and angle phase solution of the harmonic variables. It is possible to express (B.14) in a simpler way as,

$$[A]\{\tilde{X}\} = \{\tilde{b}\} \quad (\text{B.15})$$

After solving a single matrix system, the real and the imaginary parts of $\{\tilde{X}\}$ can be derived, and therefore its magnitude and phase angle in relation to $\{\tilde{b}\}$. However, we cannot include nonlinearity. If ferromagnetic materials are present, it is necessary to know a priori if the excitation current is low enough to avoid nonlinear effect such as saturation in the structure under study (Bastos 2003). If these conditions are not satisfied, the time discretization formulation can be used. For the latter, the time required for computation is longer (because an iterative calculation is performed for each step), the time discretization method is the only way to obtain results for nonlinear problems of this kind (Bastos 2003). The main results obtainable with the complex variables formulation are: a) Penetration effects can be seen graphically. b) Impedance calculation.

B.2 Time domain solution

The periodic behavior of an electrical network or a FEM equation can be calculated in the time domain, integrating the differential equation set that describe the dynamic of the system. They can be described in terms of a differential equation (Semlyen and Medina 1995), ,

$$\frac{dX}{dt} = f(X, t) \quad (\text{B.16})$$

The numerical method for the solution of (B.16) can be classified in explicit and implicit methods. They will be explained next.

B.2.1 Explicit methods

The solution of these methods depends on the solution of an earlier step. There are several implicit methods, the most widely used will be explained next. It is possible to employ several finite difference schemes to discretize x in the time domain. The explicit methods used will be explained next.

B.2.1.1 Euler method (forward difference) (Jianming 2002)

The *Euler* method is widely used. The method consists on dividing the time axis uniformly into a number of time intervals. A function $X(t+\Delta t)$ can be expanded into a Taylor series about t as follows (Jianming 2002),

$$X(t + \Delta t) = X(t) + \frac{dX}{dt} \Delta t + \frac{d^2X}{dt^2} \frac{(\Delta t)^2}{2!} + O|(\Delta t)^3| \quad (\text{B.17})$$

Where $O|(\Delta t)^3|$ denotes the sum of all the remaining terms containing $(\Delta t)^p$ with $p \geq 3$. From (B.17), we can obtain,

$$\frac{dX}{dt} = \frac{X_{(t+\Delta t)} - X_{(t)}}{\Delta t} + \mathbf{O}|\Delta t|^2| \quad (\text{B.18})$$

The equation (B.18) can also be written as (Jianming 2002),

$$\frac{dX}{dt} \approx \frac{X_{(t+\Delta t)} - X_{(t)}}{\Delta t} \quad (\text{B.19})$$

This approximation is of first order accurate in the sense that the truncation error contains $(\Delta t)^p$ with $p > 1$. Using the notation $X(t) = X(n \Delta t) = X_n$, we can rewrite (B.19) as follows ,

$$\frac{dX}{dt} \approx \frac{X_{n+1} - X_n}{\Delta t} \quad (\text{B.20})$$

Taking into account (B.20), (B.16) can be written by,

$$X_{n+1} = X_n + (\Delta t)f(X_n, t_n) \quad (\text{B.21})$$

Where x_n represents the vector that contains variables stored in the time step n ; t_n represents the time in that step; and Δt is the integration step. The calculating process of the Euler method can be seen in Figure B.1

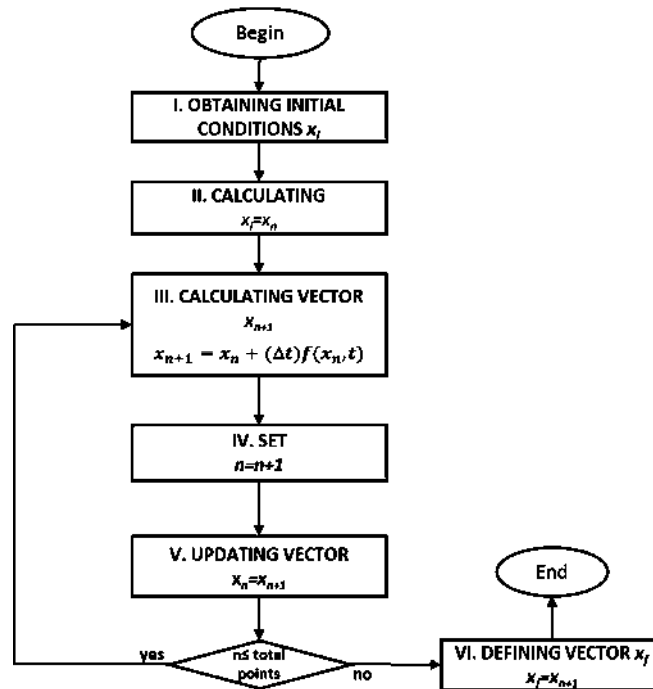


Figure B.1. Calculating process of the Euler method

The Euler Method can be used to solve the partial differential equation defined by,

$$[\mathbf{K}]\{\mathbf{X}\} + [\mathbf{G}] \frac{d}{dt}\{\mathbf{X}\} = \{\mathbf{F}\} \quad (\text{B.22})$$

If the term with derivate respect the time of (B.22) is isolated, it results on,

$$\frac{d\{\mathbf{X}\}}{dt} = [\mathbf{G}]^{-1}(\{\mathbf{F}\} - [\mathbf{K}]\{\mathbf{X}\}) \quad (\text{B.23})$$

The equation (B.23) can be approximated by the Euler method results on,

$$\frac{\{\mathbf{X}\}_{(t+\Delta t)} - \{\mathbf{X}\}_{(t)}}{\Delta t} = [\mathbf{G}]^{-1}(\{\mathbf{F}\}_{(t)} - [\mathbf{K}]\{\mathbf{X}\}_{(t)}) \quad (\text{B.24})$$

Finally (B.23) can be written by,

$$\{\mathbf{X}\}_{(t+\Delta t)} = (\Delta t)[\mathbf{G}]^{-1}(\{\mathbf{F}\}_{(t)} - [\mathbf{K}]\{\mathbf{X}\}_{(t)}) + \{\mathbf{X}\}_{(t)} \quad (\text{B.25})$$

If the notation shown of (B.21) is used on (B.25), it results on (Jianming 2002),

$$\{\mathbf{X}\}_{n+1} = (\Delta t)[\mathbf{G}]^{-1}(\{\mathbf{F}\}_n - [\mathbf{K}]\{\mathbf{X}\}_n) + \{\mathbf{X}\}_n \quad (\text{B.26})$$

B.2.1.2 Backwards Euler (backward difference) (Jianming 2002)

The *Backwards Euler* method is widely used for solving an equation which has the form of (B.1). For this method, a function $x(t-\Delta t)$ can be expanded into a Taylor series about t as (Jianming 2002),

$$\mathbf{X}(t - \Delta t) = \mathbf{X}(t) - \frac{d\mathbf{X}}{dt} \Delta t + \frac{d^2\mathbf{X}}{dt^2} \frac{(\Delta t)^2}{2!} + \mathbf{O}[(\Delta t)^3] \quad (\text{B.27})$$

From which we can obtain,

$$\frac{d\mathbf{X}}{dt} = \frac{\mathbf{X}(t) - \mathbf{X}(t-\Delta t)}{\Delta t} + \mathbf{O}[(\Delta t)^2] \quad (\text{B.28})$$

Finally (B.28) can be defined by,

$$\frac{d\mathbf{X}}{dt} \approx \frac{\mathbf{X}(t) - \mathbf{X}(t-\Delta t)}{\Delta t} \quad (\text{B.29})$$

This approximation is called the *backward difference* representation but it is also known as the *Backwards Euler* method. Using the notation $X(t) = u(n\Delta t) = X_n$, we can rewrite (B.29) as,

$$\frac{dX}{dt} \approx \frac{X_n - X_{n-1}}{\Delta t} \quad (\text{B.30})$$

Taking into account the notation used in (B.21), (B.30) can be written by,

$$X_n = X_{n-1} + (\Delta t)f(X_{n-1}, t_{n-1}) \quad (\text{B.31})$$

Where X_n represents the vector that contains variables stored in the time step n ; t_n represents the time in that step; and Δt is the integration step. The vector X_{n-1} contains the vector in an earlier step t_{n-1} . The calculating process of the *Backwards Euler* method is detailed in Figure B.2.

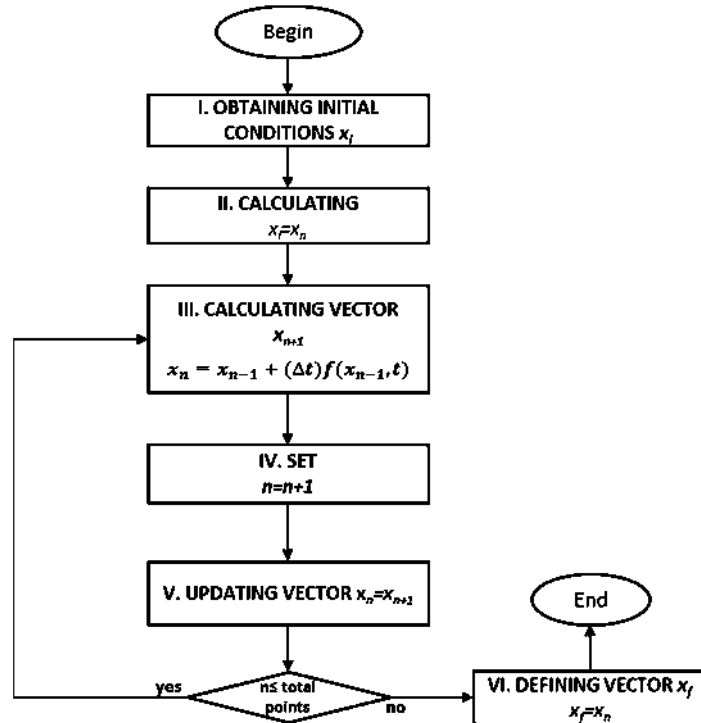


Figure B.2. Backwards Euler Method

The equation (B.22) can be approximated by the *Backwards Euler* Method. It results on,

$$\frac{\{X\}_{(t)} - \{X\}_{(t-\Delta t)}}{\Delta t} = [G]^{-1}(\{F\}_{(t-\Delta t)} - [K]\{X\}_{(t-\Delta t)}) \quad (\text{B.32})$$

Finally (B.32) can be written by,

$$\{\mathbf{X}\}_{(t)} = \left([\mathbf{K}] + \frac{[\mathbf{G}]}{\Delta t} \right)^{-1} \left(\{\mathbf{F}\}_{(t-\Delta t)} + \frac{[\mathbf{G}]}{\Delta t} \mathbf{X}_{(t-\Delta t)} \right) \quad (\text{B.33})$$

If the notation shown in (B.31) is used on (B.33), yields,

$$\{\mathbf{X}\}_{(n)} = \left([\mathbf{K}] + \frac{[\mathbf{G}]}{\Delta t} \right)^{-1} \left(\{\mathbf{F}\}_{(n-1)} + \frac{[\mathbf{G}]}{\Delta t} \mathbf{X}_{(n-1)} \right) \quad (\text{B.34})$$

B.2.1.3 Fourth order Runge Kutta method (Jianming 2002)

Another useful method is the fourth order Runge Kutta method. The method consists on calculating the variables in the time $t+\Delta t$ using,

$$\mathbf{X}_{n+1} = \mathbf{X}_n + \left(\frac{1}{6} \right) (\mathbf{k}_1 + 2\mathbf{k}_2 + 2\mathbf{k}_3 + \mathbf{k}_4) \quad (\text{B.35})$$

Where the components of (B.35) are defined by,

$$\mathbf{k}_1 = (\Delta t) f(\mathbf{X}_n, t_n) \quad (\text{B.36})$$

$$\mathbf{k}_2 = (\Delta t) f\left(\mathbf{X}_n + \frac{\mathbf{k}_1}{2}, t_n + \frac{\Delta t}{2}\right) \quad (\text{B.37})$$

$$\mathbf{k}_3 = (\Delta t) f\left(\mathbf{X}_n + \frac{\mathbf{k}_2}{2}, t_n + \frac{\Delta t}{2}\right) \quad (\text{B.38})$$

$$\mathbf{k}_4 = (\Delta t) f(\mathbf{X}_n + \mathbf{k}_3, t_n + \Delta t) \quad (\text{B.39})$$

After calculating \mathbf{X}_{n+1} , the calculating process for the next process implies that the value of \mathbf{X}_{n+1} will be become the value \mathbf{X}_n which is necessary to derivate the value for the next step. The calculating process of the fourth order Runge Kutta method is shown in Figure B.3.

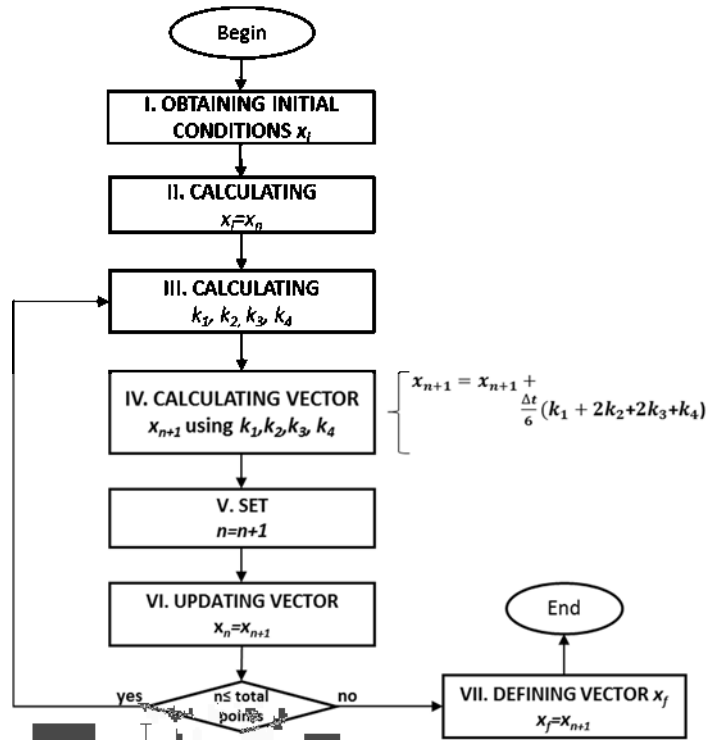


Figure B.3. Fourth order Runge Kutta method

The equation (B.22) can also be approximated by the Runge Kutta method. The values k_1 , k_2 , k_3 and k_4 will be defined by,

$$\{k_1\}_n = \Delta t [G]^{-1} (\{F\}_n - [K]\{X\}_n) \quad (B.40)$$

$$\{k_2\}_n = (t_n + \frac{\Delta t}{2}) [G]^{-1} (\{F\}_{(n)} - [K]\{X_n + \frac{k_1}{2}\}) \quad (B.41)$$

$$\{k_3\}_n = (t_n + \frac{\Delta t}{2}) [G]^{-1} (\{F\}_{(n)} - [K]\{X_n + \frac{k_2}{2}\}) \quad (B.42)$$

$$\{k_4\}_n = (t_n + \Delta t) [G]^{-1} (\{F\}_{(n)} - [K]\{X_n + k_3\}) \quad (B.43)$$

After calculating $\{k_1\}_n$, $\{k_2\}_n$, $\{k_3\}_n$ and $\{k_4\}_n$, it is possible to calculate the vector $\{X\}_{n+1}$. It yields,

$$\{X\}_{n+1} = x_n + \frac{1}{6} (\{k_1\}_n + 2\{k_2\}_n + 2\{k_3\}_n + \{k_4\}_n) \quad (B.44)$$

If the notation shown in (B.21) is used on (B.44) results on,

$$\{X\}_n = (\Delta t)[G]^{-1}(\{F\}_{n-1} - [K]\{X\}_{n-1}) + \{X\}_{n-1} \quad (\text{B.45})$$

B.2.2 Implicit methods

The method described in the section B.2.1 are known as “A-stables” because the convergence does not depend of the choice of the integration step Δt . Because of this, these are mostly used for the analysis of stiff systems. The modified *Euler* method known as *trapezoidal rule*, is an example of an implicit method. The *trapezoidal rule* can be calculated using,

$$x_{n+1} = x_n + \left(\frac{\Delta t}{2}\right) (f(t_{n+1}, x_{n+1}) + f(t_n, x_n)) \quad (\text{B.46})$$

From (B.46) can be seen that it is necessary to use a solution method to find an approximate solution to $f(t_{n+1}, x_{n+1})$ which is a feature of all the implicit methods. A good approximation to $f(t_{n+1}, x_{n+1})$ can be obtained using the *Euler* method or the *Backwards Euler* method.

B.2.2.1 Newton method (Semlyen and Medina 1995)

The traditional method to determine the stationary state of an equation, can be determined by integrating the set of differential equations that represent the dynamic of the system, over a period of time, using as a base the initial conditions. In a given period of time, the maximum error calculated between the vector of the variables at the beginning of the period and the vector of variables at the end of the period is compared against a tolerance for convergence. If the maximum error is larger, the process should be performed again. The process should be performed several times to obtain the stationary periodic time of the system. This process is named *brute force*. The method follows the steps that can be seen in Figure B.4.

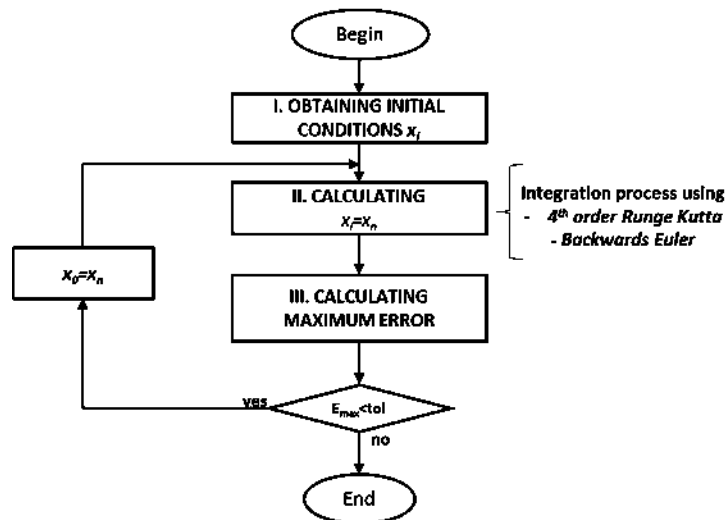


Figure B.4. Brute force method

There are several methods that permit to derive a fast solution of the periodic stationary state of a set of equations that model the dynamic of a system. This techniques can be classified as a *shooting methods* (Semlyen and Medina 1995). The main objective of these methods, is finding an solution $x(T) = x(0)$, this condition implied that the initial conditions $x(0)$ must be integrated into the equation set defined by $x=f(x,t)$ over a period of time (Semlyen and Medina 1995).

On this investigation, because of the nature of the FEM equations to be solved, the numerical differentiation method (ND) was applied, since it is amenable to the use of the *Backwards Euler* method.

The impulse functions of the differential equations to be solved are represented by voltage or current sources. These sources are assumed to be periodic. Because of this, the stable state solution $x(t)$ is also periodic and can be represented as a limit cycle for x_k in terms of another periodic element of x , or in terms of the periodic function, for example $\sin(\omega t)$.

The cycles of a transient orbit are near to the limit cycle before reaching it. The position can be properly described by a representation in the Poincare plane (Medina and Ramos-Paz 2010). A single cycle maps the starting point x_i to the final point x_{i+1} and maps a perturbing segment Dx_i to Dx_{i+1} . This can be seen in figure B.5. All the maps near from the limit cycle are quasi-linear. This permits to use the Newton methods to reach the point at the beginning of the limit cycle x_∞ (Semlyen and Medina 1995). The periodic steady state solution is irrespective of the stability of the system

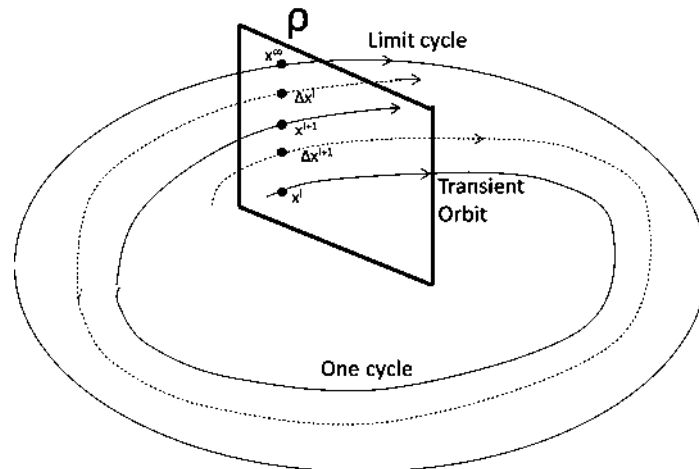


Figure B.5. Orbit of a vector X

It is possible to use linear property of the regions located near from a base cycle. Thus, the main equation can be considered to be linear in a solution $x(t)$ from t_i to t_i+T . This can be represented by a variational problem (Semlyen and Medina 1995),

$$\Delta \dot{x} = \Delta f(x(t), t) = D_x f(x_t, t) \Delta x = J(t) \Delta x \quad (B.47)$$

Where $J(t)$ is a Jacobean matrix. The initial condition is defined as,

$$\Delta \mathbf{x}(t_i) = \Delta \mathbf{x}_i \quad (\text{B.48})$$

The equation (B.47) is a linear ordinary differential equation which is time varying. Its solution is given by,

$$\Delta \mathbf{x}(t) = \exp\left(\int_{t_i}^t J(t) dt\right) \Delta \mathbf{x}_i \quad (\text{B.49})$$

It can be seen that (B.49) is a solution of (B.16). For the case of the expression $t=t_i+T$, (B.49) can be defined by (Semlyen and Medina 1995),

$$\Delta \mathbf{x}_{i+1} = \Phi \Delta \mathbf{x}_i \quad (\text{B.50})$$

Where Φ is defined by,

$$\Phi = \exp\left(\int_{t_i}^{t_i+T} J(t) dt\right) \Delta \mathbf{x}^i \quad (\text{B.51})$$

It can be seen that Φ remains almost equal for a value of t_i , if the mapping near the limit cycle presents almost a linear behavior. The equation (B.51) shows that the input segments are mapping to correspond to the output segments using the matrix defined by Φ . According to the *Poincaré* map, it can be seen that,

$$\Delta \mathbf{x}_i = \mathbf{x}_\infty - \mathbf{x}_i \quad (\text{B.52})$$

If (B.52) is isolated in terms of \mathbf{x}_∞ results on

$$\mathbf{x}_\infty = \Delta \mathbf{x}_i + \mathbf{x}_i \quad (\text{B.53})$$

Because of this, it can be concluded that,

$$\Delta \mathbf{x}_{i+1} = \mathbf{x}_\infty - \mathbf{x}_{i+1} \quad (\text{B.54})$$

If (B.54) is isolated in terms of \mathbf{x}_∞ results on

$$\mathbf{x}_\infty = \Delta \mathbf{x}_{i+1} + \mathbf{x}_{i+1} \quad (\text{B.55})$$

If the equations (B.53) and (B.54) are used, it can be concluded that,

$$\Delta x_i - \Delta x_{i+1} = x_{i+1} - x_i \quad (\text{B.56})$$

If (B.54) is substituted in (B.56) and the result is isolated in terms of the variable Δx_i , yields,

$$\Delta x_i = (I - \Phi)^{-1}(x_{i+1} - x_i) \quad (\text{B.57})$$

If (B.52) is substituted in the left side of (B.57), and the result is isolated in terms of x_∞ , yields,

$$x_\infty = x_i + (I - \Phi)^{-1}(x_{i+1} - x_i) \quad (\text{B.58})$$

The equation (B.58) represents an approximate solution of the limit cycle location. It permits to get a Newton solution if matrices Φ and $(I - \Phi)^{-1}$ are updated on each iteration. This action leads to a linear convergent process if the matrix $(I - \Phi)^{-1}$ is kept constant, or if it is updated during a state of the iterative process after the first evaluation (Semlyen and Medina 1995).

The main problem to find the limit cycle in an efficient way resides on the identification of the matrix Φ (Semlyen and Medina 1995). The ND method is now concisely described

B.2.2.2 Numerical Differentiation Method (Semlyen and Medina 1995)

The method uses the increment defined by Δf instead of $J(t)\Delta x$. This action implied that is easy to integrate the equation defined in (219) using initial conditions x_i to get the base cycle $x(t)$. At the same time, it is necessary to integrate using an initial perturbation value defined by $x_i + \varepsilon e_i$ where e_i is the i -column of the identity matrix I , ε is a small value, i.e. 1×10^{-6} . If the difference between the two values of X is calculated in the end of the cycle, it is possible to obtain the columns of ΔX_{i+1} . For this case, the calculating process of the matrix Φ calculated requires m steps. This is the case of Jacobean matrix calculating processes. Figure B.6 shows the flux diagram of the ND method.

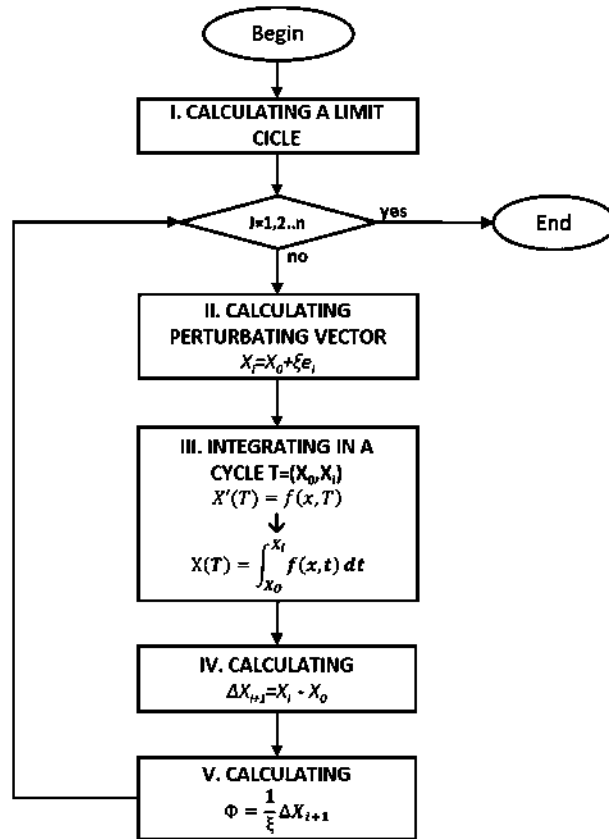


Figure B.6. Diagram of the *ND* Method.

It can be seen that the FEM field and the FEM field equations can be solved in the frequency and the time domain using the methods of solution explained in this section. Nevertheless, the FEM equations may consist on matrices of larger order, may be difficult to obtain, or it may need of a considerable computation time. It is possible to overcome this situation, by using the parallel computing platform. The CUDA parallel computing platform enables to solve these equations in an easy and efficient way.

Appendix C Main features of the CUDA programs used in case study 2 and 4

C.1 Case study 2

C.1.1 GSL program

```
// Programmer: Raul Dominguez
// December 2013
// Program name: VM185F45_6g.cu
//
// DESCRIPTION
// This program calculates the T-Slot Conductor.
// It is used the reduced equation, dimensions: 205x205
//
// PREPROCESSING STAGE: GSL AND C ROUTINES
/// CALCULATING STAGE: GSL ROUTINES
//
// PREPROCESSING STAGE
// 1. INPUT DATA:
// 1.1 ELEMENTS //
// ELEMENTS NUMBER OF ANSYS MESHING: numel=457
// 1.1.1 Element Data File: VM185F45_4_elem.txt
// Element File Structure:
// (ELEM No.) (Element Type) (NODE 1 No.) (NODE 2 No.) (NODE 3 No.)
// 1.2 NODES //
// Total Nodes of ANSYS Meshing: numnod=265
// Node number of conductor region: K11_wh=205
// Node number of non-conductor region: K22_wh=60
// 1.2.1 Nodes Data File: VM185F45_3_nod.txt
// 1.2.2 Node Data File Structure:
// (NODE No.) (Coordinate X) (Coordinate Y)
// 1.3 BOUNDARY CONDITIONS //
// Boundary conditions: numnodZ=9
// 1.3.1 Boundary Condition Structure: Node and Magnetic Vector Potential
// NODE 206---- Az(206)=0; NODE 212---- Az(212)=0
// NODE 218---- Az(218)=0; NODE 219---- Az(219)=0
```

```

//          NODE 220---- Az(220)=0; NODE 221---- Az(221)=0
//          NODE 222---- Az(222)=0; NODE 223---- Az(223)=0
//          NODE 224---- Az(224)=0;
//2.  USE OF FEM  ROUTINES  //
//    2.1 C Routine: felp2d1
//          It calculates the Finite Element Matrix of Three Nodes
//          S[3,3] Plane Symmetry (SEE APPENDIX A, EQUATION A.14)
//    2.2 C Routine: felp2d2
//          It calculates the Finite Element Matrix of Three Nodes
//          T[3,3] Plane Symmetry (SEE APPENDIX A, EQUATION A.23)
//    2.3 C Routine: felp2d4
//          It calculates the Finite Element Matrix of Three Nodes
//          F[3] Plane Symmetry (SEE APPENDIX A, EQUATION A.24)
//3.  DERIVING GLOBAL MATRICES AND VECTORS
/ Global Matrices of Plane Symmetry
// kk[numnod,numnod], gg[numnod,numnod], ff[numnod]
//4.  CALCULATING UNCOUPLED EQUATION
//    4.1 Deriving submatrices based on Global Matrices
//          kk_11[K11_wh,K11_wh], kk_12[K11_wh,K22_wh], kk_21[K22_wh,K11_wh], //
//          kk_22[K22_wh,K22_wh]
//          gg_11[K11_wh, K11_wh], gg_21[K22_wh, K11_wh]
//          ff_1[K11_wh], ff_2[K22_wh]
//    4.2 Deriving matrices of Uncoupled Equation
//          kk_11[K11_wh, K11_wh] (Use of GSL routine gsl_blas_dgemm)
//          gg_11[K11_wh, K11_wh] (Use of GSL routine gsl_blas_dgemm)
//          ff_t[K11_wh]      (Use of GSL routine gsl_blas_dgemv)
//    4.3 Forming complex Uncoupled Equation
//          freq: frequency
//          A_matrix[K11_wh]
//          X_vector[K11_wh] (Magnetic vector potentials of conductor region)
//          B_vector[K11_wh]
//
// CALCULATING STAGE //
// 1. Calculating (A_matrix)(X_vector)=B_vector
// 2. GSL routines used
//    gsl_permutation *p, gsl_linalg_complex_LU_decomp, gsl_linalg_complex_LU_solve
// 3. Calculating voltage on Conductor Uc

```


C.1.2 CUBLAS program

```
// Programmer: Raul Dominguez
// December 2013
// Program name: VM185F45_6gC.cu
//
// DESCRIPTION
// This program calculates the T-Slot Conductor.
// It is used the reduced equation, dimensions: 205x205
//
// PREPROCESSING STAGE: GSL AND C ROUTINES
// CALCULATING STAGE: CUBLAS ROUTINES
//
// PREPROCESSING STAGE
// 1. (SEE VM185F45_6c.cu)
// 2. (SEE VM185F45_6c.cu)
// 3. (SEE VM185F45_6c.cu)
// 4. CALCULATING UNCOUPLED EQUATION
//     4.1 Deriving submatrices based on Global Matrices
//         kk_11[K11_wh,K11_wh], kk_12[K11_wh,K22_wh],
//         kk_21[K22_wh,K11_wh], kk_22[K22_wh,K22_wh]
//         gg_11[K11_wh, K11_wh], gg_21[K22_wh, K11_wh]
//         ff_1[K11_wh], ff_2[K22_wh]
//     4.2 Deriving matrices of Uncoupled Equation
//         K11_cpu[K11_wh, K11_wh] (Use of CUBLAS routine CUBLASsgemm)
//         G11_cpu[K11_wh, K11_wh] (Use of CUBLAS routine CUBLASsgemm)
//         FT_cpu[K11_wh] (Use of CUBLAS routine CUBLASsgemv)
//     4.3 Forming complex Uncoupled Equation
//         freq: frequency
//         kkC_cpu[K11_wh,K11_wh] (Matrix to be decomposed in L and U)
//         bc_cpu[K11_wh]
// CALCULATING STAGE //
// 1. Performing LU decomposition: kkC_cpu=(Lc_gpu)*(Uc_gpu)
// 2. Solving [(Lc_gpu)*(Uc_gpu)]*X =bc_cpu
//     2.1 Solving (Lc_gpu)*Y=bc_cpu (Use of CUBLAS routine cublasctrsv)
//     2.1 Solving (Lc_gpu)*Y=bc_cpu (Use of CUBLAS routine cublasctrsv)
// 3. Calculating voltage and current density on Conductor
```

C.2 Case study 4

C.2.1 Air series reactor 1

C.2.1.1 GSL program

```
// Programmer: Raul Dominguez
// December 2013
// Program name: Preiss_237_53.cu
//
// DESCRIPTION
// This program calculates the 10 turns Air Series Reactor
// It is used the reduced equation, dimensions of reduced equation: 1260x1260
//
// PREPROCESSING STAGE: GSL AND C ROUTINES
// CALCULATING STAGE: GSL ROUTINES
//
// PREPROCESSING STAGE //
// 1. INPUT DATA:
```

```

//      1.1      E L E M E N T S
//      ELEMENTS NUMBER OF ANSYS MESHING: numel=6918
//      1.1.1 Element Data File: Preiss2372_elem.txt
//      Element File Structure:
//      (ELEM No.) (Element Type) (NODE 1 No.) (NODE 2 No.) (NODE 3 No.)
//      1.2      N O D E S
//      Total Nodes of ANSYS Meshing: numnod=1668
//      Node number of conductor region: K11_wh=1260
//      Node number of non-conductor region: K22_wh=2250
//      1.2.1 Nodes Data File: Preiss2372_nod.txt
//      1.2.2 Node Data File Structure:
//      (NODE No.) (Coordinate X) (Coordinate Y)
//      1.3      B O U N D A R Y   C O N D I T I O N S //
//      Boundary conditions: numnodZ=100
//      1.3.1 Boundary Conditions Data File: Preiss2372_nodZ.txt
//      1.3.2 Boundary Conditions File Structure:
//      (NODE No.) Az(NODE No.)=0
// 2.  U S E   O F   F E M   R O U T I N E S //
//      2.1 C Routine: felpaxt31
//      It calculates the Finite Element Matrix of Three Nodes
//      S[3,3] Axisymmetric Symmetry (SEE APPENDIX A, EQUATION A.43)
//
//      2.2 C Routine: felpaxt31_d
//      It calculates the Finite Element Matrix of Three Nodes
//      SII[3,3] Axisymmetric Symmetry (SEE APPENDIX A, EQUATION A.44)
//
//      2.3 C Routine: felpaxt33_a
//      It calculates the Finite Element Matrix of Three Nodes
//      T[3,3] Axisymmetric Symmetry (SEE APPENDIX A, EQUATION A.51)
//
//      2.4 C Routine: felpaxt30N
//      It calculates the Finite Element Vector of Three Nodes
//      F[3] Axisymmetric Symmetry (SEE APPENDIX A, EQUATION A.52)
//
// 3. D E R I V I N G   G L O B A L   M A T R I C E S   A N D   V E C T O R S
// Global Matrices of Axisymmetric Symmetry
//      kk[numnod+10,numnod+10], gg[numnod+10,numnod+10]
//      fg1[numnod+10], fg2[numnod+10], fg3[numnod+10], fg4[numnod+10],
//      fg5[numnod+10]
//      fg6[numnod+10], fg7[numnod+10], fg8[numnod+10], fg9[numnod+10],
//      fg10[numnod+10],
//
// 4.  C A L C U L A T I N G   U N C O U P L E D   E Q U A T I O N
//      4.1 Deriving submatrices based on Global Matrices
//      kk_11[K11_wh,K11_wh], kk_12[K11_wh,K22_wh], kk_21[K22_wh,K11_wh],
//      kk_22[K22_wh,K22_wh]
//      gg_11[K11_wh, K11_wh], gg_21[K22_wh, K11_wh]
//      ff_t[K11_wh]
//      4.2 Deriving matrices of Uncoupled Equation
//      kk_11[K11_wh, K11_wh] (Use of GSL routine gsl_blas_dgemm)
//      gg_11[K11_wh, K11_wh] (Use of GSL routine gsl_blas_dgemm)
//      ff_t[K11_wh] (Use of GSL routine gsl_blas_dgemv)
//      4.3 Forming complex Uncoupled Equation
//      freq: frequency
//      A_matrix[K11_wh]
//      X_vector[K11_wh] (Magnetic vector potentials of conductor
//      region)
//      B_vector[K11_wh]
//

```

```
// C A L C U L A T I N G   S T A G E   //
// 1. Calculating (A_matrix)(X_vector)=B_vector
// 2. GSL routines used
//   gsl_permutation *p, gsl_linalg_complex_LU_decomp,
//   gsl_linalg_complex_LU_solve
// 3. Calculating voltage on each turn Uci, Uc1, Uc2, Uc3, Uc4,
//   Uc5, Uc6, Uc7, Uc8, Uc9, Uc10
// 4. Calculating total voltage on Air Series Reactor
//   Uct=Uc1+Uc2+Uc3+Uc4+...+Uc9+Uc10
```

C.2.1.2 CUBLAS program

```
// Programmer: Raul Dominguez
// December 2013
// Program name: Preiss_237_61.cu
//
// DESCRIPTION //
// This program calculates the 10 turns Air Series Reactor
// It is used the reduced equation, dimensions: 1260x1260
//
// PREPROCESSING STAGE: GSL AND C ROUTINES
// CALCULATING STAGE: CUBLAS ROUTINES
//
// P R E P R O C E S S I N G   S T A G E   //
// 1.      (S E E   Preiss_237_53.cu)
// 2.      (S E E   Preiss_237_53.cu)
// 3.      (S E E   Preiss_237_53.cu)
// 4.  C A L C U L A T I N G   U N C O U P L E D   E Q U A T I O N
//      4.1 Deriving submatrices based on Global Matrices
//          K11_cpu[K11_wh,K11_wh], K12_cpu[K11_wh,K22_wh]
//          K21_cpu[K22_wh,K11_wh], K22_cpu[K22_wh,K22_wh]
//          G11_cpu[K11_wh, K11_wh], G21_cpu[K22_wh, K11_wh]
//          FT_cpu[K11_wh]
//      4.2 Deriving matrices of Uncoupled Equation
//          K11_cpu[K11_wh, K11_wh] (Use of CUBLAS routine CUBLASsgemm)
//          G11_cpu[K11_wh, K11_wh] (Use of CUBLAS routine CUBLASsgemm)
//          FT_cpu[K11_wh]      (Use of CUBLAS routine CUBLASsgemv)
//      4.3 Forming complex Uncoupled Equation
//          freq: frequency
//          kkC_cpu[K11_wh,K11_wh] (Matrix to be decomposed in L and U)
//          bc_cpu[K11_wh]
//
// C A L C U L A T I N G   S T A G E   //
// 1. Performing LU decomposition: kkC_cpu=(Lc_gpu)*(Uc_gpu)
// 2. Solving [(Lc_gpu)*(Uc_gpu)]*X =bc_cpu
//      2.1 Solving (Lc_gpu)*Y=bc_cpu (Use of CUBLAS routine cublasctrsv)
//      2.1 Solving (Uc_gpu)*X=bc_cpu (Use of CUBLAS routine cublasctrsv)
// 3. Calculating voltage on each turn Uci, Uc1, Uc2, Uc3, Uc4, Uc5, Uc6,
//   Uc7, Uc8, Uc9, Uc10
// 4. Calculating total voltage on Air Series Reactor /
//   Uct=Uc1+Uc2+Uc3+Uc4+...+Uc9+Uc10
```

C.2.2 Air series reactor 2

C.2.2.1 GSL program

```
// Programmer: Raul Dominguez
// December 2013
```

```

//
// Program name: Preiss_218_345.cu
//
// DESCRIPTION //
// This program calculates the 5 turns Air Series Reactor
// It is used the reduced equation, dimensions: 205x205
// PREPROCESSING STAGE: GSL AND C ROUTINES
//
// CALCULATING STAGE: GSL ROUTINES
// PREPROCESSING STAGE //
// 1. INPUT DATA:
// 1.1 ELEMENTS //
// ELEMENTS NUMBER OF ANSYS MESHING: numel=3210
// 1.1.1 Element Data File: Preiss21831_elem.txt
// Element File Structure:
// (ELEM No.) (Element Type) (NODE 1 No.) (NODE 2 No.) (NODE 3 No.)
// 1.2 NODES //
// Total Nodes of ANSYS Meshing: numnod=1668
// Node number of conductor region: K11_wh=180
// Node number of non-conductor region: K22_wh=1488
// 1.2.1 Nodes Data File: Preiss21831_nod.txt.txt
// 1.2.2 Node Data File Structure:
// (NODE No.) (Coordinate X) (Coordinate Y)
// 1.3 BOUNDARY CONDITIONS //
// Boundary conditions: numnodZ=125
// 1.2.1 Boundary Conditions Data File: Preiss21831_nodZ.txt
// 1.2.2 Boundary Conditions File Structure:
// (NODE No.) Az(NODE)=0
//
// 2. USE OF FEM ROUTINES //
// 2.1 C Routine: felpaxt31
// It calculates the Finite Element Matrix of Three Nodes
// S[3,3] Axisymmetric Symmetry (SEE APPENDIX A, EQUATION A.43)
// 2.2 C Routine: felpaxt31_d
// It calculates the Finite Element Matrix of Three Nodes
// SII[3,3] Axisymmetric Symmetry (SEE APPENDIX A, EQUATION A.44)
// 2.3 C Routine: felpaxt33_a
// It calculates the Finite Element Matrix of Three Nodes
// T[3,3] Axisymmetric Symmetry (SEE APPENDIX A, EQUATION A.51)
// 2.4 C Routine: felpaxt30N
// It calculates the Finite Element Vector of Three Nodes
// F[3] Axisymmetric Symmetry (SEE APPENDIX A, EQUATION A.52)
// 3. DERIVING GLOBAL MATRICES AND VECTORS
// Global Matrices of Plane Symmetry
// kk[numnod+5,numnod+5], gg[numnod+5,numnod+5]
// fg1[numno+5], fg2[numnod+5], fg3[numnod+5], fg4[numnod+5], fg5[numnod+5]
// 4. CALCULATING UNCOUPLED EQUATION
// 4.1 Deriving submatrices based on Global Matrices
// kk_11[K11_wh,K11_wh], kk_12[K11_wh,K22_wh], kk_21[K22_wh,K11_wh],
// kk_22[K22_wh,K22_wh]
// gg_11[K11_wh, K11_wh], gg_21[K22_wh, K11_wh]
// ff_t[K11_wh]
// 4.2 Deriving matrices of Uncoupled Equation
// kk_11[K11_wh, K11_wh] (Use of GSL routine gsl_blas_dgemm)
// gg_11[K11_wh, K11_wh] (Use of GSL routine gsl_blas_dgemm)
// ff_t[K11_wh] (Use of GSL routine gsl_blas_dgemm)
// 4.3 Forming complex Uncoupled Equation
// freq: frequency
// A_matrix[K11_wh]

```

```

//          X_vector[K11_wh] (Magnetic vector potentials of conductor region)
//          B_vector[K11_wh]
// C A L C U L A T I N G   S T A G E   //
// 1. Calculating (A_matrix)(X_vector)=B_vector
// 2. GSL routines used
//   gsl_permutation *p, gsl_linalg_complex_LU_decomp, gsl_linalg_complex_LU_solve
// 3. Calculating voltage on each turn Uci, Uc1, Uc2, Uc3, Uc4, Uc5
// 4. Calculating total voltage on Air Series Reactor Uct=Uc1+Uc2+Uc3+Uc4+Uc5

```

C.2.2.2 CUBLAS program

```

// Program name: Preiss_218_347_6.cu
// Programmer: Raul Dominguez
// December 2013

```

```

// DESCRIPTION //
// This program calculates the 5 turns Air Series Reactor
// It is used the reduced equation, dimensions: 205x205
// PREPROCESSING STAGE: GSL AND C ROUTINES
// CALCULATING STAGE: GSL ROUTINES
//
// P R E P R O C E S S I N G   S T A G E   //
// 1.      (S E E   Preiss_218_345.cu)
// 2.      (S E E   Preiss_218_345.cu)
// 3.      (S E E   Preiss_218_345.cu)
// 4.  C A L C U L A T I N G   U N C O U P L E D   E Q U A T I O N
//      4.1 Deriving submatrices and subvectors based on Global Matrices
//          K11_cpu[K11_wh,K11_wh], K12_cpu[K11_wh,K22_wh]
//          K21_cpu[K22_wh,K11_wh], K22_cpu[K22_wh,K22_wh]
//          G11_cpu[K11_wh, K11_wh], G21_cpu[K22_wh, K11_wh]
//          FT_cpu[K11_wh]
//      4.2 Deriving matrices and subvector of Uncoupled Equation
//          K11_cpu[K11_wh, K11_wh] (Use of CUBLAS routine CublasSgemm)
//          G11_cpu[K11_wh, K11_wh] (Use of CUBLAS routine CublasSgemm)
//          FT_cpu[K11_wh]      (Use of CUBLAS routine CublasSgemv)
//      4.3 Forming complex Uncoupled Equation
//          freq: frequency
//          kkC_cpu[K11_wh,K11_wh] (Matrix to be decomposed in L and U)
//          bc_cpu[K11_wh]
//
// C A L C U L A T I N G   S T A G E   //
// 1. Performing LU decomposition: kkC_cpu=(Lc_gpu)*(Uc_gpu)
// 2. Solving [(Lc_gpu)*(Uc_gpu)]*X =bc_cpu
//      2.1 Solving (Lc_gpu)*Y=bc_cpu (Use of CUBLAS routine cublasctrsv)
//      2.1 Solving (Uc_gpu)*X=bc_cpu (Use of CUBLAS routine cublasctrsv)
// 3. Calculating voltage on each turn Uci, Uc1, Uc2, Uc3, Uc4, Uc5
// 4. Calculating total voltage on Air Series Reactor Uct=Uc1+Uc2+Uc3+Uc4+Uc5

```